STRUCTURAL AND FUNCTIONAL PROPERTIES OF ENZYMATICALLY MODIFIED SLOW DIGESTING α-GLUCANS

by

Sarah Gafter Corwin

A Dissertation

Submitted to the Faculty of Purdue University

In Partial Fulfillment of the Requirements for the degree of

Doctor of Philosophy

Department of Food Science

West Lafayette, Indiana

August 2020

THE PURDUE UNIVERSITY GRADUATE SCHOOL
STATEMENT OF COMMITTEE APPROVAL

Dr. Bruce Hamaker, Chair

Department of Food Science

Dr. Bradley Reuhs

Department of Food Science

Dr. Kee Hong Kim

Department of Food Science

Dr Richard D. Mattes

Department of Nutrition Science

Dr Yuan Yao

Department of Food Science

Approved by:

Dr. Arun Bhunia

Head of the Department of Graduate Program

To my parents; and my husband.

Ricki Lee Davis Gafter, Neal Michael Gafter; and Jonathon Marc Corwin

ACKNOWLEDGMENTS

I would like to thank Professor Dr. Bruce Hamaker first and foremost for his support, encouragement, and great approach to mentorship which allowed me to focus on professional development as well as my research. Thank you as well to Drs. Lisa Lamothe and Christina Vafeiadi, and all of Nestle Nutrition Sciences for providing funding, guidance, and contribution to this body of work. I would also like to thank Drs. Lubbert Dijkhuizen, Evelien te Poele, and Joana Gangoiti of Groningen University initially and later CarbExplore for the fantastic contribution in the enzymes space to this research, this research could not have happened without you. Professor Dr. Byung-Hoo Lee served as an expert in native mammalian enzymes, as well as providing moral support and great joy in every interaction. It was truly a pleasure and an honor to work with such brilliant people, and it would be an understatement to say that I have stood on the shoulders of giants.

I would like to thank Professors Osvaldo Campanella, Bradley Reuhs, and Owen Jones, as well as Drs. Fang and Jongbin Lim, and Anton Terekhov for serving as subject matter experts whenever I needed guidance. Thank you to Anna Hayes, Rachel Jackson, Pablo Torres Aguilar, and everyone in the Hamaker lab and Purdue Food Science Department for serving as a sounding board, keeping me sane, providing moral support, and for always tasting whatever concoction I was cooking up in the Test Kitchen.

The more you know, the more you realize how much you don’t know.

TABLE OF CONTENTS

LIST OF TABLES

LIST OF FIGURES

TABLE OF EQUATIONS

LIST OF ABBREVIATIONS

CHO: Carbohydrate
DE 40: Dextrose equivalent 40 glucose syrup
DLS: Dynamic light scattering, from goniometer
DMSO: dimethyl sulfoxide
GLC DE40: Glucose syrup with 40 dextrose equivalence
HgbA1c: Hemoglobin A1c, a measure of glycated hemoglobin circulating in the blood
MALS: Multi-angle light scattering
MW: Molecular weight
PPA: Porcine pancreatic α-amylase
RDS: Rapidly digesting carbohydrates
RIAP: Rat intestinal acetone powder
RTD: Ready to drink
RS: Resistant carbohydrates
SDC: Slow digesting carbohydrate
SDS: Slow digesting starch
SLS: Static light scattering, from goniometer
WCS: Waxy corn starch

ABSTRACT

Moderating glycemic response to foods is important for the potential to control or prevent hyperglycemia-related diseases, such as diabetes and cardiovascular disease. The importance of slowly digestible carbohydrates (SDC) lies in their health effects: moderated blood glucose response, and a potential for increased satiety and reduced intake, and weight management. The research presented is on structural properties of novel, mostly soluble, α-glucans (glucose-containing oligomers and polymers with different linkage types and combinations) that are required for slow yet full digestion, and how they behave in food systems. Up to this point, little has been known regarding what structural properties of glucose-containing carbohydrates result in slow digestion, although starch structure has been well investigated and it is known that raw starch has a slowly digestible property. In addition to the structure-function aspect of the thesis work, this research contributes information about how α-glucan SDCs can be incorporated into food products that undergo heat treatment in the presence of moisture. The α-glucans maintain their SDC property while raw starch is gelatinized and becomes rapidly digestible. The rate of hydrolysis of a large number of novel α-glucans was studied using a simulated upper gastrointestinal in vitro digestion utilizing porcine pancreatic α-amylase and α-glucosidases from the rat intestine, and a subset was then evaluated in a crossover design clinical trial with blood glucose monitoring. Linkage and molecular weight analysis using gas chromatography of partially methylated alditol acetates and multi-angle light scattering and refractive index (MALS-RI) detection at time points during in vitro digestion were used to elucidate the relative rate of digestion of different linkage types in new and known α-glucan carbohydrates. Clinical results showed that resistant maltodextrin and reuteran had low initial glycemic profiles with no extended digestion, indicating rapid and resistant fractions; dextran and raw wheat starch had low initial glycemia and extended profiles, indicating a true SDC property; isomaltooligosaccharides and alternanooligosaccharides had high glycemic profiles; and alternan, as a larger polymer, was essentially undigested with a flat at-baseline glycemic profile. It was found that larger molecules with α-1,6, 1,3, and 1,2 linkages are generally more slowly digestible, though not always fully hydrolyzed within a 6 h upper GI in vitro digestion. Static and dynamic light scattering (SLS and DLS) showed the dextran sample to have a secondary structural conformation of branched or associated coils, and the Kratky

plot confirmed this finding, indicating a molecular configuration of polydisperse coils likely contributing to a slow digestion rate.

Rheological, turbidity, and SLS and DLS analyses were used to examine ingredient interaction between novel, enzymatically-modified α-glucans with slow digesting properties found most promising for inclusion in food products. A model nutritional beverage system was utilized containing proteins and salts. It was found that solvent and ion concentration of solutions were important for dictating aggregation formation with highly branched alternans and oligosaccharides in solution alone, or in the presence of soluble protein aggregates. Further, salts in solution proved to influence rheological and turbidity measures of all four α-glucans examined in the model system, indicating they may affect aggregation and structural conformation of such large carbohydrates. However, only tapioca maltodextrins showed in vitro rate of digestion affected by aggregation.

These results show the chemical and molecular properties of modified carbohydrates that contribute to slow digestion rate, which is informative to develop improved or new SDCs, as well as how these novel SDCs interact with other ingredients within a model beverage system, informing applications for the food industry.

CHAPTER 1. INTRODUCTION

1.1 Background

Highly glycemic carbohydrates are frequently looked upon negatively, and for good reason: whether low insulin sensitivity, diabetes, or obesity, it is easy to find reasons to avoid high consumption of rapidly digestible carbohydrates (RDC). While still fully digestible, there is a category of carbohydrates classified as "slowly digestible carbohydrates" (SDC), which digest in a slow fashion such that there is a prolonged digestion and absorption of glucose into the bloodstream (Englyst and Englyst, 2005). Not only does this slow digesting property mitigate the unpleasant sugar high and following dip, but there are other proposed health benefits as well, such as reduced inflammation, HgbA1c and associated diabetes complications, cardiovascular damage, overall mortality, and obesity (Jackson, Yudkin and Forrest, 1992; Meigs *et al.*, 2002; Ceriello *et al.*, 2004; Wallander *et al.*, 2005; Hanefeld and Schaper, 2007; Hasek *et al.*, 2018).

The slow rate of hydrolyses of these carbohydrates can occur at one or both of the digestive enzyme steps of: 1) α-amylase (salivary and pancreatic) that degrades starch and other glucan α-1,4 and 1,6-linkages to oligomers, and 2) at the brush border membrane of the small intestine, by the α-glucosidase enzymes maltase-glucoamylase (MGAM) and sucrase-isomaltase (SI), that degrades the different α-glucan linkages to produce glucose, or with sucrose to glucose and fructose. In this study, novel soluble α-glucans are considered that contain different types and combinations of α-linkages, to identify SDCs that could have usefulness in beverages, to understand susceptibility of different α-glucan linkages to digestive enzymes, and to test an *in vitro* assay to most accurately correlate with observed glucose digestion and absorption into the bloodstream.

It is known that raw cereal starch granules are slow digesting, although their application in manufactured food products is limited as nearly all processed starchy foods are gelatinized, which changes the starch to have a rapidly digesting property (Zhang, Ao and Hamaker, 2006; Zhang, Venkatachalam and Hamaker, 2006). Rate of hydrolysis has been correlated with starch structure, linkage type and pattern, as well as molecular size. In the following thesis studies, raw wheat starch was used as a control for slow digesting property to compare novel, enzymatically-modified

soluble α-glucans for digestion rate, glycemic profiles, structure-function relationships, functionality in food systems, and interactions with other ingredients in a model beverage system.

1.2 Research hypothesis and specific objectives

In the studies presented in Chapter 3, the objective was to investigate the rate of digestion of novel enzymatically- or process-modified carbohydrates, as well as to identify relative digestion rate of a range of α-glucan linkages and the impact of molecular size and branching on rate of digestion. We hypothesized that a combination of α-1,6, known to be slowly digestible (Shin *et al.*, 2008), and α-1,3 or α-1,4 linkages may produce the desired slow digesting affect. Larger molecular size was also hypothesized to correlate with total digestibility or rate of digestion. Chapter 4 examined novel α-glucans included in the clinical trial presented in Chapter 3 for secondary structural conformation and rheological behaviors that may influence rate of digestion or impact processing abilities. It was hypothesized that larger molecules such as the alternan may impact rate of digestion due to size and potentially may aggregate in solution, or cause double-helical structure formation, such as is found in retrograded starch (i.e. gelatinized and cooled starch). We showed that there is some helical-based agglomeration of highly branched dextran molecules that were found to be slowly digesting in Chapter 3. The final objective of this work was to investigate *in vitro* digestion rates, rheological properties, aggregation, and solubility of α-glucans with alternating α-1,6 and 1,4-linkages (i.e. alternan and alternanoligosaccharides) in a model beverage system containing spray-dried dairy and soy proteins and mineral salts. It was hypothesized that salts may have an impact on digestion rate through causing conformational changes of the carbohydrates, and we found that this was indeed the case, as well as that soluble protein aggregates likely interacted with highly branched oligo- and polysaccharides when in solution, under heat or shear stress. Overall, the goals of this research were to elucidate specific structural components necessary for slow digesting properties, as well as to determine if specific structures are appropriate for, and remain slow digesting in, manufactured food systems.

1.3 References

Ceriello, A., Hanefeld, M., Leiter, L., Monnier, L., Moses, A., Owens, D., Tajima, N., & Tuomilehto, J. (2004). Postprandial glucose regulation and diabetic complications. *Archives of Internal Medicine*, *164*(19), 2090–2095. https://doi.org/164/19/2090 [pii]

Englyst, & Englyst. (2005). Carbohydrate bioavailability. *British Journal of Nutrition*, *94*(1), 1–11. https://doi.org/10.1079/bjn20051457

Hanefeld, M., & Schaper, F. (2007). The role of alpha-glucosidase inhibitors (Acarbose). In C. E. Mogensen (Ed.), *Pharmacotherapy of Diabetes: New Developments: Improving Life and Prognosis for Diabetic Patients* (pp. 143–152). Springer US. https://doi.org/10.1007/978-0-387-69737-6_13

Hasek, L. Y., Phillips, R. J., Zhang, G., Kinzig, K. P., Kim, C. Y., Powley, T. L., & Hamaker, B. R. (2018). Dietary Slowly Digestible Starch Triggers the Gut–Brain Axis in Obese Rats with Accompanied Reduced Food Intake. *Molecular Nutrition and Food Research*, *62*(5). https://doi.org/10.1002/mnfr.201700117

Jackson, C. A., Yudkin, J. S., & Forrest, R. D. (1992). A comparison of the relationships of the glucose tolerance test and the glycated haemoglobin assay with diabetic vascular disease in the community. The Islington Diabetes Survey. *Diabetes Research and Clinical Practice*, *17*(2), 111–123. https://doi.org/10.1016/0168-8227(92)90156-L

Meigs, J. B., Nathan, D. M., D'Agostino, R. B., & Wilson, P. W. F. (2002). Fasting and postchallenge glycemia and cardiovascular disease risk: The framingham offspring study. *Diabetes Care*, *25*(10), 1845–1850. https://doi.org/10.2337/diacare.25.10.1845

Shin, J. E., Simsek, S., Reuhs, B. L., & Yao, Y. (2008). Glucose release of water-soluble starch-related alpha-glucans by pancreatin and amyloglucosidase is affected by the abundance of alpha-1,6-glucosidic linkages. *Journal of Agricultural and Food Chemistry*, *56*; 10879–10886.

Wallander, M., Bartnik, M., Efendic, S., Hamsten, A., Malmberg, K., Öhrvik, J., Rydén, L., Silveira, A., & Norhammar, A. (2005). Beta cell dysfunction in patients with acute myocardial infarction but without previously known type 2 diabetes: A report from the GAMI study. *Diabetologia*, *48*(11), 2229–2235. https://doi.org/10.1007/s00125-005-1931-z

Zhang, G., Ao, Z., & Hamaker, B. R. (2006). Slow digestion property of native cereal starches. *Biomacromolecules*, *7*(11), 3252–3258. https://doi.org/10.1021/bm060342i

Zhang, G., Venkatachalam, M., & Hamaker, B. R. (2006). Structural basis for the slow digestion property of native cereal starches. *Biomacromolecules*, *7*(11), 3259–3266. https://doi.org/10.1021/bm060343a

CHAPTER 2. REVIEW OF LITERATURE

A version of this chapter can be found published Critical Reviews in Food Science and Nutrition (© 2018 Taylor & Francis Group, LLC) (first two authors had equal contribution)

Gangoiti, J., Corwin, S. F., Lamothe, L. M., Vafiadi, C., Hamaker, B. R., & Dijkhuizen, L. (2018). Synthesis of novel α-glucans with potential health benefits through controlled glucose release in the human gastrointestinal tract. In *Critical Reviews in Food Science and Nutrition* (Vol. 60, Issue 1). https://doi.org/10.1080/10408398.2018.1516621

The glycemic carbohydrates we consume are currently viewed in an unfavorable light by many in both the consumer and medical research worlds. In significant part, these carbohydrates, mainly starch and sucrose, are looked upon negatively due to their rapid and abrupt glucose delivery to the body which causes a high glycemic response. However, dietary carbohydrates which are digested and release glucose in a slow manner are recognized as providing health benefits. Slow digestion of glycemic carbohydrates can be caused by several factors, including food matrix effect which impedes α-amylase access to substrate, or partial inhibition by plant secondary metabolites such as phenolic compounds. Differences in digestion rate of these carbohydrates may also be due to their specific structures (e.g. variations in degree of branching and/or glycosidic linkages present). In recent years, much has been learned about the synthesis and digestion kinetics of novel α-glucans (i.e. small oligosaccharides or larger polysaccharides based on glucose units linked in different positions by α-bonds). It is the synthesis and digestion of such structures that is the subject of this review.

2.1 Hyperglycemia and health

There is abundant evidence that postprandial hyperglycemia is an indicator for risk of coronary heart disease (CHD), stroke, and overall mortality (Hanefeld *et al.*, 1996); rapid rise in blood glucose levels increases low-level inflammatory effects, oxidative stress, and harmful effects on beta cells which decreases insulin sensitivity (Ceriello *et al.*, 2004; Wallander *et al.*, 2005). Hyperglycemia lasting more than 2 hours postprandial has been shown to be a better predictor of CHD, stroke, and overall mortality than hemoglobin A1c levels (Jackson, Yudkin and Forrest,

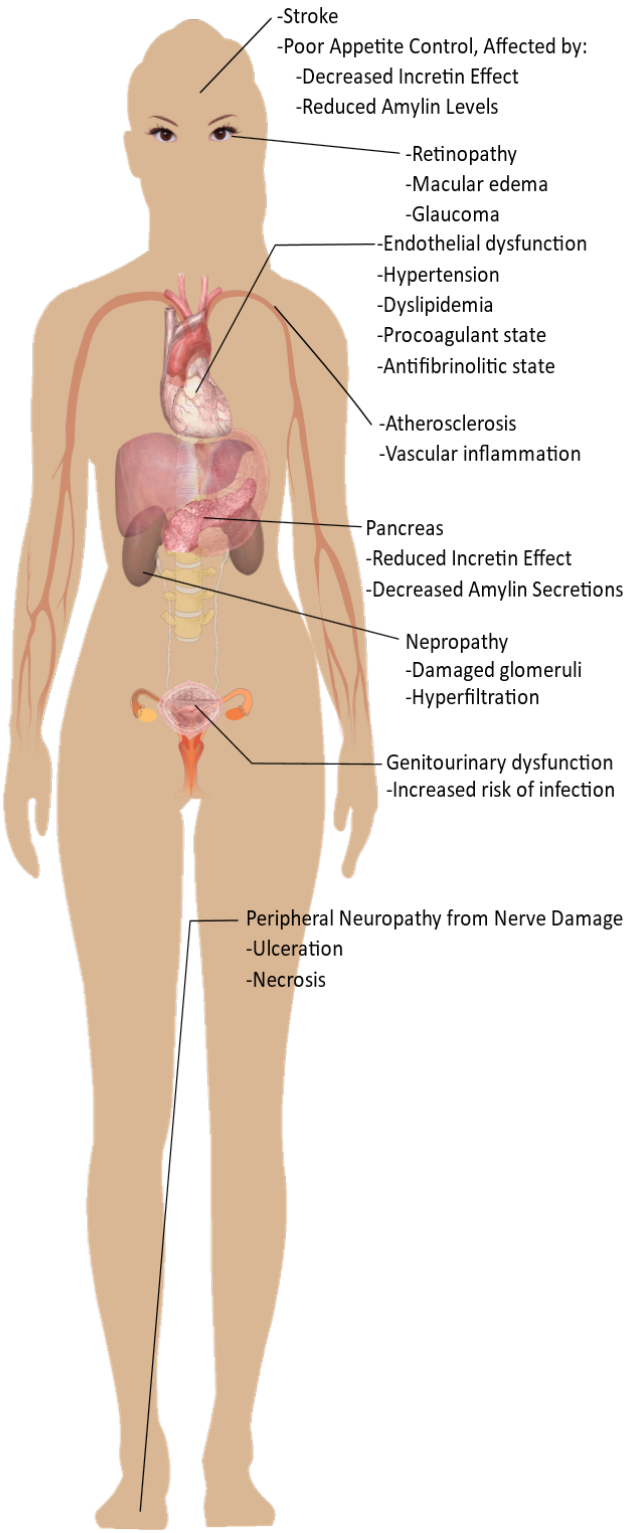

Figure 1. Effects of chronic hyperglycemia (Almdal *et al.*, 2004; Campos, 2012). Image derived from public domain.

1992; Meigs *et al.*, 2002). Many have hypothesized that postprandial hyperglycemia contributes to diabetes complications through damaging the vasculature tissue, such as retinopathy and nephropathy, which is likely why the cardiovascular disease incidence is so highly correlated to poorly controlled diabetes (Meigs *et al.*, 2002; Ceriello *et al.*, 2004). Even in non-diabetics, a meal high in rapidly digestible starches allows for some postprandial and post-challenge hyperglycemia that may contribute to cardiovascular damage (Hanefeld and Schaper, 2007). Poor insulin secretion and decreased insulin sensitivity are key characterizations of type 2 diabetes, as well as progressive beta cell dysfunction (Wallander *et al.*, 2005).

In addition to vascular damage caused by acute postprandial hyperglycemia, there may be an increase in oxidative stress when excessive blood glucose fluctuations occur pre- and postprandially, with quick absorption of glucose from meals (Monnier *et al.*, 2006). Furthermore, activation of protein kinase C, MAP-kinase, and NF-kB are promoted with intracellular hyperglycemia, increasing reactive oxygen species (Brownlee, 2001;

Monnier *et al.*, 2006). It has been reported that "overproduction of superoxide by the mitochondrial electron-transport chain" is the common factor linking the increased cell abnormalities in diabetes (Du *et al.*, 2000; Nishikawa *et al.*, 2000; Brownlee, 2001).Value of slowly digestible carbohydrates to health

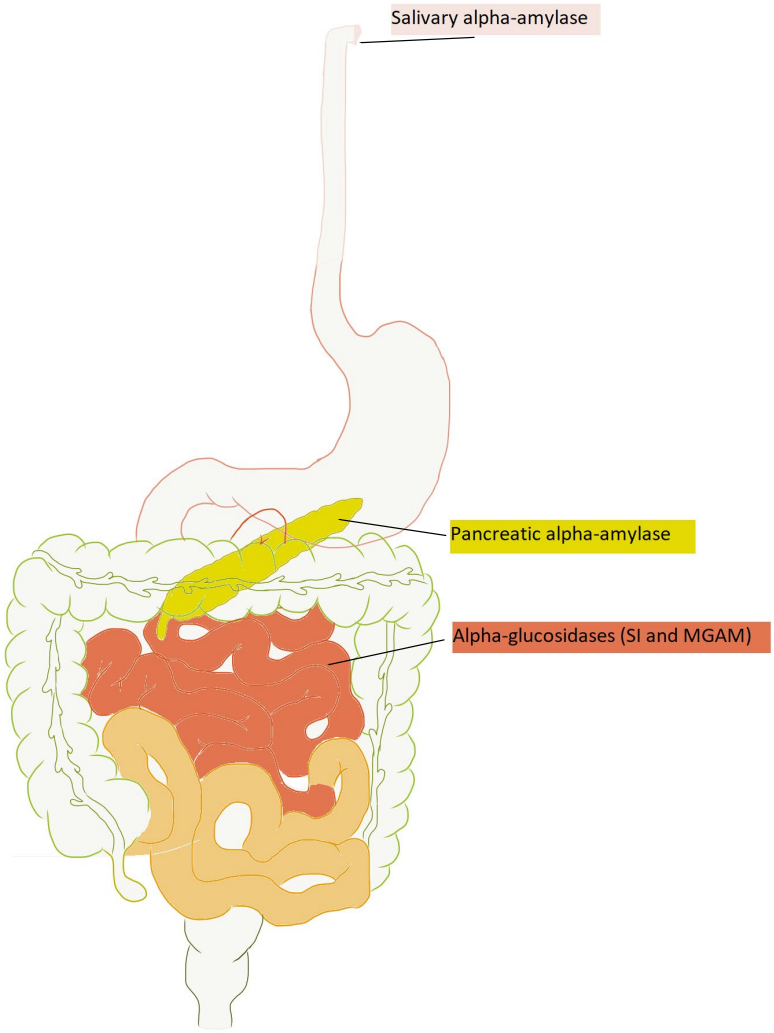

Figure 2. Location of digestive enzymes along gastrointestinal tract

Inhibition of the enzymes that digest starch, such that glucose release into the bloodstream is slowed, is one treatment method for type 2 diabetes. Currently, acarbose is used as a competitive inhibitor affecting the activities of enzymes in the human digestive tract, i.e. pancreatic α-amylase and various α-glucosidases (Figure 2) (Martin and Montgomery, 1996; Hanefeld and Schaper, 2007). While enzyme inhibition is one method clinically used to slow the glucose release of

carbohydrate digestion, as mentioned, this review will examine the potential to modulate glycemic response through the use of α-glucans with structures and glycosidic linkages that do not allow for immediate hydrolysis.

In addition to the effect of modulating glycemic response, slowly digestible carbohydrates which are digested into the ileal (distal) region of the small intestine may stimulate endocrine L-cells to reduce appetite and slow gastric emptying. This has recently been demonstrated in rats using fabricated slowly digestible carbohydrate microspheres that were shown to digest into the ileum. Long-term feeding (11 weeks) of the microspheres to diet-induced obese rats produced lower daily food intake and reduced gene expression of the hypothalamic appetite-stimulating neuropeptides (Hasek *et al.*, 2018).

2.2 **Glycemic carbohydrates and their structure**

Oligo- and polysaccharides are built of multiple sugar molecules, or monosaccharides, joined by glycosidic linkages occurring between the hydroxyl group of one monosaccharide with an anomeric carbon of another. The human digestive tract, as well as mammals in general, contains carbohydrate-digesting enzymes consisting of α-amylases secreted in salivary and pancreatic fluids that digest starch and starch products to linear oligomers (maltose, maltotriose, maltotetraose) and branched α-limit dextrins, and the small intestine mucosal α-glucosidases [maltase-glucoamylase (MGAM) and sucrase-isomaltase (SI)] that digest these and other digestible glycans to monosaccharides for absorption (Zhang and Hamaker, 2009). The human body absorbs and metabolizes glucose, fructose, and galactose. The common glycosidic bonds that are digestible by humans include (α1→4) and (α1→6) glucose-glucose that make up (iso)maltose, (iso)maltooligosaccharides, and starch; sucrose, (α1→2) glucose-fructose; and lactose, β1→4 galactose-glucose. Uncommon linkages that can be hydrolyzed by the α-glucosidases include (α1→1), (α1→2), and (α1→3) glucose-glucose; and (α1→3), (α1→4), (α1→5), and (α1→6) glucose-fructose (Lee *et al.*, 2016). When multiple monosaccharides are linked together, they form polysaccharides, which are used for energy storage and structure. For example, glycogen is a storage polysaccharide within the human body, consisting of (α1→4)-linked glucose molecules that are relatively highly branched through (α1→6) linkages. Starch, which is the glucose storage form in plants and the most common dietary polysaccharide, consists of two types of polymers: Amylose and amylopectin. Amylose is principally a linear (α1→4)-linked glucan, whereas in

amylopectin the (α1→4) linear chains are connected via (α1→6) branching points. β-Glucans (polymers of glucose with β-glycosidic linkages), such as cellulose [(β1→4)-linked] and β-glucan [in cereals, β1→4)- and β1→3)-linked], is another commonly consumed polysaccharide; humans lack cellulase enzymes to digest these β-bonds.

2.3 The enzymes responsible for mammalian α-glucan digestion

To digest the dietary available carbohydrates to the monosaccharides glucose, fructose, and galactose, the mammalian body employs the salivary and pancreatic α-amylases (EC 3.2.1.1.) and the small intestine mucosal two-enzyme complexes of maltase-glucoamylase (MGAM) (EC 3.2.1.20 and 3.2.1.3) and sucrose-isomaltase (SI) (EC 3.2.148 and 3.2.10). The α-amylases are classified in glycoside hydrolase (GH) family GH13, and the four catalytic subunits of MGAM and SI in GH31 (Nichols *et al.*, 2003). The four enzyme subunits of these α-glucosidases have different roles in the conversion of glycemic carbohydrates to glucose (and of sucrose to glucose and fructose). α-Glucans with structures and linkages that are less easily hydrolyzed by these enzymes potentially are of interest as slowly digestible carbohydrates. Following digestion of starch by salivary and pancreatic α-amylase to linear maltooligosaccharides and branched α-limit dextrins, in the small intestine the α-linked glucans and sucrose are hydrolyzed by the mucosal α-glucosidases, MGAM and SI, into free glucose (Zhang and Hamaker, 2009). Each α-glucosidase has a unique role and understanding them can aid in designing carbohydrates with low digestibility carbohydrates. The α-glucosidase dimers are composed of N- and C-terminal subunits; for MGAM the N- and C-terminal subunits are maltase and glucoamylase, and for SI these are isomaltase and sucrase, respectively (Quezada-Calvillo *et al.*, 2008). In the literature, they are also termed N- and C-terminal MGAM and SI. The N-terminal domains of both α-glucosidase complexes are connected to the enterocyte membrane, with the C-terminal subunits linked and facing the internal cavity of the intestine. The domains are anchored by an O-glycosylated stalk that branches out of the N-terminal domain (Figure 3) (Sim *et al.*, 2010; Lee *et al.*, 2014).

Glucoamylase digests (α1→4) glucosidic bonds and acts faster on longer chain α-glucans than maltase does, and even can digest native dispersed starch (Lin *et al.*, 2012). The ability of the mammalian α-glucosidases to hydrolyze different α-linked glucose-glucose disaccharides has been studied using recombinantly expressed and purified enzymes. Glucoamylase was shown to act (enzyme efficiency of glucose generation) on maltose (α1→4) (Kcat/Km 51.0 mM-1s-1), kojibiose

(α1→2) (Kcat/Km 0.9 mM-1s-1), and nigerose (α1→3) (Kcat/Km 2.7 mM-1s-1); with higher maltase activity than the maltase subunit itself (Kcat/Km 51.0 vs. 12.7 mM-1s-1) (Lee *et al.*, 2016). Glucoamylase is reported to be inhibited by maltotriose and maltotetraose at high concentrations (Quezada-Calvillo *et al.*, 2008).

In addition to digesting maltose, kojibiose, and nigerose, maltase has minor activity towards isomaltose (α1→6) (Kcat/Km 0.1 mM-1s-1). Maltase does not digest larger maltooligosaccharides well; under in vitro experimental conditions, full hydrolysis by maltase took 60 min for maltotriose, maltotetraose, and maltopentaose, while maltose was hydrolyzed in 20 min (Lee *et al.*, 2014). Compared to glucoamylase, or the SI subunits, maltase has a higher hydrolyzing activity on kojibiose and nigerose (Table 1). Per their common names, sucrase hydrolyzes sucrose (α1→2, glucose-fructose) and isomaltase hydrolyzes isomaltose (α1→6, glucose-glucose). However, the SI complex is notably responsible for the majority of mucosal maltase activity because the human intestine may contain 40-50 times more SI than MGAM (Quezada-Calvillo *et al.*, 2007; Lee *et al.*, 2013). Using individual recombinant mammalian α-glucosidase, sucrase and isomaltase had Kcat/Km values for the hydrolysis of maltose of 2.7 and 1.7 Kcat/Km, respectively; and showed some, though lesser, hydrolysis activity for kojibiose and nigerose compared to the MGAM subunits (Table 1) (Lee *et al.*, 2013).

Some sucrose hydrolyzing activity was also found for glucoamylase, and interestingly isomaltulose (α1→6, glucose-fructose) was hydrolyzed mostly by isomaltase. Both SI subunits digested longer linear maltooligosaccharides (e.g. G5 compared to G2) quite slow compared to the MGAM subunits (Lee *et al.*, 2013). Lee et al. (Lee *et al.*, 2014) proposed that selective inhibition to target MGAM subunits would slow the release of glucose to the rates of the SI subunits, as MGAM is much quicker to digest maltooligosaccharides than is SI. A study by Heymann et al. (Heymann, Breitmeier and Günther, 1995), measuring SI kinetics, proposed that the sucrase subunit has maximal activity against maltose (α1→4)-G2, and the isomaltase subunit has high activity against (α1→6) branched oligomers composed of up to 4 glucose residues (Heymann, Breitmeier and Günther, 1995). Lee et al. (Lee *et al.*, 2014) showed though that sucrase and isomaltase have similar hydrolyzing capabilities for maltose.

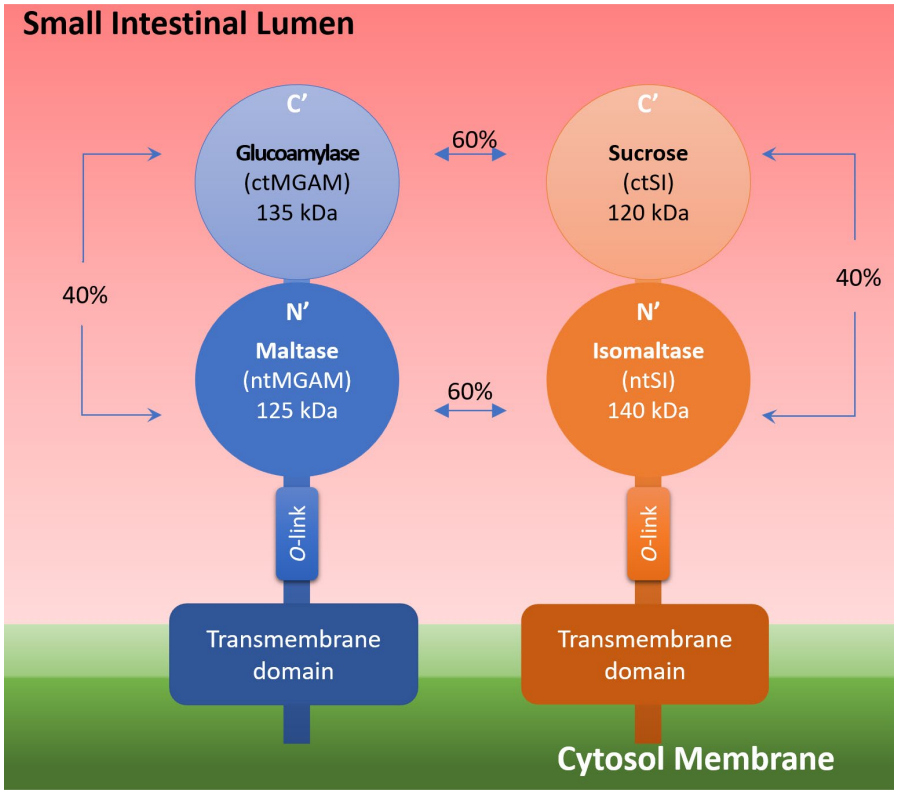

Figure 3. α-Glucosidase arrangement on the cytosol membrane. Figure modified from (Quezada-Calvillo *et al.*, 2008)

Table 1. Kinetic parameters of each recombinant mucosal α-glucosidase on differently α-linked disaccharides with two glucoses adaptation from Lee et al, 2016 (Lee *et al.*, 2016)

	ctMGAM (Glucoamylase)	ntMGAM (Maltase)	ctSI (Sucrase)	ntSI (Isomaltase)
Trehalose	Not detected	Not detected	Not detected	Not detected
	Not detected	Not detected	Not detected	Not detected
	Not detected	Not detected	Not detected	Not detected
Kojibiose	12.7 ± 2.5 [1]	11.6 ± 1.2 [1]	17.3 ± 2.2 [1]	53.7 ± 13.7 [1]
	11.5 ± 0.6 [2]	17.6 ± 0.5 [2]	0.5 ± 0.0 [2]	3.2 ± 0.3 [2]
	0.9 ± 0.2 [3]	1.5 ± 0.4 [3]	0.3 ± 0.0 [3]	0.1 ± 0.0 [3]
Nigerose	35.2 ± 3.6 [1]	27.1 ± 2.6 [1]	63.6 ± 13.0 [1]	44.4 ± 6.4 [1]
	96.0 ± 3.3 [2]	120.9 ± 3.7 [2]	11.0 ± 1.0 [2]	24.8 ± 1.3 [2]
	2.7 ± 0.9 [3]	4.4 ± 1.4 [3]	0.2 ± 0.1 [3]	0.6 ± 0.2 [3]
Maltose	2.6 ± 0.6 [1]	8.7 ± 1.3 [1]	4.2 ± 1.4 [1]	11.1 ± 1.5 [1]
	133.9 ± 4.3 [2]	110.2 ± 3.8 [2]	11.4 ± 0.8 [2]	18.3 ± 0.6 [2]
	51.0 ± 7.0 [3]	12.7 ± 3.0 [3]	2.7 ± 0.5	1.7 ± 0.4 [3]
Isomaltose	Not detected	128.0 ± 8.4 [1]	Not detected	15.2 ± 2.0 [1]
	Not detected	8.9 ± 0.3 [2]	Not detected	18.1 ± 0.7 [2]
	Not detected	0.1 ± 0.0 [3]	Not detected	1.2 ± 0.3 [3]

It is known that (α1→6)-linked branched structures, such as the α-limit dextrins, the digested products of salivary and pancreatic α-amylases, are hydrolyzed at a much slower rate than (α1 →4)-linked linear glucans (Zhang and Hamaker, 2009). Studies on α-amylase showed that optimal enzyme activity occurs when five or more (α1→4)-linked glucose molecules are in the substrate. (α1→6)-Branched linkages of amylopectin molecules hinder α-amylase activity (Quezada-Calvillo *et al.*, 2008).

The precise roles of the individual α-glucosidases are now well documented, and a synergistic picture of their concerted action seems to appear. Larger starch digestion products are effectively digested by the outer located glucoamylase enzyme and the small linear and branched maltooligosaccharide products are further digested to glucose by the inner located maltase and isomaltase (Figure 3). Glucoamylase and maltase can digest unusual α1→2- and α1→3-linked glucans, though maltase has higher capacity.

[1] K_m(mM)
[2] K_{cat} (s^{-1})
[3] K_{cat}/K_m (mM^{-1} s^{-1})

2.4 Inhibition of the α-glucosidases

While carbohydrate molecular structure influences digestion rate by α-glucosidases, phytochemical inhibitory molecules that are present at the time of digestion may also influence the rate of glucose release by these enzymes. Plant phenols (e.g. chlorogenic acid, caffeic acid gallic acid) are one such family of metabolites reported to have inhibitory effects on SI and MGAM. Chlorogenic acid has been shown to have α-glucosidase inhibitory effects when consumed with maltose or sucrose; one study by Ishikawa et al. (Ishikawa *et al.*, 2007) showed that, when consumed before a meal, leaves of *Nerium indicum* (oleander) lowered postprandial glucose levels by inhibiting α-glucosidases (Ishikawa *et al.*, 2007). Coffee contains chlorogenic acid, and green tea contains caffeic acid and catechins which are known α-glucosidase inhibitors (Adisakwattana *et al.*, 2009; Nguyen *et al.*, 2012). In a study by Simsek et al. (Simsek *et al.*, 2015), chlorogenic acid, epigallocatechin gallate, (+)-catechin, caffeic acid, and gallic acid were examined for their effect on the kinetics of maltose digestion and mechanism of inhibition against each α-glucosidase subunit. It was found that inhibition constants (K_i) for epigallocatechin gallate against glucoamylase (1.7 ± 0.7 μM) and chlorogenic acid against sucrase (1.8 ± 0.3 μM) were the lowest compared to any other phenolics acting on any other subunits (Simsek *et al.*, 2015). Therefore, there is benefit in focusing further research on the effect of epigallocatechin gallate and chlorogenic acid on slowing the α-glucosidase C-terminal subunit digestion.

Acarbose is produced by some Gram-positive bacteria and is a potent selective inhibitor of the C-terminal α-glucosidase subunits (Lee *et al.*, 2012). 1-Deoxynojirimycin which is found in the mulberry plant bark and root was shown to be a potent competitive MGAM inhibitor (Breitmeier, Günther and Heymann, 1997), but against which subunit has yet to be determined (Martin and Montgomery, 1996; Breitmeier, Günther and Heymann, 1997; Hanefeld and Schaper, 2007; Liu *et al.*, 2015). The glucoamylase C-terminal MGAM subunit acts very rapidly on smaller starch units and its inhibition could potentially be used to slow the rate of hydrolysis on longer chain maltooligosaccharides.

2.5 α-Glucans: Current and future ingredients for the food industry

Health concerns are important drivers of consumer preferences and demands on food product development are based on taste, nutritional value, and healthfulness. As mentioned,

digestible carbohydrates such as starch and its derivatives (maltodextrins and maltooligosaccharides) are the predominant α-glucans in our diets, and have recently come under scrutiny for their postulated negative impact on health, particularly when consumed in excess. α-Glucan ingredients that have slowly digestible or non-digestible profiles constitute a healthful alternative to highly processed starches and its derivatives. There is a wide range of synthetic or naturally occurring α-glucan ingredients that differ in digestibility profiles and technological properties. The α-glucans include a large group of linear, branched or cyclic oligo- and polysaccharides that are composed of glucose moieties joined via (α1→2), (α1→3), (α1→4), and (α1→6) glycosidic linkages. In this section, we describe the most prominent α-glucan ingredients with current or potential uses in the food industry.

2.6 **Commercially available α-glucan ingredients**

2.6.1 Starch

Starch is the most abundant α-glucan as it is the main storage carbohydrate in cereals, pulses, and tubers. Normal starches are composed of around 20% of amylose and 80% of amylopectin, but this ratio differs depending on the starch source (Van Der Maarel *et al.*, 2002; Van Der Maarel and Leemhuis, 2013). Also, the branching pattern and the average length of the (α1→4) chains vary with the origin of the starch. Based on the rate of digestion, starch is classified into rapidly digestible starch (RDS), slowly digestible starch (SDS) and resistant starch which largely defines its nutritional quality (Englyst, Kingman and Cummings, 1992). In its native form, starch is characterized by a granular structure that renders it slowly digestible or resistant (Oates, 1997; Valk *et al.*, 2015). It has been shown, for example, that native cereal starches are slowly digestible due to their layered structure constituted by crystalline and amorphous regions (Zhang, Ao and Hamaker, 2006). As mentioned, the health benefits of SDS mainly pertain to a slower rate of glucose release that results in a reduced postprandial glycemia (Lehman and Robin, 2007). However, as starch is cooked and gelatinized it loses its granular structure which results in a significant increase in its digestibility (Bornet *et al.*, 1989). When discussing gelatinized starches that have lost their crystalline structure, their molecular features then become the main determinant factors for digestibility. In particular, the fine structure of amylopectin (e.g. average length of (α1→4) chains and branching pattern) and the ratio of amylose to amylopectin are the main

determinants of gelatinized starch physical state and digestibility. Amylopectin molecules with either higher amounts of long or short chains were found to have a similar high content of SDS due to two different mechanisms. Whereas the presence of long chains leads to the formation of physical structures that decrease enzyme accessibility, a highly branched structure limits itself the accessibility of digestive enzymes (Zhang, Ao and Hamaker, 2008). Starches that are high in amylose content have a resistant starch character both in their native state and after gelatinization and retrogradation, the latter caused by amylose formation of long-chain double-helical crystallites that are resistant to digestion (Jiang *et al.*, 2010). Consumption of resistant starch has been shown to positively influence bowel health, blood lipids profile, and to reduce the glycemic and insulinemic responses (Nugent, 2005).

2.6.2 Isomaltooligosaccharides (IMOs)

IMOs are found naturally in various fermented foods such as miso, sake, or soy sauce but also in honey (Playne and Crittenden, 2004). Commercial IMOs are produced enzymatically and are the market leader in the dietary carbohydrate sector of functional foods (Mountzouris, Gilmour and Rastall, 2002). They are generally obtained industrially from starch hydrolysates (maltose and maltodextrins) through the action of α-transglucosidases (EC 2.4.1.24) (Yasuda, Takaku and Matsumoto, 1986; Röper and Koch, 1988), or from sucrose using dextransucrases (Paul, Francois *et al.*, 1992; Remaud-Slmeon *et al.*, 1994). IMOs, also called glucosyl saccharides, not only containing (α1→6) linkages, but also (α1→4) linkages, and nigerooligosaccharides comprised of (α1→3) and/or kojioligosaccharides comprised of (α1→2) linkages, can be found in commercially available products (Table 3) (Yun, Lee and Song, 1994; Konishi and Shindo, 1997; Chaen *et al.*, 2001; Kobayashi *et al.*, 2003; Yamamoto *et al.*, 2004).

Table 2. α-Glucan ingredients: Chemical structure, properties, and applications in food industry

α-glucan ingredient	Structure	Properties	Food application(s)
Isomaltulose (Irwin and Sträter 1991) *(α-D-glucopyranosyl-1→6-α-D-fructofuranose)*	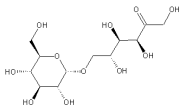	White crystalline substance Sweet	Sweetener
Isomalto-oligosaccharides (Goffin *et al.*, 2011) *(glucooligosaccharides linked with (α-1→4) and/or (α-1→6) glycosidic bonds)*[4]	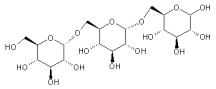 isomaltotriose 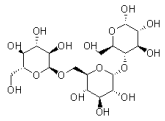 panose	White powder or syrup, water soluble, sweet	Low caloric sweetener, prebiotic[5]
Resistant dextrins (Ohkuma and Wakabayashi, 2000) *(highly-branched glucan with (α1→2), (α1→3), (α1→4), and (α1→6) in α- and β-configuration)*	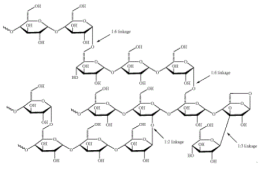 (Sr. Simpson, 2011)	White and odorless water-soluble powder	Low calorie, bulking agent
Polydextrose (Mitchell, Auerbach and Moppet, 2001) *(highly-branched glucan with (α1→2), (α1→3), (α1→4), and (α1→6) in α- and β-configuration. Contains citric acid and sorbitol.)*	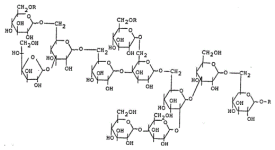 (Putaala, 2013)	White, water-soluble powder	Low calorie, bulking agent
Pullulan (Khan, Park and Kwon, 2007; Park and Khan, 2009) *(linear glucan consisting of maltotriosyl units linked with (α1→6) glycosidic linkages)*	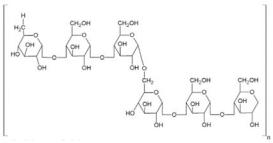 (Ferreira *et al.*, 2015)	Water-soluble, white, odorless & tasteless	Filler, glazing agent film-forming Agent, thickener, binder

[4] Commercial IMO syrup is generally accepted as a mixture of glucosyl saccharides with both (α1→6)-linkages and (α1→4) linkages and (α1→3), nigerooligosaccharides or (α1→2), kojioligosaccharides.

[5] *The prebiotic properties are under question due to recent studies* showing IMOs being digested *in the upper intestinal track* (Lin, Lee and Chang, 2016)

Table 2. continued

Cyclodextrins (Astray *et al.*, 2009) *(cyclic polymers of 6 (α), 7 (β) or 8 glucose units (γ) linked via α1→4 glycosidic linkage)*	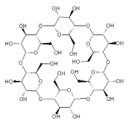 (*α-Cyclodextrin C36H60O30*, no date) 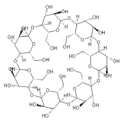 (*β-Cyclodextrin C42H70O35*, no date) 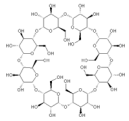 (*γ-Cyclodextrin C48H80O40*, no date)	Solubility in water: γ> α>β –cds, formation of inclusion complexes	Encapsulation of flavours, protection against oxidative degradation, heat and light induced changes, cholesterol sequestrant and preservatives.
Dextran (Jeanes *et al.*, 1954; Park and Khan, 2009; Maina *et al.*, 2011) *(glucan polysaccharides with 50 – 97% (α1→6) glycosidic linkages)*	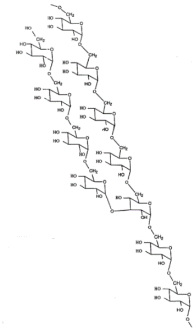 (Leathers, Hayman and Cote, 1997)	High solubility, promotes low solution viscosities[6] Molecular weight range: 1>Mw>10kDa	Sourdough baking improvers, natural thickeners in dairy products
Alternan-oligosaccharides (GmbH, 2017) *(oligosaccharides consisting of alternating (α1→6) and (α1→3) of various length)*	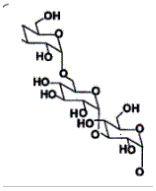 (Leathers, Hayman and Cote, 1997)	Water soluble, low viscosity and sweet syrups	Low glycemic ingredient

[6] *Depending on molecular weight and polydispersibility.*

Table 2. continued

Cyclic cluster dextrin (Takata *et al.*, 1996; Takii *et al.*, 1999; Office of Food Additive Safety (HFS-200) Center for Food Safety and Applied Nutrition (CFSAN) Food and Drug Administration (FDA), 2010) *(highly-branched cyclic dextrin consisting of (α1→4) and (α1→6)-linked glucose units.)*	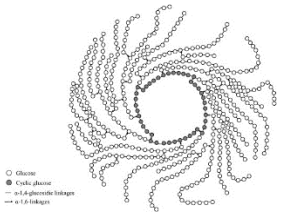 (Kadota *et al.*, 2015)	Highly water soluble, tasteless. Formation of inclusion complexes Mw 160 kDa with narrow size distribution	Slowly digestible carbohydrate that accelerates gastric emptying, spray-drying aid
Alternan (Khan, Park and Kwon, 2007; Grysman, Carlson and Wolever, 2008; Park and Khan, 2009) *(α-glucan consisting of alternating (α1→6) and (α1→3) glycosidic linkages)*	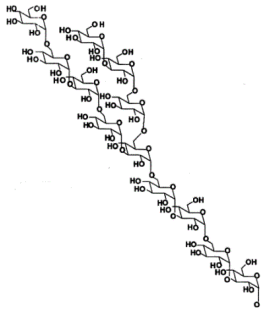 (Leathers, Hayman and Cote, 1997)	High solubility and low viscosity, hygroscopic, white, tasteless powder	Low caloric bulking agent, binder

IMOs are considered as non-digestible carbohydrates with prebiotic properties with benefit to the human microbiome (Rycroft *et al.*, 2001; Goffin *et al.*, 2011). Commercial IMO ingredients are used as a source of a soluble dietary fiber, a prebiotic and/or a low-calorie sweetener. For instance, Gu et al. (Gu *et al.*, 2003) observed an increase of reproduction of Bifidobacterium and Lactobacillus and an inhibition of growth of Clostridium perfringens after ingestion of IMOs in mice and humans. However, other studies have shown that IMOs are hydrolyzed at least partially by mammalian digestive enzymes before they reach the colon (Kohmoto *et al.*, 1992; Tsunehiro *et al.*, 1999; Hodoniczky, Morris and Rae, 2012). More specifically, in vitro studies using mammalian brush border intestinal enzymes showed that glucose disaccharides containing (α1→6), (α1→4), (α1→2) and (α1→3) are digested by the different small intestine mucosal α-glucosidases (Lin, Lee and Chang, 2016). A recent survey of commercially available IMO-based ingredients challenges current labeling as "dietary fibers", "low glycemic" and "zero calorie". The authors performed a two-subject blood glucose response acute study in which a commercial IMO ingredient proved as glycemic as glucose (Madsen *et al.*, 2017).

2.6.3 Resistant maltodextrins (RMDs)

RMDs are formed when liquefied starch is heated under acidic conditions in order to rearrange the glycosidic linkages. The treatment causes an increase in the proportion of (α1→6) linkages and introduces (α1→2) and/or (α1→3)-linkages as well as linkages of β-anomeric configuration (Deremaux, Petitjean and Wills, 2007) (Table 2). It is the combination of these linkages that render them poorly digestible. During heat treatment, starch undergoes pyroconversion, which involves hydrolysis, transglucosidation, and, in some cases, repolymerization of the branched oligosaccharides generated in the previous reactions. The rearrangement of glycosidic linkages that occurs during pyroconversion is what renders these dextrins resistant to digestion. They are popular ingredients in the food industry because they are soluble, have low viscosity, and have little to no impact on taste and color. Depending on their level of purification, resistant dextrins can contain up to 92% non-digestible carbohydrate content. In addition, they exhibit a high degree of thermal and pH stability (Ohkuma and Wakabayashi, 2000). This ingredient is predominantly used to increase the dietary fiber content of food products without conferring negatively perceived sensory attributes. RMDs are also suitable replacers of fully-caloric carbohydrates such as sucrose (4 kcal/g) since the caloric value for resistant dextrins is estimated to range between 1-2.5 kcal/g (Panasevich *et al.*, 2015). Due to this property, this ingredient can also be used to replace fully-digestible maltodextrins in the formulation of food products of medium to low glycemic index.

2.6.4 Polydextrose

Polydextrose is a synthetic, soluble, and non-viscous glucan polymer that is manufactured by melt condensation of glucose and sorbitol in acidic and vacuum conditions. This manufacturing process results in a highly-branched, low molecular weight polymer (Mw_n = 2000 Da; DP = 12) constituted by glucose units linked by (α1→2), (α1→3), (α1→4), or (α1→6) glycosidic bonds, present in both α- and β-anomeric configuration (Rennhard, 1975) (Table 2). Polydextrose is poorly digested in the small intestine and, thus, has reduced caloric availability. Its other applications in food include glazing agent, humectant, stabilizer, and thickener (Voragen, 1998; Srisuvor *et al.*, 2013). Its complex structure also results in its poor degradation by microbes making it non-cariogenic and only a small fraction is metabolized by cecal/colonic microbiota.

2.6.5 Cyclodextrins (CDs)

CDs are cyclic oligosaccharides of glucose molecules linked by (α1→4)-glycosidic linkages. They are classified depending on the number of glucose units, namely, α-, β- and γ-CDs for 6, 7, and 8 glucose units, respectively (Table 2). CDs are formed enzymatically from hydrolyzed starch by cyclodextrin glycosyltransferases (CGTases; E.C.2.4.1.19), enzymes that catalyze the cleavage of (α1→4) linkages in starch and the subsequent transfer of the newly produced reducing end to a non-reducing end of the same molecule (Thiemann *et al.*, 2004). Purified α-, β- and γ-CDs have been approved for their use as food additives (Joint FAO/WHO Expert Committee on Food Additives (JECFA), 1993, 1995, 1999, 2002, 2006; EFSA, 2005). Different applications of CDs include flavor encapsulation, taste modification by elimination of bitter or off-flavors as well as odors, food preservation, and as cholesterol sequestrants (Astray *et al.*, 2009) in a variety of food products as indicated by the Codex Alimentarius, General Standard for Food Additives (CODEX Alimentarius Commission for International Food Standards, 2017). More specifically, the use of β-CD is limited to a few food categories (i.e., chewing gum, pre-cooked pastas and noodles, starch-based snacks, water-based, and flavored drinks) (Thiemann *et al.*, 2004). α- and β-CDs are not hydrolyzed by gastrointestinal enzymes, but fermented by the colon microbiota. According to the EFSA Health Claim (Products and Allergies 2012), α-CDs have been shown to effect a significant reduction in postprandial glycemic response at a dose of at least 5 g per 50 g of starch. The reduction in glycemic response is due to the tight helix of the α-CD, the inhibitory effect of α-CD on pancreatic amylase, and that α-CD may delay gastric emptying (Koukiekolo *et al.*, 2001; Buckley *et al.*, 2006; Larson, Day and McPherson, 2010; Gentilcore *et al.*, 2011). In contrast, γ-CD is readily digested in the gastrointestinal tract yielding mainly maltose, maltotriose and glucose. Therefore, the metabolism of γ-CD closely resembles that of starch and maltodextrins. Although they are rapidly metabolized and absorbed in the small intestine, γ-CDs have also been reported to impact glycemic response with a similar inhibitory effect on pancreatic α-amylase as α-CD (Koukiekolo *et al.*, 2001; Wolf, Chow and Lai, 2006).

2.7 Novel α-glucan ingredients

2.7.1 Neo-amylose™

Neo-amylose™ is an α-glucan obtained through the polymerization of sucrose by the action of amylosucrase (E. C. 2.4.1.4) derived from *Neisseria polysaccharea* (Anand *et al.*, 1991). It is a water insoluble, unbranched polymer composed of (α1→4) glucosidic linkages with a chain length ranging from 35 up to 100 glucose units (Peters, Rose and Moser, 2010). It is an ingredient classified as a type 3 resistant starch (retrograded starch formed by cooking followed by cooling) that is around 90% non-digestible which makes it a suitable ingredient for use as a dietary fiber (Bengs and Brunner, 2000).

2.7.2 Cyclic cluster dextrin (CCD)

CCD is made from amylopectin through the cyclization reaction of glycogen branching enzyme (E.C 2.4.1.18) from the hyperthermophilic bacterium *Aquifex aeolicus* (Takata *et al.*, 2003). It has relatively long chains which adopt a helical conformation enabling the formation of inclusion complexes with guest molecules such as organic acids (Table 2). CCD is typically used in baked products, beverages, powder soups made from fruit and vegetables. It has also been used as a spray-drying aid. CCDs have received an FDA GRAS status (Takata *et al.*, 1996; Office of Food Additive Safety (HFS-200) Center for Food Safety and Applied Nutrition (CFSAN) Food and Drug Administration (FDA), 2010) and animal studies have shown that they may accelerate gastric emptying and that they are slowly digestible (Takii *et al.*, 1999).

2.7.3 Dextran

Luis Pasteur discovered dextran in wine and van Tieghem (Van Tieghem, 1878) designated the dextran-producing bacterium as *Leuconostoc mesenteroides*. Dextrans are microbial α-glucans with 50 – 97% (α1→6) linkages (Table 2). They are produced from sucrose via large scale fermentation or enzymatic synthesis involving extracellular dextransucrase (E.C. 2.4.1.5) enzymes (Jeanes *et al.*, 1954). Alternatively, these dextrans can be produced from starch by dextrin dextrinases (E.C. 2.4.1.2) (Yamamoto, Yoshikawa and Okada, 1993). Dextrans are approved as GRAS ingredients for their use in food products and feed. Also, the European Commission

approves the use of dextran in baked goods at levels up to 5%; dextrans of high molecular weight are used in sourdough baking to produce good quality bread (Scientific Committee on Food, 2000; Maina *et al.*, 2011). Furthermore, dextran was described as a thickening agent, an alternative cryostabilizer, fat replacer, or low-calorie bulking agent of interest for the food processing industry (Park and Khan, 2009). Dextran is only partially hydrolyzed to monosaccharides by small intestine α-glucosidases. The remaining dextran that escapes small intestine digestion is fermented in the colon resulting in short chain fatty acid production. Due to its low digestibility by intestinal enzymes, this polysaccharide represents a source of dietary fiber (Dahlqvist, 1961, 1963; Jeanes, 1975).

2.7.4 Alternan and alternan-oligosaccharides

Alternan is an α-glucan consisting of alternating (α1→6) and (α1→3) linkages with a low degree of branching (Table 2). It is produced from sucrose by an enzyme of the glucansucrase family, known as alternansucrase (EC 2.4.1.140), that is found mainly in *Leuconostoc mesenteroides* (Côté and Robyt, 1982; Park and Khan, 2009; Leemhuis, Pijning, *et al.*, 2013). Alternan is resistant to most known microbial and mammalian enzymes and can only be hydrolyzed by isomaltodextranases, and alternanases. Due to its resistance to digestion it can be used for production of ingredients for functional foods such as prebiotics (Leathers, Hayman and Cote, 1997; Park and Khan, 2009). It has also been reported that alternan oligosaccharides derived from alternanase activity are used as low-glycemic sweeteners. Some studies state that these oligosaccharides are potential prebiotics (Leathers, Hayman and Cote, 1997), however recent *in vivo* trials in humans showed that they are slowly but fully digestible by human digestive enzymes in the gastrointestinal track (Grysman, Carlson and Wolever, 2008; Vanschoonbeek *et al.*, 2009). A recent study on α-glucan oligomers containing (α1→6) and (α1→3) linkages with DP ranging from 3-12, showed similar glucose and insulin response curves as the dextrose control in humans. In the same study, (α1→2) branching points were introduced into these oligomers, resulting in increased resistance to digestion *in vivo* in mice. However, this observation has not been confirmed in humans (Hasselwander *et al.*, 2017).

2.7.5 Highly branched α-glucans

It has been shown that the shorter side chains make highly-branched starch less prone to α-amylase degradation resulting in a slower glucose release rate (Le *et al.*, 2009; Van Der Maarel and Leemhuis, 2013). Different enzymatic modification strategies have been successfully used to increase the degree of (α1→6) branching points in starch (e.g. treatment with branching enzymes). In experiments by Ao et al. (Z Ao *et al.*, 2007; Zihua Ao *et al.*, 2007), normal corn starch was modified through treatment with β-amylase, or β-amylase- and transglucosidase (BAMTG), or maltogenic α-amylase and transglucosidase (MAMTG). *In vitro* methods were used to analyze digestion rates of the derived starches by pancreatic α-amylase, pancreatin, and amyloglucosidase. Starch treated with MAMTG showed an *in vitro* digestion rate, measured by reducing sugars produced, after 10 (69%) and 3 hrs (55%) of digestion, compared to control untreated gelatinized corn starch (100%). Analysis of the slowest digesting starch from this experiment showed considerably greater proportions of low molecular weight starch molecules with reduced amylopectin B_1 and B_2 branch chains (short and medium linear chain lengths in amylopectin), and lower ratios of (α1→4) to (α1→6)-linkages (13% (α1→6) in BAMTG-modified starch and 23% in MAMTG-modified starch). Thus, increased (α1→6)-linkages in shorter molecular size starch molecules had a slow and extended digestion (Le *et al.*, 2009; Van Der Maarel and Leemhuis, 2013). In a study by Lee et al in 2013, rats gavaged with a highly branched maltodextrin, made with maltogenic α-amylase together with β-amylase, had higher and extended blood glucose levels 1 hour postprandial than did those gavaged with unmodified starch or starch modified with just branching enzyme alone (Lee *et al.*, 2013).

2.7.6 Pullulan

Pullulan is a linear polysaccharide consisting of maltotriose units interconnected by single (α1→6) glycosidic linkages (Table 2). This alternating pattern is responsible for the slow digestibility of pullulan in humans (Wolf *et al.*, 2003). It is a white soluble polymer without taste and odor (Khan, Park and Kwon, 2007). It is produced from starch by the fungus Aureobasidium pullulans (Bender, Lehmann and Wallenfels, 1959). As a food additive, it is known by the E number E1204.

2.8 Enzymatic tools for the synthesis of novel α-glucans from sucrose and starch

The following sections 1.8 and 1.9 were contributed by Gangoiti, J; Vafiadi, C; Dijkhuizen, L. They are relevant and provide context, but are not the focus of this body of work.

In view of the above there remains a need for novel α-glucans from sucrose and starch that are less or only slowly digestible in the human body. Microbial α-transglycosylase enzymes acting on starch and sucrose substrates are known to convert the high glycemic index sucrose and starch carbohydrates into α-glucans of interest for the food industry. Some relevant commercial examples are the dextran and CDs, described above. In general, these α-tranglycosylase enzymes are stable, they act on renewable cheap substrates, and display high regio- and stereo-selectivity. Other strategies for the production of α-glucans do not have these advantages. For example, chemical approaches require many tedious protection and deprotection steps of the hydroxyl groups in order to achieve regio- and stereo-selectivity, toxic catalysts and solvents. Other enzymatic strategies are based on the use of "Leloir" glycosyl transferases, which require expensive nucleotide-activated sugars (e.g. uridine diphosphate glucose) and will not be the focus of this review. According to the amino acid sequence-based CAZy classification system, most of these sucrose- and starch-acting α-transglycosylases (EC 2.4.) are members of families GH13, GH31, GH57, GH70 and GH77, also covering hydrolases (i.e. amylase, α-glucosidases, E.C. 3.2.) and isomerases (i.e. isomaltulose synthase, trehalose synthase, E.C. 5.4.). Despite the fact that they differ in reaction and product specificity, members of these families employ a similar double displacement α-retaining mechanism which involves the cleavage of the α-glycosidic bond of the glucose donor substrate and the formation of a covalent enzyme-glycosyl intermediate. In a second step, the enzyme-glycosyl intermediate reacts with an acceptor substrate, which can be a water molecule or an acceptor carbohydrate, yielding substrate hydrolysis or a new transglycosylation α-glucan product, respectively (Figure 4). In α-glycosidases or hydrolases (EC 3.2.), water usually acts as acceptor, whereas in α-transglycosylases the binding of an acceptor carbohydrate is favored; consequently, these latter enzymes naturally display very efficient transglycosylation activities (Light *et al.*, 2017). Although α-glycosidases/hydrolases catalyze the hydrolysis of α-glucans *in vivo*, many of these enzymes display a certain degree of transglycosylation activity that can be used for synthesis of glycosidic bonds *in vitro*. For example, the transglycosylation activity of α-glucosidases (EC 3.2.1.20), neopullulanases (EC3.2.1.135) and maltogenic amylases (EC 3.2.1.133) has been used for the production of isomaltooligosaccharides and branched

oligosaccharides (Lee *et al.*, 1995; Yoo *et al.*, 1995; Goffin *et al.*, 2011; Niu *et al.*, 2017). Many sucrose- and starch-acting enzymes have been characterized as natural α-transglycosylases with different specificities. Interestingly, protein structure studies have provided important insights in the molecular basis for product specificity of several α-transglycosylases. This also has resulted in valuable clues for subsequent steps aiming to develop tailor-made enzyme variants capable of synthesizing any desirable α-glucan structures. Most of these sucrose- and starch-acting enzymes belong to the GH13, GH70 and GH77 families that constitute the GH-H clan. Members of the GH-H clan are evolutionarily related, displaying similar protein structures and activity mechanisms. GH13, GH70 and GH77 enzymes share a catalytic $(\beta/\alpha)_8$ barrel domain and have four conserved amino acid sequence motifs containing the three catalytic Asp, Glu and Asp residues and some of the substrate binding residues (Leemhuis, Pijning, *et al.*, 2013). GH31 enzymes differ in their catalytic residues, but they adopt a similar $(\beta/\alpha)_8$ fold and were found to display a remote evolutionary relatedness with GH-H clan members (Janeček, Svensson and MacGregor, 2007). GH57 family enzymes, however, have a catalytic $(\beta/\alpha)_7$ barrel domain and possess their own five conserved motifs and catalytic machinery (Suzuki and Suzuki, 2016). The main types of natural α-transglycosylases used for the production of slowly digestible or less digestible α-glucans will be illustrated in the following sections. Particular attention will be given to the variety of existing sucrose- and starch-acting GH70 enzymes, reviewing the surge of new enzymes that have been characterized in recent years. Due to their broad product specificity, GH70 enzymes represent attractive enzymatic tools for the synthesis of tailor-made α-glucans with a defined glycemic response.

2.9 **Cyclodextrin glucanotransferases**

Cyclodextrin glucanotransferases (CGTase; EC 2.4.1.19) mainly convert starch into cyclic (α1→4)-linked oligosaccharides, named cyclodextrins (CDs). Depending on their main CD product, as discussed above, these enzymes are classified as α-, β-, and γ-CGTases, with 6, 7 and 8 glucose units, respectively. Apart from their main cyclization activity, CGTases also catalyze hydrolysis and intermolecular transglycosylation reactions using linear (α1→4) glucans (disproportionation reaction) or their own CD products (coupling reaction) as substrates, yielding linear products (Van Der Veen *et al.*, 2000; Commission and Programme, 2003; Joint FAO/WHO Expert Committee on Food Additives (JECFA), 2006). CGTases are found in Bacteria and

Archaea, and based on their sequences they are placed in the GH13 family, which is the largest family of glycoside hydrolases acting on starch and related α-glucans. Several three-dimensional structures of CGTases from bacteria of different genera (e.g. *Bacillus, Thermoanaerobacterium* and *Geobacillus*) are currently available without or complexed with several substrates (Leemhuis, Kelly and Dijkhuizen, 2010; Han *et al.*, 2014). CGTase enzymes consist of 5 domains: A, B, C, D and E. Domains A, B and C are present in most GH13 family members. Domain A comprises the catalytic $(\beta/\alpha)_8$ barrel, and together with domain B forms the substrate binding groove. Domains C and E participate in starch binding, whereas the role of domain D has remained unclear.

The reaction mechanisms and substrate-binding subsites of CGTases have been analyzed in detail allowing identification of amino acid residues determining CD size specificity (Uitdehaag *et al.*, 1999, 2000; Van Der Veen *et al.*, 2000). Most CGTases synthesize a mixture of CD of different sizes, and thus, a selective purification step is required to obtain a single type of CD only (Leemhuis, Kelly and Dijkhuizen, 2010). Using protein engineering approaches many CGTase variants with an improved α-, β-, and γ-CD selectivity have been obtained (Leemhuis, Kelly and Dijkhuizen, 2010; Han *et al.*, 2014).

2.10 **4-α-Glucanotransferases**

4-α-Glucanotransferases (4-α-GTase; EC 2.4.1.25) also designated as amylomaltases, or D-enzymes, display disproportionating activity (see below) on starch-like substrates containing consecutive (α1→4) glycosidic linkages (e.g. amylose, amylopectin, maltodextrins, and glycogen). These enzymes are distributed in plants and microorganisms, where they participate in starch biosynthesis and glycogen metabolism, respectively (Boos and Shuman, 1998; Colleoni *et al.*, 1999; Wattebled *et al.*, 2003). Enzymes with 4-α-GTase activity are distributed in the GH13, GH57 and GH77 families, only the GH77 family contains exclusively 4-α-GTases. Three-dimensional

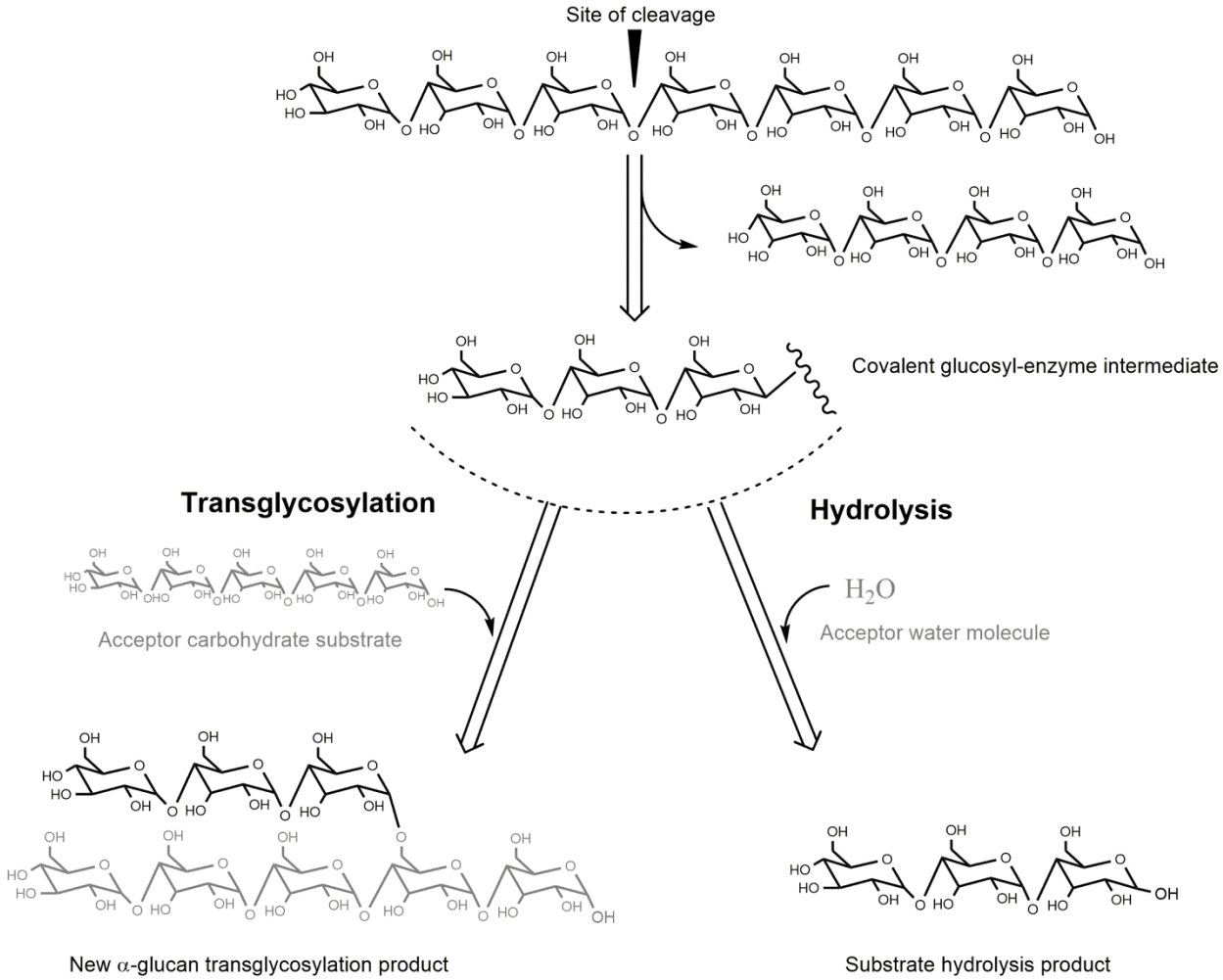

Figure 4. Examples of tranglycosylation and hydrolysis reactions.

structures in free form or in complex with substrates are available for several GH77 family enzymes, including industrially important thermostable and thermoactive enzymes from *Thermus thermophilus* HB8 (PDB codes 1FP8 and 1FP9) (Kaper et al. 2007), *Thermus aquaticus* ATCC 33923 (PDB code 1CWY (Przylas *et al.*, 2000; and *Aquifex aeolicus* VF5 (PDB code 1TZ7; Uitdehaag et al., unpublished work). The main structural feature that distinguish GH77 enzymes from the evolutionary related GH13 proteins is the lack of domain C. Crystal structures of 4-α-GTases belonging to the GH13 and GH57 protein families have also been solved from thermophilic organisms [e.g. the archaeon *Thermococcus litoralis* GH57 4-α-GTase (PDB codes 1K1W, 1K1X and 1K1Y (Imamura *et al.*, 2003); and the bacterium *Thermotoga maritima* MSB8 GH13 4-α-GTase (PDB codes 1LWH, 1LWJ, 1GJU and 1GJW) (Roujeinikova *et al.*, 2001, 2002). 4-α-GTases preferably catalyze the cleavage of an (α1→4)-glucan from the non-reducing end of a

donor substrate and its transfer to the non-reducing end of an acceptor (α1→4)-α-glucan via the formation of a new (α1→4) glycosidic linkage. Amylomaltase activity on starch results in the formation of a starch derivative free of amylose (consumed as donor substrate) and consisting of an amylopectin product with a mixture of both shortened and elongated side-chains (Van Der Maarel *et al.*, 2005). This product (e.g. Etenia) can be used as a replacement of gelatin, which is an animal-derived product widely used as a hydrocolloid in food. The presence of these relatively long chains, and its relatively high molecular weight, provide this polymer with thermoreversible gelling properties (Hansen *et al.*, 2008). 4-α-GTase treated corn starch is rather resistant to digestion (Jiang *et al.*, 2014). Some 4-α-GTases also catalyze intramolecular transglycosylation reactions resulting in the formation of large cyclic (α1→4)-glucans, designated as cycloamyloses (Terada *et al.*, 1999). Structurally, cycloamyloses resemble cyclodextrins, however, they have a higher degree of polymerization (from 16 to several hundreds of glucose units). In view of their large ring size, cycloamyloses are not expected to display the slowly digestible properties described for α- and β-cyclodextrins, however, they may have many other applications in the pharmaceutical and biotech industry due to their capacity to encapsulate hydrophobic guest molecules within their hydrophobic cavity (Roth *et al.*, 2017). Interestingly, the 4-α-GTase disproportionation activity, in combination with maltogenic amylase and pullulanase, has been used for the synthesis of starch-derived IMOs and a resistant starch-like product, respectively (Lee *et al.*, 2002; Norman *et al.*, 2007).

2.10.1 Branching enzymes

Branching enzymes (BE, EC 2.4.1.18) act on (α1→4) glucans, cleaving an internal (α1→4) linkage and transferring the cleaved-off part to the same or another (α1→4) glucan chain via an (α1→6) branch point (Shinohara *et al.*, 2001; Roussel *et al.*, 2013). BE are widespread in nature and can be found in bacterial, archaeal, and eukaryotic species, where they catalyze the formation of (α1→6)-branching points during glycogen or starch biosynthesis (Suzuki and Suzuki, 2016). BE are therefore critical determinants of the structure and properties of these intracellular storage polysaccharides. BE have gained substantial interest for the production of different starch-derived products such as highly-branched α-glucans (Kittisuban et al. 2014, Lee et al. 2013), synthetic glycogen (Kajiura *et al.*, 2006), and CCD (Takata *et al.*, 2003). In particular, thermostable glycogen BE enzymes from *Aquifex aeolicus* and *Rhodothermus obamensis* are the most

commercially exploited (Programme, 2010; Van Der Maarel and Leemhuis, 2013). BE are placed in the GH13 and GH57 family proteins, which differ in their overall 3-dimensional structures, catalytic residues, and geometry around the active site (Suzuki and Suzuki, 2016). Numerous BE have been characterized showing differences in their substrate specificity and generating products with varied frequency and branch chain length. Whereas, some BE preferentially convert amylose (Binderup, Mikkelsen and Preiss, 2000; Palomo *et al.*, 2011; Roussel *et al.*, 2013; Hayashi *et al.*, 2015), others display higher activity on amylopectin substrates (Palomo *et al.*, 2009; Jo *et al.*, 2015). Also, the minimal length of the donor glucan, the length of the transferred glucan, and the distance between two successive branch points differ from one BE to another (Takata *et al.*, 2003; Palomo *et al.*, 2009; Roussel *et al.*, 2013; Sawada *et al.*, 2014; Hayashi *et al.*, 2015; Jo *et al.*, 2015). Several experimental approaches including site-directed mutagenesis (Hayashi *et al.*, 2017; Liu *et al.*, 2017), domain-swapping and truncation experiments (Palomo *et al.*, 2009; Jo *et al.*, 2015; Welkie, Lee and Sherman, 2016) and X-ray crystallography studies (Abad *et al.*, 2002; Pal *et al.*, 2010; Palomo *et al.*, 2011; Feng *et al.*, 2015; Hayashi *et al.*, 2015; Na *et al.*, 2017) have been used to understand the mechanism of branching activity. Very recently the *Cyanothece* sp. ATCC 51142 BE1 structure with an oligosaccharide bound in the active site cleft has been solved providing a better understanding of the reaction catalyzed by these enzymes (Hayashi *et al.*, 2017). However, the relationship between the reaction specificity (e.g. preferred chain lengths transferred) and the BE protein structure remains unclear, and it is possible that variation exists in the mode of oligosaccharide binding depending on the BE species (Hayashi *et al.*, 2017). This information may allow a better control of the degree of branching and the average length of branches of the reaction product by the engineering of BE with altered specificity.

2.10.2 Amylosucrases

Amylosucrases (AS, EC 2.4.1.4) catalyze the synthesis of linear (α1→4) glucans from sucrose, and have been characterized from various bacterial sources (see below). Although most sucrose-active α-transglycosylases belong to the GH70 family (Monsan, Remaud-Siméon and André, 2010), in view of its amino acid sequence AS have been classified in the GH13 family, mostly containing starch-acting enzymes. AS activity with sucrose results in synthesis of an amylose-like polymer with a molecular weight that is significantly lower (DP up to 8) (Potocki-Veronese *et al.*, 2005) than the α-glucan polysaccharides synthesized by sucrose-utilizing GH70

members (Moulis, André and Remaud-Simeon, 2016). This (α1→4) glucan is insoluble and shows a high degree of B-type crystallinity, which makes this product resistant to hydrolysis by digestive enzymes (Norman *et al.*, 2007). In addition to the amylose-like polymer, sucrose isomers are usually also formed by AS, which reduce the α-glucan yield. It has been proposed that AS *in vivo* are involved in energy storage through glycogen elongation (Albenne *et al.*, 2004). In *in vitro* studies, when glycogen and other polymers containing (α1→4) or (α1→4) and (α1→6) linkages are used as acceptor substrates, AS elongate some of their external chains yielding polymers with higher slowly digestible and resistant starch content (Rolland-Sabaté *et al.*, 2004; Shin *et al.*, 2010; Kim *et al.*, 2014). With the aim of designing α-glucans with defined structures using only sucrose as raw material, the *Neisseria polysaccharea* AS has been combined with other α-transglycosylases, including the BE from *Rhodothermus obamensis* and the CGTase from *Bacillus macerans,* resulting in the production of glycogen and cyclodextrins, respectively (Grimaud *et al.*, 2013; Koh *et al.*, 2016). AS have been identified in various bacterial species (e.g. *Deinococcus*, *Arthrobacter, Alteromonas*, *Methylobacillus*, *Synecochococcus*); the AS from *N. polysaccharea* has been studied in most detail (Moulis, André and Remaud-Simeon, 2016). Crystal structures of AS in free form, and in complex with different substrates, have been solved (Mirza *et al.*, 2001; Jensen *et al.*, 2004; Guérin *et al.*, 2012; Skov *et al.*, 2013). In addition to the 3 domains A, B and C common to all GH13 family members, AS have 2 extra domains named N and B' that are unique to these enzymes. These 3D structures have allowed the identification of key residues involved in the polymerization process, and have guided the construction of AS mutants which produce in a controlled way either short maltooligosaccharides or insoluble amylose from sucrose (Albenne *et al.*, 2004; Schneider *et al.*, 2009; Cambon *et al.*, 2014).

2.10.3 Dextran dextrinases

Some strains of *Gluconobacter oxydans* are known to produce an intracellular enzyme named dextran dextrinase (DDase, EC 2.4.1.2) catalyzing the synthesis of dextran using maltodextrins as substrate. DDase is able to transfer the non-reducing terminal glucosyl residues of maltodextrins to an acceptor substrate forming consecutive (α1→6) linkages (Naessens *et al.*, 2005; Sadahiro *et al.*, 2015). As a result of this activity a dextran polymer is produced, which contains some (α1→4) branches and (α1→4) linkages in (α1→6) glucosyl linear chains (Yamamoto, Yoshikawa and Okada, 1993). DDase also disproportionates (α1→6) glucans

indicating that it is also active on its own products. The gene encoding the DDase from *G. oxydans* ATCC 11894 has been recently identified revealing that the protein encoded belongs to the GH15 family. With the exception of the DDase from *G. oxydans* ATCC 11894, all characterized GH15 family members employ an inverting mechanism yielding β-anomeric products (Coutinho, no date). In view of its α-retaining mechanism, the DDase enzyme is an atypical member of the GH15 family.

2.11 Generation of structurally diverse α-glucans by novel GH70 α-transglycosylases

The GH70 family was established for glucansucrases (GS), exclusively found in lactic acid bacteria (LAB), which convert sucrose into high molecular mass α-glucan polymers (Monchois, Willemot and Monsan, 1999; Leemhuis, Pijning, *et al.*, 2013). GS catalyze polymer synthesis by the successive transfer of single glucosyl units from sucrose to the non-reducing end of a growing glucan chain. Alternatively, in the presence of a low-molecular mass acceptor substrate such as maltose, GS switch from polysaccharide to low molecular mass oligosaccharide synthesis, using sucrose as donor substrate. The various characterized GS synthesize a large diversity of α-glucan products from sucrose, and with all possible linkages (α1→2), (α1→3), (α1→4), and (α1→6). Also, these α-glucans may be linear or branched and may differ in their type and degree of branching, size, and conformation, resulting in oligo- and poly-saccharides with different physicochemical properties (e.g. viscosity, adhesiveness, solubility, etc.). The α-glucans synthesized by GS are classified into four categories based on their dominant glycosidic linkage type: dextran with a majority of (α1→6) linkages, mutan with a majority of (α1→3) linkages, reuteran with a majority of (α1→4), and alternan with alternating (α1→3) and (α1→6) linkages Table 3). Three-dimensional structures are available for 5 GS proteins with different product specificity (Vujicic-Zagar *et al.*, 2010; Ito *et al.*, 2011; Brison *et al.*, 2012; Pijning *et al.*, 2012). These crystal structures show that in GS the catalytic $(\beta/\alpha)_8$-barrel domain is circularly permuted compared to GH13 and GH77 enzymes, confirming earlier predictions (MacGregor, Jespersen and Svensson, 1996). Interestingly, GS display a unique U-fold organized in five structural domains (A, B, C, IV and V) (Figure 5). The domains A, B and C form the catalytic core, and are also found in GH13 enzymes, whereas the remote domains IV and V are only present in GH70 enzymes. Thus far, 60 GS enzymes have been characterized, most of them producing dextran polymers. The industrially most relevant GS is the *Leuconostoc mesenteroides* NRR B-512F DSR-S

dextransucrase converting sucrose into a polymer with 95% (α1→6) linkages in the main chains and 5% (α1→3) branch linkages (Monchois *et al.*, 1997; Passerini *et al.*, 2015). Interestingly, GH70 enzymes displaying dextran branching specificity have been identified providing novel tools for the production of dextrans with a controlled degree of (α1→2) and (α1→3) branching points (Brison *et al.*, 2010, 2012; Vuillemin *et al.*, 2016). First, *L. mesenteroides* NRRL B-1299 was found to encode two GH70 enzymes (named DSRE and BRS-A) specialized in (α1→2) transglycosylation from sucrose to a dextran acceptor substrate (Brison *et al.*, 2012; Passerini *et al.*, 2015). The gluco-oligosaccharides containing (α1→2) linkages synthesized by *L. mesenteroides* NRRL B-1299 DSRE were found to be highly resistant to the action of digestive enzymes in both humans and animals (Valette *et al.*, 1993). Recently, genome analysis of *Leuconostoc citreum* NRRL B-742 allowed the identification of the first (α1→3) branching sucrase (named BRS-B) responsible for the high content of (α1→3) branching linkages present in the dextran produced by this strain (Vuillemin *et al.*, 2016).

In recent years, novel GH70 enzymes inactive on sucrose, but displaying clear disproportionating activity on starch/maltodextrin substrates, have been identified (Table 3) (Kralj *et al.*, 2011; Leemhuis, Dijkman, *et al.*, 2013; Gangoiti *et al.*, 2016; Gangoiti, Pijning and Dijkhuizen, 2016; Gangoiti, Lamothe, *et al.*, 2017; Gangoiti, Van Leeuwen, Gerwig, *et al.*, 2017; Gangoiti, Van Leeuwen, Meng, *et al.*, 2017). Regarding their substrate specificity, these starch-converting GH70 enzymes resemble GH13 family enzymes also acting on starch-like substrates, however, they share higher amino acid sequence similarity with GS from the GH70 family. Based on their sequences, these enzymes were classified into 3 new GH70 subfamilies designated as GtfB, GtfC and GtfD, which differ in their microbial origin, product specificity and domain organization (Kralj *et al.*, 2011; Gangoiti *et al.*, 2016; Gangoiti, Pijning and Dijkhuizen, 2016; Gangoiti, Van Leeuwen, Gerwig, *et al.*, 2017),

Whereas GtfB enzymes are mainly found in *Lactobacillus* strains and display a GS-like fold with a circularly permuted catalytic $(\beta/\alpha)_8$-barrel, GtfC and GtfD enzymes are present in non-LAB and possess a non-permuted domain organization resembling that of GH13-like enzymes (Figure 5) (Gangoiti, Pijning and Dijkhuizen, 2016; Gangoiti *et al.*, 2016; Gangoiti, Lamothe, *et al.*, 2017). In view of their intermediate position between GH13 α-amylases and GH70 GS, the emergence of GtfB, GtfC and GtfD type of enzymes have provided clues about the evolutionary history of GH70 family proteins. It has been proposed that evolution from an ancestor α-amylase to present-day GS

occurred via these GtfB-, GtfC-, and GtfD-like intermediates (Kralj *et al.*, 2011; Gangoiti *et al.*, 2016; Gangoiti, Pijning and Dijkhuizen, 2016; Gangoiti, Van Leeuwen, Gerwig, *et al.*, 2017). In addition to their scientific relevance, GtfB, GtfC and GtfD type of enzymes represent very interesting and powerful enzymatic tools for the conversion of the starch present in food matrices into soluble novel dietary fibers and/or slowly-digestible carbohydrates, and thus, they have gained substantial interest for the development of healthier starchy food products (Gangoiti, Van Leeuwen, Meng, *et al.*, 2017). However, only few starch-converting GH70 enzymes have been characterized so far. Whereas GS display a broad linkage specificity, most of the starch-converting GH70 enzymes characterized act as 4,6-α-glucanotransferases (GTases), cleaving (α1→4) linkages and synthesizing new (α1→6) linkages (Table 3). Depending on the enzyme, different products are synthesized as a result of this 4,6-α-GTase activity on starch/maltodextrin substrates. For example, the *Lactobacillus reuteri* 121 GtfB and *Exiguobacterium sibiricum* 255-15 GtfC disproportionation activity on starch-like substrates results in the synthesis of linear IsoMalto-/Malto-Polysaccharides (IMMP) and IsoMalto-/Malto-Oligosaccharides (IMMO) (Figure 6), respectively (Leemhuis *et al.*, 2014; Gangoiti, Pijning and Dijkhuizen, 2016). Both IMMP and IMMO are 'hybrid molecules' and consist of linear (α1→6) glucan chains attached to the non-reducing ends of starch or malto-oligosaccharide fragments, but they significantly differ in their molecular mass. Unlike the *L. reuteri* 121 GtfB and *E. sibiricum* GtfC enzymes, the *Azotobacter chroococcum* and *Paenibacillus beijingensis* GtfD 4,6-α-GTases are unable of forming consecutive **(**α1→6) linkages. Using these GtfD enzymes, branched polymers containing mostly (α1→4) linkages and single (α1→6) bridges in linear and branched orientations are obtained from amylose (Figure 6) (Gangoiti *et al.*, 2016; Meng, Gangoiti, *et al.*, 2016; Gangoiti, Lamothe, *et al.*, 2017). These polymers resemble the reuteran polysaccharide synthesized by the *L. reuteri* 121 GtfA GS from sucrose (van Leeuwen *et al.*, 2008b; Dobruchowska *et al.*, 2013; Meng, Dobruchowska, *et al.*, 2016; Meng, Pijning, *et al.*, 2016), described as a health-promoting food ingredient (Ekhart *et al.*, 2006; Plijter *et al.*, 2009). *In vitro* digestibility assays, using either pancreatic α-amylase and amyloglucosidase or rat intestinal maltase-glucoamylase and sucrase-isomaltase, simulating the digestive power of the gastrointestinal tract revealed that the IMMP and reuteran type of polymers have a high dietary fiber content Leemhuis *et al.*, 2014; Gangoiti, Lamothe, *et al.*, 2017). The limited diversity in linkage specificity found within these starch-converting GH70 subfamilies of enzymes recently was expanded with the discovery of the

Lactobacillus fermentum NCC 2970 GtfB displaying 4,3-α-GTase activity (Gangoiti, Van Leeuwen, Gerwig, *et al.*, 2017). This *L. fermentum* NCC 2970 GtfB converts amylose into a branched α-glucan composed of linear (α1→4) segments interconnected by single (α1→3) and (α1→3,4) linkages (Figure 6).The characterization of this *L. fermentum* NCC 2970 GtfB 4,3-α-GTase represents an important breakthrough because its 4,3-α-glucan product is unique and different from other naturally occurring, synthetic and enzymatically produced α-glucans.

Table 3. Examples of products synthesized by sucrose- and starch-active GH70 enzymes

Enzyme	Substrate	Linkage composition of the product (%)			
		(α1→2)	(α1→3)	(α1→4)	(α1→6)
Dextran					
Leuconostoc mesenteroides NRRL B-512F DSRS (Monchois *et al.*, 1997)	Sucrose		5		95
Leuconostoc citreum B-1299 DSRE[a] (Fabre *et al.*, 2005)	Sucrose	5	10	3	81
Leuconostoc citreum B-1299 BSR-A (Passerini *et al.*, 2015)	Sucrose and linear dextran	37			63
Leuconostoc citreum BSR-B (Vuillemin *et al.*, 2016)	Sucrose and linear dextran		50		50
Weissella cibaria DSRWC (Kang, Oh and Kim, 2009)	Sucrose				100
Lactobacillus reuteri 180 Gtf180 (van Leeuwen *et al.*, 2008a)	Sucrose		31		69
Streptococcus mutans GS5 GTFD (Hanada and Kuramitsu, 1989)	Sucrose		30		70
Mutan					
Streptococcus mutans GS5 GTFB (Ueda, Shiroza and Kuramitsu, 1988)	Sucrose		88		12
Lactobacillus reuteri ML1 (Kralj *et al.*, 2004)	Sucrose		65		35
Leuconostoc mesenteroides NRRL B-1118 DSRI (Côté and Robyt, 1982)	Sucrose		50		50
Alternan					
Leuconostoc mesenteroides NRRL B-1355 ASR (Côté and Robyt, 1982)	Sucrose		43		57
Reuteran					
Lactobacillus reuteri 121 GtfA (Kralj *et al.*, 2004)	Sucrose			58	42
Lactobacillus reuteri ATCC 55730 GtfO (Kralj *et al.*, 2005)	Sucrose			79	21
Azotobacter chroococcum NCIMB 8003 GtfD (Gangoiti *et al.*, 2016)	Amylose			68	32
Lactobacillus reuteri NCC 2613 GtfB (Gangoiti, Van Leeuwen, Meng, *et al.*, 2017)	Amylose			75	25
Isomalto/Malto-Polysaccharide					
Lactobacillus reuteri 121 GtfB (Leemhuis *et al.*, 2014)	Amylose			9	91
Isomalto/Malto-Oligosaccharide					
Exiguobacterium sibiricum GtfC (Gangoiti, Pijning and Dijkhuizen, 2016)	Amylose			40	60
Branched (α1→3), (α1→4)-α-glucan					
L. fermentum NCC 2970 GtfB (Gangoiti, Van Leeuwen, Gerwig, *et al.*, 2017)	Amylose		40	60	

Compared to the limited linkage specificity displayed by other sucrose- and starch-converting α- -transglycosylases, glucans with different types of glycosidic linkages can be obtained [(α1→2), (α1→3), (α1→4) and (α1→6)] by using GS. Over the years, many studies have tried to elucidate what determines the glycosidic linkage specificity in GS enzymes, resulting in synthesis of such a large variety of α-glucans. Variations in product specificity were proposed to

be determined by the way in which the acceptor α-glucan is guided into the reaction center (Vujicic-Zagar *et al.*, 2010; Leemhuis, Pijning, *et al.*, 2013). The crystal structure of GTF180-ΔN in complex with maltose revealed the residues interacting with this acceptor substrate in subsites +1 and +2 (Vujicic-Zagar *et al.*, 2010). Mutagenesis of these key residues have demonstrated that it is the interplay of different amino acid residues defining the acceptor binding subsites what determines the glycosidic linkage specificity in GS (Meng, Pijning, *et al.*, 2015; Meng, Dobruchowska, *et al.*, 2016; Gangoiti, Van Leeuwen, Meng, *et al.*, 2017). These studies also have shown that predicting the effects of mutations is still complicated. Interesting mutant variants nevertheless have been obtained producing α-glucans differing in their linkage type, degree of branching, and/or molecular weight. These studies have been recently reviewed by Meng et al., 2016 (Meng, Gangoiti, *et al.*, 2016). Overall, these efforts have significantly enlarged the panel of α-glucans that can be enzymatically produced.

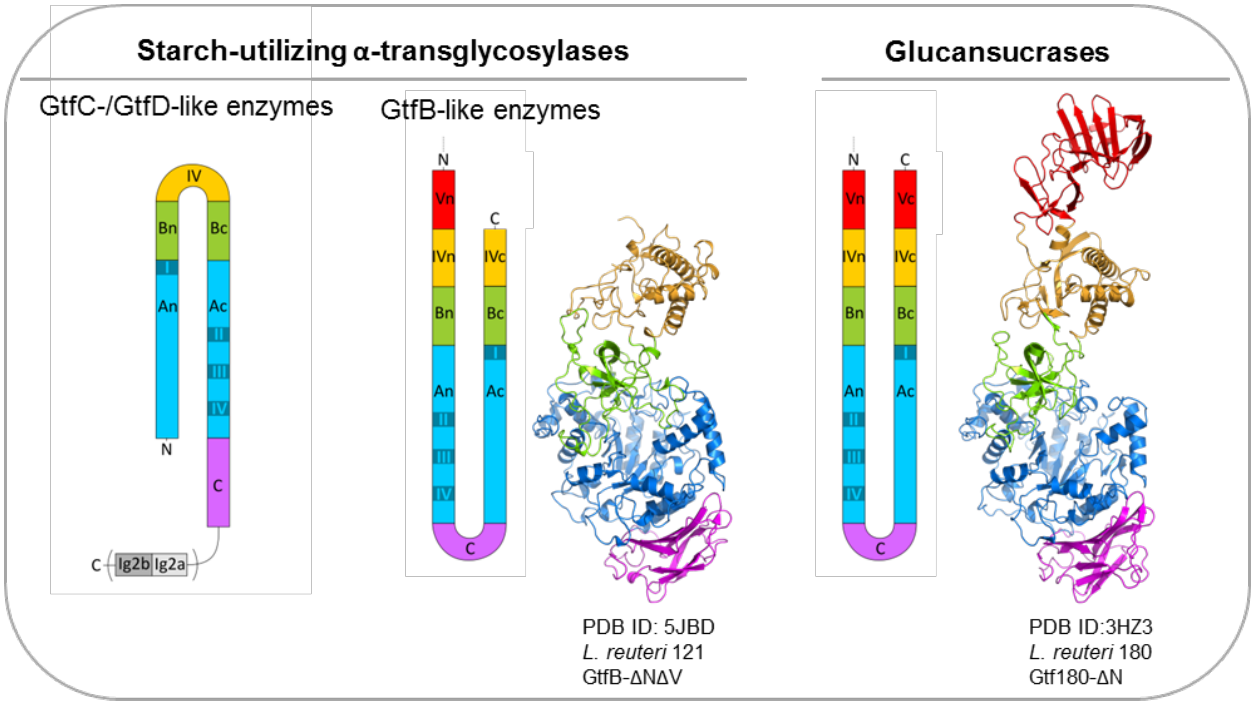

Figure 5. Domain arrangement of sucrose- and starch-converting GH70 enzymes. Crystal structures of the L. reuteri 121 GtfB 4,6-α-GTase (middle), and the L. reuteri 180 Gtf180 GS (right). Domains A, B, C, IV and V are highlighted in blue, green, magenta, yellow and red, respectively. Ig2-like domains are colored in grey. As apparent from the order of the conserved regions (indicated by grey rectangles), the catalytic barrel of the GH70 glucansucrases and GH70 GtfB-like enzymes is circularly permuted (order = II-III-IV-I).

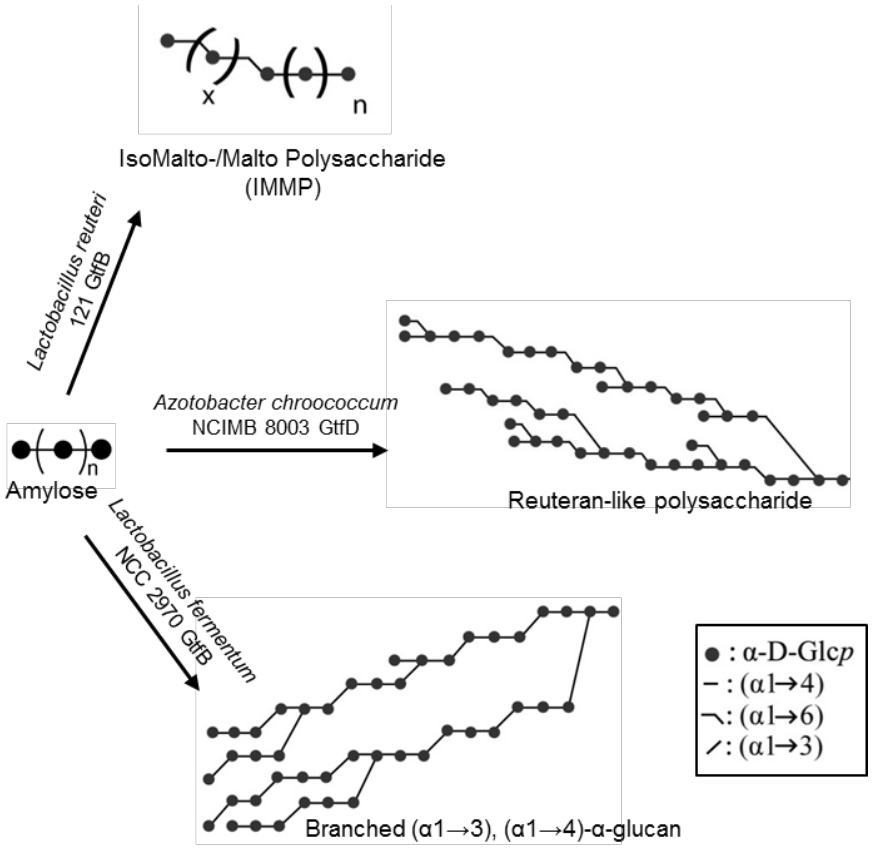

Figure 6. Composite models of representative novel α-glucans synthesized by starch-converting GH70 enzymes

Despite the lack of data related to their physicochemical properties, this structural variability is expected to result in differences in a wide range of specific properties, such as solubility, viscosity, and resistance to enzymatic hydrolysis by digestive enzymes. Another important advance in GH70 research was the elucidation of the *L. reuteri* 121 GtfB 4,6-α-GTase 3D structure (Figure 5). However, binding of oligosaccharides at the acceptor binding subsites has not been observed yet in any of the *L. reuteri* 121 GtfB crystal structures obtained (Bai *et al.*, 2017). It also remains to be studied whether the repertoire of α-glucans synthesized by the starch-converting GtfB, GtfC and GtfD GH70 enzymes could be further expanded by protein engineering approaches. Very recently, the structure of the DSR-M dextransucrase from *Leuconostoc citreum* NRRL B-1299, producing a single low molar mass dextran has been reported providing important clues about the structural features determining glucan size (Claverie *et al.*, 2017).

Attempts to diversify the structure and product size distribution of the α-glucans synthesized by GS using reaction engineering approaches already have been reported. Specifically,

the effects of sucrose and enzyme concentrations, temperature and pH have been evaluated. Studies by Robyt and co-workers have shown that the molecular size of dextran is inversely proportional to the concentration of dextransucrase, and directly proportional to the concentration of sucrose and the temperature (Robyt, Yoon and Mukerjea, 2008; Falconer, Mukerjea and Robyt, 2011). Thus, it was proposed that the best method to obtain α-glucans with a defined molecular mass was the selection of specific enzyme/sucrose concentrations and temperature values. In case of the *L. mesenteroides* B-512FMCM dextransucrase, changes in sucrose concentration and temperature were found to affect the product size distribution, whereas the pH of the reaction did not have a significant effect (Kim *et al.*, 2003). In a more recent study, synthesis of reuteran by *L. reuteri* 121 GtfA GS at different sucrose concentrations revealed that the ratio of polysaccharide versus oligosaccharide can be modulated by sucrose concentrations (Meng, Dobruchowska, *et al.*, 2015). With increasing sucrose concentrations, the production of polysaccharides decreased, while the amount of oligosaccharides increased. However, the linkage distribution and molecular mass of the polysaccharides synthesized at different sucrose concentration was not changed. Another strategy to direct the synthesis toward the production of oligosaccharides at the expense of polymer formation is by adding "good" acceptor substrates (e.g. maltose or isomaltose) to the reaction (López-Munguía *et al.*, 1993; Su and Robyt, 1993; Côté and Sheng, 2006; Meng, Gangoiti, *et al.*, 2016). In the presence of low-molecular mass acceptor sugars, GS transfers the glucosyl moieties from sucrose to the acceptor molecule, forming a series of oligosaccharides. The final product distribution can be varied by changing the reaction ratios of sucrose, acceptor substrate and enzyme. A similar approach was used for the synthesis of dextrans with a controlled degree of (α1→2) and (α1→3) linkages using branching sucrases (Brison *et al.*, 2010; Vuillemin *et al.*, 2016). As dextran is the natural acceptor of branching sucrases, the amount of (α1→2) and (α1→3) side chains was found to be directly dependent on the initial [Sucrose]/[Dextran] molar ratio. Using a suitable [Sucrose]/[Dextran] ratio, dextran polymers grafted with up to 30% of (α1→2) linkages and 50% of (α1→3) linkages, were obtained using the GBD-CD2 and BRS-B enzymes, respectively (Brison *et al.*, 2010, 2012; Vuillemin *et al.*, 2016).

2.12 **Conclusions**

The discovery of novel α-transglycosylases with diverse product specificities has provided important tools for the conversion of starch or sucrose into commercially valuable slowly

digestible or resistant α-glucans. These new carbohydrate ingredients hold a promise of providing digestion-controlled materials that can modulate glycemic response or being new dietary fiber sources. At present, α-glucans with different structures (linkage type, branching degree) can be produced by using selected α-transglycosylases. These structural differences result in different digestion rates. A further understanding of the relationship between the structure of these α-glucans and their digestibility is key for the development of α-glucans with a tailored glycemic response. In parallel, a deeper comprehension of α-transglycosylases specificities at the molecular level is still needed to guide the rational design of enzyme variants capable of synthesizing any type of desirable α-glucan regardless of size, linkage type and degree of branching of the product. These joint efforts are expected to allow the synthesis of health-promoting α-glucans of interest for the food-industry.

2.13 **References**

Abad, M. C. *et al.* (2002) 'The X-ray crystallographic structure of Escherichia coli branching enzyme', *The Journal of biological chemistry*. Department of Chemistry, Michigan State University, East Lansing 48824, USA., 277(44), pp. 42164–42170. doi: 10.1074/jbc.M205746200 [doi].

Adisakwattana, S. *et al.* (2009) 'A series of cinnamic acid derivatives and their inhibitory activity on intestinal a-glucosidase', *Journal of Enzyme Inhibition & Medicinal Chemistry*. Taylor & Francis Ltd, 24(5), pp. 1194–1200. doi: 10.1080/14756360902779326.

Albenne, C. *et al.* (2004) 'Molecular Basis of the Amylose-like Polymer Formation Catalyzed by Neisseria polysaccharea Amylosucrase', *Journal of Biological Chemistry*. Toulouse, France, 279(1), pp. 726–734. doi: 10.1074/jbc.M309891200.

Almdal, T. *et al.* (2004) 'The independent effect of type 2 diabetes mellitus on ischemic heart disease, stroke, and death: A population-based study of 13 000 men and women with 20 years of follow-up', *Archives of Internal Medicine*, 164(13), pp. 1422–1426. doi: 10.1001/archinte.164.13.1422.

Anand, C. M. *et al.* (1991) 'Variability in growth of Neisseria polysaccharea on colistin-containing selective media for Neisseria spp', *Journal of clinical microbiology*, 29, pp. 2434–2437.

Ao, Z *et al.* (2007) 'Evidence of native starch degradation with human small intestinal maltase-glucoamylase (recombinant)', *FEBS letters*, 581(13), pp. 2381–2388. doi: 10.1016/j.febslet.2007.04.035.

Ao, Zihua *et al.* (2007) 'Starch with a slow digestion property produced by altering its chain length, branch density, and crystalline structure', *Journal of Agricultural and Food Chemistry*. American Chemical Society, 55(11), pp. 4540–4547. doi: 10.1021/jf063123x.

Astray, G. *et al.* (2009) 'A review on the use of cyclodextrins in foods', *Food Hydrocolloids*, 23(7), pp. 1631–1640. doi: 10.1016/j.foodhyd.2009.01.001.

Bai, Y. *et al.* (2017) 'Crystal Structure of 4,6-α-Glucanotransferase Supports Diet-Driven Evolution of GH70 Enzymes from α-Amylases in Oral Bacteria', *Structure*. Elsevier Ltd., 25(2), pp. 231–242. doi: 10.1016/j.str.2016.11.023.

Bender, H., Lehmann, J. and Wallenfels, K. (1959) 'Pullulan, an extracellular glucan from Pullularia pullulans', *Biochimica Biophysica Acta*, 36, pp. 309–316.

Bengs, H. and Brunner, A. (2000) 'α-Amylase-Resistant Starch for Producing Foodstuff and Medicaments'. United States.

Binderup, K., Mikkelsen, R. and Preiss, J. (2000) 'Limited proteolysis of branching enzyme from Escherichia coli', *Archives of Biochemistry and Biophysics*. Department of Biochemistry, Michigan State University, East Lansing 48824, USA., 377(2), pp. 366–371. doi: S0003-9861(00)91815-0 [pii].

Boos, W. and Shuman, H. (1998) 'Maltose/Maltodextrin System of Escherichia coli: Transport, Metabolism, and Regulation', *Microbiology and Molecular Biology Reviews*. Konstanz, Germany, 62(1), pp. 204–229. doi: 10.1128/mmbr.62.1.204-229.1998.

Bornet, F. R. *et al.* (1989) 'Insulin and glycemic responses in healthy humans to native starches processed in different ways: correlation with in vitro alpha-amylase hydrolysis', *The American Journal of Clinical Nutrition*, 50, pp. 315–323.

Breitmeier, D., Günther, S. and Heymann, H. (1997) 'Acarbose and 1-Deoxynojirimycin Inhibit Maltose and Maltooligosaccharide Hydrolysis of Human Small Intestinal Glucoamylase–Maltase in Two Different Substrate-Induced Modes', *Archives of Biochemistry and Biophysics*, pp. 7–14. doi: http://dx.doi.org.ezproxy.lib.purdue.edu/10.1006/abbi.1997.0274.

Brison, Y. *et al.* (2010) 'Synthesis of dextrans with controlled amounts of α-1,2 linkages using the transglucosidase GBD-CD2', *Applied Microbiology and Biotechnology*. Toulouse, France, 86(2), pp. 545–554. doi: 10.1007/s00253-009-2241-z.

Brison, Y. *et al.* (2012) 'Functional and structural characterization of α-(1→2) branching sucrase derived from DSR-E glucansucrase', *Journal of Biological Chemistry*, 287(11), pp. 7915–7924. doi: 10.1074/jbc.M111.305078.

Brownlee, M. (2001) 'Biochemistry and molecular cell biology of diabetic complications', *Nature*. Nature Publishing Group, 414(6865), pp. 813–820. Available at: http://dx.doi.org/10.1038/414813a.

Buckley, J. D. *et al.* (2006) 'Dose-dependent inhibition of the post-prandial glycaemic response to a standard carbohydrate meal following incorporation of alpha-cyclodextrin', *Annals of Nutrition and Metabolism*, 50, pp. 108–114.

Cambon, E. *et al.* (2014) 'Essential role of amino acid position 226 in oligosaccharide elongation by amylosucrase from Neisseria polysaccharea', *Biotechnology and Bioengineering*. Toulouse, France: Wiley Periodicals, Inc, 111(9), pp. 1719–1728. doi: 10.1002/bit.25236.

Campos, C. (2012) 'Chronic hyperglycemia and glucose toxicity: Pathology and clinical sequelae', *Postgraduate Medicine*, 124(6), pp. 90–97. doi: 10.3810/pgm.2012.11.2615.

Van Can, J. G. P. *et al.* (2012) 'Reduced glycaemic and insulinaemic responses following trehalose and isomaltulose ingestion: Implications for postprandial substrate use in impaired glucose-tolerant subjects', *British Journal of Nutrition*, 108(7), pp. 1210–1217. doi: 10.1017/S0007114511006714.

Ceriello, A. *et al.* (2004) 'Postprandial glucose regulation and diabetic complications', *Archives of Internal Medicine*. Udine, Italy, 164(19), pp. 2090–2095. doi: 164/19/2090 [pii].

Chaen, H. *et al.* (2001) 'Enzymatic synthesis of kojioligosaccharides using kojibiose phosphorylase', *Journal of Bioscience and Bioengineering*, 92, pp. 177–182.

Claverie, M. *et al.* (2017) 'Investigations on the determinants responsible for low molar mass dextran formation by DSR-M dextransucrase', *ACS Catalysis*, 7(10), pp. 7106–7119. doi: 10.1021/acscatal.7b02182.
CODEX Alimentarius Commission for International Food Standards (2017) 'General standard for food additive', in, pp. 192–1995.
Colleoni, C. *et al.* (1999) 'Genetic and biochemical evidence for the involvement of alpha-1,4 glucanotransferases in amylopectin synthesis', *Plant Physiology*, 120(4), pp. 993–1004.
Commission, F. C. A. and Programme, F. F. S. (2003) *Codex alimentarius. Food hygiene, basic texts*. 3rd edn. Rome: Food and Agriculture Organization of the United Nations : World Health Organization. Available at: http://www.fao.org/DOCREP/005/Y1579E/Y1579E00.htm.
Côté, G. L. and Robyt, J. F. (1982) 'Isolation and partial characterization of an extracellular glucansucrase from Leuconostoc mesenteroides NRRL B-1355 that synthesizes an alternating (1→6), (1→3)-α-d-glucan', *Carbohydrate Research*. Ames, Iowa, 101(1), pp. 57–74. doi: 10.1016/S0008-6215(00)80795-8.
Côté, G. L. and Sheng, S. (2006) 'Penta-, hexa-, and heptasaccharide acceptor products of alternansucrase', *Carbohydrate Research*, 341(12), pp. 2066–2072. doi: 10.1016/j.carres.2006.04.044.
Coutinho, P. M. (no date) Glycoside Hydrolase Family 15, CAZypedia.
Dahlqvist, A. (1961) 'The location of carbohydrases in the digestive tract of the pig.', *The Biochemical journal*, 78, pp. 282–288. doi: 10.1042/bj0780282.
Dahlqvist, A. (1963) 'Rat-intestinal dextranase. Localization and relation to the other carbohydrases of the digestive tract.', *The Biochemical journal*, 86(1), pp. 72–76. doi: 10.1042/bj0860072.
Deremaux, L., Petitjean, C. and Wills, D. (2007) 'Soluble, highly branched glucose polymers for enteral and parenteral nutrition and for peritoneal dialysis. PAT NO US 8445460 B2'. United States.
Dobruchowska, J. M. *et al.* (2013) 'Gluco-oligomers initially formed by the reuteransucrase enzyme of Lactobacillus reuteri 121 incubated with sucrose and malto-oligosaccharides', *Glycobiology*. Groningen, The Netherlands, 23(9), pp. 1084–1096. doi: 10.1093/glycob/cwt048.
Du, X. L. *et al.* (2000) 'Hyperglycemia-induced mitochondrial superoxide overproduction activates the hexosamine pathway and induces plasminogen activator inhibitor-1 expression by increasing Sp1 glycosylation', *Proceedings of the National Academy of Sciences of the United States of America*. Albert Einstein College of Medicine, Diabetes Research Center, Bronx, NY 10461, USA., 97(22), pp. 12222–12226. doi: 10.1073/pnas.97.22.12222.
EFSA (2005) 'Opinion of the Scientific Panel on Dietetic products, nutrition and allergies [NDA] on a request from the Commission related to the Tolerable Upper Intake Level of Chloride', *EFSA Journal*, 3(6), pp. 1–21. doi: 10.2903/j.efsa.2005.210.
Ekhart, P. *et al.* (2006) 'Branched alpha-glucans for weight management. PAT NO US 20060100171 A1'.
Englyst, H. N., Kingman, S. M. and Cummings, J. H. (1992) 'Classification and measurement of nutritionally important starch fractions', *European Journal of Clinical Nutrition*. MRC Dunn Clinical Nutrition Centre, Cambridge, UK., 46(SUPPL. 2), pp. S33-50. doi: 10.1016/S0271-5317(97)00010-9.

Fabre, E. *et al.* (2005) 'Role of the two catalytic domains of DSR-E dextransucrase and their involvement in the formation of highly alpha-1,2 branched dextran', *Journal of Bacteriology*. Toulouse, France, 187(1), pp. 296–303. doi: 187/1/296 [pii].
Falconer, D. J., Mukerjea, R. and Robyt, J. F. (2011) 'Biosynthesis of dextrans with different molecular weights by selecting the concentration of Leuconostoc mesenteroides B-512FMC dextransucrase, the sucrose concentration, and the temperature', *Carbohydrate Research*, 346(2), pp. 280–284. doi: 10.1016/j.carres.2010.10.024.
Feng, L. *et al.* (2015) 'Crystal Structures of Escherichia coli Branching Enzyme in Complex with Linear Oligosaccharides', *Biochemistry*. East Lansing, Michigan, 54(40), pp. 6207–6218. doi: 10.1021/acs.biochem.5b00228.
Ferreira, L. M. *et al.* (2015) 'Pullulan: An advantageous natural polysaccharide excipient to formulate tablets of alendronate-loaded microparticles', *Brazilian Journal of Pharmaceutical Sciences*, 51(1), pp. 27–34. doi: 10.1590/S1984-82502015000100003.
Gangoiti, J. *et al.* (2016) 'The Gram-negative bacterium Azotobacter chroococcum NCIMB 8003 employs a new glycoside hydrolase family 70 4,6-α-glucanotransferase enzyme (GtfD) to synthesize a reuteran like polymer from maltodextrins and starch', *Biochimica et Biophysica Acta - General Subjects*. Elsevier B.V., 1860(6), pp. 1224–1236. doi: 10.1016/j.bbagen.2016.02.005.
Gangoiti, J., Van Leeuwen, S. S., Gerwig, G. J., *et al.* (2017) '4,3-α-Glucanotransferase, a novel reaction specificity in glycoside hydrolase family 70 and clan GH-H', *Scientific Reports*, 7, p. 39761. doi: 10.1038/srep39761.
Gangoiti, J., Lamothe, L., *et al.* (2017) 'Characterization of the Paenibacillus beijingensis DSM 24997 GtfD and its glucan polymer products representing a new Glycoside Hydrolase 70 subfamily of 4,6-Î±-glucanotransferase enzymes', *Plos One*, 12, p. e0172622.
Gangoiti, J., Van Leeuwen, S. S., Meng, X., *et al.* (2017) 'Mining novel starch-converting Glycoside Hydrolase 70 enzymes from the Nestlé Culture Collection genome database: The Lactobacillus reuteri NCC 2613 GtfB', *Scientific Reports*, 7(1). doi: 10.1038/s41598-017-07190-z.
Gangoiti, J., Pijning, T. and Dijkhuizen, L. (2016) 'The Exiguobacterium sibiricum 255-15 GtfC enzyme represents a novel glycoside hydrolase 70 subfamily of 4,6-α-glucanotransferase enzymes', *Applied and Environmental Microbiology*. Groningen, The Netherlands: American Society for Microbiology, 82(2), pp. 756–766. doi: 10.1128/AEM.03420-15.
Gentilcore, D. *et al.* (2011) 'The oligosaccharide α-cyclodextrin has modest effects to slow gastric emptying and modify the glycaemic response to sucrose in healthy older adults', *British Journal of Nutrition*, 106(4), pp. 583–587. doi: 10.1017/S0007114511000444.
GmbH, E. T. (2017) Product fibermalt syrup. Certificate of analysis. Potsdam, Germany.
Goffin, D. *et al.* (2011) 'Will isomalto-oligosaccharides, a well-established functional food in Asia, break through the European and American market? The status of knowledge on these prebiotics', *Critical Reviews in Food Science and Nutrition*, 51(5), pp. 394–409. doi: 10.1080/10408391003628955.
Grimaud, F. *et al.* (2013) 'In vitro synthesis of hyperbranched α-glucans using a biomimetic enzymatic toolbox', *Biomacromolecules*, 14(2), pp. 438–447. doi: 10.1021/bm301676c.
Grysman, A., Carlson, T. and Wolever, T. M. S. (2008) 'Effects of sucromalt on postprandial responses in human subjects', *European Journal of Clinical Nutrition*, 62(12), pp. 1364–1371. doi: 10.1038/sj.ejcn.1602890.

Gu, Q. *et al.* (2003) 'Study on the regulative effect of isomaltooligosaccharides on human intestinal flora', *Wei sheng yan jiu = Journal of hygiene research*, 32(1), pp. 54–55.
Guérin, F. *et al.* (2012) 'Structural investigation of the thermostability and product specificity of amylosucrase from the bacterium Deinococcus geothermalis', *Journal of Biological Chemistry*. Toulouse, France, 287(9), pp. 6642–6654. doi: 10.1074/jbc.M111.322917.
Han, R. *et al.* (2014) 'Recent advances in discovery, heterologous expression, and molecular engineering of cyclodextrin glycosyltransferase for versatile applications', *Biotechnology Advances*. Wuxi 214122, China: Elsevier Inc, 32(2), pp. 415–428. doi: 10.1016/j.biotechadv.2013.12.004.
Hanada, N. and Kuramitsu, H. K. (1989) 'Isolation and characterization of the Streptococcus mutans gtfD gene, coding for primer-dependent soluble glucan synthesis', *Infection and Immunity*. Chicago, Illinois, USA, 57(7), pp. 2079–2085. doi: 10.1128/iai.57.7.2079-2085.1989.
Hanefeld, M. *et al.* (1996) 'Risk factors for myocardial infarction and death in newly detected NIDDM: the Diabetes Intervention Study, 11-year follow-up', *Diabetologia*, 39(12), pp. 1577–1583. doi: 10.1007/s001250050617.
Hanefeld, M. and Schaper, F. (2007) 'The role of alpha-glucosidase inhibitors (Acarbose)', in Mogensen, C. E. (ed.) *Pharmacotherapy of Diabetes: New Developments: Improving Life and Prognosis for Diabetic Patients*. Boston, MA: Springer US, pp. 143–152. doi: 10.1007/978-0-387-69737-6_13.
Hansen, M. R. *et al.* (2008) 'Gel texture and chain structure of amylomaltase-modified starches compared to gelatin', *Food Hydrocolloids*, 22(8), pp. 1551–1566. doi: 10.1016/j.foodhyd.2007.10.010.
Hasek, L. Y. *et al.* (2018) 'Dietary Slowly Digestible Starch Triggers the Gut–Brain Axis in Obese Rats with Accompanied Reduced Food Intake', *Molecular Nutrition and Food Research*. Germany, 62(5). doi: 10.1002/mnfr.201700117.
Hasselwander, O. *et al.* (2017) 'Development of dietary soluble fibres by enzymatic synthesis and assessment of their digestibility in in vitro, animal and randomised clinical trial models', *International Journal of Food Sciences and Nutrition*, 68(7), pp. 849–864. doi: 10.1080/09637486.2017.1295027.
Hayashi, M. *et al.* (2015) 'Crystallization and crystallographic analysis of branching enzymes from Cyanothece sp. ATCC 51142', *Acta Crystallographica Section:F Structural Biology Communications*. Akita, Japan, 71, pp. 1109–1113. doi: 10.1107/S2053230X1501198X.
Hayashi, M. *et al.* (2017) 'Bound substrate in the structure of cyanobacterial branching enzyme supports a new mechanistic model', *Journal of Biological Chemistry*. Akita, Japan: by The American Society for Biochemistry and Molecular Biology, Inc, 292(13), pp. 5465–5475. doi: 10.1074/jbc.M116.755629.
Heymann, H., Breitmeier, D. and Günther, S. (1995) 'Human small intestinal sucrase-isomaltase: different binding patterns for malto- and isomaltooligosaccharides.', *Biological chemistry Hoppe-Seyler*, 376(4), pp. 249–253. Available at: https://www.scopus.com/inward/record.uri?eid=2-s2.0-0029281599&partnerID=40&md5=4e876f994bc6d6deb60aac5ed3eef7ac.
Hodoniczky, J., Morris, C. A. and Rae, A. L. (2012) 'Oral and intestinal digestion of oligosaccharides as potential sweeteners: A systematic evaluation', *Food Chemistry*, 132(4), pp. 1951–1958. doi: 10.1016/j.foodchem.2011.12.031.

Imamura, H. *et al.* (2003) 'Crystal structures of 4-α-glucanotransferase from Thermococcus litoralis and its complex with an inhibitor', *Journal of Biological Chemistry*. Tokyo 113-8657, Japan, 278(21), pp. 19378–19386. doi: 10.1074/jbc.M213134200.
Irwin, W. and Sträter, P. (1991) *Alternative Sweeteners*. New York: Marcel Dekker, Inc.
Ishikawa, A. *et al.* (2007) 'Characterization of inhibitors of postprandial hyperglycemia from the leaves of Nerium indicum', *Journal of Nutritional Science and Vitaminology*, 53(2), pp. 166–173. doi: 10.3177/jnsv.53.166.
Ito, K. *et al.* (2011) 'Crystal Structure of Glucansucrase from the Dental Caries Pathogen Streptococcus mutans', *Journal of Molecular Biology*. Shizuoka 422-8526, Japan: Elsevier Ltd, 408(2), pp. 177–186. doi: 10.1016/j.jmb.2011.02.028.
Jackson, C. A., Yudkin, J. S. and Forrest, R. D. (1992) 'A comparison of the relationships of the glucose tolerance test and the glycated haemoglobin assay with diabetic vascular disease in the community. The Islington Diabetes Survey', *Diabetes Research and Clinical Practice*. London, UK, 17(2), pp. 111–123. doi: 10.1016/0168-8227(92)90156-L.
Janeček, Š., Svensson, B. and MacGregor, E. A. (2007) 'A remote but significant sequence homology between glycoside hydrolase clan GH-H and family GH31', *FEBS Letters*. Bratislava, Slovakia, 581(7), pp. 1261–1268. doi: 10.1016/j.febslet.2007.02.036.
Jeanes, A. *et al.* (1954) 'Characterization and Classification of Dextrans from Ninety-six Strains of Bacteria1b', *Journal of the American Chemical Society*, 76(20), pp. 5041–5052. doi: 10.1021/ja01649a011.
Jeanes, A. (1975) Digestibility of Food Polysaccharides by Man: A Review, ACS Symp Ser Amer Chem Soc. doi: 10.1021/bk-1975-0015.ch022.
Jensen, M. H. *et al.* (2004) 'Crystal Structure of the Covalent Intermediate of Amylosucrase from Neisseria polysaccharea', *Biochemistry*. Structural Biology Group, Department of Medicinal Chemistry, The Danish University of Pharmaceutical Sciences, Universitetsparken 2, DK-2100 Copenhagen, Denmark., 43(11), pp. 3104–3110. doi: 10.1021/bi0357762.
Jiang, H. *et al.* (2010) 'Resistant-starch formation in high-amylose maize starch during kernel development', *Journal of Agricultural and Food Chemistry*, 58(13), pp. 8043–8047. doi: 10.1021/jf101056y.
Jiang, H. *et al.* (2014) 'Enzymatic modification of corn starch with 4-α-glucanotransferase results in increasing slow digestible and resistant starch', *International Journal of Biological Macromolecules*. Elsevier, 65(5), pp. 208–214. doi: 10.1016/j.ijbiomac.2014.01.044.
Jo, H. J. *et al.* (2015) 'Vibrio vulnificus glycogen branching enzyme preferentially transfers very short chains: N1 domain determines the chain length transferred', *FEBS Letters*. Daejeon 305-764, Republic of Korea: Federation of European Biochemical Societies. Published by Elsevier B.V, 589(10), pp. 1089–1094. doi: 10.1016/j.febslet.2015.03.011.
Joint FAO/WHO Expert Committee on Food Additives (JECFA) (1993) 'WHO Food Additives Series 32: Beta-cyclodextrin'. Available at: http://www.inchem.org/documents/jecfa/jecmono/v32je13.htm.
Joint FAO/WHO Expert Committee on Food Additives (JECFA) (1995) 'WHO Food Additives Series 35: Beta-cyclodextrin'. Available at: http://www.inchem.org/documents/jecfa/jecmono/v35je12.htm.

Joint FAO/WHO Expert Committee on Food Additives (JECFA) (1999) 'WHO Food Additives Series 42: Gamma-cyclodextrin'. Available at: http://www.inchem.org/documents/jecfa/jecmono/v042je11.htm.
Joint FAO/WHO Expert Committee on Food Additives (JECFA) (2002) 'WHO Food Additives Series 48: Alpha-cyclodextrin'. Available at: http://www.inchem.org/documents/jecfa/jecmono/v48je10.htm.
Joint FAO/WHO Expert Committee on Food Additives (JECFA) (2006) 'WHO Food Additives Series 54: Alpha-cyclodextrin'. Available at: http://www.inchem.org/documents/jecfa/jecmono/v54je01.pdf.
Kadota, K. *et al.* (2015) 'Feasibility of highly branched cyclic dextrin as an excipient matrix in dry powder inhalers', *European Journal of Pharmaceutical Sciences*, 79, pp. 79–86. doi: 10.1016/j.ejps.2015.09.006.
Kajiura, H. *et al.* (2006) 'Method of producing glycogen. PAT NO WO993532'.
Kang, H. K., Oh, J. S. and Kim, D. (2009) 'Molecular characterization and expression analysis of the glucansucrase DSRWC from Weissella cibaria synthesizing a α(1→6) glucan', *FEMS Microbiology Letters*, 292(1), pp. 33–41. doi: 10.1111/j.1574-6968.2008.01460.x.
Kawai, K., Okuda, Y. and Yamashita, K. (1985) 'Changes in Blood Glucose and Insulin after an Oral Palatinose Administration in Normal Subjects', *Endocrinologia Japonica*, 32(6), pp. 933–936. doi: 10.1507/endocrj1954.32.933.
Khan, T., Park, J. K. and Kwon, J. H. (2007) 'Functional biopolymers produced by biochemical technology considering applications in food engineering', *Korean Journal of Chemical Engineering*, 24(5), pp. 816–826. doi: 10.1007/s11814-007-0047-1.
Kim, B. K. *et al.* (2014) 'Branch chain elongation by amylosucrase: Production of waxy corn starch with a slow digestion property', *Food Chemistry*, 152, pp. 113–120. doi: 10.1016/j.foodchem.2013.11.145.
Kim, D. *et al.* (2003) 'Dextran molecular size and degree of branching as a function of sucrose concentration, pH, and temperature of reaction of Leuconostoc mesenteroides B-512FMCM dextransucrase', *Carbohydrate Research*, 338(11), pp. 1183–1189. doi: 10.1016/S0008-6215(03)00148-4.
Kobayashi, I. *et al.* (2003) 'Purification and Characterization of a New Type of α-Glucosidase from Paecilomyces lilacinus That Has Transglucosylation Activity to Produce α-1,3- and α-1,2-Linked Oligosaccharides', *Bioscience, Biotechnology and Biochemistry*, 67(1), pp. 29–35. doi: 10.1271/bbb.67.29.
Koh, D. W. *et al.* (2016) 'Efficient biocatalytic production of cyclodextrins by combined action of amylosucrase and cyclodextrin glucanotransferase', *Journal of Agricultural and Food Chemistry*. Seoul 143-747, Republic of Korea, 64(21), pp. 4371–4375. doi: 10.1021/acs.jafc.6b01080.
Kohmoto, T. *et al.* (1992) 'Metabolism of 13C-Isomaltooligosaccharides in Healthy Men', *Bioscience, Biotechnology, and Biochemistry*, 56(6), pp. 937–940. doi: 10.1271/bbb.56.937.
Konishi, Y. and Shindo, K. (1997) 'Production of Nigerose, Nigerosyl Glucose, and Nigerosyl Maltose by Acremonium sp. S4G13', *Bioscience, Biotechnology and Biochemistry*, 61(3), pp. 439–442. doi: 10.1271/bbb.61.439.
Koukiekolo, R. *et al.* (2001) 'Mechanism of porcine pancreatic α-amylase: Inhibition of amylose and maltopentaose hydrolysis by α-, β- and γ-cyclodextrins', *European Journal of Biochemistry*, 268(3), pp. 841–848. doi: 10.1046/j.1432-1327.2001.01950.x.

Kralj, S. *et al.* (2004) 'Glucan synthesis in the genus Lactobacillus: Isolation and characterization of glucansucrase genes, enzymes and glucan products from six different strains', *Microbiology*. AA Haren, The Netherlands., 150(11), pp. 3681–3690. doi: 10.1099/mic.0.27321-0.

Kralj, S. *et al.* (2005) 'Highly hydrolytic reuteransucrase from probiotic Lactobacillus reuteri strain ATCC 55730', *Applied and Environmental Microbiology*. Centre for Carbohydrate Bioengineering, TNO-University of Groningen, P.O. Box 14, 9750 AA Haren, The Netherlands., 71(7), pp. 3942–3950. doi: 10.1128/AEM.71.7.3942-3950.2005.

Kralj, S. *et al.* (2011) '4,6-α-Glucanotransferase, a Novel Enzyme That Structurally and Functionally Provides an Evolutionary Link Between Glycoside Hydrolase Enzyme Families 13 and 70', *Applied and Environmental Microbiology*, 77(22), pp. 8154–8163. doi: 10.1128/AEM.05735-11.

Larson, S. B., Day, J. S. and McPherson, A. (2010) 'X-ray crystallographic analyses of pig pancreatic α-amylase with limit dextrin, oligosaccharide, and α-cyclodextrin', *Biochemistry*, 49(14), pp. 3101–3115. doi: 10.1021/bi902183w.

Le, Q.-T. *et al.* (2009) 'Amylolytically-resistant tapioca starch modified by combined treatment of branching enzyme and maltogenic amylase', *Carbohydrate Polymers*, 75, pp. 9–14.

Leathers, T. D., Hayman, G. T. and Cote, G. L. (1997) 'Microorganism strains that produce a high proportion of alternan to dextran', *US Patent 5702942*. United States. Available at: http://www.google.com/patents/US5702942.

Lee, B. H. *et al.* (2012) 'Modulation of starch digestion for slow glucose release through "Toggling" of activities of mucosal α-glucosidases', *Journal of Biological Chemistry*, 287(38), pp. 31929–31938. doi: 10.1074/jbc.M112.351858.

Lee, B. H. *et al.* (2013) 'Enzyme-Synthesized Highly Branched Maltodextrins Have Slow Glucose Generation at the Mucosal α-Glucosidase Level and Are Slowly Digestible In Vivo', *PLoS ONE*, 8(4), p. e59745. doi: 10.1371/journal.pone.0059745.

Lee, B. H. *et al.* (2014) 'Mucosal C-terminal maltase-glucoamylase hydrolyzes large size starch digestion products that may contribute to rapid postprandial glucose generation', *Molecular Nutrition and Food Research*, 58(5), pp. 1111–1121. doi: 10.1002/mnfr.201300599.

Lee, B. H. *et al.* (2016) 'Contribution of the Individual Small Intestinal α-Glucosidases to Digestion of Unusual α-Linked Glycemic Disaccharides', *Journal of Agricultural and Food Chemistry*, 64(33), pp. 6487–6494. doi: 10.1021/acs.jafc.6b01816.

Lee, H. S. *et al.* (2002) 'Cooperative action of α-glucanotransferase and maltogenic amylase for an improved process of isomaltooligosaccharide (IMO) production', *Journal of Agricultural and Food Chemistry*. Samyang Genex Biotech Research Institute, 63-2 Hwaam-Dong, Yusung-Gu, Taejeon 305-348, Korea., 50(10), pp. 2812–2817. doi: 10.1021/jf011529y.

Lee, S. -J *et al.* (1995) 'Production and Characterization of Branched Oligosaccharides from Liquefied Starch by the Action of B. Licheniformis Amylase', *Starch - Stärke*, 47(4), pp. 127–134. doi: 10.1002/star.19950470403.

Leemhuis, H., Dijkman, W. P., *et al.* (2013) '4,6-α-Glucanotransferase activity occurs more widespread in Lactobacillus strains and constitutes a separate GH70 subfamily', *Applied Microbiology and Biotechnology*. Groningen, The Netherlands., 97(1), pp. 181–193. doi: 10.1007/s00253-012-3943-1.

Leemhuis, H., Pijning, T., *et al.* (2013) 'Glucansucrases: Three-dimensional structures, reactions, mechanism, α-glucan analysis and their implications in biotechnology and food applications', *Journal of Biotechnology*. Groningen, The Netherlands: Elsevier B.V, 163(2), pp. 250–272. doi: 10.1016/j.jbiotec.2012.06.037.

Leemhuis, H. *et al.* (2014) 'Isomalto/malto-polysaccharide, a novel soluble dietary fiber made via enzymatic conversion of starch', *Journal of Agricultural and Food Chemistry*. Groningen, The Netherlands: American Chemical Society, 62(49), pp. 12034–12044. doi: 10.1021/jf503970a.

Leemhuis, H., Kelly, R. M. and Dijkhuizen, L. (2010) 'Engineering of cyclodextrin glucanotransferases and the impact for biotechnological applications', *Applied Microbiology and Biotechnology*. Haren, The Netherlands, 85(4), pp. 823–835. doi: 10.1007/s00253-009-2221-3 [doi].

van Leeuwen, S. S. *et al.* (2008a) 'Structural analysis of the α-d-glucan (EPS180) produced by the Lactobacillus reuteri strain 180 glucansucrase GTF180 enzyme', *Carbohydrate Research*. Utrecht, The Netherlands, 343(7), pp. 1237–1250. doi: 10.1016/j.carres.2008.01.042.

van Leeuwen, S. S. *et al.* (2008b) 'Structural analysis of the α-d-glucan (EPS180) produced by the Lactobacillus reuteri strain 180 glucansucrase GTF180 enzyme', *Carbohydrate Research*. Utrecht, The Netherlands, 343(7), pp. 1237–1250. doi: 10.1016/j.carres.2008.01.042.

Lehman, U. and Robin, F. (2007) 'Slowly digestible starch - its structure and health implications: a review', *Trends in Food Science and Technology*, 18, pp. 346–355.

Light, S. H. *et al.* (2017) 'Transferase Versus Hydrolase: The Role of Conformational Flexibility in Reaction Specificity', *Structure*. Chicago, IL, USA: Elsevier Ltd, 25(2), pp. 295–304. doi: 10.1016/j.str.2016.12.007.

Lin, A. H. M. *et al.* (2012) 'Unexpected high digestion rate of cooked starch by the Ct-maltase-glucoamylase small intestine mucosal α-glucosidase subunit', *PLoS ONE*, 7(5). doi: 10.1371/journal.pone.0035473.

Lin, A. H. M., Lee, B. H. and Chang, W. J. (2016) 'Small intestine mucosal α-glucosidase: A missing feature of in vitro starch digestibility', *Food Hydrocolloids*. Elsevier, 53, pp. 163–171. doi: 10.1016/j.foodhyd.2015.03.002.

Liu, C. *et al.* (2015) 'Comparative analysis of 1-deoxynojirimycin contribution degree to α-glucosidase inhibitory activity and physiological distribution in Morus alba L', *Industrial Crops and Products*, 70, pp. 309–315. doi: 10.1016/j.indcrop.2015.02.046.

Liu, Y. *et al.* (2017) 'Met349 Mutations Enhance the Activity of 1,4-α-Glucan Branching Enzyme from Geobacillus thermoglucosidans STB02', *Journal of Agricultural and Food Chemistry*, 65(28), pp. 5674–5680. doi: 10.1021/acs.jafc.7b01227.

López-Munguía, A. *et al.* (1993) 'Production and purification of alternansucrase, a glucosyltransferase from Leuconostoc mesenteroides NRRL B-1355, for the synthesis of oligoalternans', *Enzyme and Microbial Technology*, 15(1), pp. 77–85. doi: 10.1016/0141-0229(93)90120-Q.

Van Der Maarel, M. J. E. C. *et al.* (2002) 'Properties and applications of starch-converting enzymes of the α-amylase family', *Journal of Biotechnology*, pp. 137–155. doi: 10.1016/S0168-1656(01)00407-2.

Van Der Maarel, M. J. E. C. *et al.* (2005) 'A novel thermoreversible gelling product made by enzymatic modification of starch', *Starch/Staerke*, 57(10), pp. 465–472. doi: 10.1002/star.200500409.
Van Der Maarel, M. J. E. C. and Leemhuis, H. (2013) 'Starch modification with microbial alpha-glucanotransferase enzymes', *Carbohydrate Polymers*. Veendam, The Netherlands: Elsevier Ltd, 93(1), pp. 116–121. doi: 10.1016/j.carbpol.2012.01.065.
MacGregor, E. A., Jespersen, H. M. and Svensson, B. (1996) 'A circularly permuted α-amylase-type α/β-barrel structure in glucan-synthesizing glucosyltransferases', *FEBS Letters*. Winnipeg, Canada, 378(3), pp. 263–266. doi: 10.1016/0014-5793(95)01428-4.
Madsen, L. R. *et al.* (2017) 'A Survey of Commercially Available Isomaltooligosaccharide-Based Food Ingredients', *Journal of Food Science*, 82(2), pp. 401–408. doi: 10.1111/1750-3841.13623.
Maina, N. H. *et al.* (2011) 'Structural analysis of enzyme-resistant isomaltooligosaccharides reveals the elongation of α-(1→3)-linked branches in weissella confusa dextran', *Biomacromolecules*, 12(2), pp. 409–418. doi: 10.1021/bm1011536.
Martin, A. E. and Montgomery, P. A. (1996) 'Acarbose: an alpha-glucosidase inhibitor', *American Journal of Health-System Pharmacy*, 53(19), pp. 2277–2290.
Meigs, J. B. *et al.* (2002) 'Fasting and postchallenge glycemia and cardiovascular disease risk: The framingham offspring study', *Diabetes Care*, 25(10), pp. 1845–1850. doi: 10.2337/diacare.25.10.1845.
Meng, X., Pijning, T., *et al.* (2015) 'Characterization of the functional roles of amino acid residues in acceptor-binding subsite +1 in the active site of the glucansucrase GTF180 from lactobacillus reuteri 180', *Journal of Biological Chemistry*. Groningen, The Netherlands: The American Society for Biochemistry and Molecular Biology, Inc, 290(50), pp. 30131–30141. doi: 10.1074/jbc.M115.687558.
Meng, X., Dobruchowska, J. M., *et al.* (2015) 'Synthesis of oligo- and polysaccharides by Lactobacillus reuteri 121 reuteransucrase at high concentrations of sucrose', *Carbohydrate Research*. Groningen, The Netherlands: Elsevier Ltd, 414, pp. 85–92. doi: 10.1016/j.carres.2015.07.011.
Meng, X., Pijning, T., *et al.* (2016) 'Structural determinants of alternating (α1→4) and (α1→6) linkage specificity in reuteransucrase of Lactobacillus reuteri', *Scientific Reports*. Nature Publishing Group, 6(1), p. 35261. doi: 10.1038/srep35261.
Meng, X., Gangoiti, J., *et al.* (2016) 'Structure–function relationships of family GH70 glucansucrase and 4,6-α-glucanotransferase enzymes, and their evolutionary relationships with family GH13 enzymes', *Cellular and Molecular Life Sciences*. Groningen, The Netherlands, 73(14), pp. 2681–2706. doi: 10.1007/s00018-016-2245-7.
Meng, X., Dobruchowska, J. M., *et al.* (2016) 'Synthesis of New Hyperbranched α-Glucans from Sucrose by Lactobacillus reuteri 180 Glucansucrase Mutants', *Journal of Agricultural and Food Chemistry*. Groningen, The Netherlands, 64(2), pp. 433–442. doi: 10.1021/acs.jafc.5b05161.
Mirza, O. *et al.* (2001) 'Crystal structures of amylosucrase from Neisseria polysaccharea in complex with D-glucose and the active site mutant Glu328Gln in complex with the natural substrate sucrose', *Biochemistry*, 40(30), pp. 9032–9039. doi: 10.1021/bi010706l.
Mitchell, H., Auerbach, M. H. and Moppet, F. K. (2001) 'Polydextrose', in Nabors, L. O. (ed.) *Alternative Sweetners*. Third. New York: Marcel Dekker, pp. 499–518.

Monchois, V. *et al.* (1997) 'Characterization of Leuconostoc mesenteroides NRRL B-512F dextransucrase (DSRS) and identification of amino-acid residues playing a key role in enzyme activity', *Applied Microbiology and Biotechnology*. Toulouse, France, 48(4), pp. 465–472. doi: 10.1007/s002530051081.

Monchois, V., Willemot, R.-M. and Monsan, P. (1999) 'Glucansucrases: mechanism of action and structure–function relationships', *FEMS Microbiology Reviews*. Toulouse, France, 23(2), pp. 131–151. doi: 10.1111/j.1574-6976.1999.tb00394.x.

Monnier, L. *et al.* (2006) 'Activation of oxidative stress by acute glucose fluctuations compared with sustained chronic hyperglycemia in patients with type 2 diabetes', *Journal of the American Medical Association*, 295(14), pp. 1681–1687. doi: 10.1001/jama.295.14.1681.

Monsan, P., Remaud-Siméon, M. and André, I. (2010) 'Transglucosidases as efficient tools for oligosaccharide and glucoconjugate synthesis', *Current Opinion in Microbiology*. Toulouse, France: Elsevier Ltd, 13(3), pp. 293–300. doi: 10.1016/j.mib.2010.03.002.

Moulis, C., André, I. and Remaud-Simeon, M. (2016) 'GH13 amylosucrases and GH70 branching sucrases, atypical enzymes in their respective families', *Cellular and Molecular Life Sciences*. Toulouse, France, 73(14), pp. 2661–2679. doi: 10.1007/s00018-016-2244-8.

Mountzouris, K. C., Gilmour, S. G. and Rastall, R. A. (2002) 'Continuous production of oligodextrans via controlled hydrolysis of dextran in an enzyme membrane reactor', *Journal of Food Science*, 67(5), pp. 1767–1771. doi: 10.1111/j.1365-2621.2002.tb08720.x.

Na, S. *et al.* (2017) 'Structural basis for the transglycosylase activity of a GH57-type glycogen branching enzyme from Pyrococcus horikoshii', *Biochemical and Biophysical Research Communications*. Seoul, Republic of Korea: Elsevier Inc, 484(4), pp. 850–856. doi: 10.1016/j.bbrc.2017.02.002.

Naessens, M. *et al.* (2005) 'Dextran dextrinase and dextran of Gluconobacter oxydans', *Journal of Industrial Microbiology and Biotechnology*. Ghent, Belgium, 32(8), pp. 323–334. doi: 10.1007/s10295-005-0259-5.

Nguyen, T. T. H. *et al.* (2012) 'Inhibitory effects of epigallocatechin gallate and its glucoside on the human intestinal maltase inhibition', *Biotechnology and Bioprocess Engineering*, 17(5), pp. 966–971. doi: 10.1007/s12257-012-0242-8.

Nichols, B. L. L. et al. (2003) The maltase-glucoamylase gene: Common ancestry to sucrase-isomaltase with complementary starch digestion activities, Proceedings of the National Academy of Sciences. National Academy of Sciences. doi: 10.1073/pnas.0237170100.

Nishikawa, T. *et al.* (2000) 'Normalizing mitochondrial superoxide production blocks three pathways of hyperglycaemic damage', *Nature*. Macmillian Magazines Ltd, 404(6779), pp. 787–790. Available at: http://dx.doi.org/10.1038/35008121.

Niu, D. *et al.* (2017) 'Highly efficient enzymatic preparation of isomalto-oligosaccharides from starch using an enzyme cocktail', *Electronic Journal of Biotechnology*, 26, pp. 46–51. doi: 10.1016/S0924-2244(97)01090-X.

Norman, B. *et al.* (2007) 'Production of crystalline short chain amylase. PAT NO US2007059432'.

Nugent, A. P. (2005) 'Health properties of resistant starch', *Nutrition Bulletin*, 30, pp. 27–54.

Oates, C. G. (1997) 'Towards an understanding of starch granule structure and hydrolysis', *Trends in Food Science and Technology*, 8(11), pp. 375–382. doi: 10.1016/S0924-2244(97)01090-X.

Office of Food Additive Safety (HFS-200) Center for Food Safety and Applied Nutrition (CFSAN) Food and Drug Administration (FDA) (2010) 'GRAS Notice 000358: Cyclic Dextrin, Highly Branched'.

Ohkuma, K. and Wakabayashi, S. (2000) 'Fibersol-2: A soluble, non-digestible, starch-derived dietary fibre', in *Advanced Dietary Fibre Technology*. Blackwell Science Ltd., pp. 509–523.

Pal, K. *et al.* (2010) 'Crystal structure of full-length Mycobacterium tuberculosis H37Rv glycogen branching enzyme: Insights of N-terminal β-sandwich in substrate specificity and enzymatic activity', *Journal of Biological Chemistry*, 285(27), pp. 20897–20903. doi: 10.1111/febs.13261.

Palomo, M. *et al.* (2009) 'The unique branching patterns of Deinococcus glycogen branching enzymes are determined by their N-terminal domains', *Applied and Environmental Microbiology*. Haren, The Netherlands, 75(5), pp. 1355–1362. doi: 10.1128/AEM.02141-08 [doi].

Palomo, M. *et al.* (2011) 'Thermus thermophilus Glycoside Hydrolase Family 57 Branching Enzyme', *Journal of Biological Chemistry*. Haren, The Netherlands, 286(5), pp. 3520–3530. doi: 10.1074/jbc.m110.179515.

Panasevich, M. R. *et al.* (2015) 'Evaluation of soluble corn fiber on chemical composition and nitrogen-corrected true metabolizable energy and its effects on in vitro fermentation and in vivo responses in dogs', *Journal of Animal Science*, 93(5), pp. 2191–2200. doi: 10.2527/jas.2014-8425.

Park, J. K. and Khan, T. (2009) 'Other microbial polysaccharides: Pullulan, scleroglucan, elsinan, levan, alternant, dextran', in Phillips, G. O. and Williams, P. A. B. T.-H. of H. (Second E. (eds) *Handbook of Hydrocolloids: Second Edition*. Woodhead Publishing, pp. 592–614. doi: 10.1533/9781845695873.592.

Passerini, D. *et al.* (2015) 'Inventory of the GH70 enzymes encoded by Leuconostoc citreum NRRL B-1299 - Identification of three novel α-transglucosylases', *FEBS Journal*, 282(11), pp. 2115–2130. doi: 10.1111/febs.13261.

Paul, Francois, B. *et al.* (1992) 'Method for the production of alpha-1,2 oligodextrans using Leuconostoc mesenteroides NRRL B-1299 PAT NO US 5141858 A'. US.

Pelzer, S. *et al.* (2012) 'Microorganisms having enhanced sucrose mutase activity PAT NO US 8790900 B2'.

Peters, S., Rose, T. and Moser, M. (2010) 'Sucrose: A prospering and sustainable organic raw material', *Topics in Current Chemistry*, 294, pp. 1–23. doi: 10.1007/128_2010_58.

Pijning, T. *et al.* (2012) 'Structure of the α-1,6/α-1,4-specific glucansucrase GTFA from lactobacillus reuteri 121', *Acta Crystallographica Section F: Structural Biology and Crystallization Communications*. Groningen, The Netherlands, 68(12), pp. 1448–1454. doi: 10.1107/S1744309112044168.

Playne, M. J. and Crittenden, R. G. (2004) 'Prebiotics from lactose, sucrose, starch and plant polysaccharides', in Neeser, J.-R. and German, J. B. (eds) *Bioprocesses and biotechnology for functional foods and nutraceuticals*. New York: Marcel Dekker.

Plijter, J. *et al.* (2009) 'Bread improver. US 20090297663 A1'.

Potocki-Veronese, G. *et al.* (2005) 'Amylose synthesized in vitro by amylosucrase: morphology, structure, and properties', *Biomacromolecules*. Toulouse, France, 6(2), pp. 1000–1011. doi: 10.1021/bm049326g [doi].

Programme, J. F. F. S. (2010) *Report of the 31st Session of the CODEX Committee on Nutrition and Foods for Special Dietary Uses*. CODEX committee on Nutrition and Foods for Special Dietary Uses. Available at: http://www.codexalimentarius.net/web/archives.jsp?lang=en.

Przylas, I. *et al.* (2000) 'X-ray structure of acarbose bound to amylomaltase from Thermus aquaticus: Implications for the synthesis of large cyclic glucans', *European Journal of Biochemistry*. Institut fur Chemie-Kristallographie, Freie Universitat Berlin, Germany., 267(23), pp. 6903–6913. doi: 10.1046/j.1432-1327.2000.01790.x.

Putaala, H. (2013) 'Polydextrose in Lipid Metabolism', *Lipid Metabolism*. doi: 10.5772/51791.

Quezada-Calvillo, R. *et al.* (2007) 'Luminal substrate "brake" on mucosal maltase-glucoamylase activity regulates total rate of starch digestion to glucose', *Journal of Pediatric Gastroenterology and Nutrition*, pp. 32–43. doi: 10.1097/MPG.0b013e31804216fc.

Quezada-Calvillo, R. *et al.* (2008) 'Luminal Starch Substrate "Brake" on Maltase-Glucoamylase Activity Is Located within the Glucoamylase Subunit', *The Journal of Nutrition*, 138(4), pp. 685–692. doi: 10.1093/jn/138.4.685.

Remaud-Slmeon, M. *et al.* (1994) 'Production and use of glucosyltransferases from Leuconostoc mesenteroides NRRL B-1299 for the synthesis of oligosaccharides containing α-(1→2) linkages', *Applied Biochemistry and Biotechnology*, 44(2), pp. 101–117. doi: 10.1007/BF02921648.

Rennhard, H. H. (1975) 'Polysaccharides and their preparation PAT NO US3766165'. Available at: https://www.google.com/patents/US3766165.

Robyt, J. F., Yoon, S. H. and Mukerjea, R. (2008) 'Dextransucrase and the mechanism for dextran biosynthesis', *Carbohydrate Research*. Ames, IA, USA, 343(18), pp. 3039–3048. doi: 10.1016/j.carres.2008.09.012.

Rolland-Sabaté, A. *et al.* (2004) 'Elongation and insolubilisation of α-glucans by the action of Neisseria polysaccharea amylosucrase', *Journal of Cereal Science*, 40(1), pp. 17–30. doi: 10.1016/j.jcs.2004.04.001.

Röper, H. and Koch, H. (1988) 'New Carbohydrate Derivatives from Biotechnical and Chemical Processes', *Starch - Stärke*. WILEY-VCH Verlag GmbH, 40(12), pp. 453–464. doi: 10.1002/star.19880401203.

Roth, C. *et al.* (2017) 'Amylose recognition and ring-size determination of amylomaltase', *Science Advances*. Leipzig, Germany, 3(1), p. e1601386. doi: 10.1126/sciadv.1601386.

Roujeinikova, A. *et al.* (2001) 'The crystal structure of Thermotoga maritima maltosyltransferase and its implications for the molecular basis of the novel transfer specificity', *Journal of Molecular Biology*. Sheffield, England: Academic Press, 312(1), pp. 119–131. doi: 10.1006/jmbi.2001.4944 [doi].

Roujeinikova, A. *et al.* (2002) 'Crystal structure of Thermotoga maritima 4-α-glucanotransferase and its acarbose complex: Implications for substrate specificity and catalysis', *Journal of Molecular Biology*. Sheffield, England, UK, 321(1), pp. 149–162. doi: 10.1016/S0022-2836(02)00570-3.

Roussel, X. *et al.* (2013) 'Characterization of substrate and product specificity of the purified recombinant glycogen branching enzyme of Rhodothermus obamensis', *Biochimica et Biophysica Acta - General Subjects*. Villeneuve d'Ascq, France: Elsevier B.V, 1830(1), pp. 2167–2177. doi: 10.1016/j.bbagen.2012.09.022.

Rycroft, C. E. *et al.* (2001) 'A comparative in vitro evaluation of the fermentation properties of prebiotic oligosaccharides', *Journal of Applied Microbiology*, 91(5), pp. 878–887. doi: 10.1046/j.1365-2672.2001.01446.x.

Sadahiro, J. *et al.* (2015) 'Extracellular and cell-associated forms of Gluconobacter oxydans dextran dextrinase change their localization depending on the cell growth', *Biochemical and biophysical research communications*, 456, pp. 500–505. doi: 10.1016/j.bbrc.2014.11.115.
Sawada, T. *et al.* (2014) 'Diversity of reaction characteristics of glucan branching enzymes and the fine structure of α-glucan from various sources', *Archives of Biochemistry and Biophysics*, 562, pp. 9–21. doi: 10.1016/j.abb.2014.07.032.
Schneider, J. *et al.* (2009) 'Generation of amylosucrase variants that terminate catalysis of acceptor elongation at the di- or trisaccharide stage', *Appl Environ Microbiol.*, 75(23), pp. 7453–7460. doi: 10.1128/AEM.01194-09.
Scientific Committee on Food (2000) 'Opinion of the Scientific Committee on Food on a dextran preparation, produced using Leuconostoc Mesenteroides, Saccharomyces Cerevisiae and Lactobacillus Spp as a noval food ingredient in bakery products', *Scientific Opinions*. Brussels, Belgium. Available at: http://europa.eu.int/comm/food/fs/sc/scf/index_en.html.
Shin, H. J. *et al.* (2010) 'Preparation of starches with low glycaemic response using amylosucrase and their physicochemical properties', *Carbohydrate Polymers*, 82(2), pp. 489–497. doi: 10.1016/j.carbpol.2010.05.017.
Shinohara, M. L. *et al.* (2001) 'A novel thermostable branching enzyme from an extremely thermophilic bacterial species, Rhodothermus obamensis', *Applied Microbiology and Biotechnology*. Novozymes Japan Ltd, Makuhari Techno Garden, Chiba-shi, Japan., 57(5–6), pp. 653–659. doi: 10.1007/s00253-001-0841-3.
Siddiqua, I. R. and Furhala, B. (1967) 'Isolation and characterization of oligosaccharides from honey. Part I Disaccharides.', *Journal of Apicultural Research*, 6, pp. 139–145.
Sim, L. *et al.* (2010) 'Structural basis for substrate selectivity in human maltase-glucoamylase and sucrase-isomaltase N-terminal domains', *Journal of Biological Chemistry*. Bethesda, MD, U.S.A: American Society for Biochemistry and Molecular Biology, 285(23), pp. 17763–17770. doi: 10.1074/jbc.M109.078980.
Simsek, M. *et al.* (2015) 'Dietary phenolic compounds selectively inhibit the individual subunits of maltase-glucoamylase and sucrase-isomaltase with the potential of modulating glucose release', *Journal of Agricultural and Food Chemistry*, 63(15), p. 3873. doi: 10.1021/jf505425d.
Skov, L. K. *et al.* (2013) 'The structure of amylosucrase from Deinococcus radiodurans has an unusual open active-site topology', *Acta Crystallographica Section F: Structural Biology and Crystallization Communications*. Bagsvaerd, Denmark, 69(9), pp. 973–978. doi: 10.1107/S1744309113021714.
Sr. Simpson, S. T. (2011) 'Printing Ink Base Material'.
Srisuvor, N. *et al.* (2013) 'Effects of inulin and polydextrose on physicochemical and sensory properties of low-fat set yoghurt with probiotic-cultured banana purée', *LWT - Food Science and Technology*, 51(1), pp. 30–36. doi: 10.1016/j.lwt.2012.10.018.
Su, D. and Robyt, J. F. (1993) 'Control of the synthesis of dextran and acceptor-products by Leuconostoc mesenteroides B-512FM dextransucrase', *Carbohydrate Research*, 248(C), pp. 339–348. doi: 10.1016/0008-6215(93)84139-W.
Suzuki, E. and Suzuki, R. (2016) 'Distribution of glucan-branching enzymes among prokaryotes', *Cellular and Molecular Life Sciences*. Akita, Japan, 73(14), pp. 2643–2660. doi: 10.1007/s00018-016-2243-9.
Takata, H. *et al.* (1996) 'Structure of the cyclic glucan produced from amylopectin by Bacillus stearothermophilus branching enzyme', *Carbohydrate research*, 295, pp. 91–101.

Takata, H. *et al.* (2003) 'Properties of branching enzyme from hyperthermophilic bacterium, Aquifex aeolicus, and its potential for production of highly-branched cyclic dextrin', *Journal of Applied Glycoscience*, 50, pp. 15–20.
Takazoe, I. (1985) 'New trends on sweeteners in Japan', *International Dentistry Journal*, 35, pp. 58–65.
Takii, H. *et al.* (1999) 'Enhancement of swimming endurance in mice by highly branched cyclic dextrin', *Bioscience Biotechnology and Biochemistry*, 63, pp. 2045–2052.
Terada, Y. *et al.* (1999) 'Thermus aquaticus ATCC 33923 amylomaltase gene cloning and expression and enzyme characterization: Production of cycloamylose', *Applied and Environmental Microbiology*, 65(3), pp. 910–915. doi: 10.1128/aem.65.3.910-915.1999.
Thiemann, V. *et al.* (2004) 'Characterisation of a thermoalkali-stable cyclodextrin glycosyltransferase from the anaerobic thermoalkaliphilic bacterium Anaerobranca gottschalkii', *Archives of Microbiology*, 182(2–3), pp. 226–235. doi: 10.1007/s00203-004-0717-x.
Van Tieghem, P. (1878) 'On sugar-mill gum', *Annales des Sciences Naturelles. Botanique.*, 7, pp. 180–203.
Tsuji, Y. *et al.* (1986) 'Digestion and Absorption of Sugars and Sugar Substitutes in Rat Small Intestine', *Journal of Nutritional Science and Vitaminology*, 32(1), pp. 93–100. doi: 10.3177/jnsv.32.93.
Tsunehiro, J. *et al.* (1999) 'Digestibility of the Hydrogenated Derivative of an Isomaltooligosaccharide Mixture by Rats', *Bioscience, Biotechnology and Biochemistry*, 63(9), pp. 1515–1521. doi: 10.1271/bbb.63.1515.
Ueda, S., Shiroza, T. and Kuramitsu, H. K. (1988) 'Sequence analysis of the gtfC gene from Streptococcus mutans GS-5', *Gene*, 69(1), pp. 101–109. doi: 10.1016/0378-1119(88)90382-4.
Uitdehaag, J. C. *et al.* (1999) 'X-ray structures along the reaction pathway of cyclodextrin glycosyltransferase elucidate catalysis in the alpha-amylase family', *Nature structural biology*. Groningen, The Netherlands, 6(5), pp. 432–436. doi: 10.1038/8235 [doi].
Uitdehaag, J. C. M. *et al.* (2000) 'Structures of maltohexaose and maltoheptaose bound at the donor sites of cyclodextrin glycosyltransferase give insight into the mechanisms of transglycosylation activity and cyclodextrin size specificity', *Biochemistry*. Groningen, The Netherlands, 39(26), pp. 7772–7780. doi: 10.1021/bi000340x.
Valette, P. *et al.* (1993) 'Bioavailability of new synthesised glucooligosaccharides in the intestinal tract of gnotobiotic rats', *Journal of the Science of Food and Agriculture*, 62(2), pp. 121–127. doi: 10.1002/jsfa.2740620204.
Valk, V. *et al.* (2015) 'Degradation of granular starch by the bacterium Microbacterium aurum strain B8.A involves a modular α-amylase enzyme system with FNIII and CBM25 domains', *Applied and Environmental Microbiology*, 81(19), pp. 6610–6620. doi: 10.1128/AEM.01029-15.
Vanschoonbeek, K. *et al.* (2009) 'Slowly digestible carbohydrate sources can be used to attenuate the postprandial glycemic response to the ingestion of diabetes-specific enteral formulas', *Diabetes Educator*. SAGE Publications, USA, 35(4), pp. 631–640. doi: 10.1177/0145721709335466.

Van Der Veen, B. A. *et al.* (2000) 'The three transglycosylation reactions catalyzed by cyclodextrin glycosyltransferase from Bacillus circulans (strain 251) proceed via different kinetic mechanisms', *European Journal of Biochemistry*, 267(3), pp. 658–665. doi: 10.1046/j.1432-1327.2000.01031.x.

Voragen, A. G. J. (1998) 'Technological aspects of functional food-related carbohydrates', *Trends in Food Science and Technology*, 9(8–9), pp. 328–335. doi: 10.1016/S0924-2244(98)00059-4.

Vuillemin, M. *et al.* (2016) 'Characterization of the first α-(1→3) branching sucrases of the GH70 family', *Journal of Biological Chemistry*. Toulouse, France: The American Society for Biochemistry and Molecular Biology, 291(14), pp. 7687–7702. doi: 10.1074/jbc.M115.688044.

Vujicic-Zagar, A. *et al.* (2010) 'Crystal structure of a 117 kDa glucansucrase fragment provides insight into evolution and product specificity of GH70 enzymes', *Proceedings of the National Academy of Sciences*. Groningen, The Netherlands, 107(50), pp. 21406–21411. doi: 10.1073/pnas.1007531107.

Wallander, M. *et al.* (2005) 'Beta cell dysfunction in patients with acute myocardial infarction but without previously known type 2 diabetes: A report from the GAMI study', *Diabetologia*. Berlin, Germany, 48(11), pp. 2229–2235. doi: 10.1007/s00125-005-1931-z.

Wattebled, F. *et al.* (2003) 'STA11, a Chlamydomonas reinhardtii locus required for normal starch granule biogenesis, encodes disproportionating enzyme. Further evidence for a function of α-1,4 glucanotransferases during starch granule biosynthesis in green algae', *Plant Physiology*, 132(1), pp. 137–145. doi: 10.1104/pp.102.016527.

Welkie, D. G., Lee, B. H. and Sherman, L. A. (2016) 'Altering the structure of carbohydrate storage granules in the cyanobacterium Synechocystis sp. strain PCC 6803 through branching-enzyme truncations', *Journal of Bacteriology*. American Society for Microbiology, 198(4), pp. 701–710. doi: 10.1128/JB.00830-15.

Wolf, B., Chow, J. and Lai, C.-S. (2006) 'Method for using gamma-cyclodextrin to control bood glucose and insulin secretion PAT NO WO 2009/004574A2'.

Wolf, B. W. *et al.* (2003) 'Pullulan Is a Slowly Digested Carbohydrate in Humans', *The Journal of Nutrition*, 133(4), pp. 1051–1055. doi: 10.1093/jn/133.4.1051.

Yamamoto, K., Yoshikawa, K. and Okada, S. (1993) 'Structure of dextran synthesized by dextrin dextranase from acetobacter capsulatus atcc 11894', *Bioscience, Biotechnology and Biochemistry*, 57(9), pp. 1450–1453. doi: 10.1271/bbb.57.1450.

Yamamoto, T. *et al.* (2004) 'Purification and characterization of Acremonium implicatum α-glucosidase having regioselectivity for α-1,3-glucosidic linkage', *Biochimica et Biophysica Acta - Proteins and Proteomics*, 1700(2), pp. 189–198. doi: 10.1016/j.bbapap.2004.05.002.

Yasuda, E., Takaku, H. and Matsumoto, H. (1986) 'Production of branched oligosaccharide syrup'. Japan: Japanese Patent. doi: 10.1017/CBO9781107415324.004.

Yoo, S. H. *et al.* (1995) 'Branched Oligosaccharides Concentrated by Yeast Fermentation and Effectiveness as a Low Sweetness Humectant', *Journal of Food Science*, 60(3), pp. 516–521. doi: 10.1111/j.1365-2621.1995.tb09816.x.

Yun, J. W., Lee, M. G. and Song, S. K. (1994) 'Continuous production of isomalto-oligosaccharides from maltose syrup by immobilized cells of permeabilized Aureobasidium pullulans', *Biotechnology Letters*, 16(11), pp. 1145–1150. doi: 10.1007/BF01020841.

Zhang, G., Ao, Z. and Hamaker, B. R. (2006) 'Slow digestion property of native cereal starches', *Biomacromolecules*, 7(11), pp. 3252–3258. doi: 10.1021/bm060342i.

Zhang, G., Ao, Z. and Hamaker, B. R. (2008) 'Nutritional property of endosperm starches from maize mutants: A parabolic relationship between slowly digestible starch and amylopectin fine structure', *Journal of Agricultural and Food Chemistry*. Jiangsu Province, PR China, 56(12), pp. 4686–4694. doi: 10.1021/jf072822m.

Zhang, G. and Hamaker, B. R. (2009) 'Slowly digestible starch: Concept, mechanism, and proposed extended glycemic index', *Critical Reviews in Food Science and Nutrition*. Taylor & Francis, 49(10), pp. 852–867. doi: 10.1080/10408390903372466.

α-Cyclodextrin C36H60O30 (no date) ChemSpider. doi: CSID:392705.

β-Cyclodextrin C42H70O35 (no date) ChemSpider. doi: CSID:10469496.

γ-Cyclodextrin C48H80O40 (no date) ChemSpider. doi: CSID:10469499.

CHAPTER 3. *IN VITRO* AND CLINICAL ASSESSMENT OF α-GLUCAN LINKAGES NECESSARY FOR SLOW DIGESTION AND REDUCED POSTPRANDIAL GLYCEMIC RESPONSE

3.1 Abstract

Postprandial hyperglycemia is associated with increased oxidative stress and the development of diabetes, heart disease, and other vascular damage. Slowly digestible carbohydrates (SDCs) are beneficial by providing moderated glucose response. A potentially valuable source of SDCs are α-glucans with unusual linkages and patterns that digest slowly. The current study assessed the effect of digestion of commercial and novel α-glucans on postprandial glycemia and, through *in vitro* comparisons, determined linkage types and patterns associated with SDCs. *In vitro* studies examined the rate of hydrolysis of α-glucans of varied linkage types (isomaltooligosaccharides, alternanoligosaccharides, raw wheat starch, resistant dextrin, dextran, reuteran, and alternan). Maltose and DE-40 syrup were used as controls. GC-MS and SEC were used to analyze changes in linkages and molecular size during *in vitro* digestion. α-Glucans showed a range of high to low postprandial glycemic responses. Of the different α-glucan linkages present, slowly digestible linkages were α-1,6, 1,3, and 3,6; and quickly digestible linkage types were α-1,4 and 4,6. While no α-glucans were indigestible, molecular size also was a factor affecting digestibility with the large alternan polymer with α-1,6 and 1,3 linkages being essentially indigestible. The *in vitro* digestibility assay that was optimized in the study was well correlated with *in vivo* data and may be a useful guide in SDC product development. α-Glucan 1,6 linkages were generally slowly digestible, and even more so when alternating with 1,3 or 1,4 linkages. Size matters in that alternanoligosaccharides with the same linkage patterns as alternan were more rapidly digestible, though still slowly. Notably, α-1,3 linkages digested in a slow way especially when alternating with other linkage types.

3.2 Introduction

Carbohydrates play a major role in human nutrition, supplying close to half of all calories, and facilitating numerous metabolic functions. The rate of carbohydrate release from foods, often referred to as glycemic index or response, is of nutritional and physiological importance due to its

potential to control or prevent hyperglycemia-related diseases, such as diabetes and cardiovascular disease (Frost *et al.*, 1999; Liu *et al.*, 2000; Rizkalla *et al.*, 2004; G. *et al.*, 2008). Glycemic response is dictated by changes in blood glucose in response to consumption and digestion and absorption of carbohydrates, as well as insulin response to those carbohydrates and the body's sensitivity to that insulin. Accordingly, starches as the major dietary carbohydrate can be categorized as rapidly digestible starch (RDS), slowly digestible starch (SDS), and resistant starch (RS) *in vitro* using the Englyst assay (Englyst and Englyst, 2005). Similarly, glycemic carbohydrates can be referred to as rapidly digestible carbohydrates (RDC) and slowly digestible carbohydrates (SDC). Slow digesting carbohydrate properties relate to structural properties of the food matrix, presence and manner of plant cell walls, nature of starch granules, structural aspects of starch molecules, and linkage types and combinations of non-starch α-glucans (Englyst, Kingman and Cummings, 1992; Englyst and Englyst, 2005). This article will focus on the latter linkage structures of digestible carbohydrates, and how they affect rate of digestion through measurements of human postprandial glycemia and *in vitro* of glucose hydrolysis.

Peripheral blood glucose is commonly used as the measure for glycemic response and rate of digestibility of carbohydrates. However, glycemic response does not always reflect well carbohydrate rate of hydrolysis and glucose absorption from the small intestine. For instance, lower quantities of peripheral glucose are measured if there is increased clearance due to elevated circulating insulin levels remaining from a previous bolus. The best example of this effect is with dietary protein (Westphal, Gannon and Nuttall, 1990), but other factors may also stimulate insulinemic response. Alternatively, C^{13}-labelled carbohydrates has been used to measure total and exogenous glucose kinetics, which measures total digested and absorbed carbohydrate, and is therefore a good indicator of slowly digested carbohydrates without being affected by variable inulin response (Bier *et al.*, 1977; Tissot *et al.*, 1990; Nazare *et al.*, 2010). Still, overall, blood glucose levels as a measure of glycemic response are useful in assessing dietary carbohydrate digestion and absorption, particularly when previous meals are controlled.

In addition to the important role of moderating postprandial glycemia, slowly digested carbohydrates have been linked to reduced intake and increased satiety through gut-brain axis targeting and second-meal effect, which presents the potential for SDCs to act as diet-aid for obese individuals. Hasek et al. in 2017 demonstrated that obese rats fed SDC's in a high fat diet (HF-SDC) reduced their intake to match the lean control group, whereas intake of an obese group on

high fat-RDC (HF-RDC) maintained a high intake. This observed decreased intake with SDC paralleled reduced mRNA expression levels of the hypothalamic orexigenic neuropeptide Y (NPY) and Agouti-related peptide (AgRP), whereas the anorexigenic corticotropin-releasing hormone (CRH) was increased, compared to the HF-RDC. The HF-SDC group responded similarly to the lean control group. They did not observe weight loss, likely because the treatment diets were high fat, and because decreased daily food intake in the HF-SDC group did not occur until later in the treatment phase (Hasek *et al.*, 2018). SDC intake has been linked not only to decreased intake due to increased satiety, but also to reduced body weight. A number of clinical studies have shown that low-glycemic index diets were associated with significant weight loss, (Spieth *et al.*, 2000; Ball *et al.*, 2003; Yoshinaga *et al.*, 2004; Olds *et al.*, 2010; Ogden *et al.*, 2014). These studies focused particularly on adolescents, as the rate of pediatric obesity continues to rise; this points to foods targeted at children as a good starting point for introduction of novel SDC to consumers (Spieth *et al.*, 2000; Esfahani *et al.*, 2011).

In the literature, rate of hydrolysis has been correlated with starch structure, linkage type and pattern, as well as molecular size. Zhang et al. showed that the structure in raw native cereal starch has a SDC (or slowly digestible starch, SDS) property, based on its semi-crystalline A-type structure, as well as a high proportion of short A chains with DP 5-10 (Zhang, Ao and Hamaker, 2006; Zhang, Venkatachalam and Hamaker, 2006). The SDC properties of raw starch granules are destroyed when they are gelatinized. High degree of branching density, and short terminal nonreducing ends, as well as longer chain length, lead to slow digestion properties (Ao *et al.*, 2007; Zhang, Ao and Hamaker, 2008). Some starch-protein and starch-lipid complexes also have slow digestion properties. It has been shown by Backer et al. that when amylopectin is enzymatically modified to have high proportions of α-1,6 linkages, that the resulting soluble, highly-branched glucose polymers have SDC properties (Backer and Saniez, 2004). Lee et al. enzymatically modified waxy corn starch to increase α-1,6 branching ratio and shortened amylopectin external chains, and showed that the resulting polymers had decreased rate of hydrolysis *in vitro* by human pancreatic α-amylase, as well as by individual recombinant mammalian α-glucosidases; glucogenesis decreased as branching ratio increased (Lee *et al.*, 2013). Lee et al. (Lee *et al.*, 2012) also found that glucogenesis of ctMGAM (maltase subunit) was competitively inhibited by the presence of sucrose (α-1,2), as well as confirmed that a high degree of branching and high-proportion of α-limit dextrins slowed glucogenesis (Lee and Hamaker, 2012). β-glucans, on the

other hand, are completely indigestible linkage types by mammals. There are some dietary carbohydrates that have both unusual α-linkage combinations, and are partially or fully digestible, such as processed or synthesized molecules like resistant maltodextrins (e.g. Promitor® 70 soluble corn fiber, Tate & Lyle, London, UK) and others in this article.

Larger molecular size can also contribute to slower glycose hydrolysis. Longer glucan chain length, whether due to recrystallization during retrogradation, enzymatic modification, or naturally occurrence, may be inversely related to digestibility by native enzymes (Eerlingen, Deceuninck and Delcour, 1993; Eerlingen and Delcour, 1995).

The digestion of carbohydrates in the human body by native enzymes occurs beginning in the mouth, and then continues through the terminal end of the small intestine. There are six digestive enzymes for starch in the human body: salivary and pancreatic α-amylases and four mucosal α-glucosidases. Only the mucosal α-glucosidases provide the final hydrolytic activities on various α-glucan linkages [1,4; 1,6; 1,2; 1,3; and others (33)] to produce substantial free glucose. These enzymes were the target for the *in vitro* assay protocol used in the current study (Quezada-Calvillo *et al.*, 2008; Shin *et al.*, 2019; Seo *et al.*, 2020). Most in vitro digestibility assays were developed using a-amylase and fungal amyloglucosidases, however it is not until recently that the differences in hydrolysis of glucans between fungal amyloglucosidases and mammalian α-glucosidases has come to light. Lin et al. (2012) showed that the small intestinal mucosal α-glucosidases have unique downstream digestion processes and proposed that Ct-MGAM subunit had the highest digestive capacity when hydrolyzing gelatinized starches (Lin *et al.*, 2012). Lee et al. (Lee *et al.*, 2016) showed that Nt-MGAM (or maltase) has the highly hydrolysis activity on unusual a-linkages (i.e. a-1,3 and 1,2 linkages).

In the current experiments, mammalian enzymes were used in a modified *in vitro* assay (Lee *et al.*, 2016) to obtain similar relative digestion patterns to a clinical study on various α-glucans differing in digestion rates, and to analyze digestion of different linkage types and changes in molecular sizes over time. This analysis was conducted to elucidate how a-glucans with different a-linkage types are broken down by α-glucosidases, and in turn will help form the basis of structural characteristics that contribute to slow digesting carbohydrates.

3.3 Subjects and materials

3.3.1 Materials

An initial *in vitro* digestion screening was performed on the following carbohydrates:

α-4,3 glucan, amylose (1,3 and 1,4 branched polymer from amylose fermented with *L. fermentum* GtfB) (Gangoiti, Van Leeuwen, Gerwig, *et al.*, 2017),

Alternan (Evoxx Technologies GmBH, Germany),

Alternanoligosaccharides (Fibermalt™, Evoxx Technologies GmBH, Germany),

Highly branched (HB) maltodextrin from waxy (WX) corn starch (Purdue University, West Lafayette, IN, USA) (Lee *et al.*, 2013),

Highly branched cyclic dextrin (Cluster Dextrin™ Ezaki Glico Co., Ltd., Osaka, Japan),

Isomaltooligosaccharides (Vitafiber™, BioNeutra Inc., Canada),

Isothrive metosyl-isomaltooligosaccharides (Isothrive, Manassas, VA, USA),

LF 2970 GtfB NCC wheat starch (wheat starch fermented with *L. Fermentum* 2970 GtfB University of Groningen, Groningen, Netherlands)(Gangoiti, Van Leeuwen, Gerwig, *et al.*, 2017),

LR121 GtfB -> LR2613 GtfB wheat (wheat starch fermented with *L. reuteri* 121 GtfB and subsequently *L. reuteri* 2613 GtfB, University of Groningen, Groningen, Netherlands)(Gangoiti *et al.*, 2016; Gangoiti, Lamothe, *et al.*, 2017; Gangoiti, Van Leeuwen, Meng, *et al.*, 2017),

LR121 GtfB wheat (wheat starch modified by *L. reuteri* 121 GtfB to produce isomalto/malto-polysaccharides, University of Groningen, Groningen, Netherlands) (Gangoiti *et al.*, 2016; Gangoiti, Lamothe, *et al.*, 2017; Gangoiti, Van Leeuwen, Meng, *et al.*, 2017),

LR121 IMMP *L. reuteri* 121 isomalto/malto-polysaccharides, Nestlé Nutrition Research Center, Lausanne, Switzerland),

LR121Gtf sucrose NRC (reuteran fermented from sucrose with *L. reuteri* 121 GtfA, Nestlé Nutrition Research Center, Lausanne, Switzerland),

LR121Gtf sucrose RUG (reuteran fermented from sucrose with *L. reuteri* 121 GtfA, University of Groningen, Groningen, Netherlands)(Gangoiti, Van Leeuwen, Gerwig, *et al.*, 2017),

LR180 Gtf180 dextran NRC (dextran fermented from sucrose with *L. reuteri* 180 Gtf180, Nestlé Nutrition Research Center, Lausanne, Switzerland)(Van Geel-Schutten *et al.*, 1999; Pijning *et al.*, 2008),

LR180 Gtf180, sucrose (Dextran fermented from sucrose with *L. reuteri* 180 Gtf180, University of Groningen, Groningen, Netherlands) (Van Geel-Schutten *et al.*, 1999; Pijning *et al.*, 2008),

LR2613 GtfB NCC amylose (reuteran produced from amylose fermented with *L. reuteri* 2613 GtfB, Nestlé Nutrition Research Center, Lausanne, Switzerland) (Gangoiti *et al.*, 2016; Gangoiti, Lamothe, *et al.*, 2017; Gangoiti, Van Leeuwen, Meng, *et al.*, 2017),

LR2613 GtfB NCC wheat (reuteran produced from wheat starch fermented with *L. reuteri* 2613 GtfB, Nestlé Nutrition Research Center, Lausanne, Switzerland) (Gangoiti *et al.*, 2016; Gangoiti, Lamothe, *et al.*, 2017; Gangoiti, Van Leeuwen, Meng, *et al.*, 2017),

Maltodextrin (Star-Dri 1, Tate & Lyle, London, UK),

Mutan (Mutan fermented from sucrose with *L. reuteri* GtfML Nestlé Nutrition Research Center, Lausanne, Switzerland),

Polydextrose (Litesse®, Danisco, Copenhagen, Denmark),

Raw and gelatinized wheat starch (Starch, Sigma Aldrich, St Louis, MO, USA),

Resistant maltodextrin 1 (Promitor™ 70 Soluble Corn Fiber, Tate & Lyle, London, UK),

Resistant maltodextrin 2 (Fibersol®-2, Matsutani Chemical Industry Co, Ltd, Hyogo, Japan),

Wheat dextrin (Nutriose® FB 06, Roquette, Lestrem, France),

α-Cyclodextrin (ACROS Organics™, Thermo Fisher Scientific, Waltham, MA),

β-Cyclodextrin (ACROS Organics™, Thermo Fisher Scientific, Waltham, MA),

γ-Cyclodextrin (ACROS Organics™, Thermo Fisher Scientific, Waltham, MA)

For the optimized *in vitro* digestion assay and clinical trial, as well as the remaining studies in this chapter, the following substrates were used (Table 4): Glucose DE40 syrup (DE40 syrup) (Roquette Fréres), Raw Wheat Starch (Sigma Aldrich, St Louis, MO, USA), isomaltooligosaccharides (Vitafiber™, BioNeutra Inc., Canada), alternanoligosaccharides (Fibermalt™, Evoxx Technologies GmBH, Germany), alternan (Evoxx Technologies GmBH, Germany), dextran (Pharmacosmos, Denmark), and reuteran produced enzymatically from sucrose (Nestlé Nutrition Research Center, Lausanne, Switzerland).

3.4 Methods

In vitro assays to determine rate of glucogenesis from α-glucan molecules were used to compare rate of digestion amongst the novel carbohydrates presented here. Substrates, 29 in total, were screened in an initial *in vitro* comparative assay, prior to selecting 7 α-glucans, as well as maltose and DE-40 syrup controls, for a clinical trial and further *in vitro* testing.

3.4.1 In vitro Assay for Initial Screening α-Glucans

Work from Shin et al determined a suspension of enzyme sources to have higher isomaltase and sucrase activity than supernatant alone (Shin *et al.*, 2019), and therefore necessitated a modification in a previously used assay to include suspended particles of rat intestinal acetone powder (RIAP) in the assay. Additionally, a suspension of RIAP produced increased glucose generation compared to solution retained after filtering through 100 kDa molecular weight cut off (MWCO) centrifugal filter units. This variation between suspension of whole RIAP versus solution retained after filtering could have been attributed to removal of pancreatic α-amylases, which is 45 kDa (Danielsson, 1947), as well as glucose-utilizing microorganisms for which 37°C is a favorable environment. The suspension was supplemented with 0.005% w/v ampicillin salts to inhibit growth of microorganisms in the solution (Seo *et al.*, 2018). The addition of ampicillin consequently eliminated the loss of glucose during hydrolysis of different carbohydrates after 6 h. It was also determined that across containers of RIAP powder there was varying enzyme activity. To mediate this, all containers of RIAP were pooled and thoroughly blended during the grinding stage and used as one batch of enzyme for all experiments.

Sodium phosphate buffer (100 mM) at pH 6.9, with 0.02% w/v sodium azide was prepared for all assays. RIAP (Sigma Aldrich) was stored at -20°C. A suspension of 10% w/v RIAP in buffer was made and held at 4°C for 60 min, and then centrifuged at 10,000 RPM at 4°C for 10 min. Supernatant from RIAP suspension was filtered through a 100 kDa MWCO filter membrane centrifuge tube at 4,000 G at 4°C for 30 min. Equal parts by volume of concentrated supernatant from membrane centrifuge tube and 1% w/v α-amylase from porcine pancreas suspension in buffer were combined and stored at 4°C for no more than 3 h.

One part of 1% w/v substrate solutions made with above buffer were combined with eight parts buffer, and pre-incubated while mixing for 10 min at 37°C and 600 RPM (Eppendorf

ThermoMixer® C, Eppendorf). One part above-described combined enzyme solution was added after pre-incubation. RIAP-substrate solutions were incubated at 37℃; aliquots were transferred to separate microtubes for inactivation in boiling water for 3 min at 15, 30, 60, and 120 min. Inactivated aliquots were held at 4℃ until reading. The amount of released glucose was analyzed by the glucose oxidase/peroxidase (GOPOD) reagent method (Vasanthan, 2005) using a microplate spectrophotometer (SpectraMax 190 Absorbance Microplate Reader). Digestion assays were performed in triplicate on three separate occasions (replicates), resulting in a total of nine data points from each α-glucan at each timepoint. Absorbance detected from sequential dilutions of glucose were used to create a linear equation to convert UV-Vis spectrophotometer absorbance readings to μg/ml glucose. Raw wheat starch was used for positive control of slow digesting properties in each assay.

3.4.2 Clinical evaluation of glycemic response of α-glucan substrates

Subjects

Inclusion criteria: Subjects were healthy males and females aged 18 to 45 years with a BMI between 18.5 and 29.9 kg/m2.

Exclusion criteria: Subjects were excluded if they suffered from any known metabolic disease or chronic drug intake (aspirin, vitamin C and mineral supplements, steroids, protease inhibitors, antidepressants, anxiolytic, or antipsychotics) possibly impacting (to the opinion of the medical doctor) the digestion or absorption of nutrients or the postprandial glucose and insulin response. Furthermore, subjects who had undergone major medical/surgical event requiring hospitalization within 3 months of the study, any known food allergy or intolerance, medically diagnosed cutaneous hypersensitivity to adhesives and plasters, an alcohol intake higher than 2 servings per day (1 serving = 400 mL of strong alcohols, 100 mL of red or white wine, or 300 mL of beer), smokers or any subject who could not be expected or in unwilling to comply with the protocol were also excluded.

Test products

Eight α-glucans differing in degree of polymerization and glycosidic linkage patterns were tested in this study. Maltodextrin was included within the 8 α-glucans as a positive control with a 100% digestibility.

Twenty-five g of the test products was provided to the study participants in powder forms. The powder was dissolved in 300 ml of water and consumed orally. Each product was consumed on the morning of the test visits under the fasting conditions, after a 24 h washout period. Participants were asked to be under fasting conditions starting between 19:30-20:00 hr. the evening before the test visits to maintain 12 h fasting. The 8 α-glucans with varied sources and differences in their glycosidic linkages described in Table 4 were tested.

Study design

Eligible participants were tested on separate days (after 24 h washout period) and were randomly assigned to consume a 25 g dose (total carbohydrates) of the corresponding test products mixed in 300 mL of water, including maltodextrin as a rapidly-fully digestible carbohydrate and raw wheat starch as a slowly digestible carbohydrate. The primary outcome of the study was to evaluate the postprandial glucose in the interstitial tissue of 8 α-glucan carbohydrates differing in polymer structure. The subcutaneous interstitial glucose level was obtained with a flash glucose monitoring (FGM) device (Freestyle Libre® by Abbott). The study also included secondary outcomes that consisted of: evaluating if any of the α-glucan carbohydrates tested resulted in any incidence of gut discomfort experienced by the volunteers during the trial, and visual analogue scale (VAS) hunger scoring results.

Study visits

One day before the first testing visit, participants were provided with the FGM reader and the corresponding instructions and a sensor was installed on the external side of the non-dominant arm. On each subsequent testing visit, subjects arrived at the clinic after an overnight fasting. Initial readings for glucose concentration in interstitial tissue from the FGM device were taken before and after (T=0) consumption of the test product. After the 2 readings, interstitial tissue glucose level was continuously and automatically measured every 15 min (T=15, 30, 60, 75, 90, 105, 120) for a 2 h period. A VAS was used to measure any incidence of gut discomfort during each visit.

Between each testing visit, subjects were required to continue with readings from the 24 h FGM device every 6-8 h to ensure continuous recording of interstitial glucose.

3.4.3 Optimized *in vitro* assay of 9 α-glucans

The *in vitro* digestion assay was performed as described by te Poele and Corwin, et al in 2020 (Te Poele *et al.*, 2020). Pure 0.01% α-glucans in water (without enzyme) were used for the 0 min timepoint. Digestion assays were performed in triplicate three separate times, resulting in a total of nine data points from each α-glucan at each timepoint (15, 30, 45 min, and 1, 2, 3, 6, 24 h) ; outliers more than two standard deviations from the mean were excluded. Linear dilutions of glucose fit to a linear equation were used to convert glucose UV-Vis readings from absorbance to µg/ml. Glucose DE40 and maltose were used as rapidly digesting controls, and raw wheat starch was used as a positive control of slowly digesting property in each assay.

3.4.4 Structural analysis of pure substrates after *in vitro* digestion

Sample preparation: Protein precipitation out of digested substrates

Two samples closest to the mean from each timepoint (15, 30, 60 min; 6 and 24 h) were chosen, based on GOPOD readings adjusted against a standard curve. At each timepoint, 600 µl of supernatant from inactivated and centrifuged digested substrates was used to make a 10% v/v solution in 100% ethanol. The solution was incubated at 25℃ for 30 min and then centrifuged at 10,000 RPM for 5 min. The supernatant was discarded, 600 µL dimethyl sulfoxide (DMSO) added, and then incubated at 100℃ at 600 RPM in a shaking water bath for 60 min. DMSO-substrate solution was used to make a 10% v/v solution in 100% ethanol and incubated at 25℃ for 30 min. Post-digestion steps were repeated for a total of three DMSO boils, then the pellet was rinsed in the same volume of 100% ethanol as previously used, for a total of four ethanol-only pellet washes. The pellet was dried with nitrogen gas at 35℃ to expedite evaporation, and then suspended in purified water and aliquoted appropriately for linkage and molecular size analysis.

3.4.5 Linkage analysis

Undigested pure substrates

The partially methylated alditol acetates (PMAA) derivatization method for GC-MS was used (Pettolino *et al.*, 2012). Samples (3 mg) were dissolved in 500 µl DMSO, 200 µl n-butyl lithium were added, and tubes were incubated for 40 min. Methyl iodide (300 µl) was added and stirred for 1 h. The resulting mixtures were partitioned with deionized water and chloroform. The chloroform layer was separated and dried under a stream of nitrogen. Samples were hydrolyzed with 2M TFA for 1 h at 121 °C containing 1 mg/ml inositol as an internal standard. The samples were then dried under the stream of nitrogen. Dry samples were reduced with 100 µl of 1M ammonium hydroxide with 20 mg/ml of sodium borodeuteride in DMSO for 90 min at 40 °C. The reaction was quenched with glacial acetic acid. Samples were O-acetylated with 100 µl of 1-methylimidazole and 500 µl of acetic anhydride. The resulting partially methylated alditol acetates were partitioned with deionized water and methylene chloride. The methylene chloride layer was separated and dried under a stream of nitrogen. Samples were dissolved in 1 ml acetone and analyzed by GC-MS (GC – Agilent 7890A equipped with FID detector, MS – Agilent 5975C, column SP-2330). The area under peaks was calculated using MSDI Data Analysis software (Agilent, Santa Clara, CA).

Linkage analysis of digested α-glucan substrates

RIAP in the buffer used for the digestion protocol was inactivated without substrate and analyzed as a blank standard. Linkages were identified by comparing peak mass fragments with the known mass fragmentation in the standards library (University of Georgia Complex Carbohydrate Research Center, 2019). Variance in elution times (±0.075 min) was allowed inclusion parameters for each peak identification for blank standards and linkage type. The area under peaks was calculated using MSDI Data Analysis software (Agilent, Santa Clara, CA). Inositol was used as the internal standard to normalize data, then blank standards subtracted from normalized data. Percent of total remaining area under peaks was then used to calculate percent of each linkage type detected at each timepoint. Data shown in graphs is the mean (from duplicates) of the percent of total normalized linkages detected, adjusted by percent digestibility from the *in vitro* assay. Percent digestibility was calculated by setting the DE40 syrup at 6 h equal to 100% digested. One 60-min linkage analysis was discarded due to inconsistencies with the data from timepoints before or after. A new linkage formation was observed, likely due to transferase activity of α-glucosidase after prolonged exposure to free glucose. *In vivo,* free glucose is removed through

transmembrane transporter, and would not be available for transferase activity of these enzymes. When peaks matched elution time for known linkages compared to standards in library, but mass fragmentation analysis did not confirm presence of linkage based on University of Georgia Complex Carbohydrate Research Center GC-EIMS of Partially Methylated Alditol Acetates library (University of Georgia Complex Carbohydrate Research Center, 2019), peaks were discarded.

Data were analyzed using Microsoft Excel (Excel version 1903, 2018); Differences between least square mean at each time point were evaluated using one-way ANOVA and by Tukey/Kramer tests performed with statistical significance was considered at $P < 0.05$.

3.4.6 Molecular size analysis

Undigested pure substrates

Samples were dissolved by placing 20 mg sample in 2 ml of boiling 100% DMSO for 1 h, followed by stirring for 12 h at room temperature. Then, 12 ml of ethanol was added to precipitate the carbohydrates. The supernatant was discarded and pellet was dissolved in 1 ml of water. Samples were filtered through a 25 mm diameter 5 μm nylon syringe filter (Thermo Fisher Scientific, Waltham, MA), and injected (100 μl loop) into a HPLC equipped Agilent analytical OH-60 and OH-40 or Sephacryl® S-500HR columns with detection by refractive index and multi-angle light scattering (MALS) devices (Dawn Heleos-II multi-angle laser spectrometer and Optilab® refractive index detector, Wyatt Technology Corporation, Goleta, CA, USA). The samples were then analyzed a second time using BioRad Biogel® P2 resin to separate small molecules. Results were analyzed using Astra 5.3.4.14 software. The following standards were used to convert elution time to log molecular weight, and then to molecular weight: 180, 342, 1,320, 23,000, 48,800, 113,000, 200,000, 348,000, and 805,000 Da (PSS-Polymer-Standards Service-USA Inc, Amherst, MA, USA).

Molecular size analysis after in vitro digestion at 15, 30, 60, 360 and 1440 min

Samples were prepared using protein precipitation steps as described above. Samples were then analyzed and interpreted in the same method described above for molecular size analysis of pure substrates.

3.5 Results

3.5.1 Initial *in vitro* screening & clinical trial of seven α-glucans

Seven α-glucans (Table 4) were selected for a clinical trial from an initial *in vitro* digestibility screening of 29 commercial and novel (synthesized) α-linked glucose-containing oligo- and polysaccharides (Figure 7), showing a range of glucose hydrolysis profiles. α-Glucans not showing promise for slow-digesting properties, or not currently commercially available or able to be manufactured in a method safe for consumption, were eliminated from the clinical trial inclusion list. From the remaining substrates, α-glucans were selected with the goal of obtaining the widest range of linkage types and patterns, and molecular size. Final selected α-glucans (Table 4) were isomaltooligosaccharides, alternanoligosaccharides, raw wheat starch, resistant dextrin, dextran, reuteran, and alternan. DE40 syrup was used as a highly available glucose control.

Clinical evaluation of α-glucan substrates

Sixteen healthy volunteers (7 males and 9 females) were recruited with a mean age of 28.8±1.8 years and a mean fasting glycemia of 4.5±0.2 mmol/L, and mean BMI of 24.4±0.8. Incremental area-under-curve (iAUC) for postprandial glycemic response (PPGR) of α-glucans is presented in Figure 8. iAUC is defined as the area below the blood glucose response curve, disregarding the area beneath the fasting portion of the curve. As anticipated, the DE40 syrup had the highest glycemic response out of all

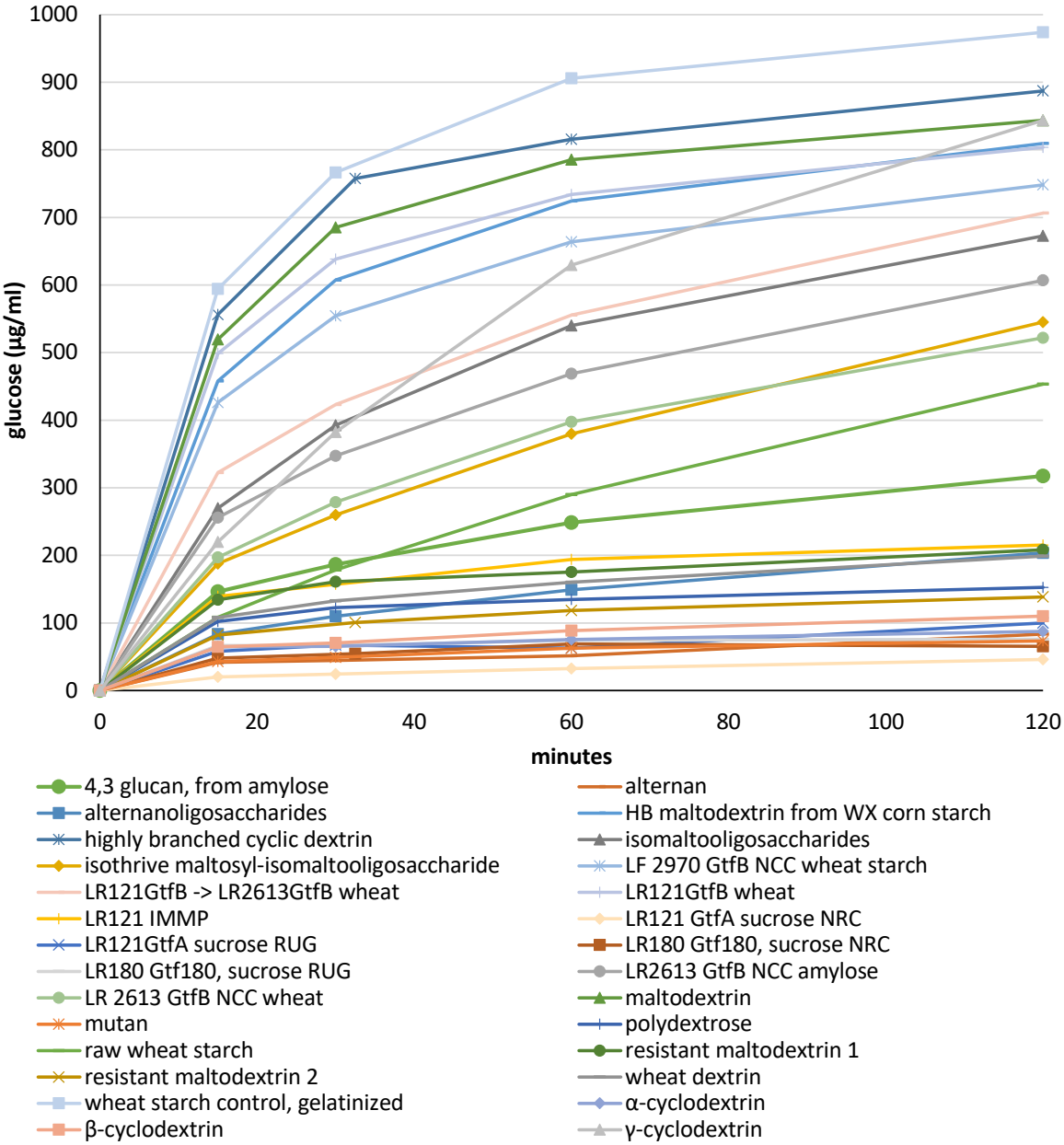

Figure 7. Original (supernatant) screening of *in vitro* digestibility of α-glucans over time.

Table 4. Description of α-glucans chosen for *in-vitro* and clinical trial.

Alternan (aevotis GmbH, Potsdam, Germany)	• Alternating α-1,3 & 1,6 glycosidic linkages
	  ○ 30% α-1,3; α-46% α-1,6; 10% α-3,6
	• 1,200,000 da: molar mass: ~40,000,000 g/mol
	• Synthesized by enzyme *alternansucrase*
	  • Raw material for bioconversion is sucrose
	• Purity depends on the dsp and can be increased up to > 99%
	• Alternan is indigestible; soluble fiber according to AOAC 2001.03

Reuteran (Kralj *et al.*, 2004)	• Alternating α-1,4 & α-1,6
	  ○ 21% α-1,6, 32% α-1,4; 2% α-3,4; 10% α-4,6
	• Synthesized using *Lactobacillus reuteri 121*
	• MW (61,100,000 Da and 380 Da)
	  • 3.0 % Tri-saccharide; 13.6% Di-saccharide; 43.7% Monosaccharide

Dextran (Van Geel-Schutten *et al.*, 1999)(Produced by CarbExplore, Groningen, Netherlands)	• Linear dextran with α-1,4,6 linkages and few α-1,3
	  ○ 83% α-1,6; 6% α-3,6; α-1,2% α-4,6; 0.2% α-1,3
	• *L reuteri 180* GTF180 dextran MW 30
	  • 100% 16,500 Da

Raw Wheat Starch (Sigma-Aldrich, St Louis, MO, USA)	• Branched α1->4 with α1->6 branching points (Sigma) ○ 2% α-1,6; 90% α-1,4; 3.2% α-4,6 • 2,100,000 Da

Isomaltooligosaccharides (Vitafiber, BioNeutra North America Inc, Edmonton, Canada)	• A1-4/α1-6 up to D12
	  ○ 29% α-1,6; 20% α-1,4; 3.6% α-4,6
	• 42 x10^6 Da MW
	  • 41.5% monosaccharide; 33.9% disaccharide; 18.3% trisaccharide

Resistant dextrin (Promitor® 70, Tate & Lyle PLC, London, UK)	• 30% α-1,4; 12% α-1,6; 10% α-4,6; 5% α-1,3 • 990 da • 7.6% glucose, 1.4% isomaltose, 2.6% maltose (12% dp 1 & 2) • Contains up to 30% other structures (Tate & Lyle, 2010)

DE40 syrup (Roquett Frères, Lestrem, France)	• Mw 590 da
	  • 12% w/w maltose
	  ○ 60% α-1,4; 32% t-glc; 4% α-4,6

Alternanoligosaccharides (EvoXX Technologies GmbH, Monheim am Rhein, Germany)	• Alternating α-1,3 & 1,6 glycosidic linkages
	  ○ 34% α-1,6; 24% α-1,3; 18% α-1,4; 11% α-3,6
	• DP range 1-20, mean DP 7
	  • 1,100 Da: 77.4% oligosaccharide (1,100 Da); 3.1% Trisaccharide; 17.5% Disaccharide; 2.0% monosaccharide

the α-glucan samples and the iAUC for isomaltooligosaccharides and alternanoligosaccharides were only 5% and 16% lower than DE40 syrup. This small decrease did not represent a significant reduction in iAUC indicating that these types of glucose-based oligosaccharides have a digestibility that is comparable to that of the DE40 syrup. On the other hand, the SDC group raw wheat starch, resistant dextrin and dextran elicited a moderately and significantly lower glycemic response, iAUC was 53%, 57% and 58%, respectively, lower that iAUC of DE40 syrup. Reuteran and alternan were the α-glucans with the lowest iAUC of all samples tested. In comparison to DE40 syrup, a 73% and 97% reduction, respectively, was observed in iAUC.

Gut discomfort

Gastrointestinal discomfort was evaluated after consumption of each α-glucan with the use of a visual analogue scale (VAS). GI symptoms, which included abdominal pain, appetite, gastric reflux, nausea, diarrhea, and headache) were scored as follows: 0 = without symptoms and 10 = maximum symptoms. No subjects reported major GI discomfort symptoms after consumption of test products (Figure 9) indicating that all α-glucans tested in the trial were well tolerated. However, a few subjects (27% of the study population) reported slight discomfort associated to abdominal pain and headache after consumption of raw wheat starch and alternan.

Postprandial glycemic profiles are presented in Figure 8. Isomaltooligosaccharides were rapidly digestible with a similar glycemic response profile as the DE40 syrup, similar to the results Gourineni et al. found when isomaltooligosaccharides was compared to a dextrose control (Gourineni *et al.*, 2018). Other α-glucans showed lower glycemic response, either with quickly decreasing profiles indicating digestible (i.e. at the beginning) and indigestible portions (i.e. to baseline and flat, indicating lack of extended glycemia) (i.e. resistant dextrin and reuteran) or with extended profiles indicating a longer slowly digestible property (i.e. dextran and wheat starch). Alternanoligosaccharides had only a slightly lower glycemic response compared to the highly digestible isomaltooligosaccharides and the DE40 syrup. Alternan, on the other hand, was almost entirely indigestible. Notably, raw wheat starch showed a significant elevated glycemic profile at 120 min, suggesting its slow digesting property as higher than the other α-glucans tested providing a sustained digestion; its postprandial glucose release showed large and significant differences in iAUC. Discomfort was elicited by some subjects, but differences between the eight carbohydrate sources were not significant (Figure 9). Interestingly, highest discomfort levels trended to alternan,

the least digestible α-glucan, and raw wheat starch which had extended digestion. Resistant dextrin, which is largely an indigestible fiber product trended to the least discomfort. Detailed questionnaire results of feeling responses after consumption of the α-glucans are presented in Table 5.

Table 5. Questionnaire results of human study, out of 100 on a visual analog scale.

	Abdominal	Appetite	Gastric Reflux	Nausea	Diarrhea	Headache	**Discomfort Total**
DE40 syrup, dried	7	0	0	0	0	7	13
Isomaltooligosaccharides	7	0	7	0	0	3	20
Alternanoligosaccharides	0	7	0	0	0	3	20
Raw wheat starch	0	3	7	3	0	7	27
Resistant dextrin	7	0	0	0	0	0	7
Dextran	7	7	0	7	0	3	13
Reuteran	7	7	0	0	7	0	20
Alternan	20	7	0	7	0	13	27

A

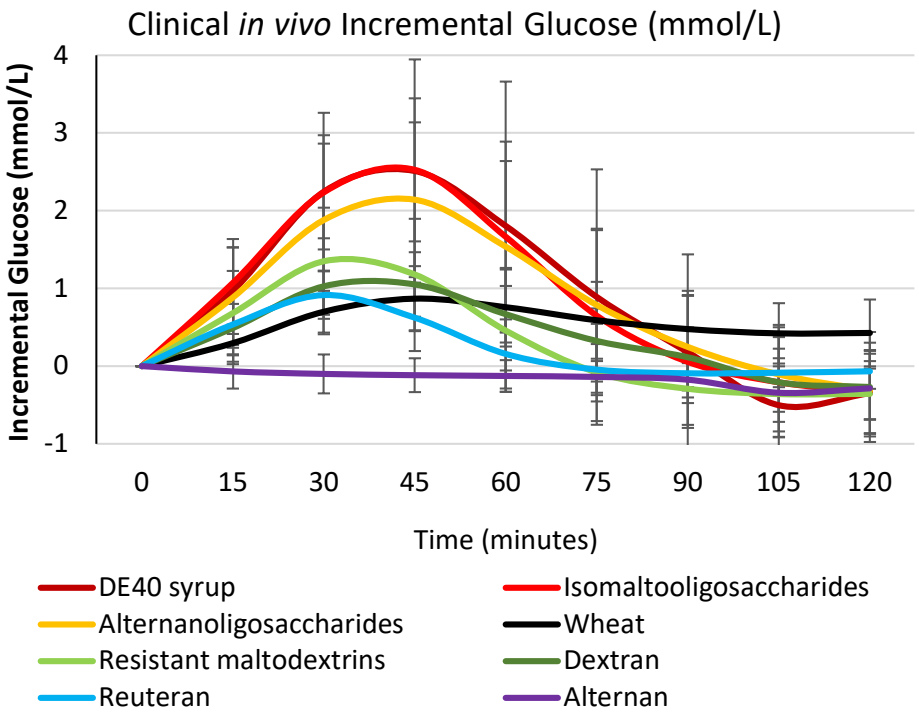

B

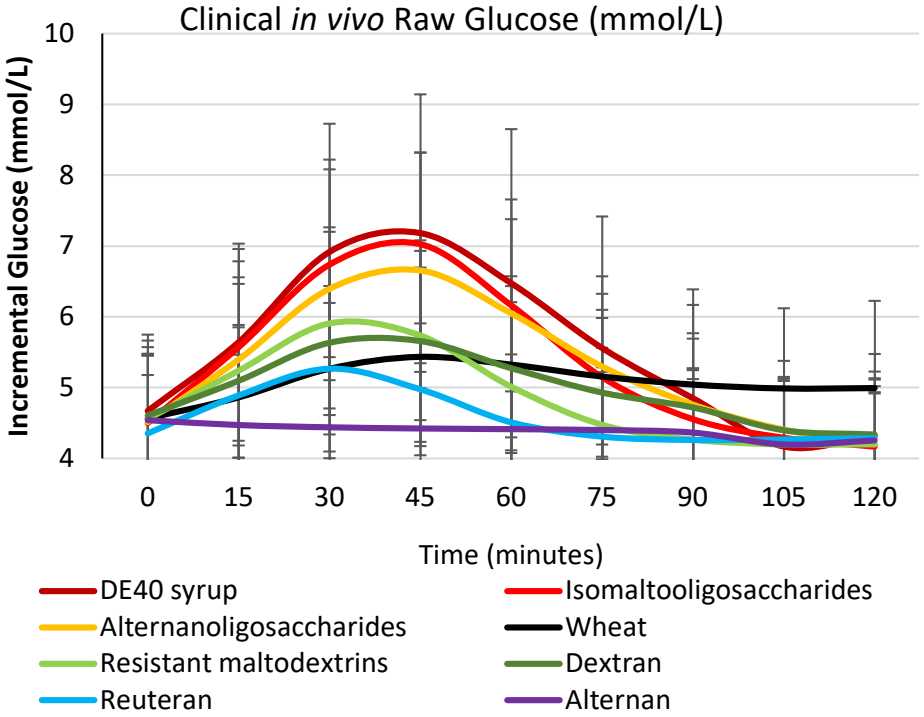

Figure 8. A: Postprandial glycemic profiles and B: Mean relative iAUC of *in vivo* digestion of 8 α-glucans.

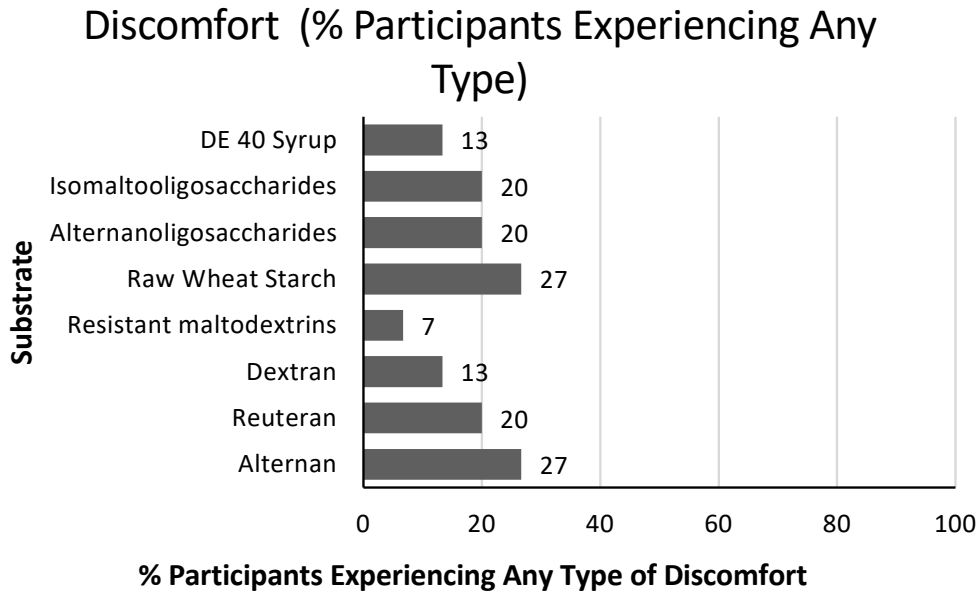

Figure 9. Recorded discomfort experienced by participants (%).

3.5.2 *In vitro* digestibility and relation of linkages and size of α-glucans to digestion: optimized *in vitro* assay of 9 α-glucans

In vitro digestion of α-glucans and relative disappearance of linkages

The clinically tested α-glucans and DE40 syrup, plus maltose as a control, were digested using an optimized *in vitro* assay protocol (Shin *et al.*, 2019) over an extended 24 h (1440 min) time period (Figure 10). Overall, *in vitro* assay results were similar to those observed in the clinical study, thus allowing the *in vitro* protocol to be used for analysis of susceptibility of different a-linkages to digestive enzymes. After 3 h (180 min) digestion (perhaps close to the time period of digestion in the upper gastrointestinal tract), the maltose control, DE40 syrup, and raw wheat starch were found to be digested to completion, indicating that the other α-glucans had portions of their structures that are indigestible within the 6 h (360 min) time period by the combination of α-amylase and α-glucosidase enzymes. At 24 h, isomaltooligosaccharides were also nearly digested to completion (~90% digested), while the other α-glucans were significantly less digested. While the total digestible portion of isomaltooligosaccharides was lower than that for raw wheat starch, the rate of change in the initial 15 min was much higher, meaning that there is a portion of isomaltooligosaccharides that is much more rapidly digesting than for raw wheat starch. This

initial rate of change helps explain the rapidly digestible *in vivo* results for isomaltooligosaccharides. At 3 h, resistant dextrins were ~40% digested, and alternanoligosaccharides, dextran, and reuteran were ~20-25% digested. Alternan had negligible digestion at 3 h. Important to its slow digestion property, raw wheat starch exhibited an approximately linear and complete digestion profile from 0 to 3 h incubation. Isomaltooligosaccharides had a fairly rapid initial digestion rate from 0 to 15 min, and afterwards was slowly digestible to 24 h. Resistant dextrin also had an initial fairly rapid digestion from 0-15 min and then a very slow digestion rate to 24 h, giving a total digestion of about 50%. Alternanoligosaccharides, dextran, and reuteran had slow initial digestion rates followed by more rapid, but still moderate, digestion rates from 1 to 24 h. A notable reduction in the maltose curve after 6 h (360 min) digestion was likely due to minor microbial hydrolytic activity and could be the explanation for similar minor reductions for raw wheat starch and DE40 syrup. This was why the assay was stopped at the 6 h time point.

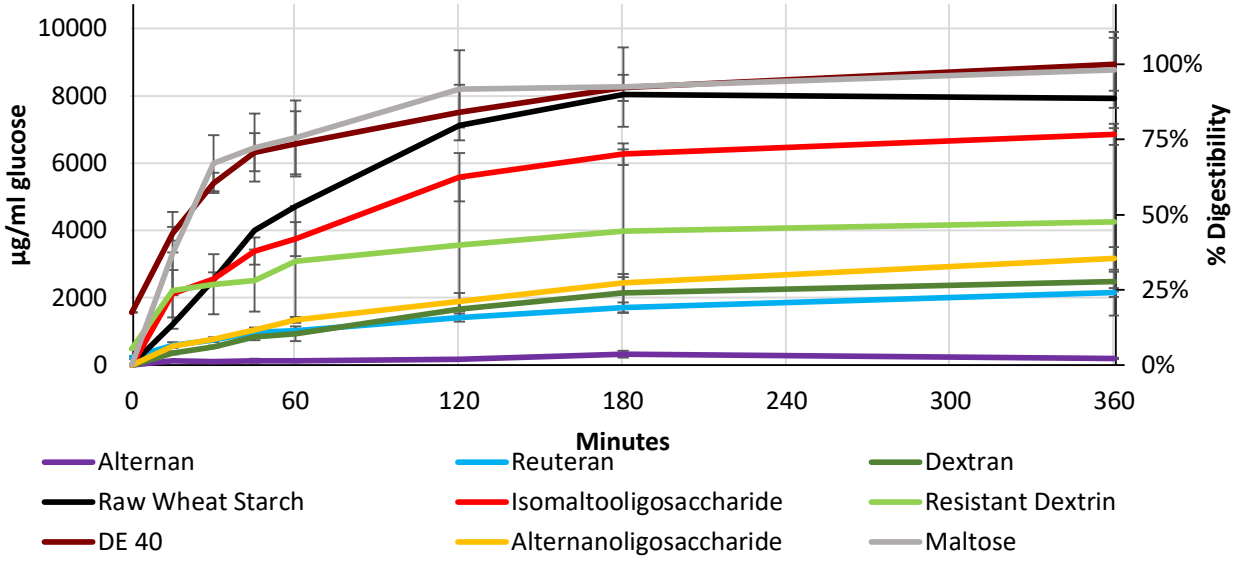

Figure 10. *in vitro* digestion profiles 6 h of the 8 α-glucans tested in the human trial using mammalian α-amylase and α-glucosidase from RIAP (mean ± SD).

Table 6. shows substrates ranked by average and initial rate of glucogenesis from the *in vitro* optimized assay (ranked by descending initial rates). ANOVA analysis among substrates of amount of glucose released as detected by GOPOD reagent at each timepoint shows p-values <0.001, showing significant differences in glucogenesis between substrates.

24 h *in vitro* assay: Rate of glucose hydrolyzation by *initial* GGR (descending) in µg/ml/min			2 h *in vivo* mean relative initial area under the curve (iAUC)
		µg/ml/min	% vs DE40 syrup
Maltose	Average rate	1.897	
	initial rate	244.683	
Isomaltooligosaccharides	Average rate	3.454	
	initial rate	157.929	95%
DE40 Syrup*	Average rate	2.273	
	initial rate	155.722	100%
Resistant dextrin	Average rate	1.958	
	initial rate	127.869	43%
Raw wheat starch	Average rate	3.675	
	initial rate	75.973	47%
Alternanoligosaccharides	Average rate	2.633	
	initial rate	41.664	84%
Dextran	Average rate	2.203	
	initial rate	27.846	42%
Reuteran	Average rate	1.163	
	initial rate	27.226	27%
Alternan	Average rate	0.193	
	initial rate	8.516	3%

*suspect erroneous, due to bacterial consumption of glucose

3.5.3 Differences in digestion of α-glucan substrate structures

The DMSO and ethanol rinses that were used to purify the α-glucans and precipitate protein from the digested samples at each timepoint also rinsed away free glucose and other small α-glucan molecules. Therefore, only miniscule amounts of free glucose were detected in the linkage and molecular size analysis. This allowed for an accurate quantitative view of digestibility different linkages by the calculated percent digestibility that is presented in the *in vitro* results section. Therefore, with some certainty, any terminal glucose (T-Glc) detected was considered part of an oligomer or polymer structure. Therefore, increasing terminal glucose over time indicates hydrolysis of glucose molecules from the interior part of a larger molecule. In the analysis, when peaks matched elution times for known linkages in the database, but mass fragmentation analysis did not confirm presence of the linkages, peaks were discarded.

Linkage analysis

Linkages and the anomeric C form of the tested α-glucan substrates are presented in Table 7. To understand which linkages and patterns of linkages found in the α-glucans were more and less susceptible to digestion, undigested α-glucans were collected at different time points of the *in vitro* digestion from the 24 h optimized protocol, and linkage analyses were done. Values were adjusted to percent digestibility against DE40 syrup at 24 h, and relative disappearance of α-glucan substrate linkages over time was calculated and is presented in Figure 11.

Alternan: There was little to no disappearance of linkages over time, which is consistent with the hypothesis from the clinical trial data that this structure was too large and too highly branched to digest significantly. A slight decrease was observed in α-1,3 (30 to 19.5%) over 24 h, indicating that while very large α-1,3 and α-1,6 alternating structures were primarily indigestible, that α-1,3 linkages are accessible for hydrolysis by native enzymes. α-3,6 linkages were found to decrease from 9.9 to 7.6% within 24 h, indicating only minimal digestion occurred. Data from one 60 min reading was discarded due to inconsistencies with previous and subsequent timepoints, and linkages present in pure substrate.

Reuteran: Decreasing amounts of terminal glucose were observed, and when coupled with observed increased relative concentrations of α-1,4 and α-1,6 over time in tangent with the hydrolysis of α-4,6 linkages, this indicated that α-4,6 linkages were fully digestible within 6 h. An

artifact at 24 hr indicated new appearance of some α-4,6 linkages based on mass fragmentation, however, for the purposes of interpreting these results, we assumed that there is no additional α-4,6 linkages that appear at 24 hr (after full disappearance at 6 hr). New α-3,4 linkages were also detected after 6 hr, and were likely due to transferase activity discussed earlier.

Dextran: α-1,6 Linkages in dextran were found to digest slowly, with some remaining after 1440 min (83 to 61.9%). Small amounts of α-3,6 (6%) were detected in the pure sample, and some (2.6%) remain at end, indicating α-3,6 is very slowly digestible, if not indigestible.

Raw wheat starch: Within raw wheat starch, α-1,4 linkages were quickly digested in the first 30 min. Some α-1,6 linkages appeared to have remained undigested at 6 h, with an increase of free glucose present after 30 min, and after 6 h. This "second wind" of glucogenesis may have been due to delayed hydrolysis of α-4,6 and α-1,6 linkages present in native raw wheat starch. The increase in α-1,6 seen in Figure 10 was likely due to variation in inositol internal standards, against which total concentrations of detected linkages were adjusted.

Isomaltooligosaccharides: A small amount of α-3,4 branching was detected after 6 h of digestion of IMO. α-4,6 quantities decreased from 30.3 to 14.2% in the first 60 min. α-1,3 and α-2,4 GLC were only present in pure substrate, and were digested within the first 15 min. New linkages appeared after 30 min were likely due to transferase activity in the presence of excess free glucose. As expected from the *in vitro* screening and clinical trial, IMOs were digested rapidly within the first 30 minutes.

Resistant dextrin: α-1,4 (28 to 8%) and α-1,6 (11.5 to 6.9%) Linkages disappeared within the first 30 min; this relatively rapid digestion of α-1,6 was likely due to the small initial quantities. A-1,4 linkages reduced in relative quantity between 30 and 1440 min (8 to 25.2% at 360 min; 16.2% at 1440 min). Digestion rate of the α-1,6 linkages was slower than for α-4,6; after 30 min α-1,6 linkages increased over time as α-4,6 linkages were hydrolyzed (6.2% at 30 min; 0.5% at 60 min; 0.6% at 360 min; 9.8% at 1440 min).

DE 40: DE40 syrup was initially composed of 48% α-1,4, <2% α-4,6, and 25.5% T-Glc. It was very rapidly digestible within the first 30 min, as expected.

Alternanoligosaccharides: 33% of α-1,6 linkages (and 7% α-3,4) remained after 24 h of digestion; this confirmed findings from other substrates that α-1,6 is resistant to digestion by native mammalian enzymes. The initially detected (10.6%) α-3,6 linkages were hydrolyzed to less than 1% within the first 30 min. We detected increased relative quantities of α-1,3 and α-1,6 linkages

after 30 min, which reflects the hydrolysis of α-3,6 after 30 min. The additional α-1,6 linkages from α-3,6 hydrolysis around the 30 min timepoint were not digested until after 360 min.

Maltose: In maltose, α-1,4 linkages were almost fully digested after 360 min (47.7 at 0 to 2.9% at 360 min)

Table 7. Linkage analysis (A) and anomeric C form (B) of tested pure substrates (% of total).

A

%	Alternan	Reuteran	Dextran	Raw Wheat Starch	Isomaltooligosaccharides	Resistant dextrin	DE 40 Syrup	Alternanoligosaccharides
T	11.7+0.6	33.0+0.9	8.4+0.3	4.2+0.1	40.8+0.9	35.2+0.7	31.8+0.1	11.3+0.1
3-Glc	30.0+2.2	1.2+0.7	0.2+0.0		2.0+0.3	4.8+1.0	0.8+0.2	24.3+1.7
2-Glc					1.8+0.1	3.2+0.1	0.3+0.0	2.2+0.3
6-Glc	46.2+1.6	21.1+0.1	83.0+0.4	2.4+0.3	29.3+0.8	12.3+0.5	2.1+0.1	33.5+0.8
4-Glc	1.1+0.5	31.5+0.9	0.3+0.3	90.0+0.5	20.2+0.4	30.4+0.2	60.2+0.4	18.1+1.6
3,4-Glc	0.4+0.2	1.9+0.5	0.4+0.0		0.5+0.1	1.1+0.1	0.4+0.0	
2,4-Glc					1.0+0.1	0.4+0.1	0.3+0.1	
3,6-Glc	9.9+0.5	1.0+0.4	6.0+0.2		0.5+0.2	1.9+0.2	0.1+0.0	10.6+0.3
4,6-Glc	0.6+0.1	10.1+0.1	1.2+0.1	3.2+0.8	3.6+0.1	10.2+0.1	3.6+0.1	

B

%	Alternan	Reuteran	Dextran	Raw Wheat Starch	Isomaltooligosaccharides	Resistant dextrin	DE 40 Syrup	Alternanoligosaccharides
α	100	90.99	100	100	82.2	71.2	81.8	92.2
β	0	9.01	0	0	17.8	28.8	18.2	7.8

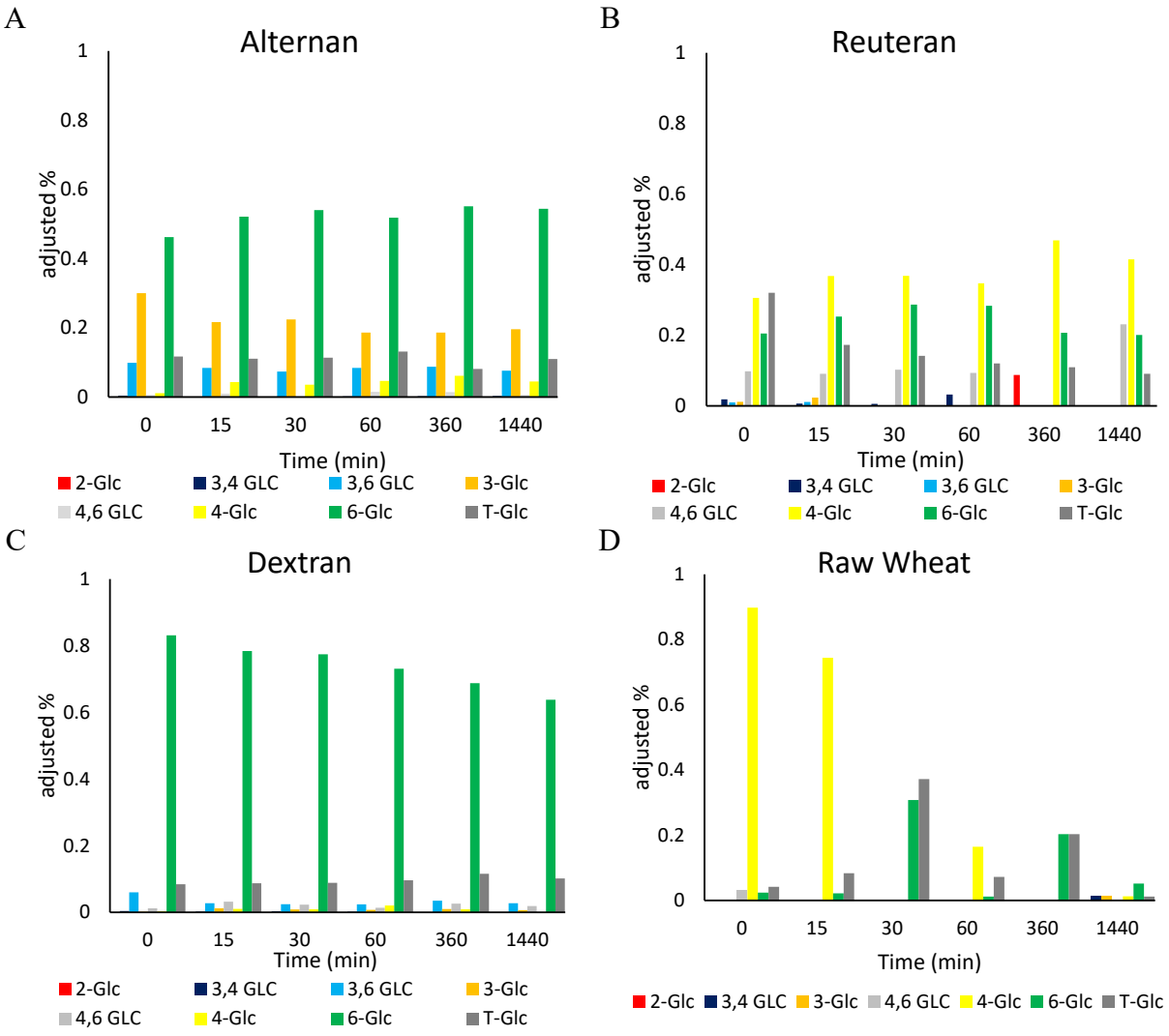

Figure 11. Linkage analysis of the α-glucan substrates at different time points of *in vitro* digestion using mammalian α-amylase and α-glucosidases from RIAP, adjusted by percent digestibility from *in vitro* digestion of DE40 Syrup at 24 h. A Alternan. B Reuteran. C Dextran. D Raw Wheat Starch. E Isomaltooligosaccharides. F Resistant dextrin. G DE 40 Syrup. H Alternanoligosaccharides. I Maltose.

Figure 11. Continued

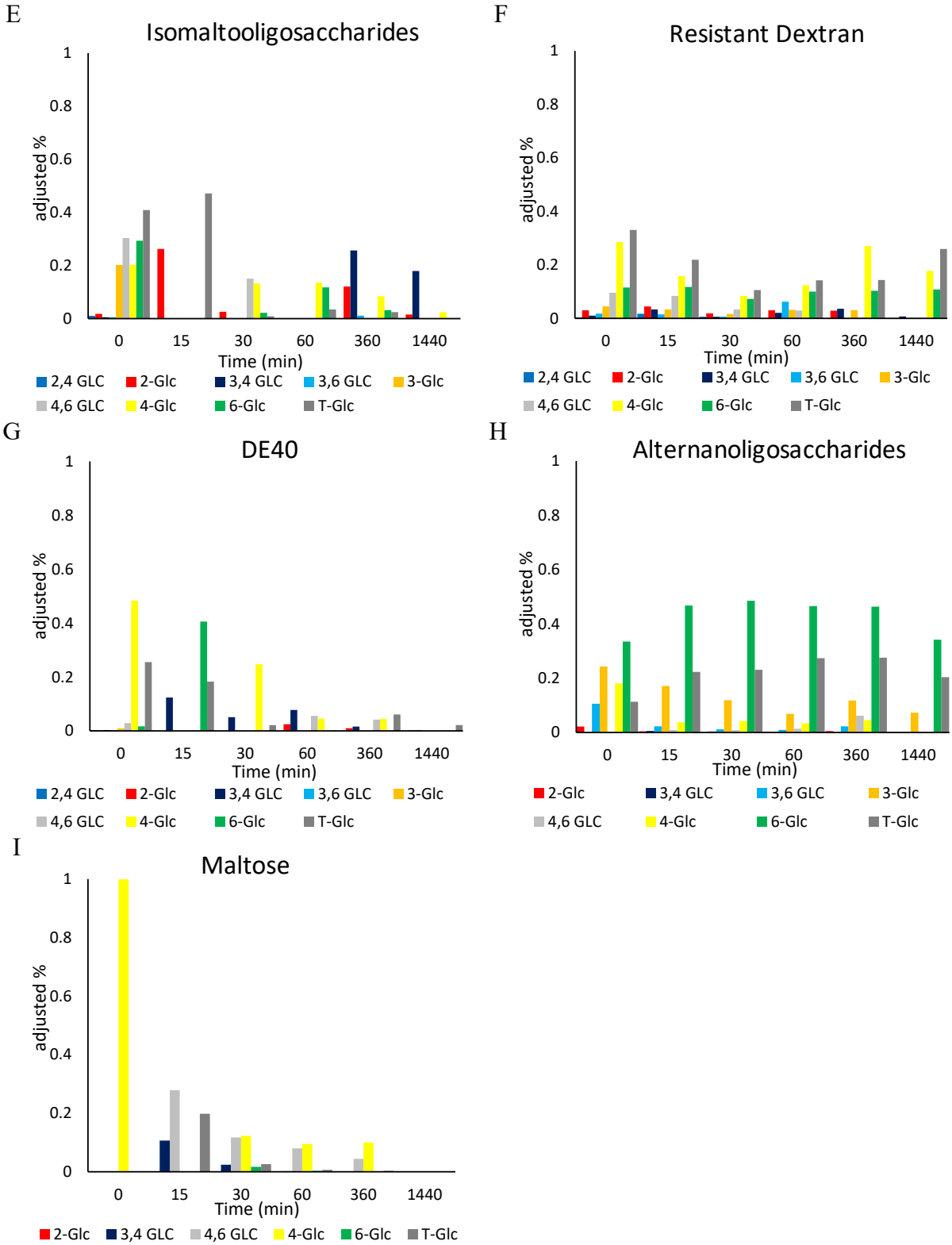

Digestion susceptibility of different linkages in selected α-glucans

Native α-glucan linkage compositions, as shown in Table 7, matched well with known structures. This formed the basis to monitor and compare digestion of individual linkages in the different α-glucans. Overall, the most resistant linkages to digestion were the non-branch point α-1,6 linkages, as they appear alternating with α-1,3 linkages in alternan, alternating with α-1,4 linkages in reuteran, in long repeated linear chains in dextran and reuteran, or alternating with α-1,3 linkages in alternanoligosaccharides. α-1,4 Linkages were well digested as evidenced in raw wheat starch and DE40 syrup, though were resistant to digestion in reuteran where in a significant part of the molecule the α-1,4 linkage alternates with the α-1,6 linkage. Perhaps somewhat unexpected was the finding that α-1,3 linkages digest in a slow way, and this was true whether found in the structure of alternan, alternanoligosaccharides, or resistant dextrin, and was even more rapidly digested in isomaltooligosaccharides. The most resistant α-glucan was alternan containing α-1,6 linkages alternating with α-1,3 linkages, and then was followed by the somewhat more digestible reuteran, dextran, and alternanoligosaccharides, all which contained significant amounts of α-1,6 linkages, either alternating with α-1,4 linkages (in a large polymer) or α-1,3 linkages (in a smaller polymer), or having consecutive α-1,6 linkages.

3.5.4 Molecular size analysis

Reductions in molecular size of α-glucans during in vitro digestion

Molecular size data is presented in Figure 12 and Figure 13. Quantities of each molecular weight category were adjusted in terms of glucose disappearance based on *in vitro* digestion from the 24 h optimized protocol. Note again that the protein precipitation step involving DMSO and ethanol rinsed away free glucose and other small soluble α-glucan molecules. This data was therefore adjusted by the calculated percent digestibility that is presented in the *in vitro* results section. The interpretation of this data is not entirely clear, especially for dextran, resistant dextrin, alternanoligosaccharide, and maltose (Figure 13)

Alternan: After 24 h of *in vitro* digestion, 64% of remaining undigested substrate was 500 -1,000 kDa, with 21.6% 0-10 Da. Quantities of 0-10 Da molecules do not change largely from 6 to 24 h digestion *in vitro*, so it is likely that these smaller molecules are not digestible either. These

results align with the glycemic profile from the human study showing poor digestibility of the polymer.

Reuteran: Reuteran showed a small increase in the 0.01-10 Da peak over time, as larger molecules were digested. Decrease was observed in molecular size over time (22% 500 -1,000 kDa at 24 h). The quantity of undigested large molecules remaining after 24 h of *in vitro* digestion aligns with the *in vivo* digestion data, showing that this reuteran is partially indigestible.

Dextran: Dextran still had large quantities of 1,6 linkages undigested after 1440 min of *in vitro* digestion, suggesting that the slow-digesting properties are due to the high initial ratio of repeating 1,6 linkages (Table 7).

Raw Wheat Starch: After 30 min of digestion, raw wheat starch was reduced to mostly 0-10 Da molecules, with complete digestion occurring after 6 h.

Isomaltooligosaccharides: Isomaltooligosaccharides were shown to be mostly digestible, with some portions being rapidly digested and releasing the majority of glucose within the first 60 min, and the remaining in the following 60 min. When compared to the iAUC curves from the clinical trial, it is clear that isomaltooligosaccharides were indeed rapidly digestible by mammalian enzymes, although they are commonly labelled as fiber due to the current AOAC methods 2002.02 and 2009.01 that utilize fungal amyloglucosidases which do not digest these linkage patterns.

DE 40: DE40 syrup was used as a positive control for rapidly digesting starch, and after adjustment by % digestibility from the optimized *in vitro* assay, insignificant quantities of large molecular sizes were detected after 30 min.

Maltose: Maltose was used as a positive control for rapidly digesting starch, and the molecular size analysis results conclude that after 30 min there were only minute quantities of any maltose remaining.

Alternan	1,200,000 Da
Reuteran	MW (61,100,000 Da and 380 Da) 3.0 % Tri-saccharide; 13.6% Di-saccharide; 43.7% Monosaccharide
Dextran 20	100% 16,500 Da
Raw Wheat Starch	2,100,000 Da

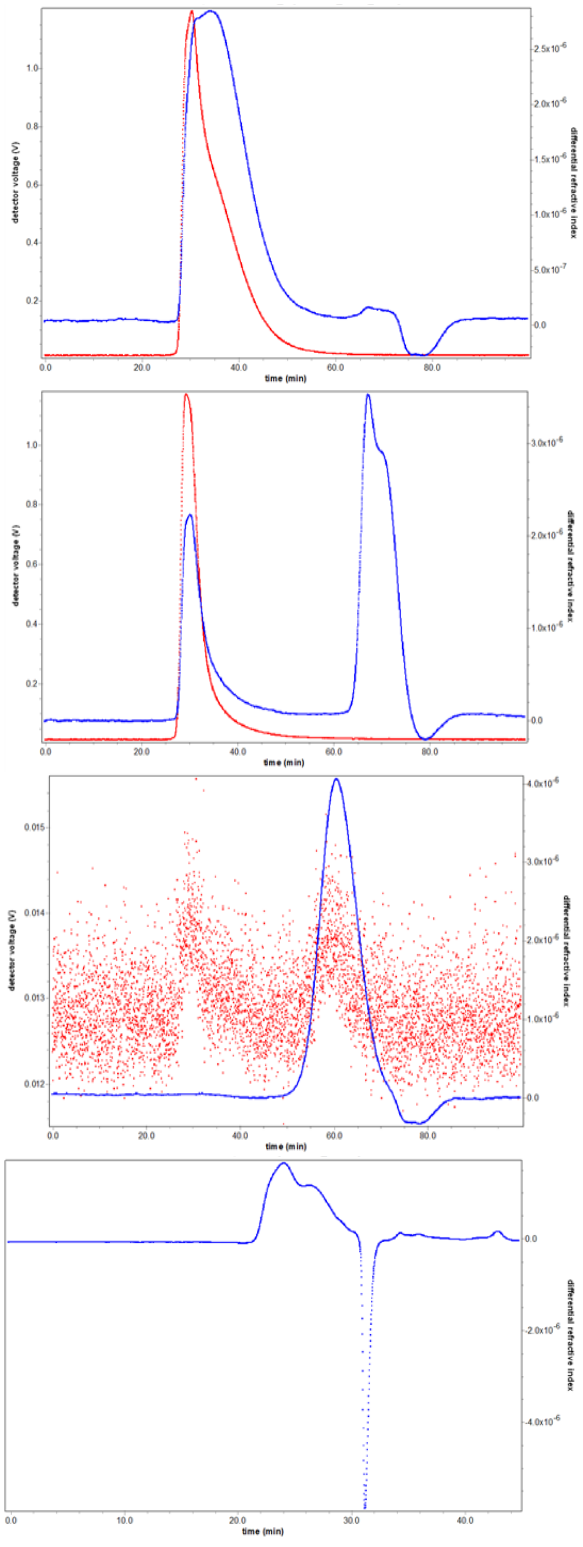

Figure 12. Molecular size of pure novel α-glucans —LS; —dRI.

Figure 12. Continued

Isomaltooligosaccharides	615 Da 41.5% monosaccharide; 33.9% disaccharide; 18.3% trisaccharide	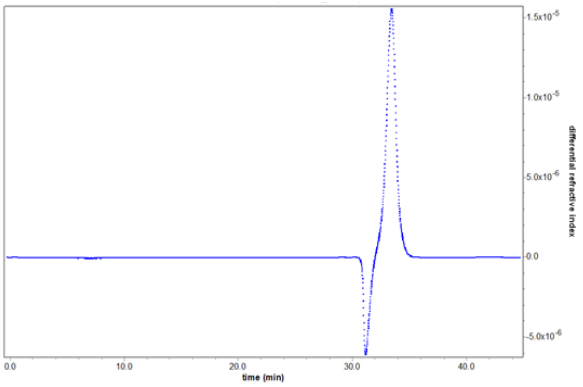
Resistant dextrin	990 Da From manufacturer: 7.6% Glucose, 1.4% isomaltose, 2.6% maltose (12% DP 1 & 2)	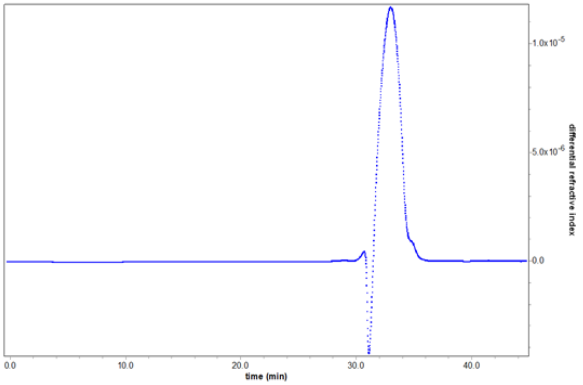
DE 40 syrup	590 Da	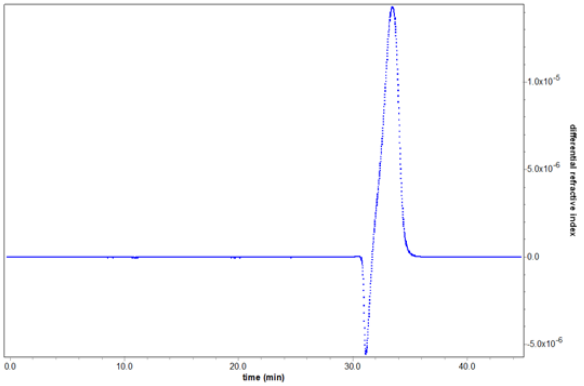
Alternanoligosaccharides	1,100 Da: 77.4% oligosaccharide (1,100 Da); 3.1% Trisaccharide; 17.5% Disaccharide; 2.0% monosaccharide	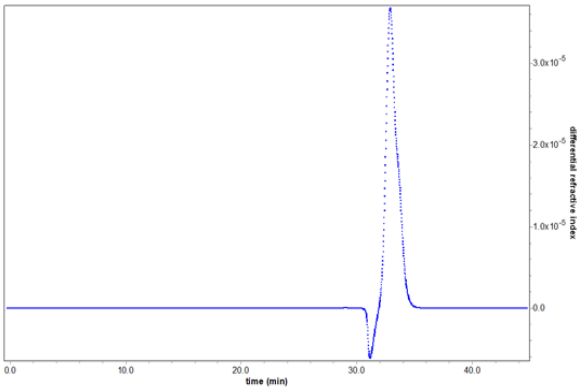

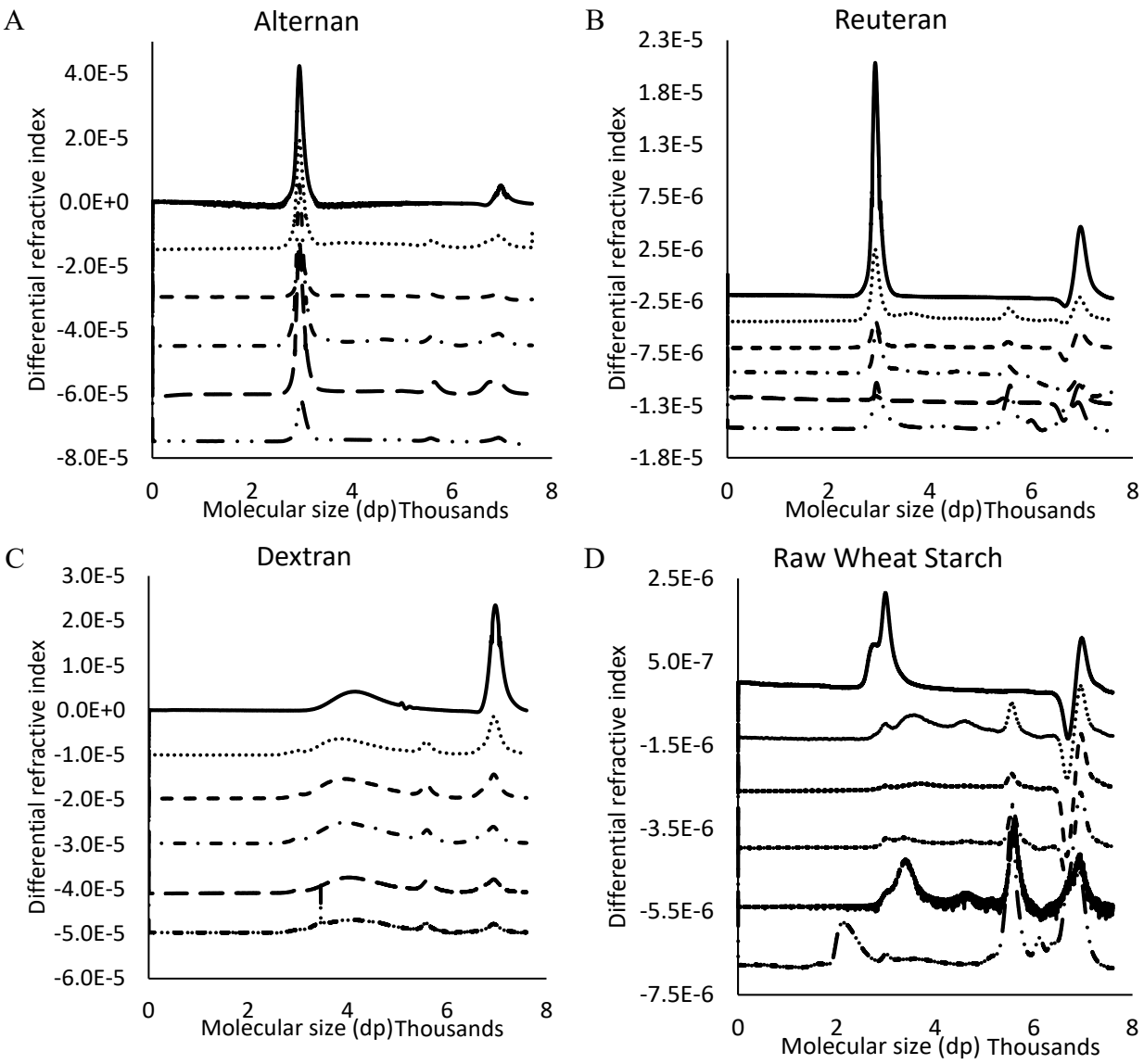

Figure 13. Molecular size analysis of the α-glucan substrates during in vitro digestion with mammalian α-amylase and α-glucosidases from RIAP. Standards were used to convert elution times to molecular size. ——0 min; ·····15 min; – – 30 min; – · –60 min; — –360 min; — · 1880 min

Figure 13. Continued

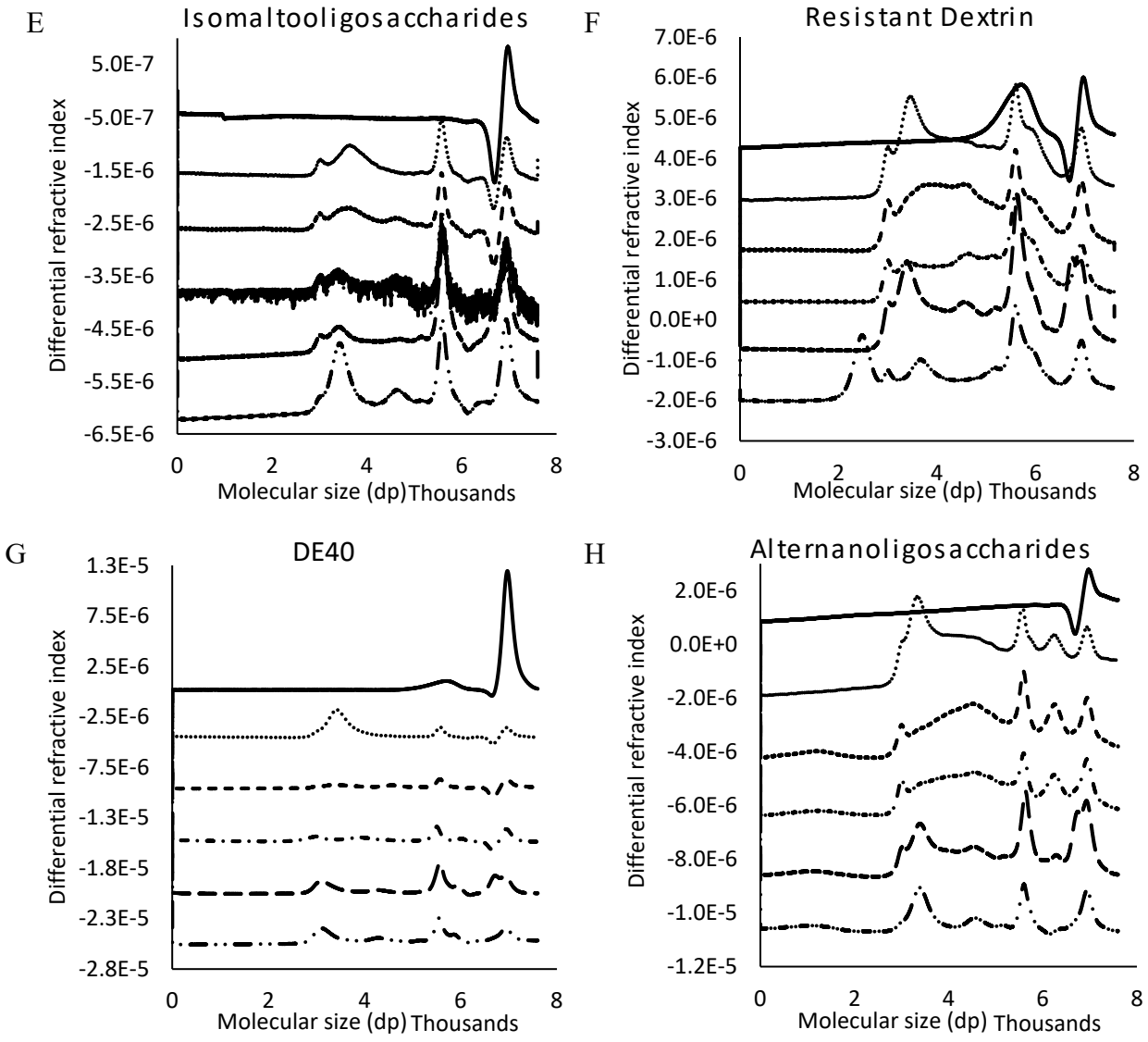

Figure 13. Continued

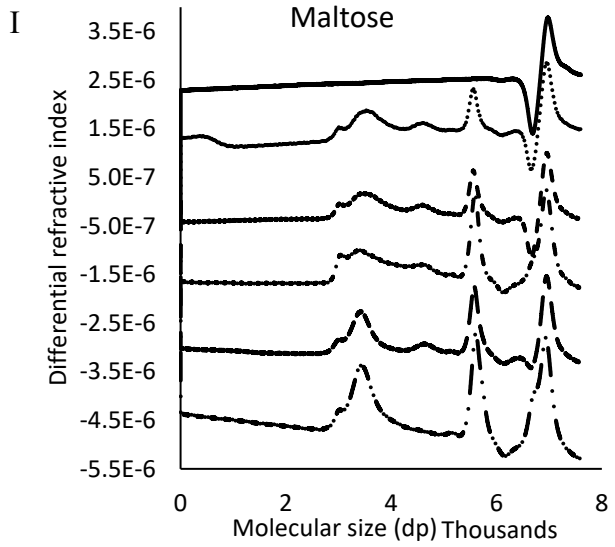

3.6 **Discussion**

Although the digestible carbohydrates in the human diet are usually relegated to starch and its various hydrolysis and modified products, and sucrose, and lactose, the mucosal brush border-bound α-glucosidases can also digest carbohydrates with other α-glucosidic linkages (Lee *et al.*, 2016). Humans and other mammals are not able to digest β-linked glucans, such as cellulose, and these pass undigested as dietary fiber to the large intestines for potential microbial degradation. Lee et al. (2016) showed that for the different Glc-Glc disaccharide forms, individual recombinant mammalian α-glucosidases effectively digest α-1,2 and α-1,3 linkages, albeit at a much slower rate than the α-1,4-linked maltose (Lee *et al.*, 2016). The N-terminal subunit of the maltase-glucoamylase complex (commonly termed "maltase") was the enzyme most able to digest the unusual α-1,2 and α-1,3 linkages with the latter being more digestible. The α-1,6 linkage between glucose molecules has a relatively low Km digestion parameter. Larger α-glucan-based oligomers and meso-size polymers synthesized mostly by microbes may have unusual linkages that are slow digesting, with combinations of linkages such that the carbohydrates are slow digesting or even indigestible within the small intestine transit time for the enzymes to act (Gangoiti *et al.*, 2018). Here, we show α-glucan linkages, patterns of linkages, and molecular sizes that are more and less susceptible to hydrolysis by mammalian enzymes with correlation to clinical trial glycemic

response results, providing guidance for development of future α-glucans with desirable digestion and glucose release patterns.

Substrates not completely digested in the *in vitro* assay within 24 h were considered to be indigestible, and if digestible in part without a rapid significant initial rise were SDCs. When compared to glycemic response *in vivo*, dextran and alternanoligosaccharides were likely the most promising as SDCs that are fully or close to fully digestible. Dextran has a high percentage (83%) of α-1,6 linkages, with 6% α-3,6 linkages and 1.2% α-4,6. Alternanoligosaccharides was slightly faster digesting than dextran. These writers hypothesize that carbohydrates with moderate to high α-1,6 and composed of some α-3,6 and α-4,6 linkages are the most likely to resemble the iAUC of raw wheat starch, which was our benchmark SDC. It is proposed that α-3,6 and α-4,6 linkages are difficult for mucosal α-glucosidases to gain access to and are accordingly slower to digest. Following that, remaining terminal glucose attached by α-1,6 linkages is slowly digested, further providing delayed glucose hydrolysis. Based on previous alternanoligosaccharides feeding studies in which the treatment group did not differ significantly from the control in body weight or intake (Dolan *et al.*, 2012), alternanoligosaccharides was not expected to be slowly digestible into the distal small intestine for activation of the gut-brain axis, and the results presented here confirm that.

Unexpectedly (but confirmed by linkage identity and mass fragmentation), there was new appearance of 40% α-1,6 after 15 min of digestion with RIAP in most samples presented here (Figure 11). The linkage data adjusted with 24 h of the DE40 syrup set to equal 100% did not show any changes to detectable linkages. However, upon close examination of only 0 to 2% of adjusted percent linkages, we can see new α-1,2, and α-1,4 linkage and new α-3,4 branching detected after 30 and 60 min that indicate there was a small amount of transferase activity of the enzymes present in RIAP. This transferase activity likely resulted from excess free glucose in the presence of mucosal α-glucosidase and α-amylase. Glucose receptors GLUT2 and SGLT1 respectively mediate basolateral exit and intestinal absorption of glucose molecules (Debnam, Denholm and Grimble, 1998; Kellet and Helliwell, 2000; Kellett and Brot-Laroche, 2005). *In vivo*, there would not be a surplus of glucose for this transferase activity unless some disease state was present.

3.6.1 *In vitro* assay for screening α-glucans

Clinical trial of 8 α-glucans

Figure 14 demonstrates a strong relationship between MW (on a log scale) and relative iAUC (r=-0.86), with only resistant dextrin and raw wheat starch unaligned – raw wheat starch is known to be slow digesting due to its crystalline (and not molecular) structure, so it is not included on this figure. Postprandial iAUC of the eight α-glucans tested in the human study was also found to be correlated to molecular size (r=-0.86) (Figure 14), with only resistant dextrin not aligned in this relationship. The most notable effect of molecular size on digestion was with alternan (large polymer) and alternanoligosaccharides (smaller oligosaccharide), which have similar compositions and linkage profiles, but very different iAUC's of 3% and 84% (of the highly available control, DE40 syrup).

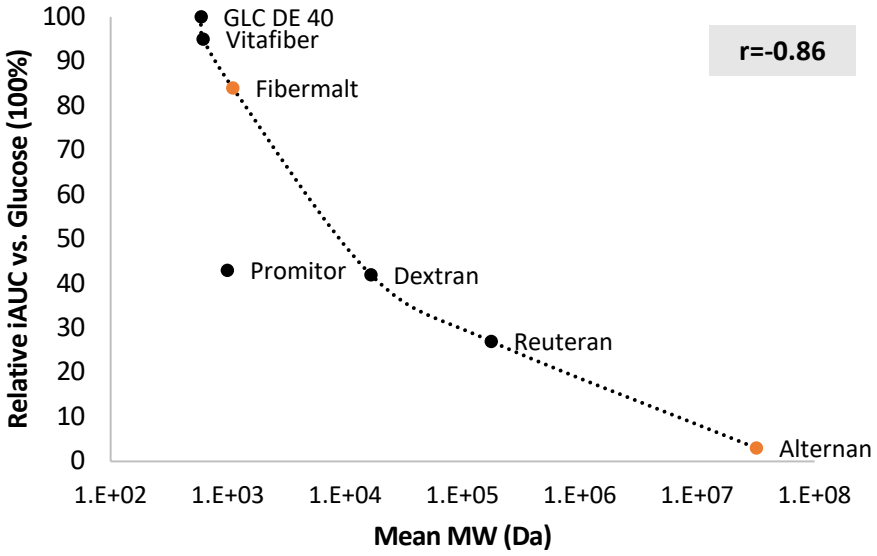

Figure 14. Correlation of iAUC and mean MW (Da) of tested α-glucans.

3.6.2 Optimized *in vitro* assay of 9 α-glucans

While the comparison of *in vitro* and *in vivo* data was justified above and used to explain relative linkage susceptibility of the SDCs, there are a few obstacles that argue against direct correlation between *in vitro* and *in vivo* models. The period of time used for *in vitro* digestion

(incubation at 37°C), and timepoints selected for examination, are best approximations intended to simulate *in vivo* digestion. However, concentrations of α-amylase and α-glucosidases *in vivo* are unknown, so it is not possible to directly compare period of digestion between *in vivo* and *in vitro* models. Further, *in vivo* feedback control mechanisms that lower glycemic index may slowed gastric emptying rate based on viscosity or slowed digestion into the ileum, which cannot be controlled in *in vitro* assays.

Other uses for the *in vitro* technique used in this study could include determining what structures will make their way to the colon by utilizing remaining carbohydrates after *in vitro* digestion for fecal fermentation studies. Determining the characteristics of structures that are not digestible by native enzymes could allow for engineering of carbohydrate substrates for colonic fermentation, and short chain fatty acid production, through partially indigestible α-glucans (Woodward *et al.*, 2012).

3.6.3 Structural analysis of undigested pure substrates

Linkage analysis

A proposed order of rate of linkage digestion is presented in Table 8. Some new linkages were observed that were not present in the linkage analysis of the pure substrate. This is likely due to the transferase activity of the Ct-SI and Nt-SI enzymes. There is past evidence that mucosal α-glucosidase has transglycosylation activity (Dahlqvist, Borgström, *et al.*, 2008). Hog Maltase Ib (CtSI) has transferase activity, transglycosylating glucose to sucrose during hydrolysis; NtSI produced oligosaccharides from isomaltose during α-glucan hydrolysis (Dahlqvist, Jensen, *et al.*, 2008). *In vitro* these products are quickly hydrolyzed, but without glucose absorbance as would occur *in vivo*, and as they remain in solution as available for transglycosylation events that products larger products. While the physiological role of transglycosylation probably small or nonexistent (Lin, Lee and Chang, 2016), these mechanisms explain the discrepancies between *in vitro* and *in vivo* findings presented in this research.

Table 8. Proposed order of linkage digestion rate, descending order.

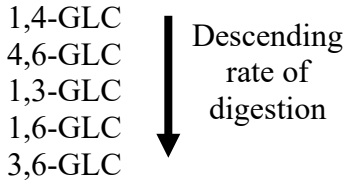

3.7 **Conclusion & future research**

As presented in Table 8, we propose an order of rate of digestion for α-linkages (descending) as: 1,4, 4,6, 1,3, 1,6, and 3,6. We also were able to confirm previous findings by Ao et al. that increased degree of branching, and likely chain length, contribute to a slow digesting property (Ao *et al.*, 2007). Further research should be done to examine the strong correlation between increasing molecular size and slowed digestion rate shown in Figure 14. We also present here an *in vitro* digestion protocol as previously proposed by Lee, et al. (Lee *et al.*, 2016; Lin, Lee and Chang, 2016; Shin *et al.*, 2019; Seo *et al.*, 2020), and demonstrated an acceptable relationship in rankings of digestibility of samples to blood glucose data from fasted clinical trial participants.

Considering the observed relationship between postprandial iAUC and MW of alternan-like carbohydrates (Figure 14), future research should find MW structures that are predicted to normally cover the relative iAUC axis between alternan and alternanoligosaccharides, and with similar linkage profiles, for enhanced slowly digesting properties.

As demonstrated using *in vitro* assay protocols that utilize mammalian enzyme sources for glucan hydrolysis, as well as the iAUC blood glucose clinical trial results, it is clear that AOAC methods 2002.02 and 2009.01 need to be re-evaluated to utilize mammalian enzyme sources rather than fungal. Without mammalian α-glucosidases included in *in vitro* total dietary fiber assays, erroneous diet recommendations and decisions are being made by dietitians, diabetes educators, and other medical professionals towards products that incorrectly appear to have increased fiber and reduced carbohydrate contents. These α-glucosidases are key to hydrolysis of α-(1,4) and (1,6)-glycosidic linkages, the most common linkages in amylose and amylopectin. Further, there are a number of unusual or new, man-made carbohydrates that are now being used in processed foods, such as isomaltooligosaccharides (Gourineni *et al.*, 2018), alternanoligosaccharides, and resistant dextrins (labelled as “soluble fiber”), which contain these structures. Many of these new or unusual-linked carbohydrates are not readily digestible by the fungal form of α-glucosidase

brush border enzymes, but they are rapidly digestible by the mammalian forms (Lee and Hamaker, 2017; Seo *et al.*, 2018; Shin *et al.*, 2019).

3.8 References

Ao, Z. *et al.* (2007) 'Starch with a slow digestion property produced by altering its chain length, branch density, and crystalline structure', *Journal of Agricultural and Food Chemistry*. American Chemical Society, 55(11), pp. 4540–4547. doi: 10.1021/jf063123x.

Backer, D. and Saniez, M.-H. (2004) 'Soluble highly branched glucose polymers and their mode of production PAT NO US7211662B2'. United States. Available at: j:%5Cmijn documenten%5Cliteratuur%5Cliteratuur in refenece manager%5Cvolledige text%5C0012.pdf.

Ball, S. D. *et al.* (2003) 'Prolongation of satiety after low versus moderately high glycemic index meals in obese adolescents', *Pediatrics*, 111(3), pp. 488–494. doi: 10.1542/peds.111.3.488.

Bier, D. M. *et al.* (1977) 'In-vivo measurement of glucose and alanine metabolism with stable isotopic tracers', *Diabetes*, 26(11), pp. 1005–1015. doi: 10.2337/diab.26.11.1005.

Dahlqvist, A., Borgström, B., *et al.* (2008) 'Characterization of Intestinal Invertase as a Glucoside-Invertase. II. Studies on Transglycosylation by Intestinal Invertase.', *Acta Chemica Scandinavica*, 13(1), pp. 1659–1667. doi: 10.3891/acta.chem.scand.13-1659.

Dahlqvist, A., Jensen, A. T., *et al.* (2008) 'Hog Intestinal Isomaltase Activity.', *Acta Chemica Scandinavica*, 14, pp. 72–80. doi: 10.3891/acta.chem.scand.14-0072.

Danielsson, C. E. (1947) 'Molecular weight of α-amylase [1]', *Nature*, 160(4078), p. 899. doi: 10.1038/160899a0.

Debnam, E. S., Denholm, E. E. and Grimble, G. K. (1998) 'Acute and Chronic Exposure of Rat Intestinal Mucosa to Dextran promotes SGLT I-mediated Glucose Transport', *European Journal of Clinical Investigations*, 28.

Dolan, L. C. *et al.* (2012) 'Safety evaluation of fibermalt', *Food and Chemical Toxicology*, 50(7), pp. 2515–2523. doi: 10.1016/j.fct.2012.03.081.

Eerlingen, R. C., Deceuninck, M. and Delcour, J. A. (1993) 'Enzyme-Resistant Starch. II. Influence of Amylose Chain Length on Resistant Starch Formation', *Cereal Chemistry*, 70(3), pp. 345–350.

Eerlingen, R. C. and Delcour, J. A. (1995) 'Formation, analysis, structure and properties of type III enzyme resistant starch', *Journal of Cereal Science*. Academic Press, 22(2), pp. 129–138. doi: 10.1016/0733-5210(95)90042-X.

Englyst and Englyst (2005) 'Carbohydrate bioavailability', *British Journal of Nutrition*, 94(1), pp. 1–11. doi: 10.1079/bjn20051457.

Englyst, H. N., Kingman, S. M. and Cummings, J. H. (1992) 'Classification and measurement of nutritionally important starch fractions', *European Journal of Clinical Nutrition*. MRC Dunn Clinical Nutrition Centre, Cambridge, UK., 46(SUPPL. 2), pp. S33-50. doi: 10.1016/S0271-5317(97)00010-9.

Esfahani, A. *et al.* (2011) 'The application of the glycemic index and glycemic load in weight loss: A review of the clinical evidence', *IUBMB Life*. Toronto, Ontario, Canada: Wiley Periodicals, Inc, 63(1), pp. 7–13. doi: 10.1002/iub.418.

Frost, G. *et al.* (1999) 'Glycaemic index as a determinant of serum HDL-cholesterol concentration', *Lancet*. Elsevier, 353(9158), pp. 1045–1048. doi: 10.1016/S0140-6736(98)07164-5.

Gangoiti, J. *et al.* (2016) 'The Gram-negative bacterium Azotobacter chroococcum NCIMB 8003 employs a new glycoside hydrolase family 70 4,6-α-glucanotransferase enzyme (GtfD) to synthesize a reuteran like polymer from maltodextrins and starch', *Biochimica et Biophysica Acta - General Subjects*. Elsevier B.V., 1860(6), pp. 1224–1236. doi: 10.1016/j.bbagen.2016.02.005.

Gangoiti, J., Van Leeuwen, S. S., Gerwig, G. J., *et al.* (2017) '4,3-α-Glucanotransferase, a novel reaction specificity in glycoside hydrolase family 70 and clan GH-H', *Scientific Reports*, 7, p. 39761. doi: 10.1038/srep39761.

Gangoiti, J., Lamothe, L., *et al.* (2017) 'Characterization of the Paenibacillus beijingensis DSM 24997 GtfD and its glucan polymer products representing a new Glycoside Hydrolase 70 subfamily of 4,6-Î±-glucanotransferase enzymes', *Plos One*, 12, p. e0172622.

Gangoiti, J., Van Leeuwen, S. S., Meng, X., *et al.* (2017) 'Mining novel starch-converting Glycoside Hydrolase 70 enzymes from the Nestlé Culture Collection genome database: The Lactobacillus reuteri NCC 2613 GtfB', *Scientific Reports*, 7(1). doi: 10.1038/s41598-017-07190-z.

Gangoiti, J. *et al.* (2018) *Synthesis of novel α-glucans with potential health benefits through controlled glucose release in the human gastrointestinal tract*, *Critical Reviews in Food Science and Nutrition*. doi: 10.1080/10408398.2018.1516621.

Van Geel-Schutten, G. H. *et al.* (1999) 'Biochemical and structural characterization of the glucan and fructan exopolysaccharides synthesized by the Lactobacillus reuteri wild-type strain and by mutant strains', *Applied and Environmental Microbiology*, 65(7), pp. 3008–3014. doi: 10.1128/aem.65.7.3008-3014.1999.

Gourineni, V. *et al.* (2018) 'Gastrointestinal tolerance and glycemic response of isomaltooligosaccharides in healthy adults', *Nutrients*. Multidisciplinary Digital Publishing Institute (MDPI), 10(3), p. 301. doi: 10.3390/nu10030301.

Hasek, L. Y. *et al.* (2018) 'Dietary Slowly Digestible Starch Triggers the Gut–Brain Axis in Obese Rats with Accompanied Reduced Food Intake', *Molecular Nutrition and Food Research*. Germany, 62(5). doi: 10.1002/mnfr.201700117.

Kellet, G. L. and Helliwell, P. A. (2000) 'The diffusive component of intestinal glucose absorption is mediated by the glucose-induced recruitment of GLUT2 to the brush-border membrane', *Biochemical Journal*, 350(1), pp. 155–162. doi: 10.1042/bj3500155.

Kellett, G. L. and Brot-Laroche, E. (2005) 'Apical GLUT2: A major pathway of intestinal sugar absorption', *Diabetes*, 54(10), pp. 3056–3062. doi: 10.2337/diabetes.54.10.3056.

Kralj, S. *et al.* (2004) 'Biochemical and molecular characterization of Lactobacillus reuteri 121 reuteransucrase', *Microbiology*. Haren, The Netherlands, 150(7), pp. 2099–2112. doi: 10.1099/mic.0.27105-0.

Lee, B.-H. and Hamaker, B. R. (2012) *Mucosal alpha-glucosidase hydrolysis properties and the control of glucogenesis*, *Dissertation*. Purdue University. doi: AAI3545304.

Lee, B. H. *et al.* (2012) 'Inhibition of maltase-glucoamylase activity to hydrolyze α-1,4 linkages by the presence of undigested sucrose', *Journal of Pediatric Gastroenterology and Nutrition*, 55(SUPPL.2). doi: 10.1097/01.mpg.0000421415.95751.f7.

Lee, B. H. *et al.* (2013) 'Enzyme-Synthesized Highly Branched Maltodextrins Have Slow Glucose Generation at the Mucosal α-Glucosidase Level and Are Slowly Digestible In Vivo', *PLoS ONE*, 8(4), p. e59745. doi: 10.1371/journal.pone.0059745.
Lee, B. H. *et al.* (2016) 'Contribution of the Individual Small Intestinal α-Glucosidases to Digestion of Unusual α-Linked Glycemic Disaccharides', *Journal of Agricultural and Food Chemistry*, 64(33), pp. 6487–6494. doi: 10.1021/acs.jafc.6b01816.
Lee, B. H. and Hamaker, B. R. (2017) 'Number of branch points in α-limit dextrins impact glucose generation rates by mammalian mucosal α-glucosidases', *Carbohydrate Polymers*, 157, pp. 207–213. doi: 10.1016/j.carbpol.2016.09.088.
Lin, A. H. M. *et al.* (2012) 'Starch source influences dietary glucose generation at the mucosal α-glucosidase level', *Journal of Biological Chemistry*, 287(44), pp. 36917–36921. doi: 10.1074/jbc.M112.378331.
Lin, A. H. M., Lee, B. H. and Chang, W. J. (2016) 'Small intestine mucosal α-glucosidase: A missing feature of in vitro starch digestibility', *Food Hydrocolloids*. Elsevier, 53, pp. 163–171. doi: 10.1016/j.foodhyd.2015.03.002.
Liu, S. *et al.* (2000) 'A prospective study of dietary glycemic load, carbohydrate intake, and risk of coronary heart disease in US women', *American Journal of Clinical Nutrition*, 71(6), pp. 1455–1461. doi: 10.1093/ajcn/71.6.1455.
Livesey, G. *et al.* (2008) 'Glycemic response and health - A systematic review and meta-analysis: The database, study characteristics, and macronutrient intakes', *American Journal of Clinical Nutrition*, 87(1), pp. 258S-268S. doi: 10.1093/ajcn/87.1.223s.
Nazare, J.-A. *et al.* (2010) 'Effect of postprandial modulation of glucose availability: short- and long-term analysis', *British Journal of Nutrition*, 103(10), pp. 1461–1470. doi: 10.1017/s0007114509993357.
Ogden, C. L. *et al.* (2014) 'Prevalence of childhood and adult obesity in the United States, 2011-2012', *Journal of the American Medical Association*, 311(8), pp. 806–814. doi: 10.1001/jama.2014.732.
Olds, T. S. *et al.* (2010) 'Trends in the prevalence of childhood overweight and obesity in Australia between 1985 and 2008', *International Journal of Obesity*, 34(1), pp. 57–66. doi: 10.1038/ijo.2009.211.
Pettolino, F. A. *et al.* (2012) 'Determining the polysaccharide composition of plant cell walls', *Nature Protocols*, 7(9), pp. 1590–1607. doi: 10.1038/nprot.2012.081.
Pijning, T. *et al.* (2008) 'Biochemical and crystallographic characterization of a glucansucrase from Lactobacillus reuteri 180', *Biocatalysis and Biotransformation*, 26(1–2), pp. 12–17. doi: 10.1080/10242420701789163.
Te Poele, E. M. *et al.* (2020) 'Development of Slowly Digestible Starch Derived α-Glucans with 4,6-α-Glucanotransferase and Branching Sucrase Enzymes', *Journal of Agricultural and Food Chemistry*, 68(24), pp. 6664–6671. doi: 10.1021/acs.jafc.0c01465.
Quezada-Calvillo, R. *et al.* (2008) 'Luminal Starch Substrate "Brake" on Maltase-Glucoamylase Activity Is Located within the Glucoamylase Subunit', *The Journal of Nutrition*, 138(4), pp. 685–692. doi: 10.1093/jn/138.4.685.
Rizkalla, S. W. *et al.* (2004) 'Improved plasma glucose control, whole-body glucose utilization, and lipid profile on a low-glycemic index diet in type 2 diabetic men: A randomized controlled trial', *Diabetes Care*, 27(8), pp. 1866–1872. doi: 10.2337/diacare.27.8.1866.

Seo, J. *et al.* (2018) 'Determination of glucose generation rate from various types of glycemic carbohydrates by optimizing the mammalian glycosidases anchored in the small intestinal tissue', in *Poster Presented at: AACC International Annual Meeting*. London, UK.

Seo, J. M. *et al.* (2020) 'Determination of glucose generation rate from various types of glycemic carbohydrates by mammalian glucosidases anchored in the small intestinal tissue', *International Journal of Biological Macromolecules*. Elsevier, 154, pp. 751–757. doi: 10.1016/j.ijbiomac.2020.03.154.

Shin, H. *et al.* (2019) 'Optimization of in vitro carbohydrate digestion by mammalian mucosal α-glucosidases and its applications to hydrolyze the various sources of starches', *Food Hydrocolloids*, 87, pp. 470–476. doi: 10.1016/j.foodhyd.2018.08.033.

Spieth, L. E. *et al.* (2000) 'A low-glycemic index diet in the treatment of pediatric obesity', *Archives of Pediatrics and Adolescent Medicine*, 154(9), pp. 947–951. doi: 10.1001/archpedi.154.9.947.

Tissot, S. *et al.* (1990) 'Use of a new gas chromatograph isotope ratio mass spectrometer to trace exogenous 13C labelled glucose at a very low level of enrichment in man', *Diabetologia*. Springer-Verlag, 33(8), pp. 449–456. doi: 10.1007/BF00405104.

University of Georgia Complex Carbohydrate Research Center (2019) *The CCRC Spectral Database for PMAA's*. Available at: https://www.ccrc.uga.edu/specdb/ms/pmaa/pframe.html (Accessed: 3 April 2019).

Vasanthan, T. (2005) 'Enzymatic Quantitation of Total Starch In Plant Products', in *Handbook of Food Analytical Chemistry*, pp. 679–687. doi: 10.1002/0471709085.ch16.

Westphal, S. A., Gannon, M. C. and Nuttall, F. Q. (1990) 'Metabolic response to glucose ingested with various amounts of protein', *American Journal of Clinical Nutrition*. Narnia, 52(2), pp. 267–272. doi: 10.1093/ajcn/52.2.267.

Woodward, A. D. *et al.* (2012) 'Slowly digestible starch influences mRNA abundance of glucose and short-chain fatty acid transporters in the porcine distal intestinal tract', *Journal of Animal Science*, 90(SUPPL4), pp. 80–82. doi: 10.2527/jas.53877.

Yoshinaga, M. *et al.* (2004) 'Rapid increase in the prevalence of obesity in elementary school children', *International Journal of Obesity*, 28(4), pp. 494–499. doi: 10.1038/sj.ijo.0802608.

Zhang, G., Ao, Z. and Hamaker, B. R. (2006) 'Slow digestion property of native cereal starches', *Biomacromolecules*, 7(11), pp. 3252–3258. doi: 10.1021/bm060342i.

Zhang, G., Ao, Z. and Hamaker, B. R. (2008) 'Nutritional property of endosperm starches from maize mutants: A parabolic relationship between slowly digestible starch and amylopectin fine structure', *Journal of Agricultural and Food Chemistry*. Jiangsu Province, PR China, 56(12), pp. 4686–4694. doi: 10.1021/jf072822m.

Zhang, G., Venkatachalam, M. and Hamaker, B. R. (2006) 'Structural basis for the slow digestion property of native cereal starches', *Biomacromolecules*. American Chemical Society, 7(11), pp. 3259–3266. doi: 10.1021/bm060343a.

CHAPTER 4. RHEOLOGICAL AND STRUCTURAL PROPERTIES OF SLOW DIGESTING α-GLUCANS

4.1 Abstract

α-Glucans were previously screened *in vitro* and in humans for slowly digestible properties. To incorporate these slow digesting carbohydrates into food products, material and structural characteristics were analyzed to determine potential effects on processing. Slowly digestible carbohydrates were analyzed for rheological properties and secondary structural conformations. It was determined that alternan exhibited polydisperse coil conformation by the Kratky plot, and self-assembled into dense spherical secondary conformations in water at low concentrations; shear thinning was observed at 10% concentration and may be due to entanglement. Dextran exhibited a shear thickening behavior at 50°C, potentially due to helical agglomeration or association of many dextran molecules, and possibly due to branching, as when analyzed by light scattering with goniometer were more open structured compared to the other α-glucans analyzed. Agglomeration of carbohydrates in foods could affect processability, as well as rate of hydrolysis into glucose in the body, and this research suggests that the shear thickening behavior of alternan and dextran indicate that these interactions need to be considered when including these ingredients in food systems.

4.2 Introduction

The impact of dietary carbohydrates on blood glucose, often referred to as glycemic index or response, is of nutritional and physiological importance. This is due to the influence on controlling and preventing hyperglycemia-related diseases, such as diabetes and cardiovascular diseases (Frost *et al.*, 1999; Liu *et al.*, 2000; Rizkalla *et al.*, 2004; G. *et al.*, 2008). Slowly digestible carbohydrates (SDCs) is a broad term for all digestible or available dietary carbohydrates with a slow digestion property. The most studied slowly digestible carbohydrate is starch and this term relates in this case to structural properties of the food matrix, presence and type of plant cell walls, as well as nature of starch granules (Englyst, Kingman and Cummings, 1992; Englyst and Englyst, 2005). It has previously been shown that larger molecular size contributes to slower glucose hydrolysis (Eerlingen, Deceuninck and Delcour, 1993; Eerlingen and Delcour, 1995). Increased

glucan size, whether due to retrogradation, enzymatic modification, or natural occurrence is inversely related to digestibility by gastrointestinal tract enzymes. It is known that rheological behavior of digesting polysaccharides impacts gastric emptying rate, which if slowed modulates glycemic response and prolongs satiety (Lentle and Janssen, 2008). In addition to physiological effects related to dietary carbohydrate rheological properties and structural conformations, processing conditions must be considered when evaluating new ingredients for a food product. Low viscosity and high flow behavior are important to achieve good processing of materials, as well as in taste and texture for consumer acceptance.

This chapter focuses on the functional and structural characteristics of α-glucan oligo- and polysaccharides screened in Chapter 3 for slow digesting properties. Shear viscosity and light scattering (goniometric and multi-angle) were measured to determine if there are molecular interactions or agglomeration that would impact the rate of digestion, or processing capacity in a food or beverage system. Below critical concentrations, most polysaccharides form random coils in a disordered fashion that behaves as a Newtonian fluid (Phillips, 2009). At higher concentrations, molecules come into contact and become less mobile by restricted movements, generating entangled molecules with larger aggregate size (Sworn, 2004). We hypothesized that molecular interactions at higher concentrations in solution could result in these entangled and aggregated structures with larger sizes. Molecular interaction and entanglement could result in impeded digestion rate by native α-amylase and α-glucosidases, as well as resulting in a change in viscosity that would affect function of these novel glucans in a finished product after processing. This effect is observed in the research presented here, and these results must be considered for successful incorporation of these slowly digestible α-glucans into food products.

4.3 Materials and methods

Eight carbohydrates were selected based on *in vitro* and clinical trials resulting in a set of α-glucans with a range of digestion profiles, utilizing raw wheat starch (Sigma Aldrich, St Louis, MO, USA) as a slow digesting control as well as a glucose-containing syrup with a dextrose equivalence (DE) of 40 (DE40). Molecular size and linkage (Table 7 , Figure 12, and Figure 13) information was previously gathered from experiments using MALS and GC-MS. Test α-glucans included reuteran, dextran, raw wheat starch, isomaltooligosaccharides (Vitafiber™, BioNeutra Inc., Canada), resistant dextrins (Promitor® 70, Tate & Lyle PLC, London, UK),

alternanoligosaccharides (Fibermalt™, Evoxx Technologies GmBH, Germany), and alternan (Evoxx Technologies GmBH, Germany) (Table 4).

4.3.1 Experiment 1: Sheer viscosity analysis of novel α-glucans

Sample preparation

Solutions of each glucan (10 and 20%, w/v) were prepared in purified water with 0.002% sodium azide and stirred with magnetic stir bar at 27℃ for 1 h to ensure full dissolution. alternan solutions (5 and 10%, w/v) were prepared in purified water with 0.002% sodium azide and stirred with magnetic stir bar for 3 h at 27℃.

Experimental apparatus and measurement procedure

A rheometer (ARG2 from TA Instruments, USA) fitted with a Peltier steel plate and using a cone and plate geometry with a 60 mm diameter cone (54 µm truncation; Cone angle 2°) was used to measure viscosities of the above solutions at temperatures 25, 50, and 70℃. The system temperature was controlled via a water bath system, to aid the control of the Peltier plate. Flow sweep tests using shear rate changes were set by a logarithm ramp in a range 0.1 to 500 s^{-1} and 500 to 0.1 s^{-1} for each temperature selected. A solvent trap filled with water was used to minimize water loss during the experiment.

4.3.2 Experiment 2: Secondary structural conformation of three novel α-glucans using light scattering

Fraction collection by HPSEC

Solutions 1%, w/v) were made of substrates (alternan, reuteran, dextran) in sodium phosphate buffer (100 mM, pH 6.0, 0.005% sodium azide). Substrate solutions were passed through a 1.2 µm nylon filter and injected into a 200 µl loop of the HPSEC system equipped with degasser (Shimadzu, Japan) and a Sephacryl® S-500HR (GE Healthcare Life Sciences, USA) column. Fractions were collected at the highest point of the first eluted peak, in order to collect the largest MW fraction of each α-glucan.

Z-average radius of gyration analysis by multi-angle light scattering (MALS)

Z-average mean square radius (R_z) from MALS was analyzed and used as a comparison to confirm light scattering radius of gyration (R_g). Samples were purified by dissolving 20 mg sample in 2 ml of boiling DMSO for 1 h, followed by stirring for 12 h at room temperature. Then, 12 ml of ethanol was added to precipitate the carbohydrates. The supernatants were discarded, and the pellets were dissolved in 1 ml of water. Samples were filtered through a 5 μm filter and injected into a 100 μl loop of the Wyatt DAWN HELEOS-II/OPTILAB MALS system (Wyatt Technology, USA) equipped with Agilent analytical OH-60 and OH-40 (Agilent, USA) or Sephacryl® S-500HR (GE Healthcare Life Sciences, USA) columns. The results were analyzed using Astra 5.3.4.14 software (Wyatt Technology, USA).

Static and dynamic light scattering measurements by goniometer (SLS and DLS)

R_g, R_z, hydrodynamic radius (R_h), Rho, and secondary structural conformation were analyzed with light scattering using Kratky and Zimm plots. Light scattering measurements were performed at 25°C with a goniometer (CGS-3, ALV, Germany) at angles 30-150° and a correlator (ALV-5000, Germany). The light source was a helium-neon laser (λ_0=633 nm, 22 mW). R_h and R_z measurements were taken over 10 s in 3 sets at each angle and values are extrapolated to zero angle. The effective diameter was determined using the method of cumulants. R_g measurements were taken at angles 30-150°, as well in 10° steps. All light scattering analyses were repeated a minimum of three times, using the same sample.

4.4 Results and discussion

4.4.1 Shear viscosity

The Power Law model was used to describe the flow curves (either shear stress vs shear rate or viscosity vs shear rate flow curves), which is given by the equation below:

$$\text{Equation 1:} \tau = k\dot{\gamma}^n$$

or its equivalent form in terms of the apparent viscosity, μ_{app}

$$\text{Equation 2:} \mu_{app} = k\dot{\gamma}^{n-1}$$

Two parameters are involved in the model, the flow index, n, and the consistency index, k. The flow behavior index provides an indication of the rheological behavior of the liquid, where values of n=1 indicate a linear behavior between the shear stress, τ and the shear rate $\dot{\gamma}$ or by examining Equation 2, a constant apparent viscosity which in this case agrees with the consistency index. Liquids with this behavior are known as Newtonian liquids. If $n < 1$, the behavior of the liquid is known as pseudoplastic or shear thinning and is experimentally observed when the viscosity of the liquid decreases with the shear rate. Conversely, a value of $n > 1$ indicates a viscosity that increases with increases of shear rate. Although it is a rheological behavior fairly rare among biological liquids, it has been observed in other type of liquids, which have been classified as shear thickening or dilatant fluids. Regardless of the type of behavior, the value of flow index n indicates a deviation from the Newtonian behavior (i.e. when n=1) whereas the consistency index, k, provides an indication of the viscosity of the liquid. Flow curves were obtained for all solutions. Results are presented in Table 9 and Figure 15.

Alternan solutions had a Newtonian behavior at a concentration of 5% and temperatures measured, and values of viscosities decreased with increasing temperature. At very low shear rates, only a slight shear thinning behavior was observed likely due to limitations in the instrument to measure viscosities at low shear rates. Thus. those values were not considered in the analysis. However, viscosity curves show that slight shear thinning continues at shear rates above 100 s^{-1}. n values, or flow behavior index, were very close to 1, and thus alternan can be considered Newtonian (as explained above). At 5% w/v, the consistency index, k, decreased when the temperature of the solution increased from 25 to 50°C. The behavior of the 5% liquid had a different pattern when the temperature increased from 50 to 70°C showing a more shear thickening behavior (increase of n) and an slight decrease in the viscosity (k value). 10% alternan exhibited increasing apparent viscosity (k) at shear rates 1 s^{-1}, and viscosity curves (Figure 15) show the same result. Fluid behavior as described by n (flow behavior index) is close to Newtonian at 25°C, though decreases with higher temperatures, indicating that shear thinning properties increase with increasing temperature.

Dextran k values decreased with increasing temperatures at both 10% and 20% concentrations. Slight shear thickening was observed at 10% 70ºC; n values and viscosity curves

indicate Newtonian behavior at 20% for all temperatures measured. Apparent viscosity (*k*) at shear rate 1 s^{-1} decreased with increasing temperatures for both 10 and 20%.

Alternanoligosaccharides exhibited shear thickening fluid behavior at 10% at 25 and 70°C, as well as at 20% 25°C; other temperatures and concentrations measured showed shear thinning behavior. Apparent viscosity at a shear rate of 1 s^{-1} (*k)* was very low for all measurements taken. This interesting viscosity profile of elevated initial viscosity and shear thinning behavior observed at 10% and 20%, but only at 50°C, could be due to molecular entanglement that occurs in that temperature range. This is an important consideration when choosing this as an ingredient for a processed food product that might undergo shearing during processing at or near 50°C.

DE40 exhibited a very low apparent viscosity with little variation at both concentrations and all temperatures. Flow behavior index indicated shear thinning at 10% w/v at 50°C and 20% concentration at 70°C, however viscosity curves (Figure 15) showed shear thickening. When plotted as shear stress vs shear rate, a slight shear thickening was observed with an upward opening parabola shape (not included) for all concentrations and temperatures. Shear stress measurements of DE40 syrup showed likely precipitation of the sample - perhaps due to water binding capacity of the glucose syrup at higher percentages.

Resistant Dextrins showed slight shear thinning behavior at 25°C at 20% concentration; all other temperatures at 20% w/v and all temperatures at 10% showed shear thickening behavior at shear rates above 50 (s^{-1}). At 10% resistant dextrin, solution showed minor decreasing apparent viscosity at shear rate 1 s^{-1} with increasing temperature. 20% resistant dextrin solutions also exhibited decreasing apparent viscosity at shear rate 1 s^{-1} with increasing temperature, Newtonian at 20°C and shear thickening at higher temperatures.

Raw Wheat Starch was shear thickening at 25 and 50°C and shear thinning at 70°C for both 10 and 20% concentrations, as indicated by flow behavior index (*n*) (Table 9) as well as viscosity curves. Apparent viscosity at shear rate 1 s^{-1} markedly increased at 70°C for both 10 and 20% w/v solutions, which was attributed to gelatinization occurring near 65°C, causing a phase transition (Allan, Rajwa and Mauer, 2018). Additionally, the initial apparent viscosity, as well as viscosity curves of wheat starch show much higher viscosity at 70°C and 20% than at 10% concentration at the same temperature. This is likely due to evaporation occurring during the experiment, despite the use of a solvent cap.

Reuteran was shear thinning and higher viscosity at all temperatures at 20%, and shear thickening and relatively lower viscosity at 10% w/v. At 10%, reuteran exhibited close to Newtonian behavior at 25°C, with more dramatic shear thickening behavior observed at 50 and 70°C. Shear stress data confirms 10% reuteran apparent viscosity at shear rate 1 s^{-1} remains relatively stable at all temperatures, Newtonian behavior is confirmed from shear stress data at 10 and 20%, with slight dilatant behavior at 10% and slight pseudoplasticity at 20% w/v.

Isomaltooligosaccharides showed slight shear thickening at both 10 and 20% at all temperatures. At 10 and 20% at all temperatures, Isomaltooligosaccharides exhibited slight dilatant behavior with increasing temperatures for both concentrations, likely due to unavoidable evaporation occurring at those higher temperatures. Apparent viscosity at shear rate 1 s^{-1} remained very low for all conditions and isomaltooligosaccharide solution concentrations.

As evidenced in Figure 15 and Table 9, while some of the substrates included in this report exhibited weak shear thickening behavior, the majority of the α-glucans considered were near to Newtonian fluid in their behaviors. Wheat starch was the exception, exhibiting shear thickening behavior at higher temperatures to the point that shear force disrupted starch granules past the shear thinning point (Bagley and Christianson, 1982; Steeneken, 1989). It is hypothesized that the slight shear thickening behavior of these substrates is due to the asymmetricity of their molecular conformation in aqueous solutions, or that the concentrations of the substrates measured were insufficient to affect viscosity. Further, shear thickening could be due to molecular entanglement. Secondary structural conformation in aqueous solutions, including radius of gyration, are reported below in DLS results for reuteran, dextran, and alternan, as these were the most promising novel α-glucans for slow digestion.

Table 9. The Power Law parameters for novel α-glucan solutions. k: consistency coefficient (Pa sn); n: flow behavior index (mean ± SD).

Samples		k(Pa s^n)	*n*	R^2	*k*(Pa s^n)	*n*	R^2
		5% w/v			10% w/v		
Alternan	25°C	0.022±0.000	1.018±0.001	1.000±0.000	0.033±0.001	0.901±0.016	1.000±0.000
	50°C	0.000±1.039	1.039±0.006	0.999±0.000	0.042±0.012	0.846±0.050	0.999±0.001
	70°C	0.000±1.044	1.044±0.036	0.998±0.000	0.101±0.050	0.630±0.068	0.993±0.004
		10% w/v			20% w/v		
Dextran	25°C	0.003±0.000	1.003±0.006	1.000±0.000	0.011±0.003	0.958±0.035	1.000±0.000
	50°C	0.002±0.000	1.028±0.017	0.999±0.001	0.006±0.002	0.951±0.048	0.999±0.001
	70°C	0.001±0.000	1.054±0.009	0.998±0.000	0.003±0.000	1.000±0.005	1.000±0.000
Alternanol igosaccharides	25°C	0.001±0.000	1.055±0.047	0.998±0.002	0.002±0.000	1.034±0.005	0.999±0.000
	50°C	0.012±0.001	0.627±0.009	0.968±0.006	0.004±0.002	0.825±0.032	0.328±0.560
	70°C	0.001±0.000	1.093±0.084	0.990±0.007	0.001±0.000	0.964±0.024	0.001±0.000
DE40	25°C	0.001±0.000	1.044±0.014	0.997±0.000	0.002±0.000	1.028±0.002	0.999±0.000
	50°C	0.001±0.000	0.974±0.006	0.979±0.002	0.001±0.000	1.040±0.002	0.994±0.000
	70°C	0.000±0.000	1.103±0.010	0.991±0.001	0.001±0.000	0.980±0.059	0.985±0.006
Resistant Dextrin	25°C	0.002±0.001	0.993±0.055	0.998±0.001	0.004±0.001	0.925±0.065	0.999±0.001
	50°C	0.001±0.002	1.026±0.138	0.973±0.039	0.001±0.000	1.046±0.024	0.995±0.002
	70°C	0.000±0.000	1.133±0.013	0.992±0.001	0.001±0.000	1.036±0.011	0.993±0.003
Raw Wheat Starch	25°C	0.001±0.000	1.111±0.018	0.994±0.002	0.002±0.000	1.066±0.046	0.993±0.005
	50°C	0.001±0.000	1.167±0.030	0.994±0.001	0.001±0.000	1.148±0.029	0.992±0.004
	70°C	0.236±0.079	0.877±0.029	0.988±0.003	108.210±3.340	0.314±0.011	0.990±0.012
Reuteran	25°C	0.002±0.000	1.032±0.000	0.999±0.000	0.032±0.003	0.885±0.011	0.998±0.000
	50°C	0.001±0.000	1.064±0.004	0.998±0.000	0.015±0.005	0.926±0.045	0.999±0.000
	70°C	0.001±0.000	1.071±0.024	0.997±0.001	0.019±0.002	0.841±0.003	0.999±0.000
Isomaltooligosaccharides	25°C	0.001±0.000	1.044±0.015	0.997±0.001	0.002±0.000	1.014±0.019	0.998±0.001
	50°C	0.001±0.000	1.114±0.009	0.996±0.001	0.001±0.000	1.081±0.006	0.997±0.000
	70°C	1.000±1.732	1.145±0.019	0.992±0.002	0.001±0.000	1.091±0.007	0.994±0.002

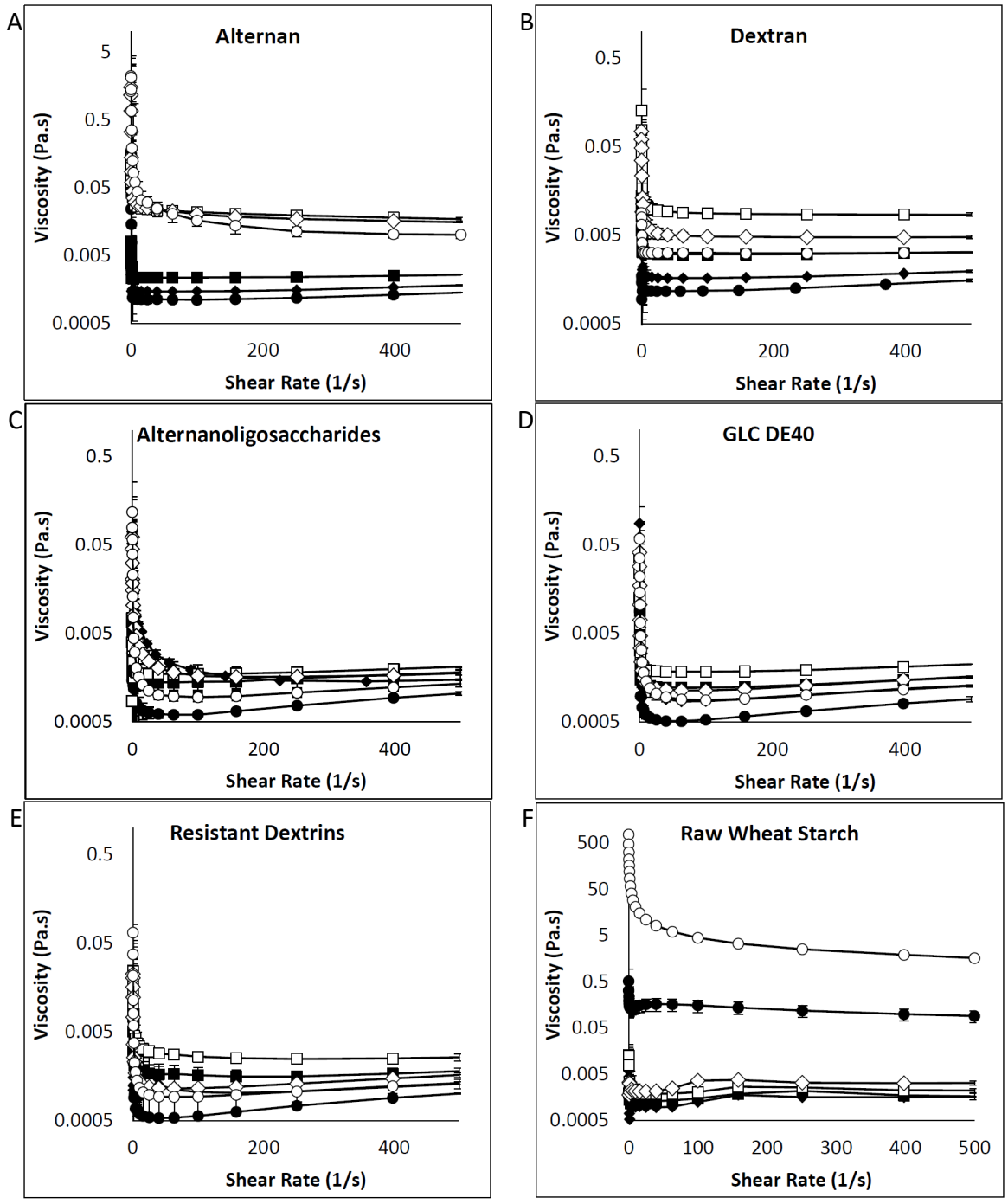

Figure 15. Viscosity versus shear rate plots for A: 5 and 10% Alternan, B: 10 and 20% Dextran, C: 10 and 20% Alternanoligosacharides, D: 10 and 20% DE40, E: 10 and 20% Resistant dextrin, F: 10 and 20% Raw wheat starch, G: 10 and 20% Reuteran, H: 10 and 20% IMO Isomaltooligosaccharides (mean ± SD).

Legend: Alternan: ■ 25˚C 5%; ♦ 50˚C 5%; ● 70˚C 5%; □ 25˚C 10%; ◊ 50˚C 10%; ○ 70˚C 10%.

All other glucans: ■ 25˚C 10%; ♦ 50˚C 10%; ● 70˚C 10%; □ 25˚C 20%; ◊ 50˚C 20%; ○70˚C 20%

Figure 15. continued.

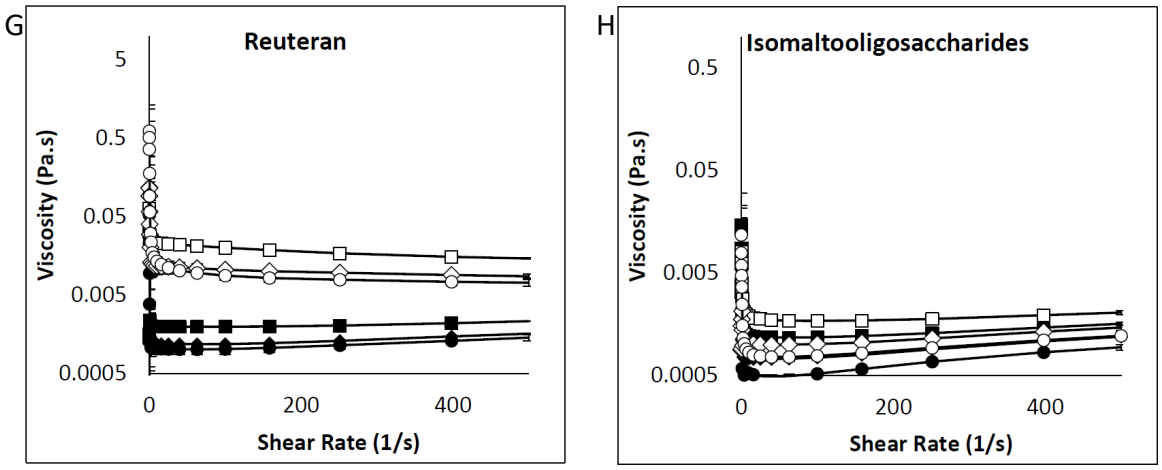

4.4.2 Structural conformation with light scattering

Light scattering was previously shown by Gallant et. al. (Gallant, Bouchet and Baldwin, 1997) to be useful in determining the angular dependence of light scattered from starch solutions. Size information at a specific angle can be determined by a cumulants analysis. Dynamic scattering provides R_h of a molecule (Gallant, Bouchet and Baldwin, 1997), but not R_g $(S^2)\frac{1}{2}$ as calculated by SLS. The relationship between R_h and R_g is complex and depends on the polymer type, solvent, and conformation; therefore R_h and $(S^2)\frac{1}{2}$ are essentially independent indicators of the starch conformation, branching, and connectivity (Sheridan *et al.*, 2002). Table 10 shows hydrodynamic radius, radius of gyration, and Rho for the three α-glucans.

Alternan exhibited polydisperse coil conformation when examined by Kratky plot, and self-assembled into dense spherical secondary conformations in water at low concentrations (Rho 0.762613), as shown in Figure 16. These results show that there is likely a diffusion coefficient, a way to parameterize the area of a spherical surface, over the angles the sample was analyzed at. This self-assembly into larger conglomerates explains the shear thinning behavior observed at 10% concentration at 70°C.

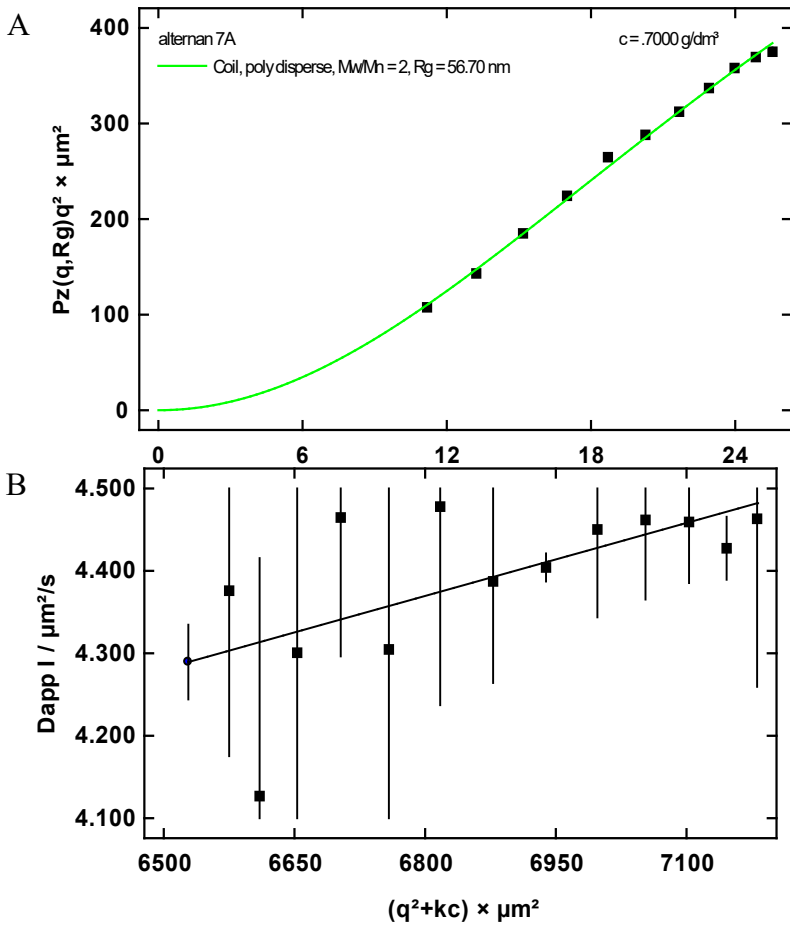

Figure 16. Alternan light scattering analysis shows polydisperse coils by Kratky plot

Light scattering analysis of reuteran (Figure 17) provided inconclusive information regarding secondary structural conformation, and better scattering is needed to have any confidence in results; it is likely that the structure conforms in a spherical fashion (Rho 0.708179) close to a coil.

By Kratky plot, reuteran follows a dense spherical structure, however this could be erroneous due to the small Rho value obtained in this analysis. As reuteran was found to be Newtonian at all temperatures and concentrations measured, it is unlikely that there is significant inter-molecular interaction at play that would need to be considered when incorporating it into a new food system or matrix.

Table 10. Hydrodynamic radius (R_h) (nm), Radius of gyration (R_g) (nm) calculated, and Rho for three novel α-glucans by DLS measurement.

	Alternan	Reuteran	Dextran
R_h dynamic (nm)	57.657	64.334	100.39
R_g static (nm) 1st observation	47.51	50.74	78.83
2nd	43.97	45.56	100.6
3rd	56.7	60.91	114.9
Rho	0.7626	0.7081	1.0020

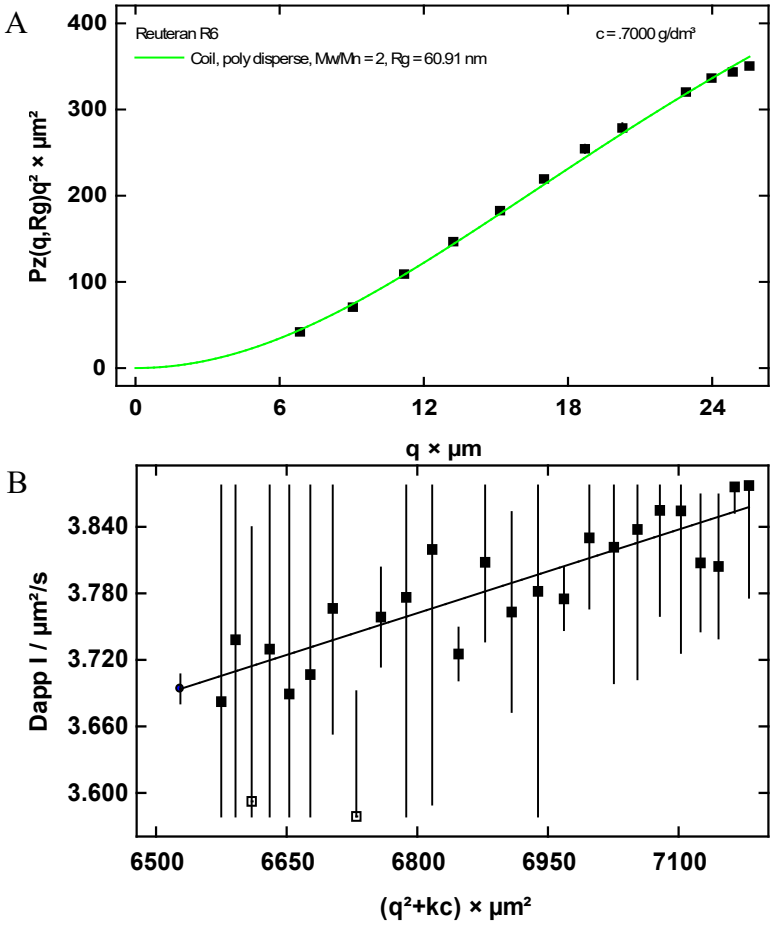

Figure 17. Reuteran light scattering analysis reveals dense spherical structure, but with a small Rho (0.718179) that indicates results to be inconclusive

Analysis of the largest fraction of dextran by light scattering showed a secondary structural conformation of branched or associated coils (Rho 1.002092 & 1.111728) (Figure 18). Kratky plot analysis confirmed this finding, indicating molecular configuration of polydisperse coils. Dextran samples analyzed were much more open structured compared to the other α-glucans analyzed, and with a shape factor greater than 1, a large molecular aggregation is indicated. This is potentially

due to helical formation or association of many dextran molecules together, possibly due to branching. Previous experiments showed that dextran is about 8% branching, with a molecular weight of 16,500 Da (Sections 3.5.2 and 3.5.4) The shape factor also indicates an outwardly radiating tertiary structural conformation, with agglomerated complex possibly reaching a size in the millions of daltons. This agglomeration of branched molecules into a larger structure explains the shear thickening at 50°C that was observed in 10 and 20% concentrations. This shear thickening due to association would need to be considered when incorporating dextran into a processed food, so that machinery such as blenders or nozzles with small sizes are not jammed due to increased viscosity under higher temperatures and shear rates.

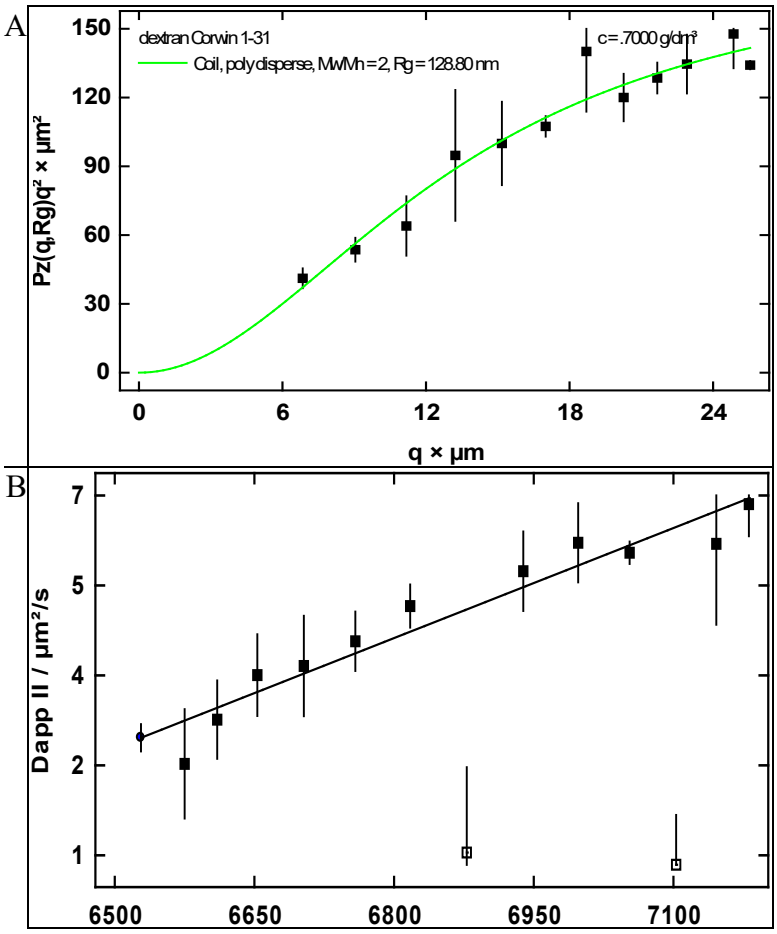

Figure 18. Dextran light scattering analysis reveals branched, polydisperse coils with larger agglomerations of molecules together into an outwardly radiating tertiary structure

This research, specifically the goniometric light scattering measurements, could be improved in future studies through denaturation of these α-glucan structures in NaOH/urea aqueous solution, as described by L. Zhang (Zhang, Zhang and Cheng, 2000; Fang *et al.*, 2015). This would provide a better understanding into the shape factor, double helical crystallinity, and agglomeration when there is less molecular entanglement and helical structure formation when in water as a solvent. Specifically, light scattering analysis of dextran after denaturation would provide further information on helical association of multiple molecules together.

Overall, the agglomeration of certain α-glucan helical structures into dense spherical structures could affect their processability as well as rate of hydrolysis by native α-amylase and α-glucosidase. Processing adjustments might need to be taken to adjust for molecular aggregation of alternan and dextrin because of their shear-thickening behaviors. Research presented in the next chapter will focus on examining potential changes in molecular conformation and interaction inter- and intra-molecularly of α-glucans in a model beverage system with other macronutrients to determine feasibility of incorporation into processing on conventional equipment typically used in food manufacturing, such as mixers, pasteurizers, and aseptic lines. It focuses on alternan and alternanoligosaccharides, due to the novelty of the chemical structures as well as the initial rheological results suggesting that intermolecular interaction does occurs.

4.5 References

Allan, M. C., Rajwa, B. and Mauer, L. J. (2018) 'Effects of sugars and sugar alcohols on the gelatinization temperature of wheat starch', *Food Hydrocolloids*. Elsevier B.V., 84, pp. 593–607. doi: 10.1016/j.foodhyd.2018.06.035.

Bagley, E. B. and Christianson, D. D. (1982) 'Swelling Capacity of Starch and Its Relationship To Suspension Viscosity-Effect of Cooking Time, Temperature and Concentration', *Journal of Texture Studies*, 13(1), pp. 115–126. doi: 10.1111/j.1745-4603.1982.tb00881.x.

Eerlingen, R. C., Deceuninck, M. and Delcour, J. A. (1993) 'Enzyme-Resistant Starch. II. Influence of Amylose Chain Length on Resistant Starch Formation', *Cereal Chemistry*, 70(3), pp. 345–350.

Eerlingen, R. C. and Delcour, J. A. (1995) 'Formation, analysis, structure and properties of type III enzyme resistant starch', *Journal of Cereal Science*. Academic Press, 22(2), pp. 129–138. doi: 10.1016/0733-5210(95)90042-X.

Englyst and Englyst (2005) 'Carbohydrate bioavailability', *British Journal of Nutrition*, 94(1), pp. 1–11. doi: 10.1079/bjn20051457.

Englyst, H. N., Kingman, S. M. and Cummings, J. H. (1992) 'Classification and measurement of nutritionally important starch fractions', *European Journal of Clinical Nutrition*. MRC Dunn Clinical Nutrition Centre, Cambridge, UK., 46(SUPPL. 2), pp. S33-50. doi: 10.1016/S0271-5317(97)00010-9.

Fang, Y. *et al.* (2015) 'Intermolecular Interaction and the Extended Wormlike Chain Conformation of Chitin in NaOH/Urea Aqueous Solution', *Biomacromolecules*. American Chemical Society, 16(4), pp. 1410–1417. doi: 10.1021/acs.biomac.5b00195.

Frost, G. *et al.* (1999) 'Glycaemic index as a determinant of serum HDL-cholesterol concentration', *Lancet*. Elsevier, 353(9158), pp. 1045–1048. doi: 10.1016/S0140-6736(98)07164-5.

Gallant, D. J., Bouchet, B. and Baldwin, P. M. (1997) 'Microscopy of starch: Evidence of a new level of granule organization', *Carbohydrate Polymers*. Elsevier, 32(3–4), pp. 177–191. doi: 10.1016/S0144-8617(97)00008-8.

González-Pérez, S. and Arellano, J. B. (2009) *Vegetable protein isolates*, *Handbook of Hydrocolloids: Second Edition*. Edited by G. O. Phillips and P. A. B. T.-H. of H. (Second E. Williams. Woodhead Publishing. doi: 10.1533/9781845695873.383.

Lentle, R. G. and Janssen, P. W. M. (2008) 'Physical characteristics of digesta and their influence on flow and mixing in the mammalian intestine: A review', *Journal of Comparative Physiology B: Biochemical, Systemic, and Environmental Physiology*, 178(6), pp. 673–690. doi: 10.1007/s00360-008-0264-x.

Liu, S. *et al.* (2000) 'A prospective study of dietary glycemic load, carbohydrate intake, and risk of coronary heart disease in US women', *American Journal of Clinical Nutrition*, 71(6), pp. 1455–1461. doi: 10.1093/ajcn/71.6.1455.

Livesey, G. *et al.* (2008) 'Glycemic response and health - A systematic review and meta-analysis: The database, study characteristics, and macronutrient intakes', *American Journal of Clinical Nutrition*, 87(1), pp. 258S-268S. doi: 10.1093/ajcn/87.1.223s.

Rizkalla, S. W. *et al.* (2004) 'Improved plasma glucose control, whole-body glucose utilization, and lipid profile on a low-glycemic index diet in type 2 diabetic men: A randomized controlled trial', *Diabetes Care*, 27(8), pp. 1866–1872. doi: 10.2337/diacare.27.8.1866.

Sheridan, P. F. *et al.* (2002) 'Computer simulations of hyperbranched polymers: The influence of the Wiener index on the intrinsic viscosity and radius of gyration', *Journal of Chemical Physics*, 117(16), pp. 7802–7812. doi: 10.1063/1.1507774.

Steeneken, P. A. M. (1989) 'Rheological properties of aqueous suspensions of swollen starch granules', *Carbohydrate Polymers*, 11(1), pp. 23–42.

Sworn, G. (2004) *Gums and stabilisers for the food industry*. Oxford: RSC Publishing.

Zhang, P., Zhang, L. and Cheng, S. (2000) 'Effects of urea and sodium hydroxide on the molecular weight and conformation of α-(1→3)-D-glucan from Lentinus edodes in aqueous solution', *Carbohydrate Research*. Elsevier, 327(4), pp. 431–438. doi: 10.1016/S0008-6215(00)00077-X.

CHAPTER 5. INTERACTIONS IN A BEVERAGE MODEL SYSTEM OF SLOWLY DIGESTIBLE ALTERNATING 1,3 AND 1,4-LINKED α-GLUCANS OF DIFFERENT SIZES

5.1 Introduction

The functional and physiological properties of modified carbohydrates greatly dictate their applicability in today's world of manufactured food products, especially as consumers become more focused on health effects of what they consume. Glycemic carbohydrates are ones that are fully digestible, completely hydrolyzed into monosaccharides by native salivary, pancreatic, and small intestinal mucosal enzymes. Carbohydrates with the largest impact on immediate blood sugar are α-glucans, comprised solely of glucose monomers linked only by fully digestible α-linkages. There are several diseases and co-morbidities associated with rapid fluctuations of blood sugar, which can be affected by the rate of digestion of carbohydrates. In individuals with poor glycemic control, pre-diabetes, and types I and II diabetes mellitus, this rate of α-glucan hydrolysis becomes even more important to management of health. It is well known that raw starch granules are slow digesting due to their crystalline structure (Englyst, Kingman and Cummings, 1992; Seal *et al.*, 2003; Tester, Karkalas and Qi, 2004), however raw starch is not a favorable ingredient in food that does not undergo heat treatment for microbial safety; it is very difficult to maintain crystalline structures of raw starch in products that do undergo heat treatment with any sort of moisture present. For these reasons, alternative ingredients with slow digesting properties that are not affected by heat or moisture during processing, and have a desirable mouthfeel, are a desirable addition to today's packaged foods.

Most commonly touted as containing slowly digestible carbohydrates (SDC) are nutritional food products marketed towards pre-diabetics and diabetics, especially ready to drink (RTD) nutritional beverages; these commonly contain tapioca maltodextrin. It is important to continuously examine new ingredients for functionality, physically and physiologically – in this study we examine novel enzymatically-modified α-glucans previously shown to be slow digesting in both *in vitro* and human studies, without offensive mouthfeel or texture. There are alternating α-glucan chains of 1,6-1,3, above a certain molecular weight we have previously shown to digest too slowly to be classified as SDC (Zhang and Hamaker, 2009; Lee and Hamaker, 2017). This may

be due to double helical conformation or aggregation that occurs with longer molecular chains, which impedes digestion.

It is important to consider hydrolysis rate as impacted by other ingredients in processed foods, as often ingredient-ingredient interaction can effect enzymes such as in amylo-lipid complexes (Tester, Karkalas and Qi, 2004; Ahmadi-Abhari *et al.*, 2013). The objective of the *in vitro* upper GI digestion portion of this study was to examine the rate of glucose hydrolysis by native α-glucosidases and α-amylases from novel α-glucans, as effected by the presence of salts in solution such as in a RTD nutritional beverage product.

Previously, the authors utilized an *in vitro* assay with rat intestinal acetone powder (RIAP) as a source of α-glucosidases and α-amylase. In the experiments presented below, α-amylase from porcine pancreas (PPA) (porcine pancreatic α-amylase; Megazyme, Wicklow, Ireland) is used with RIAP as an α-hydrolytic enzyme solution to ensure the rate of glucose generation mimics *in-vivo* processes as closely as possible.

This study also examined aggregation or chain length of SDC that may affect mouthfeel and texture, as well as interaction with other ingredients in a model beverage system that may impact rate of digestion. A simple model system (salts, carbohydrates, and soluble proteins) was utilized to determine if there is a change in material physical or functional property resulting from ingredient interaction.

It is well known that salt, depending on pH, can increase solubility resulting in dissociation, or decrease solubility of proteins often resulting in aggregation when solubility is decreased (Green, 1931). This phenomenon is very important for biological systems, but also is important to consider in the design of food and beverage systems. When proteins are strongly charged in solution due to pH, salts weaken electrostatic interactions by screening charges and consequently have an effect of electrostatic screening on protein properties (Xiong, 1992; Dahal and Schmit, 2018). Similarly, when in solution at pH near the isoelectric point with the net charge on a protein is small, salt weakens intermolecular interactions, thus increasing solubility (Tanford, 1961; Dahal and Schmit, 2018). In this experiment, dynamic and static light scattering were used to determine if molecular interactions (i.e. agglomeration) occurred with the alternan, tapioca maltodextrin, and alternanoligosaccharides with DP 7 and 15. Also, turbidity measurements of these glucans in water and DMSO were compared to determine differences in solubility. Decreasing solubility resulting

in increasing aggregation may influence rate of hydrolysis of native α-glucosidases and α-amylases through increasing entanglement impacting access enzyme catalytic sites to glucans.

5.2 Materials & methods

5.2.1 Novel α-glucan materials

Alternanoligosaccharides with DP 7 and DP 15 were generously gifted from Evoxx (Fibermalt® Evoxx Technologies GmbH, Monheim, Germany), alternan was created by CarbExplore (Groningen, Netherlands) with methods previously described, and Tapioca Maltodextrin was purchased from Ingredion, Inc (N-DULGE Ca1, Ingredion Inc, Westchester, IL, USA).

5.2.2 Molecular weight

Samples were dissolved in a 0.05 w/w Lithium bromide in DMSO solution, then filtered through a 0.45 μm filter and injected into a 100 μl loop of the Wyatt DAWN HELEOS-II/OPTILAB Multi Angle Laser Spectrometer system equipped with Shimadzu LC-10AT Vp Pump, Shimadzu SCL-10A Vp System Controller, Shimadzu SPD-10AV Vp UV/Vis Detector, and PSS 10,000 Å, 3,000 Å, and 30 Å columns (PSS Polymer Standards Service-USA Inc. Amherst, MA, USA) at a flow rate of 0.3 ml/min. The results were analyzed using Astra 5.3.4.14 software. R_z from MALS as described previously was analyzed and used as a comparison to hydrodynamic radius (R_h) from static and dynamic goniometric light scattering (SLS and DLS).

Specific refractive index increment, *dn/dc* was obtained from MALS with RI, but due to very small molecular weights of alternanoligosaccharides DP 7 and 15, are only presented for alternan (0.066 ml/g) and tapioca maltodextrin (0.066 ml/g).

5.2.3 Light scattering measurements

One percent solutions of alternan, tapioca maltodextrin, and alternanoligosaccharides were prepared in purified filtered water with 0.002% sodium azide, stirred with a magnetic stir bar at 75°C for 30 min to ensure full dissolution. Solutions of alternan, tapioca maltodextrin, alternanoligosaccharides were also prepared using the same methods with the addition of 0.133%

salts prior to stirring at 75°C for 30 min. Salt solution was comprised of dimagnesium phosphate, sodium chloride, and tricalcium phosphate (Sigma Aldrich, Darmstadt, Germany) in a ratio of 11:33:56. Solutions were made based on RTD nutritional beverages, using a ratio of 3% carbohydrate to 0.4% total salts.

Solutions were passed through a 0.45µm, nylon syringe filter prior to injection (200 µl loop) of an HPSEC system equipped with degasser (Shimadzu, Japan) and Sephacryl S-500 HR (GE Healthcare Life Sciences, USA) column. The largest molecular weight fraction of each α-glucan was then collected at the highest point of the first peak eluted. Solutions were diluted further as necessary to adjust for the correct light scattering sensitivity range.

Sample preparation & fraction collection by HPSEC

Hydrodynamic radius, R_g, R_z, Rho, and secondary structural conformation were analyzed with light scattering using Zimm, Berry, and angle-dependent plots. Measurements were taken with a goniometer (CGS-3, ALV, Germany) at 25°C at angles 30-150° and a correlator (ALV-5000, Germany); a helium-neon laser (λ_0=633 nm, 22 mW) was used as a light source.

Measurements of R_h using DLS were determined by the z-averaged diffusion coefficient of samples using the viscosity of water as the continuous phase. Measurements of R_h and R_z were taken over 10 seconds in 3 sets at each angle, and values were extrapolated to zero angle. Effective diameter was determined with the method of cumulants. Measurements of R_g were taken at 30-150° angles, in 10° increments. Berry plots were used for tapioca maltodextrin, and Zimm plots for all other analyses. Analyses were collected in triplicate, using the same sample.

5.2.4 Hysteresis loop areas and viscoelastic measurements.

Samples were dissolved in purified DI water, and solubilized at 70ºC for 30 min, using a magnetic stir bar and plate, and then allowed to cool at 4ºC 24 h to eliminate air bubbles, as well as to allow for potential aggregation to occur. Model system solutions were made from carbohydrates (variable), proteins, and salts solutions. Protein solutions consisted of a 28:55:17

w/w/w ratio of calcium caseinate[7], 85% milk protein concentrates[8], and soy protein[9], respectively. Salt solution was comprised of dimagnesium phosphate, sodium chloride, and tricalcium phosphate in a 11:33:56 w/w/w ratio. Carbohydrates examined within the model system for ingredient interaction included tapioca maltodextrin, alternan, alternanoligosaccharide DP7, and alternanoligosaccharide DP15. Solutions were made based on aseptically packaged nutritionally fortified beverages marketed for blood glucose control, using 3% carbohydrate, 7% total protein, and 0.4% total salts.

A rheometer (ARG2 from TA Instruments, USA) fitted with a vane Peltier steel (28mm diameter, 42 mm height) and cup (30.4 mm diameter) geometry with a 4,000 µm operating gap was used to measure viscosities of the above solutions at 27 ℃. The system temperature was controlled via a water bath system, to aid the temperature control of the Peltier system. Two subsequent flow ramp tests using shear rate changes set by a linear ramp in a range 1 to 300 s^{-1} in a period of 300 seconds, following a linear decrease from 300 to 1 s^{-1} in 300 seconds, were used to collect a hysteresis loop, a characteristic of viscoelastic systems having shear dependent structure. This time dependent flow behavior was described by fitting forward ramp of shear stress versus shear rate experimental data to the Power law model.

5.2.5 Turbidity in water and DMSO

Samples were prepared in the same method as described above for rheological measurements. A linear reading range was determined using serial dilutions of the protein solutions from 0.01% to 1% (Figure 21). Model system solutions were then diluted 29x to obtain best accuracy of absorbance, based on the protein solution alone (~1.0 Abs at 450 nm).

Turbidity measurements for all solutions were determined using a SpectraMax 190 Absorbance Microplate Reader at wavelengths of 400 nm (Ryan *et al.*, 2012; Guo, Wang and Wang, 2018) and 450 nm (Rayate, 2018). Analysis of the samples was performed with disposable polypropylene microplates with 300 µl solution per well. Purified DI water was included in all readings as a blank well.

---

[7] Generous gift from The Milky Whey International, Inc, Missoula, MT, USA
[8] Purchased from The Milky Whey International, Inc, Missoula, MT, USA
[9] PROFAM825, Generous gift from Archer Daniel Midlands Company, Chicago, IL, USA

One percent (w/v) solutions of the four glucans in purified filtered water or 100% DMSO were prepared and stirred at 75°C, 1,000 RPM for 30 min to ensure samples were fully dissolved. A microplate spectrophotometer (SpectraMax 190 Absorbance Microplate Reader, Molecular Devices, LLC, San Jose, CA, USA) was used to detect absorbance of 300 µl of each solution at 400 and 450 nm.

5.2.6 Effect of α-amylase on carbohydrate digestion

Red Starch Assay kit (Megazyme, Wicklow, Ireland) was used to measure the activity of α-amylase in the crude and purified α-glucosidase solutions derived from rat intestinal powder. Pre-incubated at 37°C, red starch solution (50 µL, 2% w/v in 0.5 M KCl) was mixed with the α-glucosidase solution (100 µL) and incubated at 37°C for 10 min. The reaction was terminated by adding ethanol (250 µL, 95% v/v). The reaction tube was equilibrated at room temperature for 10 min and centrifuged at 1000 × *g* for 10 min. The change of absorbance was measured at 510 nm, and the α-amylase activity of the enzyme solutions was calculated using a standard curve of the activity of α-amylase from *Aspergillus niger* as a control. One unit of α-amylase activity was defined as the amount of enzyme required to generate 1 µmol of *p*-nitrophenol hydrolyzed from blocked *p*-nitrophenyl-maltoheptaoside per minute at pH 6.9 and 40°C.

To determine the effect of α-amylase on glucose generation during hydrolysis by α-glucosidases, different concentrations of porcine pancreatic α-amylase (PPA; Megazyme, Wicklow, Ireland) were added to the purified α-glucosidase solution and used together as an α-hydrolytic enzyme solution. WCS, maltodextrin DE10, and maltose were used as substrates for the α-hydrolytic enzyme solution. The sample solution (1% w/v) was prepared in 100 mM phosphate buffer (pH 6.8) and 6.7 mM NaCl, and then carbohydrate digestion was initiated by adding the α-hydrolytic enzyme solution at 37°C for 48 h, with shaking (160 rpm). For each sample, reactions were quenched at various time points, 1 h, 2 h, 4 h, 8 h, 12 h, 24 h, 36 h, and 48 h, by boiling. The amount of glucose released by hydrolysis was measured by the glucose assay kit at 510 nm.

5.2.7 Impact of salts on *in vitro* rate of glucose hydrolysis

To study the rate of hydrolysis by native mammalian mucosal α-glucosidases and pancreatic α-amylase as impacted by the presence of salts, α-glucan solutions were digested at 37˚C for 6 h, with shaking (160 RPM). *In vitro* digestion was performed using methods previously described (Shin *et al.*, 2019) using a suspension of crude ground RIAP, as described by Shin et al, as a source for mammalian mucosal α-glucosidases. 50 U/ml PPA as a source of α-amylase and 0.005% ampicillin salts to prevent microbial consumption of glucose were also included (Seo *et al.*, 2020). Digestia was comprised of 5% (w/v) RIAP, 50 U/ml PPA, 1% carbohydrate, and 0.005% ampicillin in a sodium phosphate buffer at pH 6.7; for each glucan, a variation with 0.133% salts (dimagnesium phosphate, sodium chloride, tricalcium phosphate in a ratio of 11:33:56) was also assayed. For each reaction, samples were collected at 15, 30, 45, 60, 120, 180, and 360 min and boiled for 5 min to inactivate enzymes. Inactivated samples were then centrifuged (Microfuge 20R Centrifuge, Beckman Coulter, Indianapolis, IN, USA) at 9160 × g for 10 min, and supernatant diluted 10x with DI water. The amount of glucose released during the reactions was measured using GOPOD Glucose Assay Kit (Megazyme, Wicklow, Ireland). Raw wheat starch was included as a slow digesting control, and maltose as a rapidly digesting control (Tester, Karkalas and Qi, 2004; Wang and Copeland, 2013).

5.2.8 Statistical treatment

Statistical analyses were conducted using Microsoft Excel (2005, Microsoft, Redmond, WA, USA) and TRIOS Software (v2.3.1.1477, TA Instruments, New Castle, DE, USA). Data is expressed as mean ± standard deviation. In all figures, error bars displayed represent the standard deviation from independent sample measurements. Turbidity measurements were performed in triplicate, with three wells per solution per reading; results presented are means with standard deviation error bars. *In-vitro* digestions were performed in triplicate, two times on two separate days; results presented include mcg/ml glucose as well as percent digestibility, calculated by adjusting mcg/ml glucose against glucose detected when maltose was digested for 180 minutes (to completion).

5.3 Results and discussion

5.3.1 Molecular weight and structural conformation with light scattering

When examined by light scattering, angular dependence of light scattering of starch has previously been shown (Gallant, Bouchet and Baldwin, 1997) to be helpful in determining internal rotation of branched polysaccharides. At a specific angle, size information can be determined by a cumulants analysis; dynamic scattering can provide R_h of a molecule, but not R_g $(S^2)\frac{1}{2}$ as calculated by SLS. R_h and R_g have a complex relationship that depends on the polymer, solvent, and conformation of the molecule examined. As such, R_h and $(S^2)\frac{1}{2}$ can be viewed as independent indicators of the structural conformation, branching, and connectivity of the molecule (Sheridan *et al.*, 2002).

Results indicated that 1% alternan exhibited a hard sphere form factor (R_g 35.29 nm, Rho 0.76261) in water with salts, with dense spherical secondary conformation (R_g 33.97 nm, Rho 0.69789) previously measured alternan in water without salts using the goniometer SLS. R_z from MALS with RI of alternan in DMSO, 34.9 nm, was close to the R_g from the goniometer SLS, indicating unlikely inter-molecular interactions at 1% concentration in water or DMSO.

One percent Tapioca maltodextrin samples with and without salts were analyzed using Berry model due to non-linear results with Zimm plot. Tapioca maltodextrin without salt displayed a spherical shape factor with Rho values illogical and indicative of an excessively large R_h for a single molecule. However, the R_z from MALS (21.4 nm) was significantly smaller than the R_g (89.94 nm) determined by DLS, and much smaller than what would be expected for a molecule of this size (942,300 Da). Tapioca maltodextrin in solution with salts (R_h 204.579 nm) had a shape factor indicating a spherical molecule, but the hydrodynamic radius was far too large for the radius of gyration indicated from MALS with DMSO. These results indicate there are likely intermolecular interactions that occurred resulting in aggregation when water was used as a solvent, further confirming the likelihood that aggregates were formed in water as it is not as strong a solvent as DMSO, as well as that there was likely increased aggregation of tapioca maltodextrin when in the presence of the salts used in this model system.

Alternanoligosaccharide DP 7 (coil shape factor, Rho 1.60492) and DP 15 (sphere shape factor, Rho 0.89171) in water both show hydrodynamic radii (17.303 and 37.4 nm) much larger

than the respective molecular weights obtained from HPSEC with MALS in DMSO would predict, and much smaller than in solution with salts. Results from light scattering of salt solutions with alternanoligosaccharide DP7 (R_h 23.459, Rho 1.31208, coil shape factor) and alternanoligosaccharide DP 15 (R_h 41.787 nm, Rho 0.81245, sphere shape factor) are appropriate for the MW observed from MALS. We can infer from this the likelihood of assemblies in water and not individual molecules. Scattering observed was low, and could contribute to error, where R_h and R_g could be reflecting a small sub-population of assemblies while the majority of alternanoligosaccharide structures were not assembled, but scattering was too little to contribute significantly to the signal.

DMSO, the eluent used for obtaining molecular weight of these structures, is well known to be a strong solvent of maltodextrins (Divers *et al.*, 2007) compared to water.

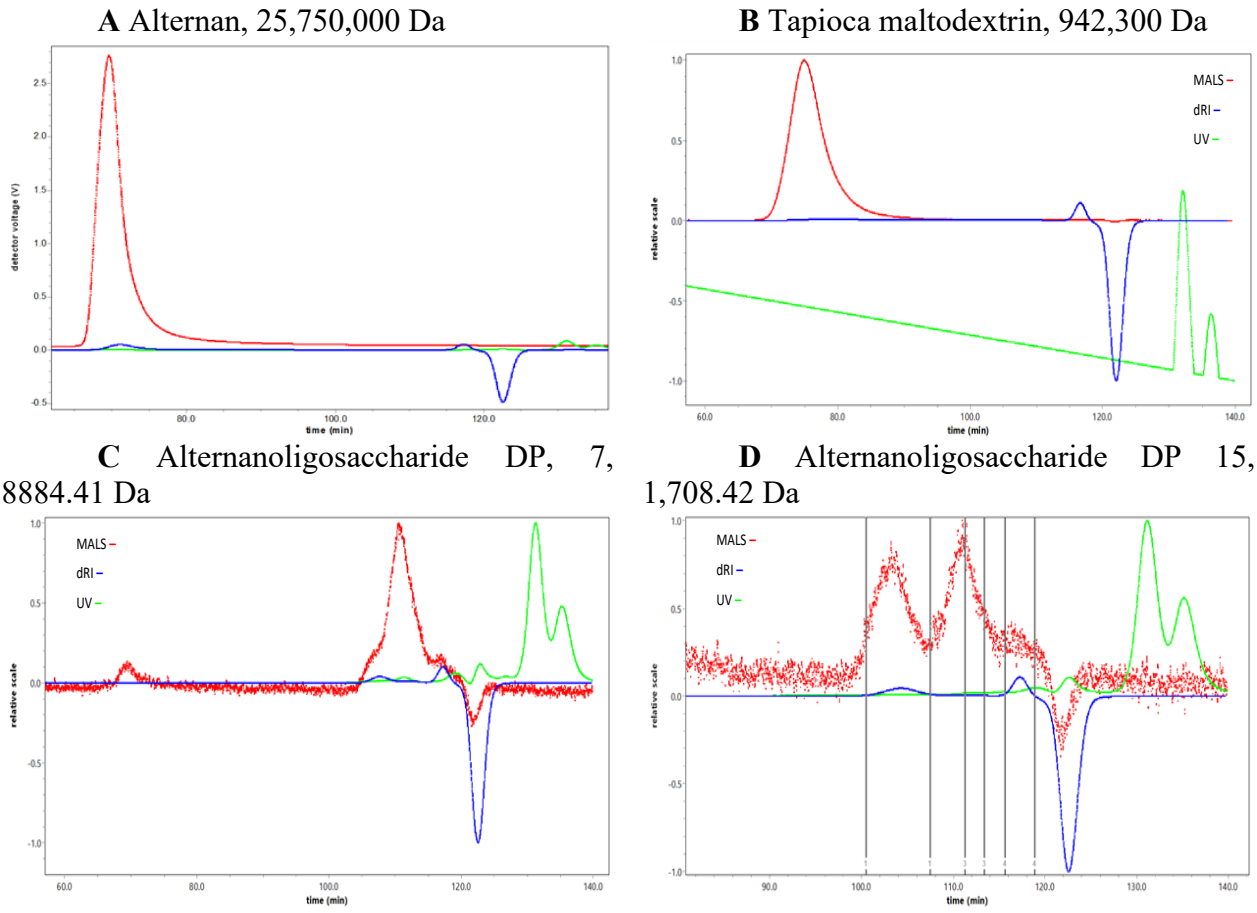

Figure 19. Molecular weight analyses by MALS with RI —LS; —dRI; —UV

Hysteresis loop area and shear viscosity

To describe the flow curves (shear stress v. shear rate or viscosity v. shear rate), the power model was used:

$$\text{Equation 3: } \tau = K\dot{\gamma}^n$$

Alternatively, its equivalent form in relation to apparent viscosity, μ_{app}

$$\text{Equation 4: } \mu_{app} = K\dot{\gamma}^{n-1}$$

The model involves the flow index, n which gives characterizing information about the deviation from the Newtonian behavior (i.e. when n=1), and the consistency index, K, which indicates the apparent viscosity of the sample at a shear rate of 1 s^{-1}.

When the value of n=1, a linear relationship between the shear stress τ and shear rate $\dot{\gamma}$ is noted and liquids with this behavior is known as Newtonian. The behavior of the liquid is known as pseudoplastic, or has shear thinning properties, if n<1 and is observed in a test in which the viscosity of the liquid decreases with increasing shear rate. When n>1, dilatant, or shear thickening, behavior is indicated such that the viscosity increases with increasing shear rate. While the occurrence of shear thickening or dilatant fluids is typically rare between naturally occurring bio-organic fluids, this behavior has been documented to occur with other types of liquids (Green, 1931; Barnes, 1989). The value of the flow index n indicates a departure away from Newtonian behavior (when n=1), whereas the consistency index K provides an indication of the viscosity of the liquid (Goodeve, 1939).

Viscosity data below shear rate 50 1 s^{-1} were discarded as they were below the lower limits of the equipment's accuracy. All data presented is representative of triplicates, with the exception of the following permutations of the model system solutions, for which duplicates are presented as one of the triplicates falls outside two standard deviations for the majority of data points collected in the flow ramps: proteins, alternan proteins and salts, tapioca maltodextrin, alternanoligosaccharides DP15. As evidenced in Table 11 and Figure 20, all solutions exhibited some shear thickening behaviors for which n >1. It is hypothesized that the shear thickening behavior of these substrates is due to the asymmetricity of the material molecular conformation in aqueous solutions. Further, shear thickening could be due to molecular entanglement occurring between carbohydrate ingredients and proteins in solution. Interestingly, for all glucans present in the model system shear thickening behavior of the glucan alone in solution was significantly

greater than glucan in the presence of salts. It has previously been shown that the presence of NaCl ions lower viscosity and yield stress while increasing solubility of soluble aggregates of thermally treated whey protein isolates (Xiong, 1992; Ryan *et al.*, 2012). Ryan et al. (2012) proposed a mechanism for the formation of denser aggregate particles with larger apparent hydrodynamic radii and particle size, in denatured proteins obtained from the spray drying process when salt is not present. However, when salt is present, soluble aggregates are less prone to have secondary interactions when heated because of their overall negative charge, more compact structure with less branching, and small size (Ryan *et al.*, 2012).

Rheological results from solutions containing only 0.4% salts were discarded due to limitations of the instrument at such low viscosities close to that of water; hysteresis was observed in these solutions despite the high improbability of it occurring, likely due to vortexes and turbulence (Taylor eddies) occurring during measurements. This solution is expected to have viscosity larger than water, which was used as a solvent for all model system permutations.

Smaller values of *K* were observed in the downward flow curve than in the upward flow curve, indicating a lower viscosity in the down phase. However, the *n* values for the downward flow ramps were significantly higher, indicating a stronger shear thickening effect with decreasing shear rate, *n*-values of the down curve were significantly greater than those of the upwards flow curve, indicating that it is likely that with increasing shear rate, further entanglement of long and/or highly branched protein and carbohydrate chains occurs, and as a result the intermolecular resistance to flow is increased (Barnes, 1989; Martínez *et al.*, 2015).

The hysteresis loop area was calculated by Equation 5 and indicates the area between the up-ramp (extending) and down-ramp (retracting) shear stress versus shear rate data, where *K* and *K'* are consistency coefficients, and *n* and *n'* are the flow behavior indices for up and down ramp measurements, respectively.

Equation 5: $$Hysteresis\ loop\ area = \int_{\gamma_1}^{\gamma_2} k\gamma^n - \int_{\gamma_1}^{\gamma_2} Kk'\gamma^{n'}$$

Structural bonds are destroyed with increasing shear stress, which leads to lower viscosity, indicated by the lower consistency indexes, during the down ramp (decreasing shear). The hysteresis loop area marks the difference between the structures at the beginning of the measurement procedure and the structure remaining after shear stress has been applied, and represents the energy consumed during breakdown and reformation of the structure of the samples. Equivalently, this can be applied to structural or aggregate breakdown (Sweeny and Geckler, 1954;

Horne, 1986; Sedlmeyer and Kulozik, 2006; Vicent, De, 2012). The hysteresis loop area for all model systems containing a glucan, proteins, and salts was higher, though not significantly, than any glucan alone in solution, or with either proteins or salts- this effect was especially pronounced in the model system using Alternan. Further, the area of hysteresis was much greater in a solution containing proteins alone than salt or proteins and salts. From these results we may infer that when large and highly branched glucans are in solution in the presence of soluble protein and salt, the large and highly branched carbohydrate structures could interact with the proteins as the solubility of proteins improve with increased electrolytes in solution resulting in structures that are more affected by the shear applied during the test.

These findings may help better inform formulation of beverages containing ionic salts, soluble aggregates of proteins, such as those produced by spray drying, and highly branched carbohydrate molecules that are likely to interact with such soluble protein aggregates.

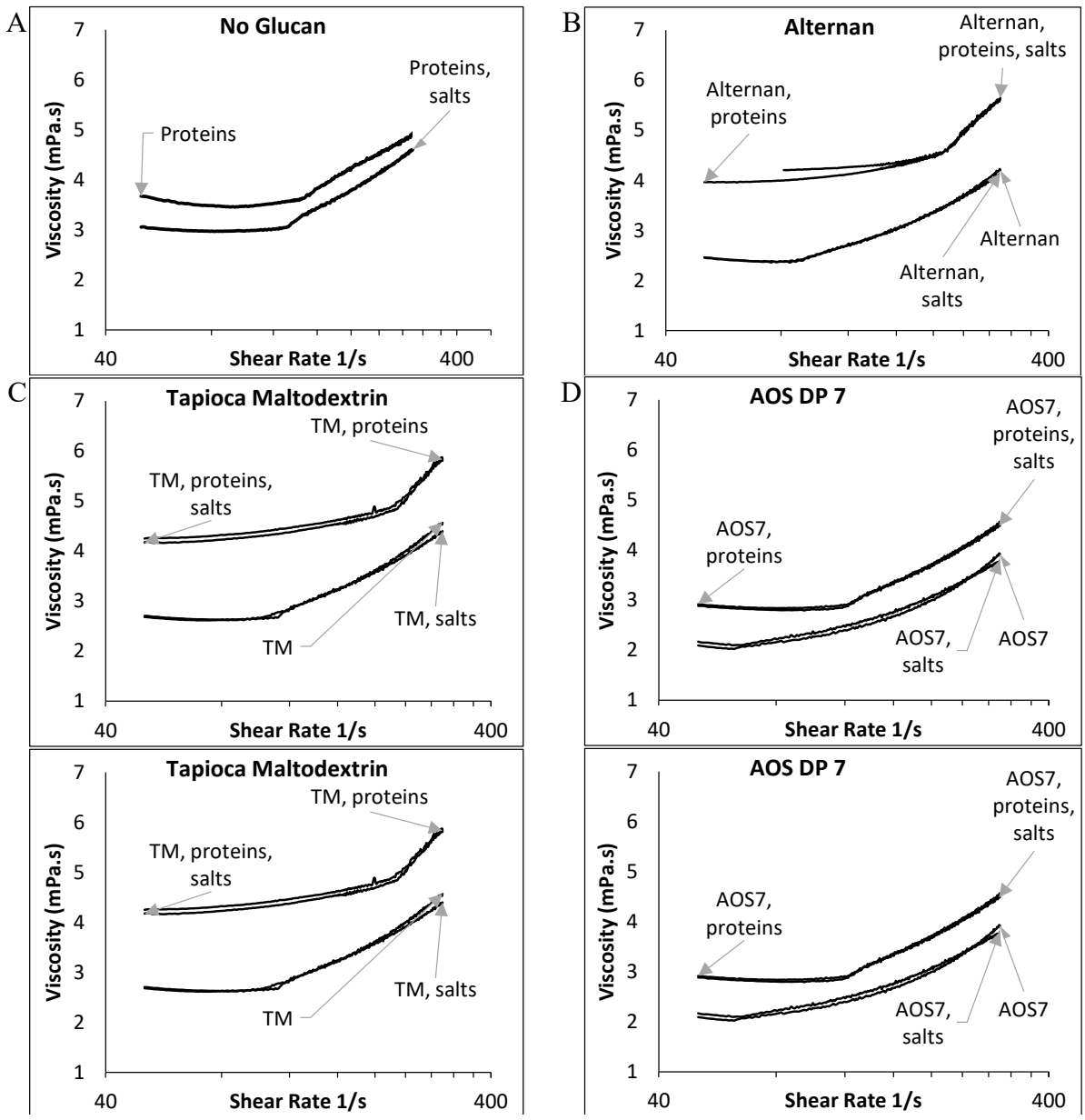
A
No Glucan
Proteins
Proteins, salts
B
Alternan
Alternan, proteins, salts
Alternan, proteins
Alternan
Alternan, salts
C
Tapioca Maltodextrin
TM, proteins
TM, proteins, salts
TM, salts
TM
D
AOS DP 7
AOS7, proteins, salts
AOS7, proteins
AOS7, salts
AOS7
Viscosity (mPa.s)
Shear Rate 1/s
40
400

E

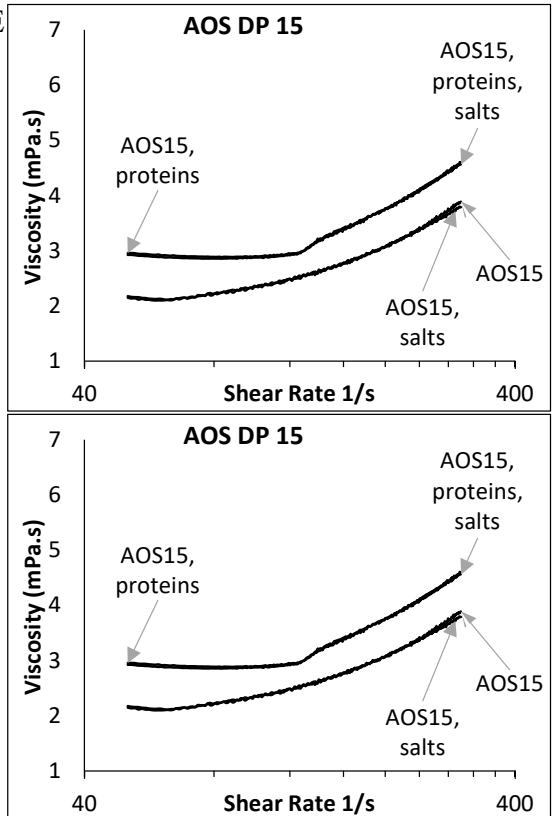

Figure 20. Up-ramp viscosity of model system solutions. A Alternan; B Tapioca Maltodextrin (TM); C Alternanoligosaccharides DP 7 (AOS7); D Alternanoligosaccharides DP 15 (AOS15). The coefficient of variance was below 5% and error bars are not included in the figures.

Table 11. The power law parameters for starch and model system component solutions. Assays were performed in triplicate, mean ± SD values. K: consistency coefficient (Pa.sn); n: flow behavior. Alternan, Tapioca Maltodextrin (TM), Alternanoligosaccharides DP 7 (AOS7), and Alternanoligosaccharides DP 15 (AOS15).

Samples		Hysteresis Loop Area	Upward Curve			Upward Curve		
Glucan	Model System Components	(Pa/s)	K (mPa.s^n)	n	R^2	K (mPa.s^n)	n	R^2
	7% PROTEIN	30.936 ± 0.535	1.000 ± 0.849	1.226 ± 0.007	0.992	0.200 ± 0.000	1.564 ± 0.001	0.999
	0.4% SALT AND 7% PROTEIN	23.230 ± 0.696	0.633 ± 0.208	1.293 ± 0.020	0.991	0.100 ± 0.000	1.603 ± 0.002	0.999
3% ALTERNAN		18.551 ± 0.692	2.000 ± 2.598	1.371 ± 0.007	0.995	0.070 ± 0.000	1.711 ± 0.002	0.999
3% ALTERNAN	0.4% SALT	21.582 ± 0.012	0.467 ± 0.058	1.363 ± 0.004	0.996	0.060 ± 0.000	1.744 ± 0.001	0.999
3% ALTERNAN	7% PROTEIN	22.439 ± 0.668	1.233 ± 0.723	1.200 ± 0.007	0.993	0.500 ± 0.000	1.408 ± 0.004	0.998
3% ALTERNAN	0.4% SALT AND 7% PROTEIN	26.783 ± 3.091	1.400 ± 1.414	1.161 ± 0.041	0.991	0.400 ± 0.000	1.428 ± 0.003	0.998
3% TM		13.934 ± 13.857	0.450 ± 0.071	1.369 ± 0.001	0.993	0.095 ± 0.007	1.650 ± 0.037	1.000
3% TM	0.4% SALT	22.025 ± 0.400	0.533 ± 0.115	1.345 ± 0.002	0.993	0.080 ± 0.000	1.690 ± 0.003	2.000
3% TM	7% PROTEIN	21.712 ± 2.695	1.533 ± 0.981	1.173 ± 0.009	0.995	0.633 ± 0.058	1.372 ± 0.007	0.999
3% TM	0.4% SALT AND 7% PROTEIN	22.493 ± 0.253	1.400 ± 0.866	1.178 ± 0.003	0.994	0.600 ± 0.000	1.375 ± 0.010	0.998
3% AOS DP7		15.773 ± 0.998	0.367 ± 0.058	1.401 ± 0.021	0.995	0.037 ± 0.006	1.818 ± 0.015	0.998
3% AOS DP7	0.4% SALT	21.631 ± 0.332	0.400 ± 0.000	1.370 ± 0.002	0.997	0.040 ± 0.000	1.796 ± 0.002	0.997
3% AOS DP7	7% PROTEIN	23.175 ± 0.052	0.600 ± 0.173	1.316 ± 0.006	0.992	0.100 ± 0.000	1.650 ± 0.004	0.999
3% AOS DP7	0.4% SALT AND 7% PROTEIN	23.258 ± 1.015	0.633 ± 0.208	1.318 ± 0.033	0.993	0.100 ± 0.000	1.666 ± 0.001	1.000
3% AOS DP15		18.199 ± 0.313	0.400 ± 0.000	1.385 ± 0.002	0.996	0.040 ± 0.000	1.787 ± 0.006	0.998
3% AOS DP15	0.4% SALT	20.729 ± 0.721	0.433 ± 0.058	1.369 ± 0.009	0.997	0.040 ± 0.000	1.798 ± 0.005	0.997
3% AOS DP15	7% PROTEIN	23.334 ± 0.185	0.600 ± 0.173	1.313 ± 0.008	0.992	0.100 ± 0.000	1.647 ± 0.000	0.999
3% AOS DP15	0.4% SALT AND 7% PROTEIN	23.320 ± 0.334	0.600 ± 0.173	1.318 ± 0.012	0.992	0.100 ± 0.000	1.654 ± 0.004	1.000

5.3.2 Turbidity to examine aggregation in water or DMSO solvents

Reduced turbidity of mixed samples at 450 nm typically indicates the domain of the solution had decreased scattering contrast, compared to individual domains of either solution (Figure 22) - this is a result of more solute and less aggregate in solution (Doty and Steiner, 1950; Horne, 1986). Due to differences observed of molecular weight and R_g between DLS, where water was used as a solvent, and MALS, where DMSO was the solvent, turbidity of the α-glucans studied in this work was examined at 1% concentration (w/v) in the different solvents, water or DMSO.

Turbidity of carbohydrates with salts or salts and protein when measured at 450 nm was higher than for either solution independently, suggesting there is an increase in aggregate formation among the test carbohydrates. Decreased turbidity observed with salts and proteins (lower than protein or salt alone) indicates likely interaction between the two solutes, resulting in improved solubility of the protein from the addition of salts weakening attractive interactions. Turbidity of samples containing tapioca maltodextrin, salts, and proteins (i.e. ingredients in the complete model system) resulted in lower observed absorbance than tapioca maltodextrin and protein alone, suggesting interaction between salts and proteins when tapioca maltodextrin is present that causes improved solubility (decreased aggregation). Hernandez et al (Gloria Hernández *et al.*, 2011) suggested a possibility of weak associative interactions between dextrans and caseinates, potentially a reduction in protein-protein aggregation, which may explain this result.

Interaction between maltodextrin and protein is likely exacerbated by salts in solution, potentially due to protein secondary structural conformation changes due to the presence of salts causing a change in ionic environment that further improves solubility (Tanford, 1961; Rendleman, 1967; Rayate, 2018). It is known that these inter-molecular interactions are driven by hydrogen bonding, and it isit likely that the initial attraction driving aggregation is hydrophobic interactions (Damodaran, Parkin and Fennema, 2008).

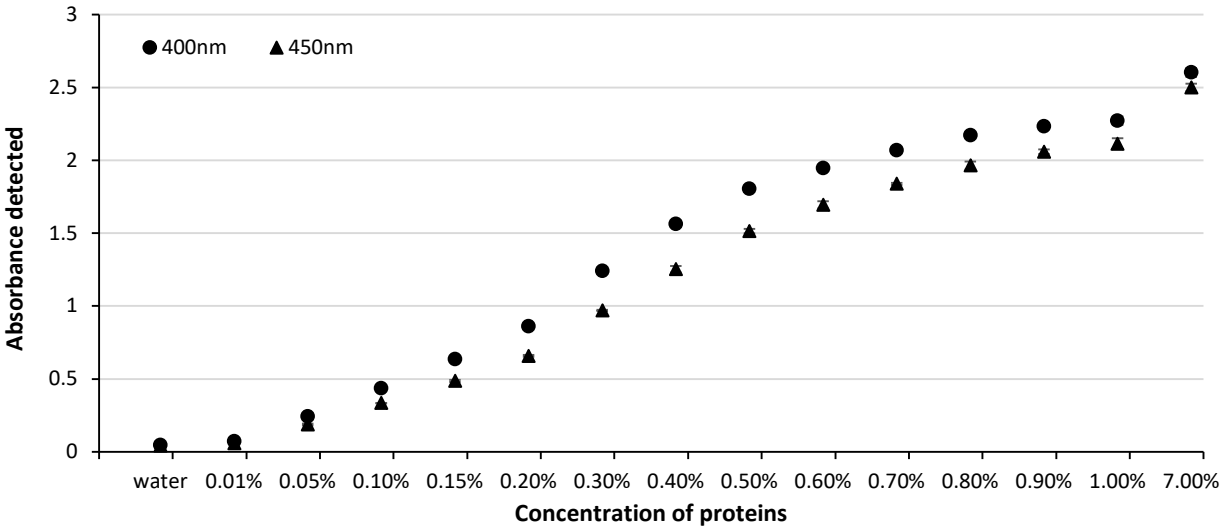

Figure 21. Linear Test for validity of absorbance range using protein solutions made from serial dilutions of a 1% protein solution.

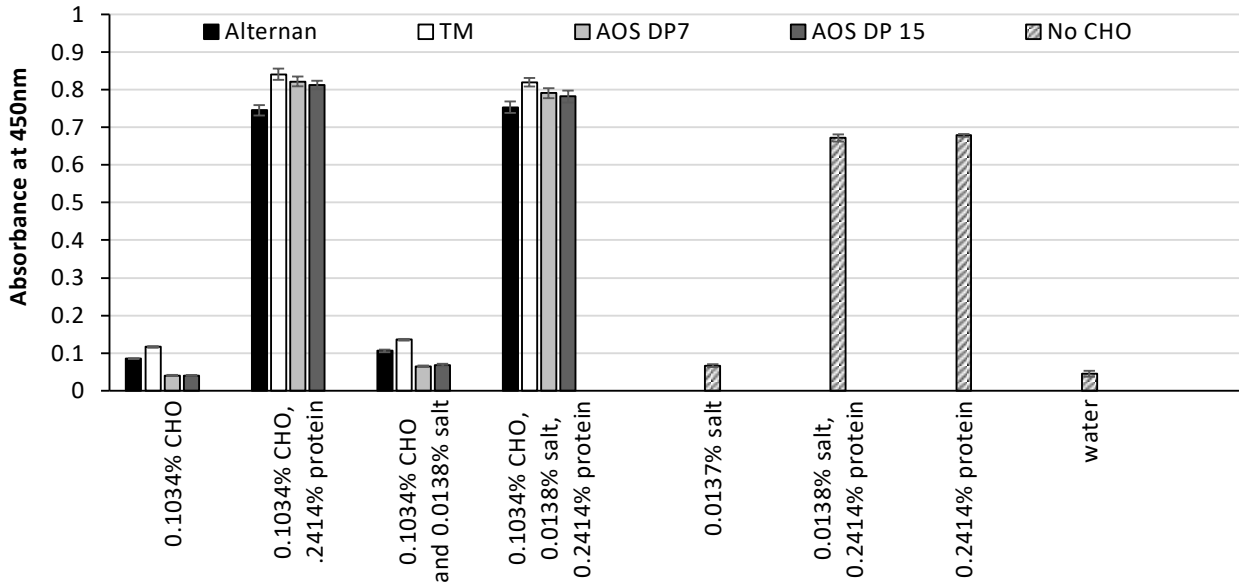

Figure 22. Turbidity of carbohydrate (CHO), protein, and salt mixtures measured at 450 nm for alternan, tapioca maltodextrin (TM), alternanoligosaccharides (AOS) DP 7 and 15, and no carbohydrate (no CHO).

When absorbance of solvents alone was accounted for (Figure 23), All of the α-glucans in DMSO showed significantly lower levels of turbidity than when water was the solvent. This effect was especially pronounced for alternan and tapioca maltodextrin, with absorbance of alternan in water nearly 4x higher than in DMSO, and the absorbance for tapioca maltodextrin in water over 10x higher than that in DMSO. As expected from little to no variation between results of

alternanoligosaccharides DP 7 and 15 from DLS and HPLC with MALS, there were very small but significant differences between absorbances detected when water versus DMSO was the solvent, with both oligosaccharides dissolving more completely in DMSO than water resulting in lower absorbances detected when absorbance of solvents was accounted for (Figure 23 B).

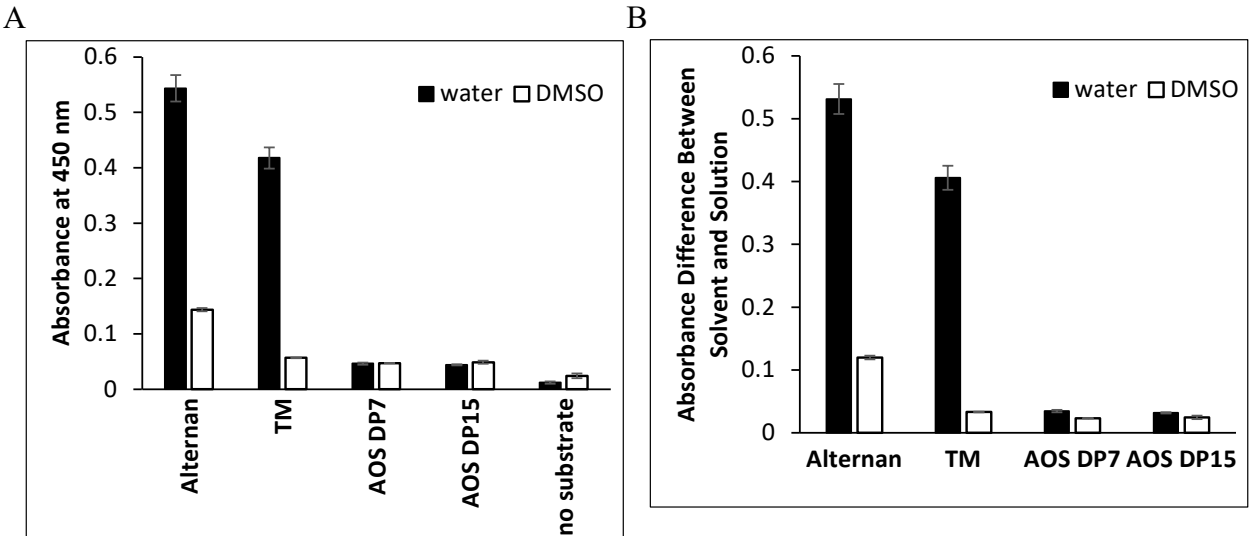

Figure 23. A: Absorbance detected at 450 nm for 1% (w/v) glucan solutions in water or DMSO. B: Difference in absorbance detected at 450 nm between glucan solutions in water or DMSO.

5.3.3 Effect of α-amylase on carbohydrate digestion

α-Amylase plays an important function in starch digestion to produce linear maltooligosaccharides, primarily maltose and maltotriose, and α-limit dextrins, which are subsequently converted into glucose in the small intestine by mucosal α-glucosidases (Lee and Hamaker, 2017). The α-amylase activity of the enzyme solution was reduced from 150.7 ± 0.2 U to 101.9 ± 0.2 U after purifying the solution twice with filter units with MWCO of 100 kDa as the molecular size (ca. 55 kDa) of α-amylases is lower than filter size (Table 12) (Darnis *et al.*, 1999). The effect of different concentrations of additional porcine pancreatic α-amylase (PPA) to produce the α-amylolyzed starch products were shown in Figure 24. Furthermore, the addition of PPA to the purified α-glucosidase solution increased the hydrolysis rate of WCS and maltodextrin DE10 to glucose molecules, which a kind of α-glucan composed with α-1,4 and α-1,6-linked glucose polymers. However, there was no changes due to increasing concentrations of PPA as maltose was already fully digested by purified mammalian mucosal α-glucosidases (PRIE) although PPA was

not added. Therefore, our results suggested that the loss of α-amylase activity during α-glucosidase purification decreased the hydrolysis activity of large sized carbohydrates such as starches and maltodextrins, and PPA supplementation made hydrolysis rate of PRIE similar with crude mammalian mucosal α-glucosidases (CRIE) at 50 U PPA supplement. Thus, we concluded that it was necessary to adjust and supplement the purified α-glucosidase solution with PPA (50 U/ml).

Table 12. α-Amylase activity of purified mammalian mucosal α-glucosidases

	30 K AMICON	100 K AMICON
Control	150.66 ± 0.24	
Centrifuge x 1	131.26 ± 0.33	129.26 ± 0.18
Centrifuge x 2	115.26 ± 0.42	101.86 ± 0.2

5.3.4 Impact of salts on *in vitro* digestion

In vitro digestion showed large and significant differences in the amount of glucose hydrolyzed from the different α-glucans over time (Figure 25). Tapioca maltodextrin with salts was the only solution that was digested to a different (higher) degree than without salts; however, there was no statistical differences between the two solutions at any timepoint besides 180 min. From these results, we can conclude no effect from salts on digestibility of these novel α-glucans studied, signifying they should provide similar slow release of glucose when consumed in RTD nutritional products as results previously observed during *in vivo* study of pure α-glucans.

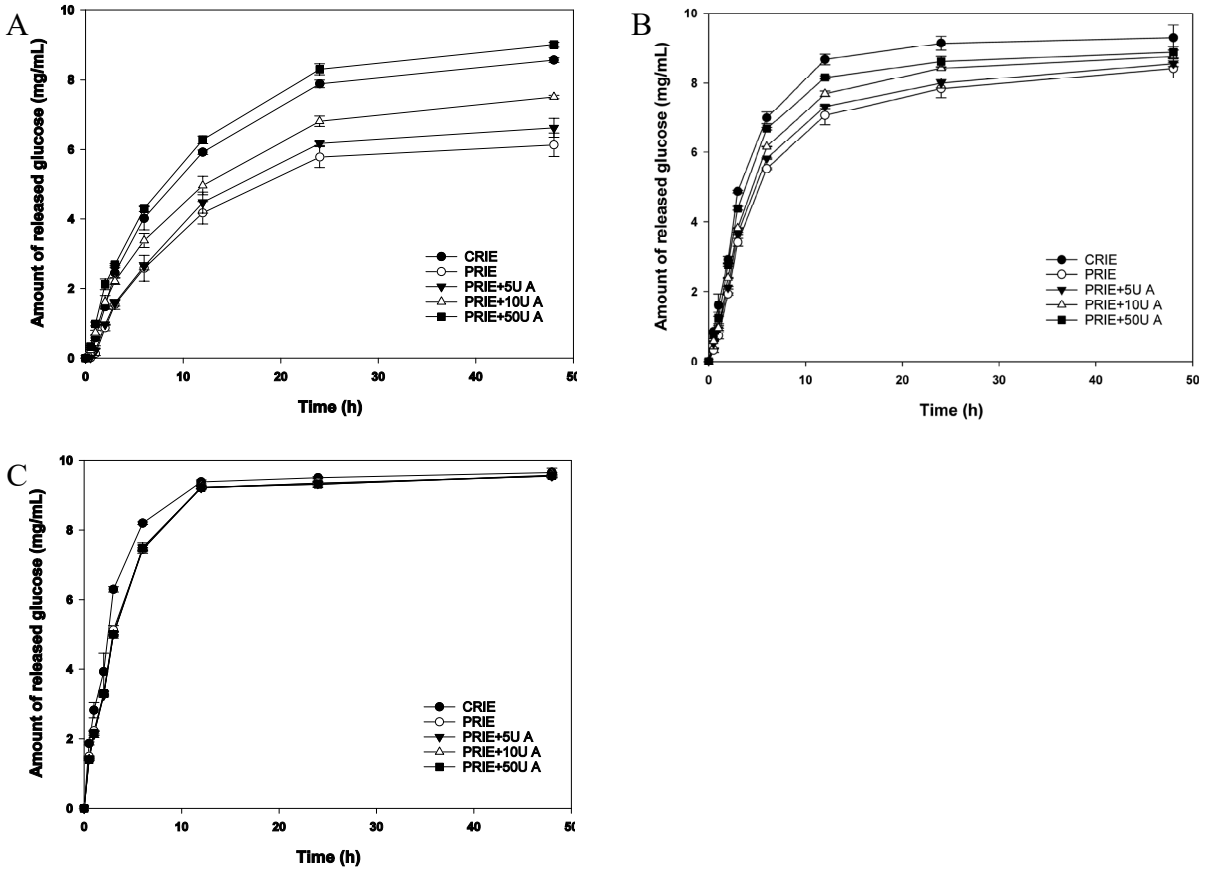

Figure 24. Glucose generation (mg/mL) of mammalian α-glucosidases (100 U) supplemented with different concentrations of porcine pancreatic α-amylase (PPA). A) Waxy corn starch (WCS), B) maltodextrin DE10, and C) maltose were hydrolyzed with crude mammalian mucosal (mean ± SD)

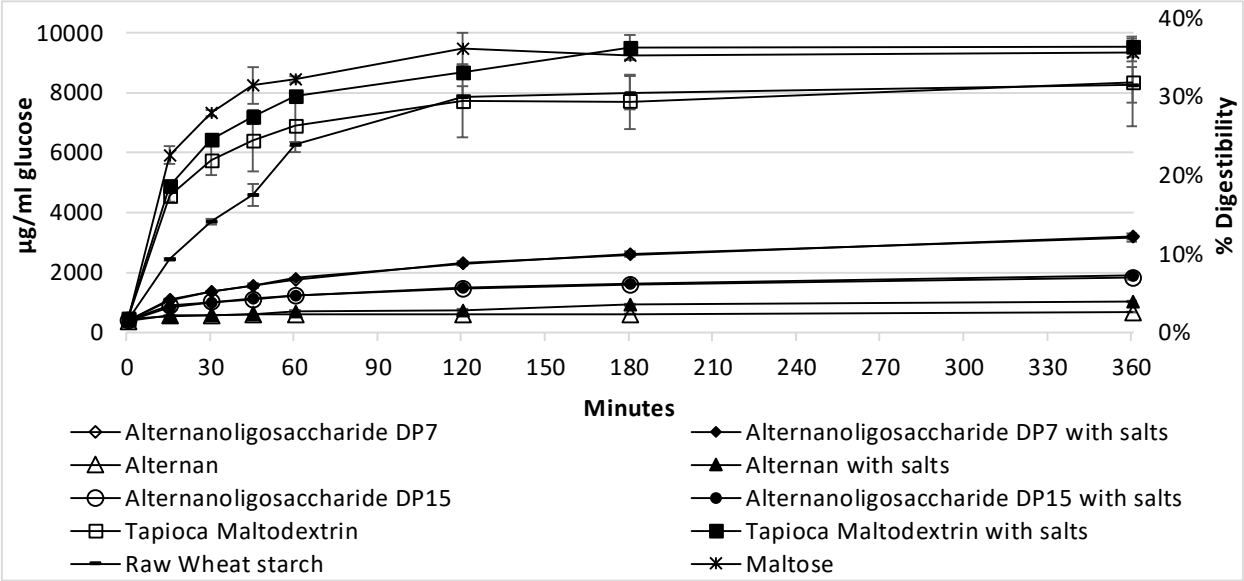

Figure 25. *In vitro* digestion: glucose released over time and percent digestibility compared to maltose after 6 h (assuming 100% digestion of maltose after 6 h) (maltose, and raw wheat starch controls) (mean ± SD)

5.3.5 Future research

The tendency of highly branched molecules to aggregate with soluble proteins when salts are in solution should be considered when designing beverage formulations that will undergo heat treatment. Attention to aggregate is important to prevent large aggregates from clogging nozzle heads. Further, attention should be taken when designing food products with intended slow digesting properties that contain these components, as large aggregations may further inhibit or prevent digestion of an already slowly digesting α-glucan. Future research should include a comparison of the hydrodynamic radius from light scattering of these structures in water versus in DMSO to better explain the variance between the very large hydrodynamic radius observed in water when molecular weight and R_g from MALS and RI in DMSO is considered. Further, errors in fit for shape factors from SLS and DLS results should be evaluated. Additionally, examining a range of salt concentrations in carbohydrate solutions could help inform whether the salt level used in this model system is close to the "salting out" or solubility point of the novel slow digesting α-glucans described in this work. Understanding the electrolyte concentration at which these carbohydrates decrease in solubility could help inform development of future beverages utilizing them as a delivery mechanism for a slow release of glucose into the bloodstream. Further studies

could also include macroscopy to examine the size and arrangement of the aggregates created when highly branched carbohydrates, soluble proteins, and salts are in solution.

5.4 References

Ahmadi-Abhari, S. *et al.* (2013) 'The influence of amylose-LPC complex formation on the susceptibility of wheat starch to amylase', *Carbohydrate Polymers*, 97(2), pp. 436–440. doi: 10.1016/j.carbpol.2013.04.095.

Barnes, H. A. (1989) 'Shear-Thickening ("Dilatancy") in Suspensions of Nonaggregating Solid Particles Dispersed in Newtonian Liquids', *Journal of Rheology*, 33(2), pp. 329–366. doi: 10.1122/1.550017.

Dahal, Y. R. and Schmit, J. D. (2018) 'Ion Specificity and Nonmonotonic Protein Solubility from Salt Entropy', *Biophysical Journal*. Biophysical Society, 114(1), pp. 76–87. doi: 10.1016/j.bpj.2017.10.040.

Darnis, S. *et al.* (1999) 'Molecular cloning and primary structure analysis of porcine pancreatic α-amylase', *Biochimica et Biophysica Acta - Protein Structure and Molecular Enzymology*, 1430(2), pp. 281–289. doi: 10.1016/S0167-4838(99)00011-4.

Divers, T. *et al.* (2007) 'The influence of O-formylation on the scale of starch macromolecules association in DMSO and water', *Carbohydrate Polymers*, 68(1), pp. 136–145. doi: 10.1016/j.carbpol.2006.07.026.

Doty, P. and Steiner, R. F. (1950) 'Light scattering and spectrophotometry of colloidal solutions', *The Journal of Chemical Physics*, 18(9), pp. 1211–1220. doi: 10.1063/1.1747913.

Englyst, H. N., Kingman, S. M. and Cummings, J. H. (1992) 'Classification and measurement of nutritionally important starch fractions', *European Journal of Clinical Nutrition*. MRC Dunn Clinical Nutrition Centre, Cambridge, UK., 46(SUPPL. 2), pp. S33-50. doi: 10.1016/S0271-5317(97)00010-9.

Damodaran, S., Parkin, K. L. (Kirk L. and Fennema, O. R. (2008) *Fennema's Food Chemistry, Fourth Edition*. 4th ed. Edited by S. Damodaran, K. L. (Kirk L. Parkin, and O. R. Fennema. Boca Raton: Taylor & Francis (Food science and technology (Taylor & Francis)).

Gallant, D. J., Bouchet, B. and Baldwin, P. M. (1997) 'Microscopy of starch: Evidence of a new level of granule organization', *Carbohydrate Polymers*. Elsevier, 32(3–4), pp. 177–191. doi: 10.1016/S0144-8617(97)00008-8.

Gloria Hernández, H. *et al.* (2011) 'Phase transitions of dairy proteins, dextrans and their mixtures as a function of water interactions', *Food Hydrocolloids*, 25(5), pp. 1311–1318. doi: 10.1016/j.foodhyd.2010.12.006.

Goodeve, C. F. (1939) 'A general theory of thixotropy and viscosity', *Transactions of the Faraday Society*, 35, pp. 342–358. doi: 10.1039/tf9393500342.

Green, A. A. (1931) 'Studies in the Physical Chemistry of the Proteins: Ix. the Effect of Electrolytes on the Solubility of Hemoglobin in Solutions of Varying Hydrogen Ion Activity With a Note on the Comparable Behavior of Casein', *The Journal of Biological Chemistry*, 93, pp. 495–516. Available at: http://www.jbc.org/ (Accessed: 4 July 2020).

Guo, M., Wang, H. and Wang, C. (2018) 'Interactions between whey protein and inulin in a model system', *Journal of Food Science and Technology*, 55(10), pp. 4051–4058. doi: 10.1007/s13197-018-3331-7.

Horne, D. S. (1986) 'Steric stabilization and casein micelle stability', *Journal of Colloid And Interface Science*, 111(1), pp. 250–260. doi: 10.1016/0021-9797(86)90024-X.

Lee, B. H. and Hamaker, B. R. (2017) 'Number of branch points in α-limit dextrins impact glucose generation rates by mammalian mucosal α-glucosidases', *Carbohydrate Polymers*, 157, pp. 207–213. doi: 10.1016/j.carbpol.2016.09.088.

Martínez, O. *et al.* (2015) 'Mecanismo de gelatinização do amido nativo de banana exportável do Equador (Gelatinization mechanism of native exportable banana starch from Ecuador)', *Revista Colombiana de Quimica*, 44(2), pp. 16–21. doi: 10.15446/rev.colomb.quim.v44n2.55215.

Rayate, A. (2018) *Interactions Between Sodium Caseinate and Polyglucose in Aqueous Solutions*. Purdue University.

Rendleman, J. A. (1967) 'Complexes of Alkali Metals and Alkaline-Earth Metals with Carbohydrates', *Advances in Carbohydrate Chemistry*, 21(C), pp. 209–271. doi: 10.1016/S0096-5332(08)60318-5.

Ryan, K. N. *et al.* (2012) 'Stability and mechanism of whey protein soluble aggregates thermally treated with salts', *Food Hydrocolloids*, 27(2), pp. 411–420. doi: 10.1016/j.foodhyd.2011.11.006.

Seal, C. J. *et al.* (2003) ' Postprandial carbohydrate metabolism in healthy subjects and those with type 2 diabetes fed starches with slow and rapid hydrolysis rates determined in vitro ', *British Journal of Nutrition*, 90(5), pp. 853–864. doi: 10.1079/bjn2003972.

Sedlmeyer, F. and Kulozik, U. (2006) 'Impact of process conditions on the rheological detectable structure of UHT treated milk protein-carrageenan systems', *Journal of Food Engineering*, 77(4), pp. 943–950. doi: 10.1016/j.jfoodeng.2005.08.023.

Seo, J. M. *et al.* (2020) 'Determination of glucose generation rate from various types of glycemic carbohydrates by mammalian glucosidases anchored in the small intestinal tissue', *International Journal of Biological Macromolecules*. Elsevier, 154, pp. 751–757. doi: 10.1016/j.ijbiomac.2020.03.154.

Sheridan, P. F. *et al.* (2002) 'Computer simulations of hyperbranched polymers: The influence of the Wiener index on the intrinsic viscosity and radius of gyration', *Journal of Chemical Physics*, 117(16), pp. 7802–7812. doi: 10.1063/1.1507774.

Shin, H. *et al.* (2019) 'Optimization of in vitro carbohydrate digestion by mammalian mucosal α-glucosidases and its applications to hydrolyze the various sources of starches', *Food Hydrocolloids*, 87, pp. 470–476. doi: 10.1016/j.foodhyd.2018.08.033.

Sweeny, K. H. and Geckler, R. D. (1954) 'Rheology of Suspensions in Polymeric', *Rheology of Suspensions Journal of Rheology*, 25, p. 287. doi: 10.1063/1.1721828.

Tanford, C. (1961) *Physical chemistry of macromolecules*, *Journal of Pharmaceutical Sciences*. Edited by I. John Wiley & Sons. Hoboken, New Jersey, New Jersey. doi: 10.1002/jps.2600510233.

Tester, R. F., Karkalas, J. and Qi, X. (2004) 'Starch structure and digestibility Enzyme-Substrate relationship', *World's Poultry Science Journal*, 60(2), pp. 186–195. doi: 10.1079/wps200412.

Vicent, De, J. (ed.) (2012) *Rheology*. Rijeka, Croatia. Available at: www.intechopen.com (Accessed: 6 July 2020).

Wang, S. and Copeland, L. (2013) 'Molecular disassembly of starch granules during gelatinization and its effect on starch digestibility: A review', *Food and Function*, pp. 1564–1580. doi: 10.1039/c3fo60258c.

Xiong, Y. L. (1992) 'Influence of pH and Ionic Environment on Thermal Aggregation of Whey Proteins', *Journal of Agricultural and Food Chemistry*, 40(3), pp. 380–384. doi: 10.1021/jf00015a004.

Zhang, G. and Hamaker, B. R. (2009) 'Slowly digestible starch: Concept, mechanism, and proposed extended glycemic index', *Critical Reviews in Food Science and Nutrition*. Taylor & Francis, 49(10), pp. 852–867. doi: 10.1080/10408390903372466.

CHAPTER 6. OVERALL CONSLUSIONS AND FUTURE WORK

The works presented aimed to investigate the relationship between α-glucan linkage type and pattern, molecular size, and structural conformation on slow digesting properties, and to understand how the investigated novel α-glucans behave in different solvents and in a model system. Based on the results from the studies presented here, the following conclusions and suggestions for future research can be made with respect to hypotheses and results presented in Chapter 1.

In Chapter 3 we hypothesized that a combination of α-1,6 linkages, known to be slow digesting, with more rapidly digesting linkages such as α-1,4, or oligosaccharides containing rare linkages such as α-1,3, would produce a desired slow hydrolysis affect similar to that of raw wheat starch due to its crystalline structure. These ideas originated from previous work in our laboratory (Lee et al., 2016). We also hypothesized that in these structures, increasing molecular size would be associated with decreasing or extended digestibility. In both *in vitro* studies and a clinical trial, the hypotheses were validated and, as well, represent the first report of a structure-function relationship of α-glucan linkage type for SDCs and their ultimate application in the human. Results showed the relative rate of digestion of the most common naturally and enzymatically occurring α-linkages. It was found that dextran, high in repeating α-1,6-linkages, was slowly and likely only partially digestible; highly branched alternanoligosaccharides composed of roughly an equal ratio of α-1,3 and α-1,6 were good SDCs and digested only slightly faster that dextran, despite large differences in molecular size. This prompted further investigation in Chapter 5 into examining how varying MWs, from small to large, of the alternating α-1,3 and α-1,6-linked structures of alternanoligosaccharides and alternan affect rate of digestion. The results also provide guidance for development of future α-glucans with desirable digestion and glucose release patterns.

In Chapter 4, the novel α-glucans included in the clinical trial presented in Chapter 3 were examined for structural conformation and rheological behavior that might affect rate of digestion or processing abilities. The hypothesis presented was that larger molecules such as the alternan examined may impact rate of digestion due to the structural size, and potential aggregation in solution, or double helical structure formation such as is found in crystalline raw starch granules. Indeed, alternan with polydisperse coil conformation by the Kratky plot was observed to self-assemble into dense spherical structures in water at low concentrations, when examined using a

DLS goniometer. Alternan also exhibited shear thinning behavior at 10% but not 5%, likely due to entanglement of these large branched molecules. Dextrans examined by DLS with the Kratky plot were much more open in structure compared to the other α-glucans studied, and at 50°C demonstrated a shear thickening behavior, which may be due to helical agglomeration of many molecules together due to the high degree of branching of these structures.

Chapter 5 observed the impact of alternanoligosaccharides and alternan of increasing MWs alone in water and DMSO solvents, as well as in a model nutritional protein and electrolyte beverage system. The objective of the studies presented in Chapter 5 were to examine *in vitro* rate of digestion for comparison based on MW, as well as secondary structures, rheological behaviors, and if aggregates are formed with these molecules that may impact digestion rate or application for food processing systems. The hypotheses for these studies were that salts in the solution, effect ionic environment and, in turn, conformation change may impact rate of digestion. The hypothesis presented was confirmed, and we also found that soluble protein aggregates likely interact with these highly branched oligo- and polysaccharides, especially under heat or shear stress.

These findings are important to consider when designing enzymatically carbohydrate structures with the end goal of slow rate of digestion, as well as when including highly branched soluble carbohydrates in food or beverage formations. Future research should include further examination of the relationship between iAUC and MW as presented in Figure 14, as well as considering other alternating branched α-glucans for slow digesting properties. Because it was found that alternans and alternanoligosaccharides interact with soluble protein aggregates in solution, it is important to further explore the effect these carbohydrate-protein agglomerates might have on the rate of carbohydrate digestion and glucogenesis. Further research is planned to compare the hydrodynamic radii from goniometric light scattering of the α-glucan structures presented in Chapter 5 when in water versus DMSO solvents, to further investigate the variance between the very large R_h in water compared to the MW and R_g results obtained from MALS and RI when in DMSO. Additionally, a range of salt concentrations should be applied to these alternan and alternanoligosaccharides to advise what the ideal salt concentration range should be considered for this system so that solubility of these structures will be maximized in water.

6.1 **References**

Lee, B. H., Rose, D. R., Lin, A. H. M., Quezada-Calvillo, R., Nichols, B. L., & Hamaker, B. R. (2016). Contribution of the Individual Small Intestinal α-Glucosidases to Digestion of Unusual α-Linked Glycemic Disaccharides. *Journal of Agricultural and Food Chemistry*, *64*(33), 6487–6494. https://doi.org/10.1021/acs.jafc.6b01816

APPENDIX - PUBLICATION

Note: The following manuscript describes the process to synthesize enzymatically modified carbohydrates, their digestibility by *in vitro* study, and molecular and structural characterizations. Primary contribution of S. Corwin to this work was the *in vitro* study and related writings. The following manuscript is copyright the American Chemical Society (ACS) 2020 and further permissions related to the material excerpted should be directed to the ACS.

Te Poele, E. M. *et al.* (2020) 'Development of Slowly Digestible Starch Derived α-Glucans with 4,6-α-Glucanotransferase and Branching Sucrase Enzymes', *Journal of Agricultural and Food Chemistry*, 68(24), pp. 6664–6671. doi: 10.1021/acs.jafc.0c01465. Available at https://pubs.acs.org/doi/10.1021/acs.jafc.0c01465

DEVELOPMENT OF SLOWLY DIGESTIBLE STARCH DERIVED ALPHA-GLUCANS WITH 4,6-A-GLUCANOTRANSFERASE AND BRANCHING SUCRASE ENZYMES

6.1 Abstract

Previously, we have identified and characterized 4,6-α-glucanotransferase enzymes of Glycosyl Hydrolase (GH) family 70 (GH70) that cleave (α1→4)-linkages in amylose and introduce (α1→6)-linkages in linear chains. The 4,6-α-glucanotransferase of *Lactobacillus reuteri* 121, for instance, converts amylose into an Isomalto/Malto-Polysaccharide (IMMP) with 90% (α1→6)-linkages. Over the years, also branching sucrase enzymes belonging to the GH70 family have been characterized. These enzymes use sucrose as donor substrate to glucosylate dextran as acceptor substrate, introducing single -(1→2,6)-α-D-Glcp-(1→6)- (*Leuconostoc citreum* enzyme) or -(1→3,6)-α-D-Glcp-(1→6)-branches (*Leuconostoc citreum, Leuconostoc fallax, Lactobacillus kunkeei* enzymes). In this work we observed that the catalytic domain 2 of the *L. kunkeei* branching sucrase not only used dextran but also IMMP as acceptor substrate, introducing -(1→3,6)-α-D-Glcp-(1→6)-branches. The products obtained have been structurally characterized in detail, revealing the addition of single (α1→3)-linked glucose units to IMMP (resulting in a comb-like structure). The *in vitro* digestibility of the various α-glucans was estimated with the Glucose Generation Rate (GGR) assay that uses rat intestinal acetone powder to simulate the digestive

enzymes in the upper intestine. Raw wheat starch is known to be a slowly digestible carbohydrate in mammals and was used as a benchmark control. Compared to raw wheat starch, IMMP and dextran showed reduced digestibility, with partially digestible and indigestible portions. Interestingly, the digestibility of the branching sucrase modified IMMP and dextran products considerably decreased with increasing percentages of (α1→3)-linkages present. Treatment of amylose with 4,6-α-glucanotransferase and branching sucrase/sucrose thus allowed synthesis of amylose/starch derived α-glucans with markedly reduced digestibility. These starch derived α-glucans may find applications in the food industry.

6.2 Introduction

It is well known that sugar reduction is a major challenge for the food industry. In many cases maltodextrins, glucose syrups, and other starch derivatives are proposed and used as alternatives. Their consumption results in rapid and abrupt glucose delivery to the body and consequently causes a high glycemic response. Therefore, like sugars, these glycemic carbohydrates are viewed in an unfavorable light by consumers, the scientific community, and regulatory bodies (Gangoiti, Corwin, et al., 2018).

In recent years we have characterized various novel starch modifying enzymes of Glycosyl Hydrolase family 70 (GH70) that cleave (α1→4)-linkages and introduce (α1→6)-linkages, resulting in the synthesis of α-glucans with various ratios of these linkage types, either in linear chains or with different degrees of branching. Such modified starches are likely to be digested slowly or to a lesser degree, releasing glucose less abruptly, turning them into more healthful carbohydrates compared to the original rapidly digestible starch ingredients (Gangoiti et al., 2016, 2017; Gangoiti, Corwin, et al., 2018; Gangoiti, Pijning, et al., 2018; Meng et al., 2016).

One example is the 4,6-α-glucanotransferase GtfB-ΔN-ΔV of Lactobacillus reuteri strain 121; it cleaves (α1→4)-linkages in amylose and introduces (α1→6)-linkages, resulting in synthesis of linear IsoMalto/Malto-Polysaccharides (IMMP) (Dobruchowska et al., 2012; Gu et al., 2018; Kralj et al., 2011; Leemhuis et al., 2014; van der Zaal et al., 2018). Another example is the 4,6-α-glucanotransferase GtfB of Lactobacillus reuteri NCC 2613 that modifies amylose/starch into a branched glucan with (α1→4)- and (α1→6)-linkages (Gangoiti et al., 2017). Lactobacillus aviarius subsp. aviarius DSM 20655 encodes both types of 4,6-α-glucanotransferase GtfB enzymes from adjacent genes (Meng, Gangoiti, de Kok, et al., 2018). The differences in product and substrate

specificity between these GtfB enzymes are understood in molecular detail, involving a closed (L. reuteri 121 GtfB, acting on amylose, producing a linear α-glucan) or an open (L. reuteri NCC 2613 GtfB, acting on amylose, amylopectin, starch, producing a branched α-glucan) active site cavity (Bai et al., 2017; Pijning et al., n.d.). Differences in digestibility between these various α-glucan products with (α1→4)- and (α1→6)-linkages remained to be studied.

To digest the dietary available carbohydrates to the monosaccharides glucose, fructose, and galactose, the mammalian body employs the salivary and pancreatic α-amylases (EC 3.2.1.1.) and the small intestine mucosal two-enzyme complexes of maltase-glucoamylase (MGAM) (EC 3.2.1.20 and 3.2.1.3) and sucrose-isomaltase (SI) (EC 3.2.148 and 3.2.10). The α-amylases are classified in glycoside hydrolase (GH) family GH13, and the four catalytic subunits of MGAM and SI in GH31 (Nichols et al., 2003). The four enzyme subunits of these α-glucosidases have different roles in the conversion of glycemic carbohydrates to glucose (and of sucrose to glucose and fructose). α-Glucans with structures and linkages that are less easily hydrolyzed by these enzymes potentially are of interest as slowly digestible carbohydrates (Gangoiti, Corwin, et al., 2018). It is the synthesis and digestibility of such α-glucan structures that is the subject of this work.

The α-glucans with (α1→4)- and (α1→6)-linkages may still be digestible to some (considerable) extent by human oral-, pancreatic- and intestinal tract enzymes (Gangoiti, Corwin, et al., 2018; Leemhuis et al., 2014). Therefore, we also looked at the possible synthesis of α-glucans with (α1→3)-linkages. The characterized family GH70 branching sucrase enzymes use sucrose as donor substrate to glucosylate dextran as an acceptor substrate, introducing single -(1→2,6)-α-D-Glcp-(1→6)- (Leuconostoc citreum enzyme) or -(1→3,6)-α-D-Glcp-(1→6)-branches (Leuconostoc citreum, Leuconostoc fallax, Lactobacillus kunkeei enzymes) (Figure 26) (Brison et al., 2012; Meng, Gangoiti, Wang, et al., 2018; Passerini et al., 2015; Vuillemin et al., 2016). Interestingly, our results show that the GtfZ-CD2 catalytic domain of the L. kunkeei DSM 12361 branching sucrase not only uses dextran but also IMMP as an acceptor substrate, introducing -(1→3,6)-α-D-Glcp-(1→6)-branch points. A detailed structural analysis, and the *in vitro* digestibility, of such novel linear and branched α-glucans are reported in this paper.

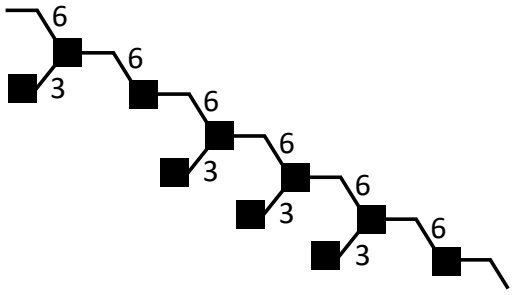

Figure 26. Incubation of dextran (70 kDa)16 and IMMP (18.3 kDa) (this study) with GtfZ-CD2 and 200 mM sucrose resulted in synthesis of comb-like structures consisting of single (α1→3)-branched glucose units on a linear (α1→6) glucose chain (adapted from Meng et al. (Meng, Gangoiti, Wang, et al., 2018)

6.3 Materials and methods

6.3.1 Production of the enzymes

The GtfZ-CD2 enzyme used in this study is the (α1→3)-branching sucrase (EC 2.4.1.362) catalytic domain CD2 (amino acids 121-2264) of the GtfZ protein of *Lactobacillus kunkeei* DSM 12361 (Meng, Gangoiti, Wang, et al., 2018). The 4,6-α-glucanotransferase enzyme GtfB-ΔN-ΔV (EC 2.4.1.B34) is a truncated variant (amino acids 761 to 1619) of GtfB of *L. reuteri* 121 lacking both the N-terminal variable domain and domain V (Bai et al., 2017). Both GtfZ-CD2 and GtfB-ΔN-ΔV carried a C-terminal His-tag, were expressed from *E. coli* BL21 DE3 cells and purified by $Ni2^{+}$ -nitrilotriacetic acid (NTA) affinity chromatography as described by Meng *et al*. (2018b) (Meng, Gangoiti, Wang, et al., 2018).

6.3.2 Standard reaction buffer and conditions

All GtfZ-CD2 enzyme reactions were performed at 30 °C in 25 mM sodium acetate (pH 5.5), containing 1.5 mM $CaCl_2$. GtfB-ΔN-ΔV reactions were at 37 °C in 25 mM sodium acetate (pH 5.0), containing 1.0 mM $CaCl_2$.

6.3.3 Enzyme activity assays

Enzyme activity assays with 0.12 mg/mL GtfZ-CD2 were performed with 7-20 g/L dextran (M_w 10.2 kDa or M_w 70 kDa) (Sigma Aldrich, The Netherlands) or IMMP (see below), in both cases with 200 mM sucrose. Samples of 25 µL were taken every min over a period of 7 min and

immediately inactivated with 12.5 µL 0.4 M NaOH; after enzyme inactivation the samples were neutralized by adding 12.5 µL 0.4 M HCl. The glucose and fructose concentrations in these samples were enzymatically determined by monitoring the reduction of NADP with the hexokinase and glucose-6-phosphate dehydrogenase/phosphoglucose isomerase assays (Roche Nederland BV, Woerden, The Netherlands) (Mayer et al., 1981). Determination of the release of glucose and fructose from sucrose allowed calculation of the total activity of the glucansucrase enzymes (Van Geel-Schutten et al., 1999). One unit (U) of enzyme is defined as the amount of enzyme required for producing 1 µmol fructose per min in reaction buffer.

The total enzyme activity of GtfB-ΔN-ΔV was determined by the amylose-iodine staining method as described by Bai *et al*. (2015) (Bai et al., 2015) using 0.125% (w/v) Amylose V from potato starch (M_w 170 kDa) (AVEBE, Foxhol, The Netherlands). The decrease in absorbance of the α-glucan-iodine complex resulting from transglycosylation and/or hydrolytic activity was monitored at 660 nm for 7 min at 40 °C. One unit of activity was defined as the amount of enzyme converting 1 mg of substrate per min.

6.3.4 Synthesis of isomalto/malto-polysaccarides (IMMP) from starch

A 4% amylose stock solution was prepared by solubilizing amylose V in 1 M NaOH. The stock was set to pH 5.0 with 1 M HCl and diluted to a concentration of 1% (w/v) in buffer. For the production of IMMP from amylose V, 40 µg/mL GtfB-ΔN-ΔV was incubated with 500 mL 1% amylose V for 72 h at 37 ºC. After incubation, the enzyme was heat-inactivated at 95 ºC for 20 min. The incubation was dialyzed against 25 L running tap water for 72 h in 3.5 kDa snake skin tubing (ThermoFisher), then dialyzed for 48 h in 25 L demineralized water, and finally dialyzed for 24 h against 22 L MilliQ water. The dialyzed IMMP was lyophilized to dryness.

6.3.5 Synthesis of α-(1→3)-branched IMMP and dextran

The (α1→3)-branched polymers were synthesized by incubating 0.5 U/mL GtfZ-CD2 for 24 h with 20 g/L IMMP or dextran (Mw 70 kDa) with 200 mM sucrose. To obtain partially branched polymers, 20 g/L IMMP or dextran (Mw 10.2 kDa) were incubated with 0.5 U/mL GtfZ-CD2 for 24 h with different sucrose concentrations ranging from 0 to 200 mM. The concentration of 10.2 and 70 kDa dextran and IMMP was expressed as the molar concentration of the

anhydroglucosyl units in the polymer. The 20 g/L polymer (dextran (Mw 70 kDa), dextran (Mw 10.2 kDa) and IMMP (Mw 18.3) used in each case thus corresponds to a concentration of 123 mM anhydroglucosyl units. The incubations were heat-inactivated at 95 ºC for 20 min and subsequently dialyzed as described above for IMMP synthesis.

6.3.6 High-pH anion-exchange chromatography

High-performance anion-exchange chromatography (HPAEC) was performed on an ICS-3000 workstation (Dionex, Amsterdam, The Netherlands), equipped with an ICS-3000 ED pulsed amperometric detection system (PAD). Samples were diluted 1:100 in MilliQ water, filtered through a 0.2 µm cellulose filter prior to injection (25 µL injection volume). The oligosaccharides were separated on a CarboPac PA-1 column (Dionex; 250 × 4 mm) by using a linear gradient of 10–240 mM sodium acetate in 100 mM NaOH over 57 min at a flow rate of 1 mL/min. Commercial oligosaccharide standards were used to identify the peaks.

6.3.7 Methylation analysis

Analysis of the glucosyl linkage composition of the (α1→3)-branched polymers of the 24 h incubations of 20 g/L (123 mM anhydroglucose) dextran (Mw 70 kDa) or IMMP with 200 mM sucrose was done as follows. Samples were permethylated using CH_3I and solid NaOH in $(CH_3)_2SO$, as described previously (Ciucanu & Kerek, 1984), then hydrolyzed with 2 M trifluoroacetic acid (2 h, 120 °C) to give the mixture of partially methylated monosaccharides. After evaporation to dryness, the mixture, dissolved in H_2O, was reduced with $NaBD_4$ (2 h, room temperature). Subsequently, the solution was neutralized with 4 M acetic acid and boric acid was removed by repeated co-evaporation with methanol. The obtained partially methylated alditol samples were acetylated with 1:1 acetic anhydride-pyridine (30 min, 120 °C). After evaporation to dryness, the mixtures of partially methylated alditol acetates (PMAA), dissolved in dichloromethane, were analyzed by GLC-EI-MS on an EC-1 column (30 m x 0.25 mm; Alltech), using a GCMS-QP2010 Plus instrument (Shimadzu Kratos Inc., Manchester, UK) and a temperature gradient (140-250 °C at 8 °C/min) (Kamerling & Gerwig, 2007).

6.3.8 NMR spectroscopy

One-dimensional ^{1}H nuclear magnetic resonance (NMR) spectra were recorded on a Bruker 600-MHz spectrometer (NMR Center, University of Groningen), using D_2O as solvent at a probe temperature of 300K. Before analysis, 3 mg of freeze-dried polymer sample was exchanged twice in 500 µL D_2O (99.9 atom% D, Cambridge Isotope Laboratories, Inc., Andover, MA) with intermediate lyophilization, and finally dissolved in 650 µL D_2O spiked with 0.005% acetone as an internal standard. The NMR data were processed using the MestReNova 12 program (Mestrelab Research SL, Santiago de Compostella, Spain). Chemical shifts (δ) were expressed in ppm by reference to internal acetone (δ_H 2.225 for ^{1}H). The ratio of different glycosidic linkages was determined by integration of the surface areas of the respective signal peaks in the ^{1}H NMR spectra.

6.3.9 High-performance size-exclusion chromatography

The molecular mass distribution of the products were determined by high-pressure size-exclusion chromatography (HPSEC) as described previously (Bai et al., 2015). The HPSEC system (Agilent Technologies 1260 Infinity) was equipped with a multi angle laser light scattering detector (SLD 7000 PSS, Mainz, Germany), a viscometer (ETA-2010 PSS, Mainz) and a differential refractive index detector (G1362A 1260 RID Agilent Technologies). Separation was performed by using three PFG-SEC columns with porosities of 100, 300 and 4000 Å, coupled with a PFG guard column. DMSO-LiBr (0.05 M) was used as eluent at a flow rate of 0.5 mL/min. The system was calibrated and validated using a standard pullulan kit (PSS, Mainz, Germany) with M_w ranging from 342 to 708 000 Da. The specific RI increment (dn/dc) value for pullulan was determined as 0.072 mL/g (PSS, Mainz). We assumed that the specific RI increment (dn/dc) values for the IMMP and dextran polysaccharides were the same as for pullulan. The molecular weight of the low molecular weight products ($< 1 \times 10^5$ Da) was determined by the universal calibration method. WinGPC Unity software (PSS, Mainz) was used for data processing.

6.3.10 *In vitro* glucose generation rate (GGR) assay using rat intestinal acetone powder

Based on the protocol of Shin *et al*. (2019) (Shin et al., 2019), 100 mM sodium phosphate buffer at pH 6.0 with 0.005% w/v ampicillin salts (Seo et al., 2018) was freshly prepared for each

experiment. Rat intestinal acetone powder (RIAP) (Sigma Aldrich, Burlington, MA, USA) was ground using a cell grinder (IKA A-10 Homogenizer, IKA Works, Inc, Wilmington, NC, USA), then pressed through a #20 standard (850 µm) sieve and stored at -20 ℃. Sufficient quantities of RIAP needed for all assays were ground and pooled together to ensure consistent enzyme activity. A suspension of 5.55% w/v RIAP was created and held at 4 ℃ for 60 min prior to beginning incubation of the samples. Substrate solutions (10% w/v) made with the above buffer were pre-incubated for 10 min at 37 °C, 600 rpm (Eppendorf ThermoMixer® C, Eppendorf, Hauppauge, NY, USA). Quantities of 1% substrate solutions sufficient to dilute RIAP to 5% w/v and substrate to 0.1% w/v were added. RIAP-substrate suspensions were incubated at 37 °C; aliquots were taken and inactivated at 100 °C and 600 rpm for 5 min at 15, 30, and 45 min, and 1, 2, 3, and 6 h. Inactivated aliquots were centrifuged (Microfuge 20R Centrifuge, Beckman Coulter, Indianapolis, IN, USA) at 9160 × *g* for 10 min, and held at 4 °C until time of analysis. Pure 0.1% α-glucans in water were used for the 0 min timepoint. The amount of released glucose in digested and inactivated supernatant was diluted 10 times, then analysed using the glucose oxidase/peroxidase (GOPOD) method and a microplate spectrophotometer (SpectraMax 190 Absorbance Microplate Reader, Molecular Devices, LLC, San Jose, CA, USA) (Vasanthan, 2005), using glucose to prepare the standard curve. Digestion assays were performed in triplicate at each timepoint. Raw wheat starch was used as a positive slowly digestible carbohydrate benchmark control (Englyst et al., 1992), and was digested fully in 6 h with RIAP containing residual α-amylase and α-glucosidases. Percent digestibility was determined based on full hydrolysis of raw wheat starch to glucose (100%) at 360 min.

6.4 Results and discussion

6.4.1 IMMP synthesis and structural characterization

To synthesize IMMP, amylose V (M_w 170 kDa) was incubated for 72 h with the GtfB-ΔN-ΔV enzyme. After inactivation of the GtfB-ΔN-ΔV enzyme, the reaction products were purified from glucose, oligosaccharides, and salts by dialysis. Structural analysis of the GtfB-ΔN-ΔV reaction products with 1D ^{1}H NMR revealed that the amylose V was almost completely converted into IMMP, showing an NMR profile nearly identical to that of dextran (M_w 70 kDa) (Figure 27). The (α1→4) signal (δ 5.41), corresponding to linear (α1→4)-linked glucose units, had disappeared

and a peak corresponding to linear (α1→6)-linked glucose units had appeared at δ 4.98. Methylation analysis showed that the IMMP product consisted of terminal [Glcp(1→], 4-substituted [→4)Glcp(1→], and 6-substituted [→6)Glcp(1→] glucosyl units in a molar ratio of 3.8, 6.8 and 89.4%, respectively (Table 13). The molar ratio of terminal [Glc*p*(1→] and 6-substituted [→6)Glc*p*(1→] glucosyl units in 70 kDa dextran was nearly identical to that of IMMP, i.e 3.9, and 89%, respectively, but consisted of 6.2% 3,6-substituted [→3,6)Glc*p*(1→] glucosyl units instead of 4-substituted [→4)Glc*p*(1→] glucose units (Table 13). HPSEC analysis of the IMMP and 10.2 kDa dextran showed monodisperse peaks with M_w of 18.30 kDa and 9.75 kDa, respectively (Table 14).

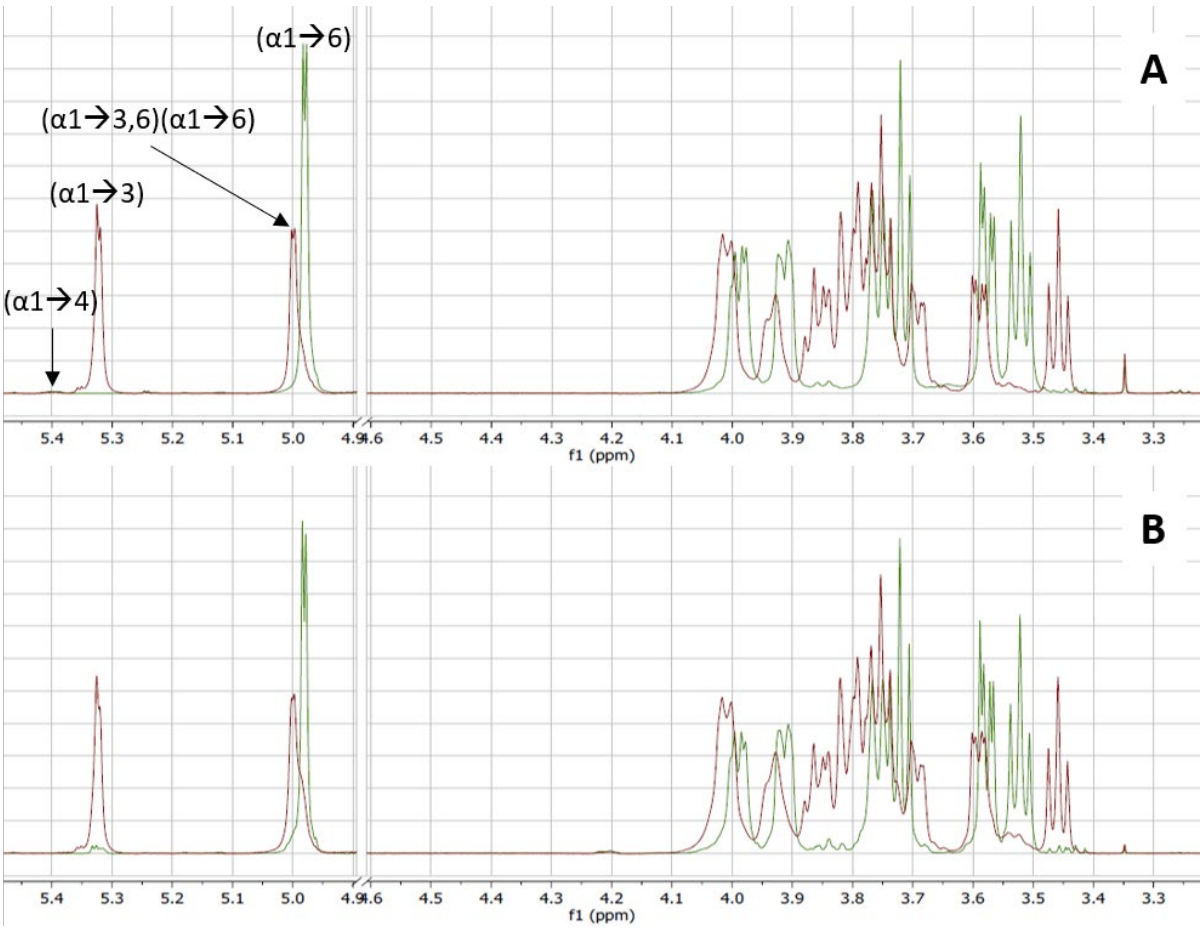

Figure 27. 1H NMR spectra (D2O, 300 K) of branched polymers formed by the incubation of GtfZ-CD2 with 20 g/L (123 mM anhydroglucose) (A) IMMP (18.3 kDa) and (B) dextran (70 kDa) with (red lines) or without (green lines) 200 mM sucrose. Chemical shifts are shown in parts per million (ppm) relative to the signal of internal acetone (δ 2.225).

Table 13. Methylation analysis (%) of the carbohydrate moieties in IMMP (18.3 kDa), dextran (70 kDa) and their branched derivatives. These branched polymers were produced during a 24-h incubation of the GtfZ-CD2 enzyme with 20 g/L (123 mM anhydroglucose) IMMP or d extran (70 kDa) and 200 mM sucrose.

PMAA	R_t	IMMP GtfZ-CD2	IMMP -	dextran GtfZ-CD2	dextran -
Glc(1→	1.00	50.8	3.8	39.4	3.9
→3)Glc(1→	1.16			1.5	
→4)Glc(1→	1.19		6.8		
→6)Glc(1→	1.23	5.5	89.4	12.9	89
→3,6)Glc(1→	1.38	43.7		46.2	6.2
→4,6)Glc(1→	1.40				0.9

R_t = relative retention time to Glc(1→

Table 14. Molecular weights (Mw) of a range of purified branched polymers derived from IMMP (18.3 kDa) and dextran (10.2 kDa) as determined by HPSEC analysis (also see Figure 31). The branched polymers were produced during a 24-h incubation of the GtfZ-CD2 enzyme with 20 g/L (123 mM anhydroglucose) IMMP or dextran (Mw 10.2 kDa) at increasing molar ratios of [sucrose]/[IMMP or dextran anhydroglucose]. Sucrose was provided at 0-200 mM.

[sucrose] (mM)	ratio [suc]/[IMMP or dextran]	M_w (kDa) IMMP products	M_w (kDa) dextran products	M_w increase (%) IMMP	M_w increase (%) dextran
200	1.63	25.50	13.10	39.34	34.36
150	1.22	23.00	12.20	25.68	25.13
100	0.81	23.20	12.30	26.78	26.15
75	0.61	21.30	11.90	16.39	22.05
50	0.41	21.00	11.40	14.75	16.92
25	0.20	19.00	10.40	3.83	6.67
12.5	0.10	18.70	10.10	2.19	3.59
6.25	0.05	18.50	9.90	1.09	1.54
0	0.00	18.30	9.75	0.00	0.00

6.4.2 Branching sucrase activity of GtfZ-CD2 on IMMP

GtfZ-CD2 of *L. kunkeei* (Meng, Gangoiti, Wang, et al., 2018), and the related branching sucrase enzymes of *L. citreum* and *L. fallax* (Passerini et al., 2015; Vuillemin et al., 2016), use sucrose as a glucose donor to decorate dextran molecules, adding single (α1→3)-branched glucose units on the linear (α1→6) glucose chain (Figure 26). Here we show that GtfZ-CD2 also had (α1→3)-branching activity on the IMMP product (with ~90% (α1→6. The effects of (α1→3)-branching on the digestibility of the dextran and IMMP derived products subsequently were analyzed. To determine whether GtfZ-CD2 had (α1→3)-branching activity on IMMP, enzyme activity assays were performed with IMMP, with and without 200 mM sucrose. Assays with 70 kDa dextran with and without 200 mM sucrose served as controls. GtfZ-CD2 had clear transglucosylating activity on both dextran and IMMP; a somewhat lower initial rate was observed with IMMP, i.e 10.4 and 14.8 U/mg protein for IMMP (M_w 18.3 kDa) and dextran (M_w 70 kDa), respectively (Figure 28). In the absence of sucrose as a glucosyl donor, no activity was observed with dextran or IMMP alone. With sucrose alone, GtfZ-CD2 showed minor transglucosylase activity and mainly catalyzed sucrose hydrolysis and synthesis of leucrose, as reported before (Figure 28) (Meng, Gangoiti, Wang, et al., 2018).

6.4.3 Structural analysis of the GtfZ-CD2 reaction products with dextran and IMMP

Using dextran (M_w 70 kDa) as acceptor substrate, Meng *et al*. (2018b)(Meng, Gangoiti, Wang, et al., 2018) showed that at a molar ratio of [sucrose]/[dextran] of 0.65 and higher, the dextran glucosylation products obtained maximally had 41% (α1→3) linkages. In this work we used both IMMP (M_w 18.3 kDa) and 70 kDa dextran (M_w 70 kDa) (as positive control) as substrates for GtfZ-CD2, incubated with 200 mM sucrose for 24 h (molar ratio of [sucrose]/[dextran] of 4.63). Structural analysis of the reaction products with 1D ^{1}H NMR showed that GtfZ-CD2 indeed also decorated IMMP with (α1→3)-branched glucosyl units. The NMR profiles of the products from the IMMP and dextran incubations with GtfZ-CD2 were almost identical (Figure 27), suggesting that the branched polymers produced from IMMP and from dextran were very similar. Treatment with the GtfZ-CD2 enzyme in the presence of sucrose resulted in disappearance of the (α1→6) signal (δ 4.98), corresponding to linear (α1→6)-linked glucose units, in both the IMMP and dextran products. Instead, a structural unit -(1→3,6)-α-D-Glc*p*-(1→6)- at δ 5.00, corresponding to

an (α1→3) branch point on linear (α1→6)-linked glucose units, appeared in the profiles of both polymer products. The high intensity of H-4 signals (δ 3.40~3.45) stemming from terminal glucose units in the IMMP product indicated a high percentage of branching linkages, as seen previously for the dextran product (Figure 26) (Meng, Gangoiti, Wang, et al., 2018). Furthermore, a peak appeared at δ 5.32 that is typical for (α1→3) linkages. Integration of the surface areas of the (α1→3)-linkage signal at δ 5.32 and the −(1→3,6)-α-D-Glc*p*-(1→6)-linkage signal at δ 5.00 revealed that their ratios were close to one, 0.85 and 0.72 for IMMP and dextran, respectively (Figure 27). This indicates that the (α1→3) signal stems from branched (α1→3)-linkages and not from consecutive (α1→3)-linkages and that most of the (α1→6)-linked glucose units were decorated with an (α1→3)-linked glucose (Figure 26). The absence of the [→6)-α-D-Glc*p*-(1→3)-] epitope at δ 4.20(van Leeuwen et al., 2008) suggests that the (α1→3) glucosyl units were not elongated with (α1→6)-linked glucose units. Methylation analysis showed that the branched IMMP and 70 kDa dextran polymers consisted of 44 and 46% (α1→3) linkages (Table 13) respectively, representing comb-like structures consisting of single (α1→3)-branched glucose units on a linear (α1→6) glucose chain (Figure 26). The branched IMMP polymer had terminal [Glc*p*(1→], 6-substituted [→6)Glc*p*(1→], and 3, 6-substituted [→3,6)Glc*p*(1→] glucosyl units in a molar ratio of 50.8, 5.5 and 43.7%, respectively. No detectable levels of 3-substituted [→3)Glc*p*(1→] glucosyl units were observed, confirming the absence of linear (α1→3) stretches (Table 13, Figure 26).

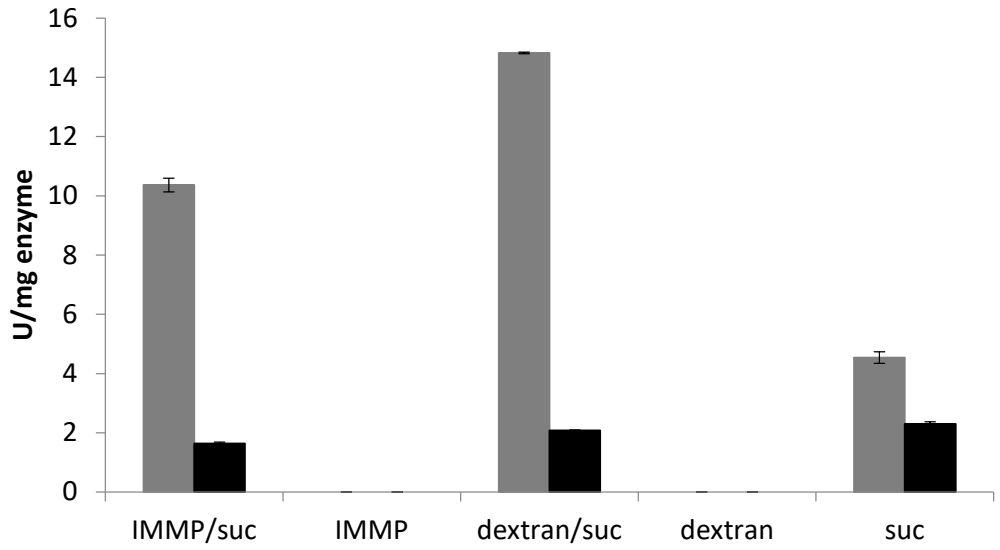

Figure 28. Enzyme activities of GtfZ-CD2 on 7 g/L IMMP (18.3 kDa) or dextran (70 kDa) with and without 200 mM sucrose. Transglucosylation activity (grey bars); sucrose hydrolysis (black bars). Hydrolysis standard deviations were very small and therefore not apparent in this figure.

6.4.4 Synthesis of partially branched IMMP and dextran with GtfZ-CD2

The degree of (α1→3)-branching may well influence the digestibility of the branched IMMP and dextran polymers. To test this, GtfZ-CD2 incubations were performed with fixed IMMP or dextran concentrations and a varying sucrose concentration to modulate the degree of (α1→3)-branching in the polymer products. For comparison, 10.2 kDa dextran was used in this experiment since its molecular weight is more similar to that of IMMP (18.3 kDa) than 70 kDa dextran. Incubation of GtfZ-CD2 with 20 g/L (123 mM anhydroglucose) 10.2 or 70 kDa dextran and 200 mM sucrose (molar ratio of [sucrose]/[dextran anhydroglucose] of 1.63) resulted in 57 and 46% of (α1→3) linkages in the end products, respectively.

NMR analysis of purified reaction products showed that GtfZ-CD2 was also able to partially branch IMMP and dextran (Figure 29, Figure 30). As observed with 70 kDa dextran, branching of the 10.2 kDa dextran leveled off at [sucrose]/[dextran] molar ratios above 0.65, whereas with IMMP the decoration with (α1→3) linkages was less at lower [sucrose]/[IMMP] molar ratios, and had not reached a maximum at a ratio of 1.63. HPSEC analysis of the polymers indeed showed that the M_w of the branched dextran (10.2 kDa) products increased less above a ratio of 0.61, while the M_w of the branched IMMP (18.3 kDa) products displayed a linear increase from 0 to 1.63 (Table 14, Figure 31). This suggests a lower branching efficiency of GtfZ-CD2 with

IMMP compared to dextran, which is also reflected by its lower initial transglucosylase activity with IMMP. Based on linkage type distributions, the (branched) IMMP and dextran (products) are rather similar, but there may be other structural differences that affect the branching efficiency of GtfZ-CD2, e.g. the presence of 6.8% 4-substituted [→4)Glc*p*(1→] linkages in IMMP.

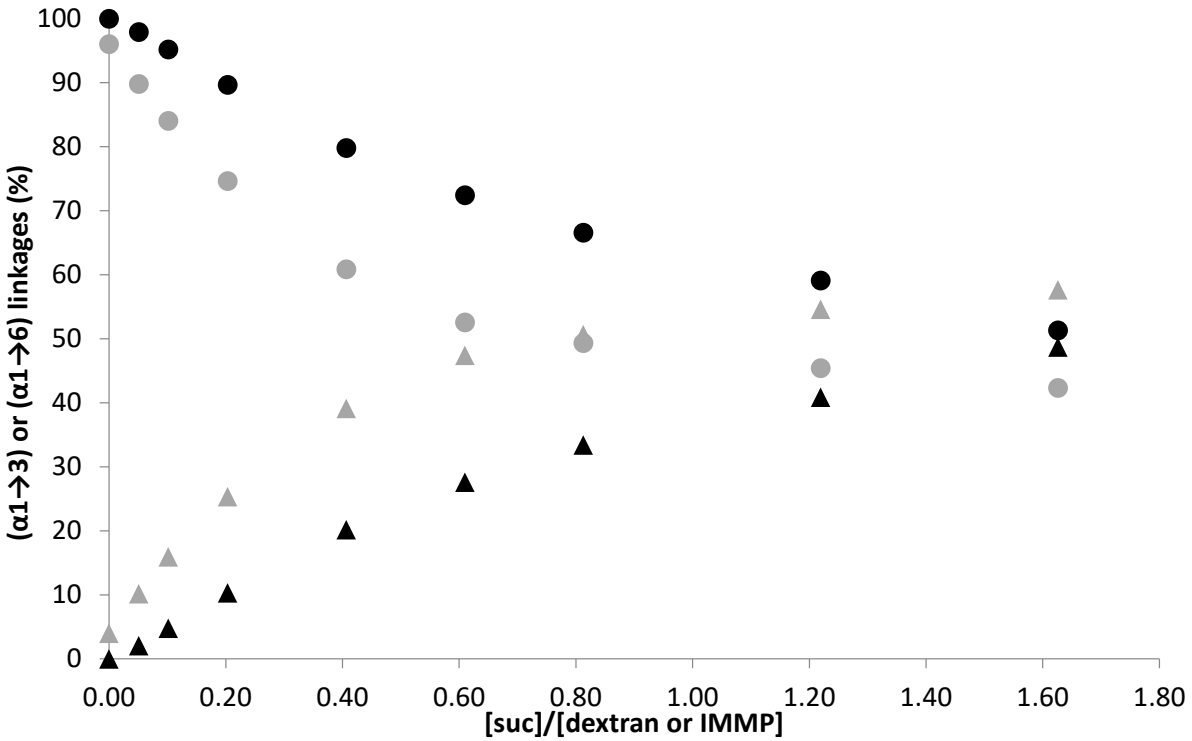

Figure 29. The percentages of (α1→3) (△) and (α1→6) (○) linkages in a range of purified branched polymers, derived from IMMP (18.3 kDa) (black) and dextran (10.2 kDa) (grey), based on the integrated peak areas of their 1D 1H NMR profiles. The polymers were produced during a 24-h incubation of the GtfZ-CD2 enzyme with 20 g/L (123 mM anhydroglucose) IMMP or dextran (Mw 10.2 kDa) at increasing molar ratios of [sucrose]/[IMMP or dextran anhydroglucose]. Sucrose was provided at 0-200 mM. For ratios, also see Table 14

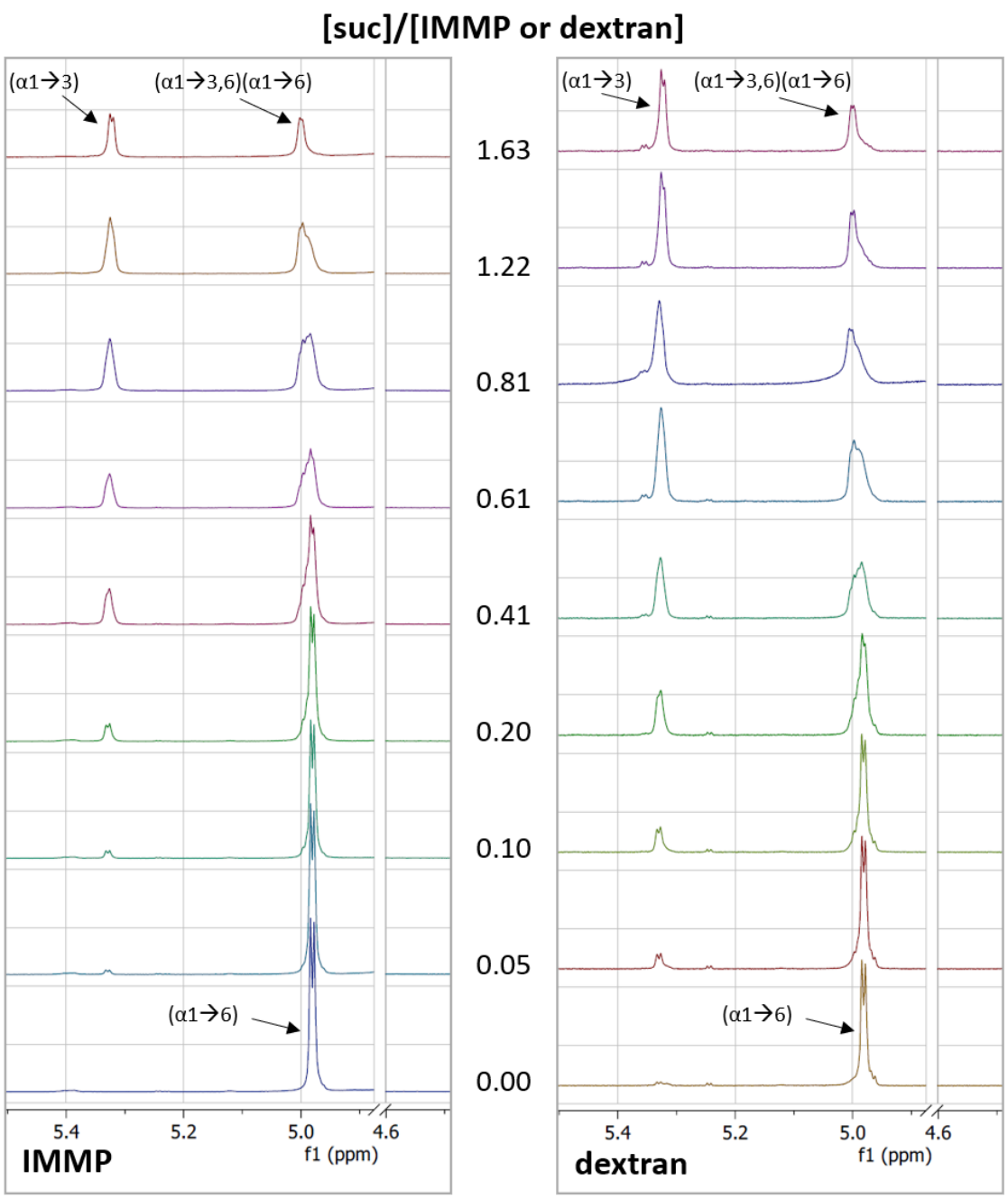

Figure 30. 1H NMR spectra (D2O, 300 K) of polymers formed by the incubation of GtfZ-CD2 and 20 g/L (123 mM) IMMP (18.3 kDa) or dextran (10.2 kDa) with different [sucrose]/[IMMP or dextran] ratios. Chemical shifts are shown in parts per million (ppm) relative to the signal of internal acetone (δ 2.225).

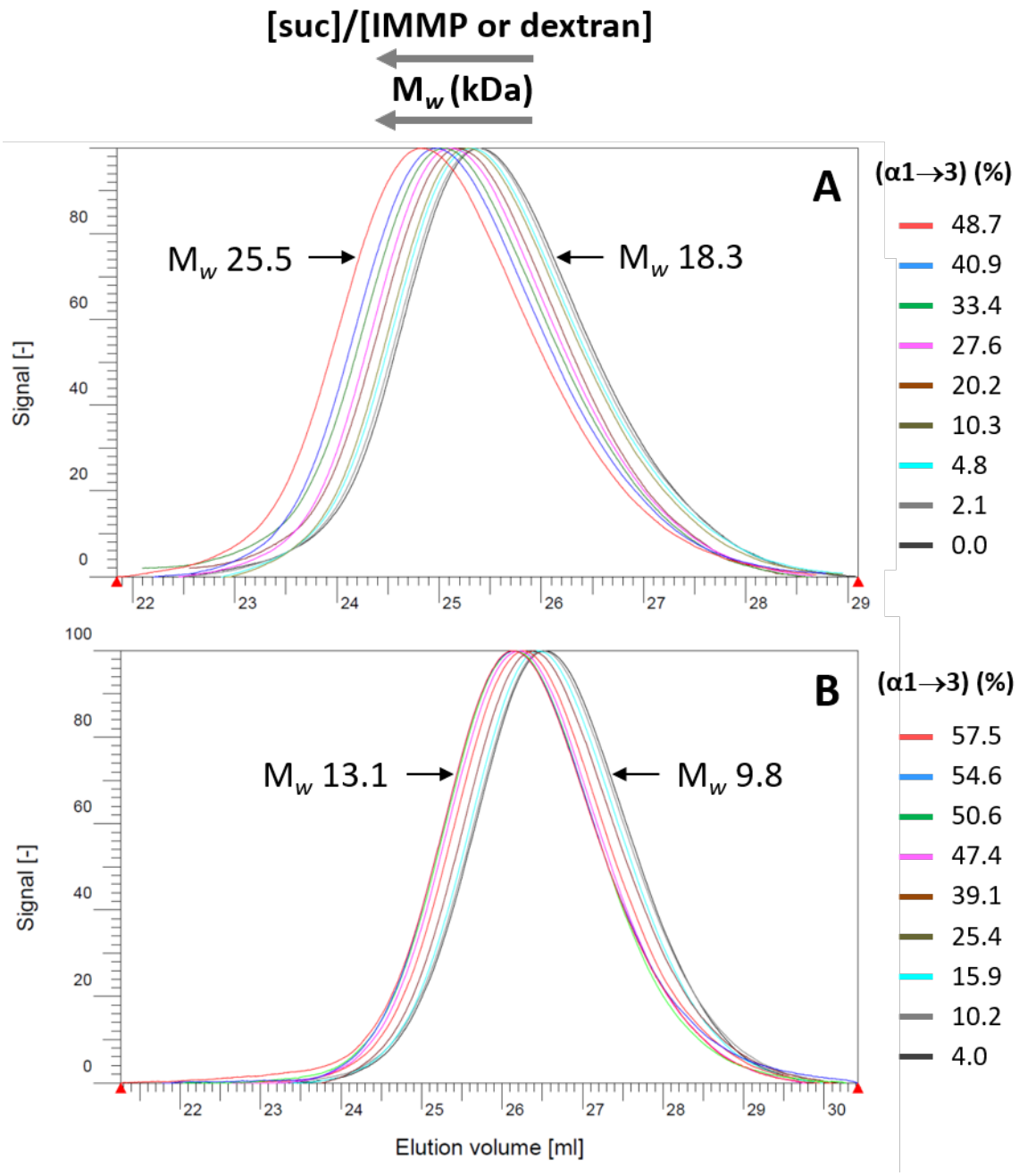

Figure 31. HPSEC chromatograms of a range of purified branched polymers derived from IMMP (18.3 kDa) (A) and dextran (10.2 kDa) (B). The percentages of (α1→3) linkages in the branched polymers are based on the integrated peak areas of their 1D 1H NMR profiles (see % color coding on the right). The polymers were produced during a 24-h incubation of the GtfZ-CD2 enzyme with 20 g/L (123 mM anhydroglucose) IMMP or dextran (Mw 10.2 kDa) at increasing molar ratios of [sucrose]/[IMMP or dextran anhydroglucose]. Sucrose was provided at 0-200 mM. For ratios, also see Table 14.

6.4.5 *In vitro* glucose generation rate (GGR) assay using rat intestinal acetone powder (RIAP)

The digestibility of the branched polymers was tested using the *in vitro* RIAP assay. This assay simulates the digestive power of the human gastrointestinal tract, by using rat intestinal maltase-glucoamylase and sucrase-isomaltase enzymes that digest (α1→6) and (α1→3) linkages (Lee et al., 2016), and residual α-amylase. Digestibility was measured by the release of free glucose from enzymatic hydrolysis of the polymers over time. Polymers that are slowly digestible are less easily hydrolyzed by these enzymes, thus resulting in a decreased glucose release over time. Raw wheat starch was found to be a good representative of a slowly digestible carbohydrate (Zhang, Ao, et al., 2006; Zhang, Venkatachalam, et al., 2006), and was used here as a benchmark.

In vitro digestion analysis showed that, compared to the slowly digestible raw wheat starch benchmark, the unmodified dextran and IMMP α-glucans [0 mM sucrose] had a reduced digestibility (Figure 32). Introduction of (α1→3)-linked branching decreased their digestibility even further, displaying an incremental effect with a greater degree of branching correlating to lower digestibility. Highly branched polymers were essentially not digested. Of interest, IMMP [0 mM sucrose] reached 44% digestion by 6 h; dextran [0 mM sucrose] reached 53% digestion by 6 h. Note that [200 mM sucrose] and [150 mM sucrose] dextran, and [200 mM sucrose] and [0 mM sucrose] IMMP were very hygroscopic and viscous when hydrated and required additional heat and shear application to create homogenous mixtures in solution. These solutions were incubated at 37 ℃ at 1000 rpm for 30 min prior to the digestion assay.

A 6 h timeline was used for the *in vitro* studies in view of the observation that RDS and SDS controls were 100% digested at 6 h *in vitro* digestion (Lee et al., 2016; Shin et al., 2019). Alignment of digestion times between an *in vitro* assay and human digestion is difficult for a number of reasons, including unknown α-glucosidase expression and activity levels along the course of the small intestine, and unknown concentrations of pancreatic α-amylase relative to types of food ingested and location in the small intestine. Thus, it is not possible to directly compare 1 h of *in vivo* digestion to 1 h of *in vitro* digestion, hence digestions of carbohydrates were considered over 6 h in this *in vitro* model (Figure 32).

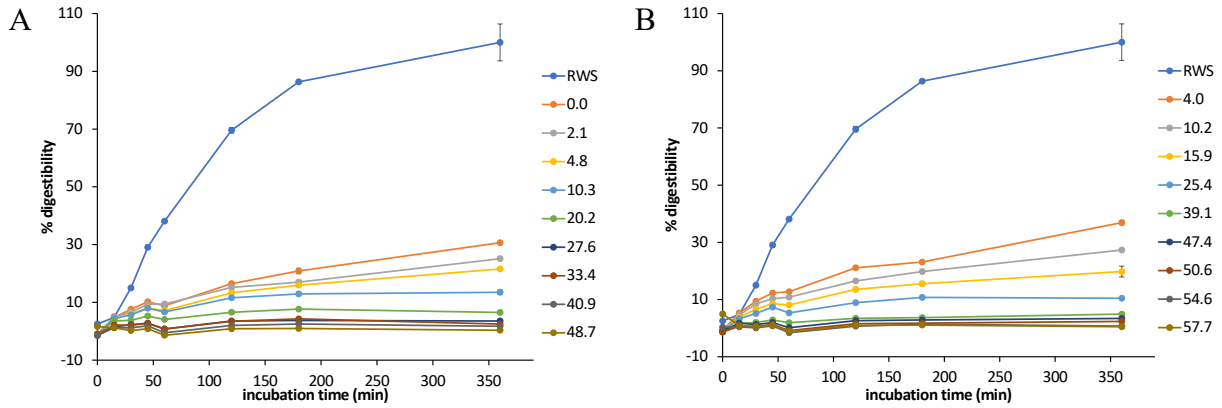

Figure 32. Digestibility of raw wheat starch (RWS), and a range of purified branched polymers derived from IMMP (A) and dextran (B), in an in vitro digestion assay (6 h) with rat intestinal acetone powder enzymes. Digestibility was measured by the release of free glucose from enzymatic hydrolysis of the polymers over time (in triplicate). Standard deviations were very small and therefore in most cases not apparent in this figure. The percentages of (α1→3) linkages in the branched polymers are based on the integrated peak areas of their 1D 1H NMR profiles (see % color coding on the right). The polymers were produced during a 24-h incubation of the GtfZ-CD2 enzyme with 20 g/L (123 mM anhydroglucose) IMMP or dextran (Mw 10.2 kDa) at increasing molar ratios of [sucrose]/[IMMP or dextran anhydroglucose]. Sucrose was provided at 0-200 mM. For ratios, also see Table 14

In conclusion, treatment of amylose with 4,6-α-glucanotransferase and branching sucrase/sucrose allowed synthesis of starch derived α-glucans with markedly reduced digestibility. These starch derived α-glucans may find application in the food industry.

6.5 References

Bai, Y., Gangoiti, J., Dijkstra, B. W., Dijkhuizen, L., & Pijning, T. (2017). Crystal Structure of 4,6-α-Glucanotransferase Supports Diet-Driven Evolution of GH70 Enzymes from α-Amylases in Oral Bacteria. *Structure*, *25*(2), 231–242. https://doi.org/10.1016/j.str.2016.11.023

Bai, Y., van der Kaaij, R. M., Leemhuis, H., Pijning, T., Leeuwen, S. S. van, Jin, Z., & Dijkhuizen, L. (2015). Biochemical characterization of the Lactobacillus reuteri glycoside hydrolase family 70 GTFB type of 4,6-α-glucanotransferase enzymes that synthesize soluble dietary starch fibers. *Applied and Environmental Microbiology*, *81*(20), 7223–7232. https://doi.org/10.1128/AEM.01860-15

Brison, Y., Pijning, T., Malbert, Y., Fabre, É., Mourey, L., Morel, S., Potocki-Véronèse, G., Monsan, P., Tranier, S., Remaud-Siméon, M., & Dijkstra, B. W. W. (2012). Functional and structural characterization of α-(1→2) branching sucrase derived from DSR-E glucansucrase. *Journal of Biological Chemistry*, *287*(11), 7915–7924. https://doi.org/10.1074/jbc.M111.305078

Ciucanu, I., & Kerek, F. (1984). A simple and rapid method for the permethylation of carbohydrates. *Carbohydrate Research*, *131*(2), 209–217. https://doi.org/10.1016/0008-6215(84)85242-8

Dobruchowska, J. M., Gerwig, G. J., Kralj, S., Grijpstra, P., Leemhuis, H., Dijkhuizen, L., & Kamerling, J. P. (2012). Structural characterization of linear isomalto-/malto-oligomer products synthesized by the novel GTFB 4,6 α-glucanotransferase enzyme from Lactobacillus reuteri 121. *Glycobiology*, *22*(4), 517–528. https://doi.org/10.1093/glycob/cwr167

Englyst, H. N., Kingman, S. M., & Cummings, J. H. (1992). Classification and measurement of nutritionally important starch fractions. *European Journal of Clinical Nutrition*, *46*(SUPPL. 2), S33-50. https://doi.org/10.1016/S0271-5317(97)00010-9

Gangoiti, J., Corwin, S. F., Lamothe, L. M., Vafiadi, C., Hamaker, B. R., & Dijkhuizen, L. (2018). Synthesis of novel α-glucans with potential health benefits through controlled glucose release in the human gastrointestinal tract. In *Critical Reviews in Food Science and Nutrition* (Vol. 60, Issue 1). https://doi.org/10.1080/10408398.2018.1516621

Gangoiti, J., Pijning, T., & Dijkhuizen, L. (2018). Biotechnological potential of novel glycoside hydrolase family 70 enzymes synthesizing α-glucans from starch and sucrose. *Biotechnology Advances*, *36*(1), 196–207. https://doi.org/10.1016/j.biotechadv.2017.11.001

Gangoiti, J., Van Leeuwen, S. S., Meng, X., Duboux, S., Vafiadi, C., Pijning, T., & Dijkhuizen, L. (2017). Mining novel starch-converting Glycoside Hydrolase 70 enzymes from the Nestlé Culture Collection genome database: The Lactobacillus reuteri NCC 2613 GtfB. *Scientific Reports*, *7*(1). https://doi.org/10.1038/s41598-017-07190-z

Gangoiti, J., Van Leeuwen, S. S., Vafiadi, C., & Dijkhuizen, L. (2016). The Gram-negative bacterium Azotobacter chroococcum NCIMB 8003 employs a new glycoside hydrolase family 70 4,6-α-glucanotransferase enzyme (GtfD) to synthesize a reuteran like polymer from maltodextrins and starch. *Biochimica et Biophysica Acta - General Subjects*, *1860*(6), 1224–1236. https://doi.org/10.1016/j.bbagen.2016.02.005

Gu, F., Borewicz, K., Richter, B., van der Zaal, P. H., Smidt, H., Buwalda, P. L., & Schols, H. A. (2018). In Vitro Fermentation Behavior of Isomalto/Malto-Polysaccharides Using Human Fecal Inoculum Indicates Prebiotic Potential. *Molecular Nutrition and Food Research*, *62*(12). https://doi.org/10.1002/mnfr.201800232

Kamerling, J. P. P., & Gerwig, G. J. J. (2007). Strategies for the Structural Analysis of Carbohydrates. In J. Kamerling, G. Boons, Y. Lee, A. Suzuki, N. Taniguchi, & A. Voragen (Eds.), *Comprehensive Glycoscience: From Chemistry to Systems Biology* (Vols. 2–4, pp. 1–68). Elsevier Ltd. https://doi.org/10.1016/B978-044451967-2/00032-5

Kralj, S., Grijpstra, P., van Leeuwen, S. S., Leemhuis, H., Dobruchowska, J. M., van der Kaaij, R. M., Malik, A., Oetari, A., Kamerling, J. P., & Dijkhuizen, L. (2011). 4,6-α-Glucanotransferase, a Novel Enzyme That Structurally and Functionally Provides an Evolutionary Link Between Glycoside Hydrolase Enzyme Families 13 and 70. *Applied and Environmental Microbiology*, *77*(22), 8154–8163. https://doi.org/10.1128/AEM.05735-11

Lee, B. H., Rose, D. R., Lin, A. H. M., Quezada-Calvillo, R., Nichols, B. L., & Hamaker, B. R. (2016). Contribution of the Individual Small Intestinal α-Glucosidases to Digestion of Unusual α-Linked Glycemic Disaccharides. *Journal of Agricultural and Food Chemistry*, *64*(33), 6487–6494. https://doi.org/10.1021/acs.jafc.6b01816

Leemhuis, H., Dobruchowska, J. M., Ebbelaar, M., Faber, F., Buwalda, P. L., Van Der Maarel, M. J. E. C., Kamerling, J. P., & Dijkhuizen, L. (2014). Isomalto/malto-polysaccharide, a novel soluble dietary fiber made via enzymatic conversion of starch. *Journal of Agricultural and Food Chemistry*, *62*(49), 12034–12044. https://doi.org/10.1021/jf503970a

Mayer, R. M., Matthews, M. M., Futerman, C. L., Parnaik, V. K., & Jung, S. M. (1981). Dextransucrase: Acceptor substrate reactions. *Archives of Biochemistry and Biophysics*, *208*(1), 278–287. https://doi.org/10.1016/0003-9861(81)90150-8

Meng, X., Gangoiti, J., Bai, Y., Pijning, T., Van Leeuwen, S. S., & Dijkhuizen, L. (2016). Structure–function relationships of family GH70 glucansucrase and 4,6-α-glucanotransferase enzymes, and their evolutionary relationships with family GH13 enzymes. *Cellular and Molecular Life Sciences*, *73*(14), 2681–2706. https://doi.org/10.1007/s00018-016-2245-7

Meng, X., Gangoiti, J., de Kok, N., van Leeuwen, S. S., Pijning, T., & Dijkhuizen, L. (2018). Biochemical characterization of two GH70 family 4,6-α-glucanotransferases with distinct product specificity from Lactobacillus aviarius subsp. aviarius DSM 20655. *Food Chemistry*, *253*, 236–246. https://doi.org/10.1016/j.foodchem.2018.01.154

Meng, X., Gangoiti, J., Wang, X., Grijpstra, P., van Leeuwen, S. S., Pijning, T., & Dijkhuizen, L. (2018). Biochemical characterization of a GH70 protein from Lactobacillus kunkeei DSM 12361 with two catalytic domains involving branching sucrase activity. *Applied Microbiology and Biotechnology*, *102*(18), 7935–7950. https://doi.org/10.1007/s00253-018-9236-6

Nichols, B. L. L., Avery, S., Sen, P., Swallow, D. M. M., Hahn, D., & Sterchi, E. (2003). The maltase-glucoamylase gene: Common ancestry to sucrase-isomaltase with complementary starch digestion activities. In *Proceedings of the National Academy of Sciences* (Vol. 100, Issue 3). National Academy of Sciences. https://doi.org/10.1073/pnas.0237170100

Passerini, D., Vuillemin, M., Ufarté, L., Morel, S., Loux, V., Fontagné-Faucher, C., Monsan, P., Remaud-Siméon, M., & Moulis, C. (2015). Inventory of the GH70 enzymes encoded by Leuconostoc citreum NRRL B-1299 - Identification of three novel α-transglucosylases. *FEBS Journal*, *282*(11), 2115–2130. https://doi.org/10.1111/febs.13261

Pijning et al., in preparation. (n.d.). *Pijning et al., in preparation*.

Seo, J., Lamothe, L. M., Austin, S., & Lee, B.-H. (2018). Determination of glucose generation rate from various types of glycemic carbohydrates by optimizing the mammalian glycosidases anchored in the small intestinal tissue. *Poster Presented at: AACC International Annual Meeting*.

Shin, H., Seo, D. H., Seo, J., Lamothe, L. M., Yoo, S. H., & Lee, B. H. (2019). Optimization of in vitro carbohydrate digestion by mammalian mucosal α-glucosidases and its applications to hydrolyze the various sources of starches. *Food Hydrocolloids*, *87*, 470–476. https://doi.org/10.1016/j.foodhyd.2018.08.033

van der Zaal, P. H., Schols, H. A., Bitter, J. H., & Buwalda, P. L. (2018). Isomalto/malto-polysaccharide structure in relation to the structural properties of starch substrates. *Carbohydrate Polymers*, *185*, 179–186. https://doi.org/10.1016/j.carbpol.2017.11.072

Van Geel-Schutten, G. H., Faber, E. J., Smit, E., Bonting, K., Smith, M. R., Ten Brink, B., Kamerling, J. P., Vliegenthart, J. F. G., & Dijkhuizen, L. (1999). Biochemical and structural characterization of the glucan and fructan exopolysaccharides synthesized by the Lactobacillus reuteri wild-type strain and by mutant strains. *Applied and Environmental Microbiology*, *65*(7), 3008–3014. https://doi.org/10.1128/aem.65.7.3008-3014.1999

van Leeuwen, S. S., Kralj, S., van Geel-Schutten, I. H., Gerwig, G. J., Dijkhuizen, L., & Kamerling, J. P. (2008). Structural analysis of the α-d-glucan (EPS180) produced by the Lactobacillus reuteri strain 180 glucansucrase GTF180 enzyme. *Carbohydrate Research*, *343*(7), 1237–1250. https://doi.org/10.1016/j.carres.2008.01.042

Vasanthan, T. (2005). Enzymatic Quantitation of Total Starch in Plant Products. In *Handbook of Food Analytical Chemistry* (Vols. 1–2, pp. 679–687). https://doi.org/10.1002/0471709085.ch16

Vuillemin, M., Claverie, M., Brison, Y., Séverac, E., Bondy, P., Morel, S., Monsan, P., Moulis, C., & Remaud-Siméon, M. (2016). Characterization of the first α-(1→3) branching sucrases of the GH70 family. *Journal of Biological Chemistry*, *291*(14), 7687–7702. https://doi.org/10.1074/jbc.M115.688044

Zhang, G., Ao, Z., & Hamaker, B. R. (2006). Slow digestion property of native cereal starches. *Biomacromolecules*, *7*(11), 3252–3258. https://doi.org/10.1021/bm060342i

Zhang, G., Venkatachalam, M., & Hamaker, B. R. (2006). Structural basis for the slow digestion property of native cereal starches. *Biomacromolecules*, *7*(11), 3259–3266. https://doi.org/10.1021/bm060343a